The Dissertation Committee for Niti Bhushan Mishra Certifies that this is the approved version of the following dissertation:

CHARACTERIZING ECOSYSTEM STRUCTURAL AND FUNCTIONAL PROPERTIES IN THE CENTRAL KALAHARI USING MULTI-SCALE REMOTE SENSING

Committee:

Kelley A. Crews, Supervisor

Kenneth R. Young

Jennifer A. Miller

Mark T. Simmons

Gregory S. Okin

CHARACTERIZING ECOSYSTEM STRUCTURAL AND FUNCTIONAL PROPERTIES IN THE CENTRAL KALAHARI USING MULTI-SCALE REMOTE SENSING

by

Niti Bhushan Mishra, M.A.; M.S.

Dissertation

Presented to the Faculty of the Graduate School of

The University of Texas at Austin

in Partial Fulfillment

of the Requirements

for the Degree of

Doctor of Philosophy

The University of Texas at Austin

May 2014

Dedication

To my loved ones and the Kalahari.

Acknowledgements

CHARACTERIZING ECOSYSTEM STRUCTURAL AND FUNCTIONAL PROPERTIES IN THE CENTRAL KALAHARI USING MULTI-SCALE REMOTE SENSING

Niti Bhushan Mishra, PhD

The University of Texas at Austin, 2014

Supervisor: Kelley A. Crews

Understanding, monitoring and managing savanna ecosystems require characterizing both functional and structural properties of vegetation. Due to functional diversity and structural heterogeneity in savannas, characterizing these properties using remote sensing is methodologically challenging. Focusing on the semi-arid savanna in the central Kalahari, the objective of this dissertation was to combine *in situ* data with multi-scale satellite imagery and two image analysis approaches (i.e. Multiple Endmember Spectral Mixture Analysis (MESMA) and Object Based Image Analysis (OBIA)) to : (i) determine the superior method for estimating fractional photosynthetic vegetation (f_{PV}), non-photosynthetic vegetation (f_{NPV}) and bare soil (f_{BS}) when high spatial resolution multispectral imagery is used, (ii) examine the suitability of OBIA for mapping vegetation morphology types using a Landsat TM imagery, (iii) examine the impact of changing spatial resolution on magnitude and accuracy of fractional cover and (iv) examine how the fractional cover magnitude and accuracy are spatially associated with vegetation morphology.

Using the GeoEye-1 imagery, MESMA provided more accurate fractional cover estimates than OBIA. The increasing segmentation scale in OBIA resulted in a consistent increase in error. While areas under woody cover produced lower errors even at coarse segmentation scales, those with herbaceous cover provided low errors only at the fine segmentation scale. Vegetation morphology type mapping results suggest that classes with dominant woody life forms attained higher accuracy at fine segmentation scales, while those with dominant herbaceous vegetation reached higher classification accuracy at coarse segmentation scales. Contrarily, for bare areas accuracy was relatively unaffected by changing segmentation scale. Multi-scale fractional cover mapping results indicate that increasing pixel size caused consistent increases in variance of and error in fractional cover estimates. Even at a coarse spatial resolution, f_{PV} was estimated with higher accuracy compared to f_{NPV} and f_{BS}. At a larger pixel size, in areas with dominant woody vegetation, f_{PV} was overestimated at the cost of mainly underestimating f_{BS}; in contrast, in areas with dominant herbaceous vegetation, f_{NPV} was overestimated with a corresponding underestimation of both f_{PV} and f_{BS}. These results underscore that structural and functional heterogeneity in savannas impact retrieval of fractional cover, suggesting that comprehensive remote sensing of savannas needs to take both structure and cover into account.

Table of Contents

xi

List of Tables

xiii

List of Figures

xix

List of Illustrations

Chapter 1: Introduction

Research motivation

Anthropogenic activities over the last few decades have affected Earth's ecosystems more rapidly and extensively than ever before (Adeel et al. 2005; Werger 1973). To meet the growing demand for food, fresh water and fuel, humans have utilized a variety of goods and services of terrestrial ecosystems resulting in substantial changes in the ecosystem processes and number of negative consequences (Lambin et al. 2001; Peters et al. 2006; Poole 2002). The expansion and intensification of land use has resulted in, among many others, destruction of natural habitats and biodiversity loss, soil erosion and nutrient loss (Aplin 2005; Southworth et al. 2002; Turner et al. 2007; Wiegand et al. 2005). Under these circumstances the future sustainability of terrestrial ecosystems and their ability to meet the needs of growing human population is threatened.

For understanding and managing terrestrial ecosystems, characterizing land cover and land use change (LCLUC) has emerged as a key research area. In this regard, increasing research emphasis on land cover land use related research has resulted in the emergence of land change science as an interdisciplinary research theme (Gutman 2004; Turner et al. 2007). Changes in land cover directly impact carbon and hydrological cycles that have significant implications for climate at the local and regional scales (Aplin 2005; Bhattacharya et al. 2003; Brock and Kelt 2004; Wu 2007). Information on land cover and land use dynamics is not only considered a key resource for environmental and socio-economic planning but also constitutes an essential parameter for environmental modeling at all scales (Lambin and Geist 2006; Turner et al. 2007). Over the last two decades, substantial progress in various disciplines has resulted in increased availability of environmental data. Significant increases in the number of satellite and airborne Earth

observation sensors has enabled monitoring LCLUC at different spatio-temporal scales (Andrews 1990; Develey and Stouffer 2001; Gutman 2004; Knight and Morris 1996; Van Rooyen et al. 1990). As a result of increases in the number of users and producers of remotely sensed land cover data during the last decade, the Earth observation technologies have found their way into wide range of scientific disciplines. In interdisciplinary scientific disciplines, information exchange implicates the association of different conceptual views and thematic descriptions on the same research theme. For the land change science community the result was an increase of land cover information and the need to integrate interpretations, definitions and understandings from different perspectives (Hüttich et al. 2011a; Turner et al. 2007).

Due to the increasing importance of land cover information for monitoring global change, several earth observation data archives have been created (e.g. images acquired from Landsat, Advanced Very High Resolution Radiometer (AVHRR), and Moderate Resolution Imaging Spectroradiometer (MODIS)). Utilizing these archived datasets several important research projects have been conducted for characterizing land cover at the global scale (e.g. IGBP DISCover (Heilman et al. 2002), Global Land Cover (GLC2000) (Gelbard and Belnap 2003), University of Maryland Global Land Cover (Forman and Alexander 1998) (Table 1). Comparative studies accessing the relative accuracy of global land cover datasets in various terrestrial ecosystems have found that drylands/semi-arid savanna ecosystems have the lowest mapping accuracy compared to other biomes (e.g. tropical/temperate rainforests, boreal forests) (Fahrig and Rytwinski 2009; Flather and Bevers 2002; Jaeger et al. 2005). Comparison of land cover types related to savanna biomes show low spatial agreement and comparatively low mapping accuracies with 60.3% for herbaceous vegetation and 65.8% for shrublands (Herold et al. 2008). Studies in these ecosystems have attributed such low mapping accuracy to high

structural heterogeneity and functional diversity in the spatial distribution of life forms (e.g. trees, shrubs and grasses as shown in figure 1.1) forming zones of fuzzy transition (Hill et al. 2012; Hüttich et al. 2011b; Shugart et al. 2004). The coexistence of woody and herbaceous life forms and the different phenological characteristics of these contrasting life forms have been found to influence the remote sensing based analysis approaches that are largely based on statistical analysis of spectral and temporal features derived from remotely sensed datasets (Guerschman et al. 2009; Huete and Jackson 1988; Steen and Gibbs 2004; Van Rooyen et al. 1990). Furthermore, while the majority of scientific research and methodological development has focused on forest ecosystems under different climatic regimes worldwide, dryland ecosystems, in spite of their considerable area, have comparatively received limited scientific attention (Adeel et al. 2005; Watkins et al. 2003; Werger 1973).

Global drylands that include tropical and sub-tropical savanna ecosystems are one of the largest biomes covering over 40% of terrestrial area globally and nearly 60% of sub-Saharan Africa. In addition to their main geographical distribution in Africa, savannas also cover significant areas in South America, Australia and Asia (Mistry 2000; Watkins et al. 2003). Due to their geographical extent, savanna ecosystems play a significant role in global land-atmosphere energy balance as well as carbon and nutrient cycles (Hill et al. 2011a; Mistry 2000). They provide a variety of ecological goods and services and also have high socio-economic importance. Although, savannas are areas of low productivity, they have been a source of biotic, social and scientific innovation. Savanna ecosystems contain one third of the global biodiversity hotspots with diversity of large mammals, endemic vascular plants, amphibians, reptiles and birds (Addicott et al. 1987; Jane et al. 2006; Lal 2004). Many tropical savannas are found in semi-arid climates where a constantly changing distribution of soil moisture is supplied by predominantly

convective storms that vary considerably in both frequency and depth (McCown and Williams 1990; Sala and Lauenroth 1982). In southern Africa, semi-arid savannas are extensive but varied, ranging from partially closed woodlands to sparsely covered shrublands (Scholes et al. 2002). Southern Africa savanna ecosystems are economically significant as they offer the basis of economic activity by supporting high populations of livestock as well as wildlife-based tourism in several developing economies (Boyce et al. 2003; Thomas and Shaw 1991; Werger 1973).

Over the last few decades, the impact of global change on savanna ecosystems has been mainly driven by the expansion and intensification of land use and increasing climatic variability. Particularly in southern Africa savanna ecosystems, increasing anthropogenic pressure coupled with changing government policies that seek to improve livelihood opportunities for the population are facilitating the conversion of large parts of previously natural savanna areas into pastures for commercial livestock ranching or pastoral/rain fed agriculture (Adeel et al. 2005; Furley 2004; Thomas and Shaw 1991). As a result of this changing land use and altered fire regimes over large geographical extents in southern Africa, savanna vegetation is undergoing changes in structural and functional properties (Dougill et al. 1999; Hudak and Wessman 1998; Moleele et al. 2002; Skarpe 1990; Thomas and Sporton 1997; Thomas and Twyman 2004; Zhu and Southworth 2013). This in turn is affecting biogeochemical processes and the availability of habitat-related key structural resources (e.g. solitary nesting trees, foraging grounds, breeding zones, hiding places and safe migration routes) also leading to increased human-animal conflict (Blaum et al. 2007; McDermid et al. 2005; Tews et al. 2004; Tews et al. 2006; Wiegand et al. 2006). The changing structural and functional characteristics of vegetation assemblages observed in southern Africa are also a global phenomenon encountered in Sahelian Africa (Warren and Agnew 1988), North America and Mexico

(Archer et al. 1988), Australia (Andrew 1988) and South America (Medina and Silva 1991). Additionally, climatic predictions suggest that under current climatic developments, southern African arid and semi-arid systems will experience an increased aridity due to higher mean temperatures and more highly variable mean annual precipitation (Hulme and Arntzen 1996; Solomon et al. 2007; Thomas et al. 2005), further aggravating the resource base and livelihood options for the increasing local population.

Decreasing vegetation cover and changing species composition are sensitive indicators of land degradation in southern Africa savanna areas (Adeel et al. 2005; Archer et al. 1988; Homewood 1996; Southworth et al. 2013). While vegetation cover is treated as an important indicator in savanna systems, it is also a determinant of landscape function as it is related to the ability of the landscape to capture rainfall or lose it through surface runoff (Caylor et al. 2003; Ludwig et al. 2007). Furthermore, in semi-arid savanna ecosystems the exchange of energy and water balance is controlled by transpiration and evaporation through the proportion of photosynthetically active vegetation (f_{PV}), non-photosynthetically active vegetation (f_{NPV}) and bare soil (f_{BS}) (Asner et al. 2011; Scanlon et al. 2002). In semi-arid savannas, f_{PV} can be directly related to above ground carbon dynamics (Hill et al. 2012), f_{NPV} is intimately related to fire frequency and intensity and also contributes to the total biomass (Edwards et al. 2013; Roy et al. 2011). Similarly, f_{BS} is also significant as it controls wind and water erosion (Edwards et al. 2013; Ludwig et al. 2004; Okin et al. 2009). Thus in savanna ecosystems, f_{PV}, f_{NPV} and f_{BS} can serve as key state variables and by accurately quantifying and monitoring their temporal dynamics can help understand ecosystem functional dynamics and shed light on ecological processes in these systems (Asner et al. 2011; Guerschman et al. 2009; Hill 2013; Okin 2007a).

5

Besides vegetation functional properties, vegetation in savanna ecosystems also shows substantial variation in terms of vegetation structural/morphological properties. Savannas are structurally diverse ecosystems where vegetation morphology can range from dense shrubland and woodland to medium dense shrubland with grasses and open grassland with little shrub cover (Caylor et al. 2003; Privette et al. 2004; Sankaran et al. 2005). Unlike f_{PV}, f_{NPV} and f_{BS} that highlight ecosystem functional dynamics, vegetation morphology can reveal ecosystem structural properties. Accurately characterizing vegetation morphological properties (vegetation density, height, floristic composition) is also essential in semi-arid savannas as it will not only help understand vegetation structural properties but will enable detection of woody plant encroachment and associated changes in savanna ecological processes (Archer et al. 1994; Laliberte et al. 2004; Levick and Rogers 2006).

The assessment of both ecosystem structural and functional properties in savannas is possible following a field based approach. However, field assessments are limited in scope and scale in savannas that are geographically extensive, remote and wild (Hill et al. 2011a). Remote sensing provides an important alternative tool for characterizing and monitoring these critical ecosystem properties and can not only complement field measurements but also provide much larger spatial coverage including areas that would be inaccessible on ground (Huete et al. 2003). Most field based studies in savannas have been focused on local scales to examine interaction of biotic and abiotic savanna determinants and resulting spatial patterns (Hill et al. 2011a; Scholes and Walker 1993). There have only been a few studies that compiled field data from several field locations and attempted relating savanna spatial patterns to ecological processes at regional scales (Sankaran et al. 2005). However, more recent ecological questions in savannas related to global climate change and ecosystem functioning have motivated researchers to

investigate how local processes are transferred across scales and how regional vegetation patterns and processes influence and are influenced by large scale dynamics and energy exchanges (Bucini and Hanan 2007; Hanan and Lehmann 2010; Hill 2013). More recent investigations and focus on these research questions in savanna ecosystems have been possible due to the availability of variables derived from remotely sensed data at multiple spatial and temporal scales that are comparable with field derived parameters (Hill 2013).

The use of remotely sensed imagery for characterizing structural and functional properties of savanna ecosystems has been proven to be effective and suitable as demonstrated by number of landscape to regional scale studies conducted within the southern Africa savanna system in general (Chamaille-Jammes and Fritz 2009; Gessner et al. 2013; Hüttich et al. 2011b; Justice et al. 1996; Privette and Roy 2005; Steenkamp et al. 2008; Swap et al. 2003) and the semi-arid Kalahari savanna system of Botswana in particular (Caylor et al. 2003; Cui et al. 2013; Jin et al. 2013; Ringrose et al. 2005; Scanlon et al. 2007; Scholes et al. 2002; Shugart et al. 2004; Southworth et al. 2013; van Bommel et al. 2006). Ecological studies in savanna ecosystems focus on the assessment of ecosystem structure, function at local, landscape and regional scales or on the calibration and validation programs for remote sensing derived bio-physical parameters and estimates (Hill et al. 2011a). Important research activities in the southern Africa savanna that have focused on these research objective include the Southern Africa Regional Science Initiative (SAFARI 2000) (Swap et al. 2003), Biodiversity Transect Monitoring Program (BIOTA) (Krug et al. 2006) and studies along the Kalahari Transect established under the International Geosphere Biosphere Program (IGBP) (Caylor et al. 2003). This trend suggests that in southern Africa savanna ecosystems, the number, value and importance of ecological applications using remotely sensed imagery have increased during the last two decades. Both field-based ecological studies and satellite remote

sensing application in semi-arid savanna systems have, in particular, focused on monitoring and assessment of land degradation and associated loss of biodiversity which is a major ecosystem service in the southern Africa savanna systems (Archibald et al. 2010; Huntley 1982; Scholes and Walker 1993). The value of functional diversity is given by (a) the balanced coexistence of woody and herbaceous life forms (to prevent bush encroachment) and maintain a sustainable carrying capacity of livestock, (b) the economic benefit for a diverse and healthy plant and animal life since large proportion of the local economy is tourism dependent and (c) the knowledge of the spatial distribution of numerous savanna vegetation types that are important for rangeland management and conservation purposes (Adeel et al. 2005; Huttich et al. 2009).

Compared to other terrestrial ecosystems (e.g. tropical rain forests), due to the functional diversity and structural heterogeneity in savannas, f_{PV}, f_{NPV} and f_{BS} have been considered ecologically more important land surface bio-physical property that related to ecosystem dynamics (Asner et al. 2011). Hence for the last two decades, remote sensing based fractional cover estimation in savannas and drylands has been a major research theme within environmental remote sensing (Asner and Heidebrecht 2002; Asner et al. 2011; Asner and Lobell 2000; Gessner et al. 2013; Guerschman et al. 2009; Numata et al. 2007; Okin 2007a; Okin et al. 2013; Roberts et al. 1998; Smith et al. 1990; Xiao and Moody 2005). In spite of the significant research interest there exist number of questions and methodological challenges pertaining to our current ability to accurately estimate f_{PV}, f_{NPV} and f_{BS} in savanna ecosystems at the landscape to regional scale. These methodological changes are perhaps due to the set of trade-offs observed in remote sensing science. A limited number of photons arriving at a sensor require trade-off between bandwidth, pixel size and noise. Furthermore, orbital mechanics limit spaceborn platforms requiring trade-offs between repeat time and swath width.

Besides vegetation functional properties, vegetation in savanna ecosystems also show significant variation in terms of vegetation structural or morphological properties i.e. dominant or co-dominant life forms, vegetation density and height. Savannas are structurally diverse ecosystems where vegetation morphology can range from dense shrubland and woodland to medium dense shrubland with grasses and open grassland with little shrub cover (Caylor et al. 2003; Privette et al. 2004; Sankaran et al. 2005). Characterizing vegetation morphological properties (vegetation density, height, and floristic composition) is also important in savannas but unlike f_{PV}, f_{NPV} and f_{BS} that highlight ecosystem functional dynamics, vegetation morphological properties reveal ecosystem structural properties. A significant part of southern Africa's- and in particular Botswana's- natural and semi-natural land is not surveyed in terms of vegetation morphological properties and community composition (Reed and Dougill 2010). Spatially explicit information about vegetation morphological properties in savannas and its temporal dynamics in response to changing biotic and abiotic drivers at suitable spatial scale is critical for resource management and ecologically informed decision making by governmental authorities (DWNP 2003; Reed et al. 2007; Thomas and Sporton 1997). Currently, there is a lack of wall to wall environmental geodata on vegetation physiognomic and floristic composition in Botswana. More than two thirds area of the country is covered by the Kalahari sands and livestock ranching is the dominant land use. Land-use designations are established considering the availability of natural resources such as biodiversity richness and physiographic and geological conditions (Dahlberg 2000). North and south-eastern Botswana has more fragmented land use than other parts of the country (Herremans 1998). Certain areas such as the Okavango Delta have been studied more intensively than others (e.g. central Kalahari) (Thomas 2002)

Previous studies in savanna have shown that low spatial resolution dataset faces significant challenges in accurately characterizing vegetation functional as well as morphological properties due to relatively low niche differentiation and inherent structural heterogeneity. While high spatial resolution multi-spectral datasets provide the required spatial detail, they are unsuitable for landscape to regional scale monitoring due to limited spatial coverage and large data size. The increasing availability of multi-scale remotely sensed datasets has motivated researchers to improve upon the existing image analysis methods and also develop new techniques for extracting environmentally or ecologically relevant information from remotely sensed data. Findings from several studies using remotely sensed data for multiple spatio-temporal scales have confirmed that a signal image analysis approach (e.g. per-pixel analysis) may not be suitable for images acquired at different spatial/spectral resolution. To improve upon the limitations of per-pixel analysis approach, studies have utilized new image analysis approaches (e.g. sub-pixel analysis following techniques such as Multiple Endmember Spectral Mixture Analysis (Asner et al. 2011; Guerschman et al. 2009; Hamada et al. 2011; Okin 2007a; Okin and Roberts 2004; Scanlon et al. 2002) or Object Based Image Analysis (Asner et al. 2011; Blaschke 2010; Laliberte et al. 2007; McGlynn and Okin 2006) depending upon the spatial or spectral resolution of the imagery. While sub-pixel image analysis approach as MESMA have been utilized for analyzing medium (e.g. Landsat, ASTER) and low spatial resolution multispectral imagery (e.g. MODIS), (Guerschman et al. 2009) OBIA approach has been favored with high spatial resolution multi-spectral imagery (e.g. Quickbird, IKONOS) (Laliberte et al. 2004).

Research questions/hypotheses

Based on the research motivations mentioned above the research questions and hypothesis examined in this dissertation are:

(i) What are the strength and weaknesses of OBIA and MESMA approaches for deriving f_{PV}, f_{NPV} and f_{BS} in semi-arid central Kalahari savanna using high spatial resolution multi-spectral imagery?

Hypothesis (i) – In semi-arid central Kalahari savanna both MESMA and OBIA produce equally accurate fractional cover estimates using high spatial resolution imagery and there is no significant difference.

Due to their structural heterogeneity and function diversity remote sensing in dry savanna systems faces several methodological challenges. To address these challenges studies have been developing and testing new image analysis methods for accurately characterizing savanna bio-physical characteristics. Comparison and evaluation of such image analysis approaches are important and informative.

ii) How suitably can different vegetation morphological associations in the semi-arid central Kalahari savanna be mapped by integrating in-situ information with high and medium resolution images (i.e. GeoEye, Landsat) in the central Kalahari? What is the impact of changing segmentation scale in OBIA on the mapping accuracy of different vegetation morphology classes in the semi-arid central Kalahari?

Hypothesis (ii) - Integrating in-situ information on vegetation morphological properties with those interpreted from high spatial resolution imagery for training data collection will significantly improve the accuracy of vegetation morphology types in semi-arid savannas. Mapping accuracy of classification for different vegetation morphology types in savannas is dependent on the segmentation scale used in OBIA.

Considering the existing insufficient user accuracies of savanna land cover classes (Fortin et al. 2003), a synergistic approach is required for improving the alienability of vegetation associations by integrating field information (e.g. land type, vegetation composition and physiognomy) with predictor variables derived using remotely sensed datasets available at different spatio-temporal scales. At a finer spatial scale, rather than using per pixel classifiers, integrated land cover related object attributes, such as shape and neighborhood that enhance thematic depth and mapping accuracies should also be considered. Further, products with higher temporal resolution should be used to derive phonological and intensity based time-series matrices that are more suitable for distinguishing savanna vegetation associations and thus exploiting the capability of different remotely sensed datasets to the fullest.

(iii) How does changing spatial and spectral resolution of satellite imagery impact the estimation accuracy of f_{PV}, f_{NPV} and f_{BS} in the semi-arid central Kalahari?

Hypothesis (iii) – Reducing spatial/spectral resolution of imagery will lead to decreased accuracy in fractional cover estimation and different cover types (i.e. f_{PV}, f_{NPV} and f_{BS}) will also vary in terms of mapping accuracy.

Since the ability to detect ecological patterns is scale dependent, it is important to examine the effect of changing spatial/spectral resolution on the level of uncertainty in variables under a nested hierarchical approach. This is necessary especially in structurally heterogeneous and functionally complex savanna systems (Giri et al. 2005; Guerschman et al. 2009; Okin and Roberts 2004). With fractional cover controlling evapotranspiration rate and relating directly to above ground carbon stocks and biomass in low vegetation cover areas (Scholes and Walker 1993), the use of finer scale products to train and validate results obtained at coarser scale (but covering much larger spatial extents) is expected to not only examine the suitability of employed technique, but also improve the reliability of coarse resolution derived estimates for the entire central Kalahari.

(iv) How is the distribution of fractional cover (i.e. f_{PV}, f_{NPV} and f_{BS}) spatially associated with vegetation morphological properties in semi-arid savannas? How do vegetation morphological properties in the semi-arid savanna impact the accuracy of the retrieval of fractional cover?

Hypothesis (iv) - Fractional cover is spatially associated with vegetation type in the central Kalahari and different vegetation associations have significantly different fractional cover pattern. Vegetation morphological properties influence the fractional cover estimation and different vegetation morphology types have also comparatively different mapping accuracies.

Since niche differentiation and alienability of vegetation associations is low in semi-arid savannas, examination of spatial association between savanna vegetation

13

morphological properties and pattern of fractional cover is important to understand how distribution of above ground carbon and biomass varies among the different vegetation associations. This will also highlight if vegetation associations with poor accuracy have also low reliability in terms of fractional cover estimates and *vice-versa* and thus furthering the understanding of savanna structure and function. Considering the principle research questions above, the research framework of this dissertation contributes to the three key issues as described in the figure 1.2.

Dissertation structure

This dissertation utilizes field derived information on vegetation physiognomy/morphology and fractional land cover and those mapped using multi-scale remotely sensed data to examine the impact of spatial heterogeneity and observation scale on characterization results. The dissertation is organized into seven main chapters. Chapter 1 describes the objectives and structure of the research based on the mentioned research framework. Chapter 2 provides the description of the geomorphology, climate, vegetation, soil and land use of the study area in central Kalahari of Botswana. Chapter 3 provides a review of the existing literature on ecology of savanna systems including determinants of savanna ecosystem structure and function, overview of various ecological theories that attempt to explain the coexistence and variation in tree-grass ratio. This chapter also provides a research literature review of field data collection and environmental remote sensing data and methods that are implemented to test the research hypotheses. In addition, this chapter reviews the methods used in remote sensing community for upscaling field derived bio-physical measurements by linking them with multi-scale remotely sensed imagery. Following the described assumptions and research hypothesis, the research presented in chapters' four to six are presented in the form of

research articles, which have been published or submitted to peer-reviewed scientific journals and international scientific conferences. Chapter 4 of this dissertation addresses the first research question/hypothesis mentioned above and compares the relative suitability of OBIA and MESMA approaches for estimating fractional land cover among different vegetation morphology types using high spatial resolution imagery (Mishra and Crews 2014a). Chapter 5 addresses the second research question/hypothesis mentioned earlier. This chapter describes the mapping of vegetation morphology types in the study area by combining hierarchical object based image analysis with an ensemble machine learning approach (Mishra and Crews 2014b). In particular, this chapter examines the impact of changing the segmentation scale in object based classification on the mapping accuracy of different vegetation morphology types. Chapter 6 addresses the third and fourth research questions/hypotheses mentioned above and examines the spatial association of fractional land cover and its estimation error using three different remote sensing datasets with vegetation morphology types to examine the impact of changing spatial resolution as well as vegetation morphology on fractional land cover estimation accuracy in the study area (Mishra et al. 2014). Finally, Chapter 7 finalizes the methodologies/results used in this research and described their contribution to the literature. Furthermore, the contribution of the results to the central Kalahari and its stakeholders are presented. Additionally, the last chapter also calls for continued monitoring of the Kalahari ecosystem by integrating field data with multi-scale and multi-source remotely sensed data.

Illustration 1.1: This picture was taken inside the Central Kalahari Game Reserve (CKGR) in the central Kalahari of Botswana during the beginning of dry season (June 2011). The picture shows the landscape of the semi-arid central Kalahari characterized by coexistence of herbaceous and woody life forms with different structural and functional properties.

Dataset	Data	Production methodology
Global Land Cover Map, (GLC 2000)	SPOT Vegetation (2000) 1km	This product included 19 regional products and each of them used a regionally specified legend. These regional products were merged to develop the Global Land Cover Map, 2000
IGBP DIScover	AVHRR (1992-93) 1 km	Land cover product created from multi-temporal unsupervised classification of NDVI data
University of Maryland Global Land Cover product	AVHRR (1992-93), 1 km, 8 km, 1 degree	Unsupervised classification approach applied on phenological metrics to map Land Cover
MODIS Continuous Fields Tree Cover	MODIS (available from 2000 – 2005) 500 m	Using training data from Landsat ETM+ in combination with IKONOS were used under a regression tree algorithm to predict continuous tree cover using phenological metrics derived from MODIS
MODIS Land Cover product (MOD 12)	MODIS (since 2000) 1 km	Training and validation data derived from Landsat TM images to train a supervised classification using decision tree approach

Table 1.1: Summary of some important existing Land Cover products created using different Earth Observation datasets.
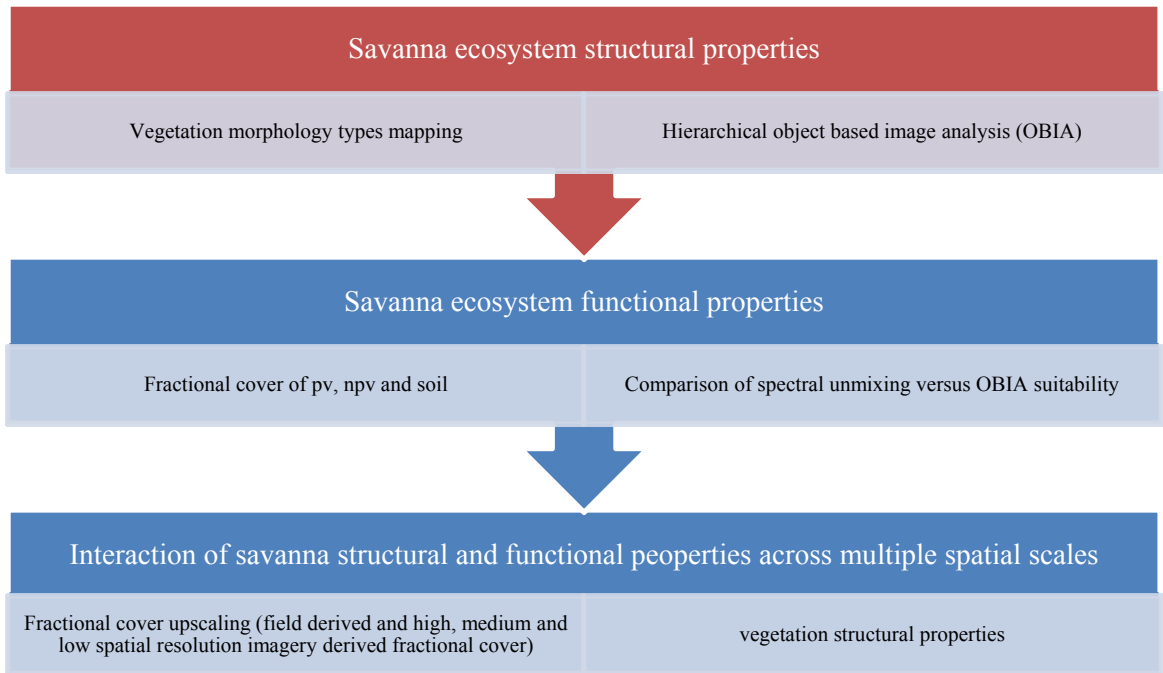
Figure 1.1: Overview of the research framework for this dissertation.

Chapter 2: Study Area

The Kalahari system and the central Kalahari

This study was conducted in the central Kalahari region of Botswana. Central Kalahari is part of the extensive Kalahari system or the 'Mega Kalahari' (Thomas 1984), which is a physiographically and sedimentologically unified system (Figure 2.1). The Kalahari system is an elevated, flat, sand covered plain area that occupies around 2.5 million km^2 area in southern Africa extending from the vineyards on the margin of the orange river at Upington in South Africa (29° S) to the north of Congo river into the south-eastern corner of equatorial Gabon (1° S) (Barker 1982; Thomas and Shaw 1993) (Figure 2.1). The Kalahari system is composed of series of contiguous sub-basins into which continental sediments have been deposited since the Jurassic age (Baillieul 1975). The most common surface unit of the Kalahari group of sediments is the Kalahari sand. The Kalahari system which encompasses the Kalahari Desert impinges on the territories of nine countries and embraces a wide range of climates and vegetation communities. Moving away from the equator within the Kalahari system, the climate becomes more seasonal with decreasing precipitation. Located in the Central district of Botswana, Central Kalahari experiences a semi-arid climate with relatively low anthropogenic pressure (Makhabu et al. 2002) (Figure 2.2). Ecosystem structure and processes in the central Kalahari are mainly determined by natural processes (e.g. rainfall, fire, edaphic properties). More than 70 percent of the study area falls under protected area (i.e. the Central Kalahari Game Reserve or CKGR) and the rest is private game farms and open

access commercial ranching (Figure 2.3). While CKGR is Africa's largest stand-alone protected area that serves as an important wildlife habitat and supports wildlife based tourism; commercial ranches support pastoral agriculture that is the basis of subsistence economy (DWNP 2003). Historical explorations in the central Kalahari area started after the 1850s and during the early 20th century. Early expeditions by explorers such as Thomas Baines and James Chapman (1861), Siegfried Passarge (between 1896 and 1898), F. Seiver (during1906-1907) and Sir F. G. Lugard (1905) provided site specific descriptions of flora, landscape conditions and soil properties for different parts of the central Kalahari (Thomas and Shaw 1993). These earlier studies covered relatively small parts of the central Kalahari region and expected the floristic and landscape properties to be fairly uniform in the unvisited areas mainly due to uniformity of pedological properties and climatic conditions (Thomas and Shaw 1991).

Climate of the Central Kalahari Region

The central Kalahari lies within the southern African summer (i.e. October to March) rainfall zone. Due to its proximity to the inter-tropical convergence zone, summer months brings moisture-bearing air masses. The moisture source for these air masses is the Indian Ocean and hence both the precipitation amount and duration decreases in a south-westerly direction within the Kalahari system. The rainy season is restricted between October-April (Thomas 2002). There is a lack of meteorological data for the central Kalahari region and general meteorological measurements are recorded at Maun (located in the north) and in Ghanzi (located west of the study area). Averages from these

20

two sites are used to represent the climate of the central Kalahari. The north and the west tip of CKGR receive up to 400 mm of rainfall whereas the rest receives a mean annual precipitation (MAP) of 350 mm (Makhabu et al. 2002). High spatial and temporal variability is an important characteristic of rainfall in the study area (Figure 2.4 and Figure 2.5). Although Kalahari rainfall is associated with convection, it is important to note that over three quarters of rain events are of low intensity and half of the storms generate less than 10 mm rainfall (Thomas 2002). Also, event-to-event difference in rainfall amount and marked interannual variability occurs too. The rainy season is frequently broken by dry spells and studies have shown that in north-eastern Botswana this irregularity can result in interannual rainfall variation of up to 35 percent and well over 45 percent in the extreme south-west of Botswana (Dougill et al. 1999; Scanlon et al. 2002). This variability leads to conditions of droughts that are frequent in the Kalahari system.

The temporal variability of precipitation in the central Kalahari is reported to follow precipitation cycles common to southern Africa. Like most of southern Africa, Botswana's precipitation is highly cyclical. Tyson et al. (1975) reported precipitation cycles of 16 – 20 years. Botswana's position within the African continent means the ENSO phenomenon has a negligible (Hulme et al. 2005) to weak (Low 2005) influence on the climate of Botswana, with below normal precipitation occurring during the warm phase of ENSO (El Niño). Botswana experienced droughts during the 1960s, to which the deaths of numerous wild animals are partially attributed (Ross 1987). Botswana endured a significant drought during 1982 – 1988 and below average precipitation during 1993 –

21

1994 and 1996 – 1999. A quasi-twenty year cycle has also been noted in Southern Africa with wet periods centered in 1921, 1940, 1958, and 1975 (Dyer and Tyson 1977). This approximate 18-year rainfall oscillation for southern Africa has been confirmed in other geophysical data well as dendrochronological data dating back at least 600 years (Tyson et al. 2002). Further analysis of climate patterns using tree ring dendrochronology and $\delta_{18}O$ dating of cave stalactites show that the most pronounced climate pattern is an 80-year oscillation dating over the past 3500 years (Tyson et al. 2002). Similarly, solar sun spot activity has been found to follow a short term 11-year cycle coupled with this long term 80-year oscillation (Friis-Christensen and Lassen 1991). The coincidence of solar activity cycles "may be the underlying cause of many climatic cycles that are preserved in the geophysical record" (Perry and Hsu 2000, pg. 12433).

In the central Kalahari, the range of temperature is high in dry and wet seasons, with the maximum temperatures being recorded in November and minimum in June (Pike 1971; Thomas and Twyman 2004). Maximum temperature during the summer could easily exceed 40°C resulting in high evapotranspiration losses. Annual potential evapotranspiration values in the south-west Kalahari in Botswana can reach 4000 mm decreasing to about 3000 mm in Maun (DWNP 2003). Actual losses are low and mainly constrained as the porous Kalahari sand favors rapid infiltration. The lack of a perennial surface has been a major hindrance to the economic and agricultural development of the area (Makhabu et al. 2002). Surface water does accumulate seasonally in pan depressions and may last days, weeks or even months into the dry season serving as a water source for herbivores and their predators, among others.

For utilizing groundwater resources, boreholes have been sunk in the Kalahari and their numbers have been increasing consistently ever since 1960s (Dougill et al. 1999). Although the initial boreholes were for the relief purpose of wildlife, changing government policies have allowed their number to increase in order to utilize groundwater and thereby start livestock ranching over a large area. More recently, the increasing rates of groundwater use has raised concerns regarding long term sustainability in the central Kalahari due to the lowering of the groundwater table and very limited natural recharge ability of the aquifers (Thomas 2002).

Topography/Geology/Soils

With the extensive spread of nutrient-poor Kalahari sand (average thickness: 80-100 meters), the central Kalahari is also termed as sandveld (Parris 1971). Geologically, the Kalahari formation is underlain by sandstone, shale and basalt of the Karroo Subgroup and forms the basement and sporadic outcrops of calcrete (Fagan 2002). In a mineralogical analysis of soil samples throughout the central Kalahari, Moore and Attwell (2002) found Toumaline to be the most common mineral. In general, a high percentage of tourmaline is associated with areas of dominant coarse sand. An exception to this generalization exists at the edge of several fossil river valleys, where a high percentage of tourmaline is associated with fine sand.

Pans are a principal geomorphological feature of the study area. Pans are mostly contained in isolated sub circular to sub elliptical depressions with distinct saline clay or sandy clay soils that retain rainwater for a comparatively longer duration than the

surrounding sandy areas. As in the rest of southern Africa, pans are important as they provide mineral licks (Parris 1971; Parris and Child 1973) as well as a relatively nutrient-rich vegetation attracting large herbivores and their associated predators (DHV 1980). Due to the geomorphological distinctiveness of pans, previous studies have either debated their origin or classified them as grassed, ungrassed or saline pans (Parris and Child 1973). In the study area, many pans are remnants of ancient sand-chocked drainage lines (also called fossil river valleys) and lie in belts that could be related to a pattern of drainage lines and divides (Thomas and Shaw 1991).

The altitude of the study area ranges between 880-1130 meters above mean sea level and follows a gentle gradient from a slightly lower altitude in the east to increasingly higher towards the west (Figure 2.6). The semi-arid savannas in the central Kalahari are characterized by low soil moisture and water intake levels combined with often very heavy rainfall events. As a consequence the aeolian and fluvial soils in the study area are generally poorly developed (Parris 1971). The north and north-eastern parts of the study area are marked by a few immobile longitudinal sand dunes (Makhabu et al. 2002). Predominant soil types in the study area range from Arenosols that are poorly drained and have more than 75% sand content to less dominant Vertisols in pans that are well drained and have more than 50% clay content (Figure 2.7).

Vegetation/Animals

Considering the eco-region classification of terrestrial surfaces (Forman et al. 2002), the study area falls under two eco-regions: Kalahari Acacia Baikiaea Woodland and Kalahari Xeric Savanna (Figure 2.7). The vegetation in the central Kalahari is

characterized by a spatially complex and structurally heterogeneous mixture of woody and herbaceous species that exhibit temporally distinct phenological patterns. Compared to the nutrient limited vegetation of the northern Kalahari, plant available moisture has been found to exert more control on vegetation structure and function in the central and southern Kalahari (Ringrose et al. 2003; Sankaran et al. 2005). Plant species diversity is relatively low for all plant communities in the study area. Differences between communities are related to changes in species dominance rather than occurrence of different species and thus vegetation boundaries based on plant species are often unclear (DWNP 2003; Makhabu et al. 2002). Following the rainfall gradient in general, the study area represents an ecotone with the north and central parts dominated by broad-leafed species that are gradually replaced by fine-leafed species in the southern part (Fagan 2002; Weare and Yalala 1971) (Figure 2.9).

While broadleaved savanna species have been reportedly dominant the north-east Botswana, vegetation in the central Kalahari is composed of mixture of microphyllous (fine-leafed) and broadleafed species (DHV 1980). In general, the central Kalahari represents a transition zone between northern and southern Kalahari. While in general, the dominance of broad-leafed species decreases towards south, there are several areas of exceptions due to fine scale variation in plant available nutrients. Notable broadleaf woody species in the study area includes *Lonchocarpus nelsi, Ziziphus mucronata, Terminalia sericea, Grewia flava, Croton gratissimus, Combretum hereroense, Colophospermum mopane* and *Boscia albitrunca*. Important fine-leaved woody species in the study area are *Dichrostachyas cinerea, Acacia mellifera, Acacia tortilis, Acacia erioloba, Acacia nigrescens, Acaic karroo and Catophractes alexandrii* (DHV 1980; Wyk 1997). Exploring the relation of vegetation/species type to soil grain size, Moore and Attwall (1999) found that while most broadleaf species occupied areas with large soil

grain sizes, *Boscia albitrunc*a was ubiquitous tree species that showed no preference to soil grain size throughout the central Kalahari.

Based on photo interpretation and selective ground truthing, DHV consulting engineers (1980) produced the first vegetation map of Botswana in which they recognized five main plant association types in the central Kalahari. *Broad-leafed tree savanna type* was associated mainly with the longitudinal sand dunes in the northern part of the study area where deep sands supported growth of dominant *Lonchocarpus nelsi* and *Terminalia sericea*. In the east and north-east of the study area the dominant woody components were formed by *Burkea africana* and *Combretum spp. Broad-leafed shrub savanna* consisted of the same woody species as found in *broad-leafed tree association* but was dominated by shrub and sparse tree cover. *Thorn savanna* is dominant in the south and south west with lesser sand depth and is characterized by *Acacia erioloba, Acacia luederiziit* and *Ziziphus mucronata. Mixed broad-leafed and thorn savanna* is dominant in the north western parts of the central Kalahari and also occupies edge areas of fossil river valley systems in the area. *Mopane woodland* is a vegetation association dominated by *Colophospermum mopane* and co-dominated by *Lonchocarpus nelsii* and is found exclusively in the extreme eastern part of the central Kalahari.   Important large herbivores of CKGR includes oryx, kudu, springbok, giraffe, eland, wildebeest, hartebeest and carnivores population is represented by lion, cheetah, leopard, wild dog (Thouless 1998).

As the result of spatio-temporal variability in rainfall, fire history and edaphic properties, vegetation physiognomic characteristics in the study area also show high variation ranging from dense wooded shrubland to open grassland (Figure 2.10).

Woodland generally occurs on dunes where coarser sands allow greater penetration of tree roots and moisture. While upper dune slopes and crests are often tree-covered, lower slopes tend to support mixed stands of shrubs where sand is more compacted. Woodlands provide abundant plants for browsing, shade and underground storage organs for drought tolerance and thus represent an important dry season habitat type for herbivores and their predators. Open and very open shrubland are mixed shrub and grass areas generally found in inter-dunal valleys with slightly smaller soil particle size. Grasslands with mixed shrubs predominate on plains where smaller soil particle size limits tree root penetration, and a general lack of compacted sub-surface soil layers limits near-surface soil moisture availability. Since very few large trees occur in grasslands, they are occupied less by wildlife during the dry season than at other times of the year. Pans and fossil river valleys are predominantly clay, which results in occurrence of grasses interspersed with occasional clumps of trees known as "tree islands" (Parris and Child 1973; Thomas and Shaw 1991). At pan edges where sands overlay pan and valley floors, shrub communities dominate. The clay soils have good moisture-retaining qualities and high mineral contents and support relatively nutritious plants (Thomas 2002). Fossil river valleys and pans are the most important areas for Kalahari wildlife, especially during the wet season.

Fire

As with other parts of the southern Africa savanna, fire is an important determinant of vegetation structure in the central Kalahari (Sankaran et al. 2005; Thomas and Shaw 1993). Most fire activity takes place during the dry season and fires can start as

early as April with the last fire activity as late as early November. Most fires are surface fires burning senescent grasses and shrubs and can spread rapidly due to the hot, windy, low humidity conditions of the dry season. Early dry season fires are generally less intense than late dry season fires and the patch size of a burned area can range from less than a hectare to several hundred square kms (Thomas and Shaw 1991). The spatio-temporal distribution of fire is expected to be highly correlated to the available fuel load that is in turn determined by rainfall history as well as fire activity during previous years (DWNP 2003; Thomas and Twyman 2004). Since grasses and shrubs can grow rapidly post-fire, the same region can burn every year. Analysis of the MODIS monthly burned area product for the period 2003-2009 suggests that for a large part of the study area the fire return interval is between 3-6 years (Figure 2.11).

Most fires inside the CKGR are expected to be natural in origin (DWNP 2003). Currently, there is no policy of practicing controlled burning for management of fires inside CKGR. However, controlled burning is practiced in private game farms outside the CKGR (DWNP 2003). Previous studies in the Kalahari system have reported both negative as well as positive effects of fire activity on savanna vegetation and ecosystem structure. The negative effects of fire include loss of pasture and grazing resources, shrub encroachment by fire resistant shrubs and woody vegetation species, and the formation of hardened soil horizons (Scholes and Archer 1997; Scholes and Walker 1993; Zimmermann et al. 2010). In contrast, there are numerous ecological studies in semi-arid savannas that demonstrate the positive effects of fire on vegetation (Avon et al. ; Eigenbrod et al. 2008; Flory and Clay 2006; Milton and Dean 1998; Trombulak and

Frissell 2000). Using field data from 854 sites in African savanna systems, Shankaran et al (2005) showed that woody cover in savanna system increases linearly up to precipitation below 650 mm. In areas with mean annual precipitation above 650 mm, the balance of woody versus herbaceous components of the ecosystems is maintained mainly by fire activity and grazing pressure.
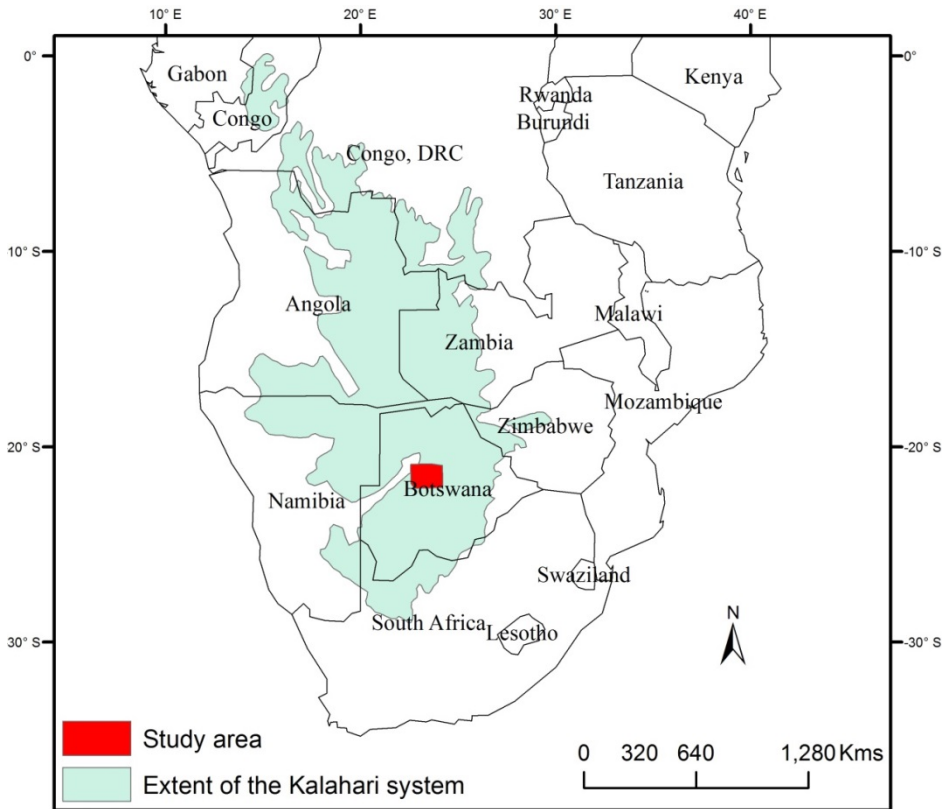
Figure 2.1: Extent of the Kalahari system in Africa (modified from Thomas and

Shaw, 1991) and location of the current study area in the central Kalahari of Botswana.
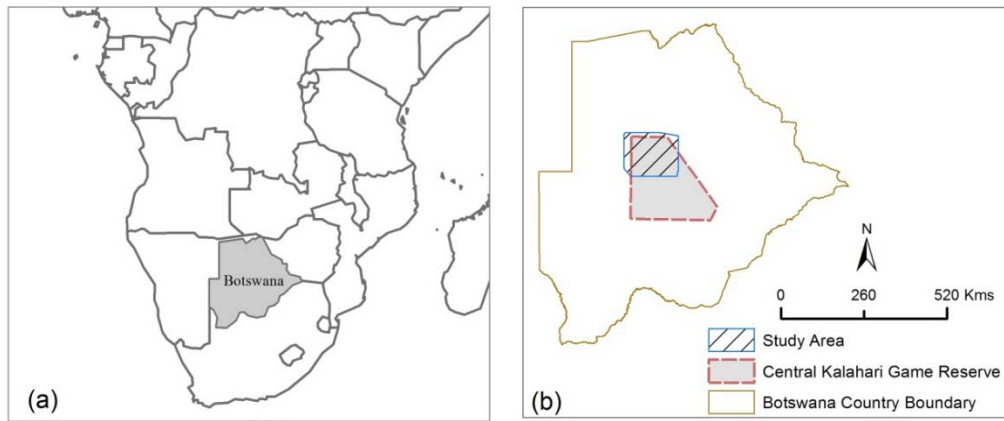
Figure 2.2: (a) location of Botswana in southern Africa, (b) location of study area

in the central Kalahari of Botswana.
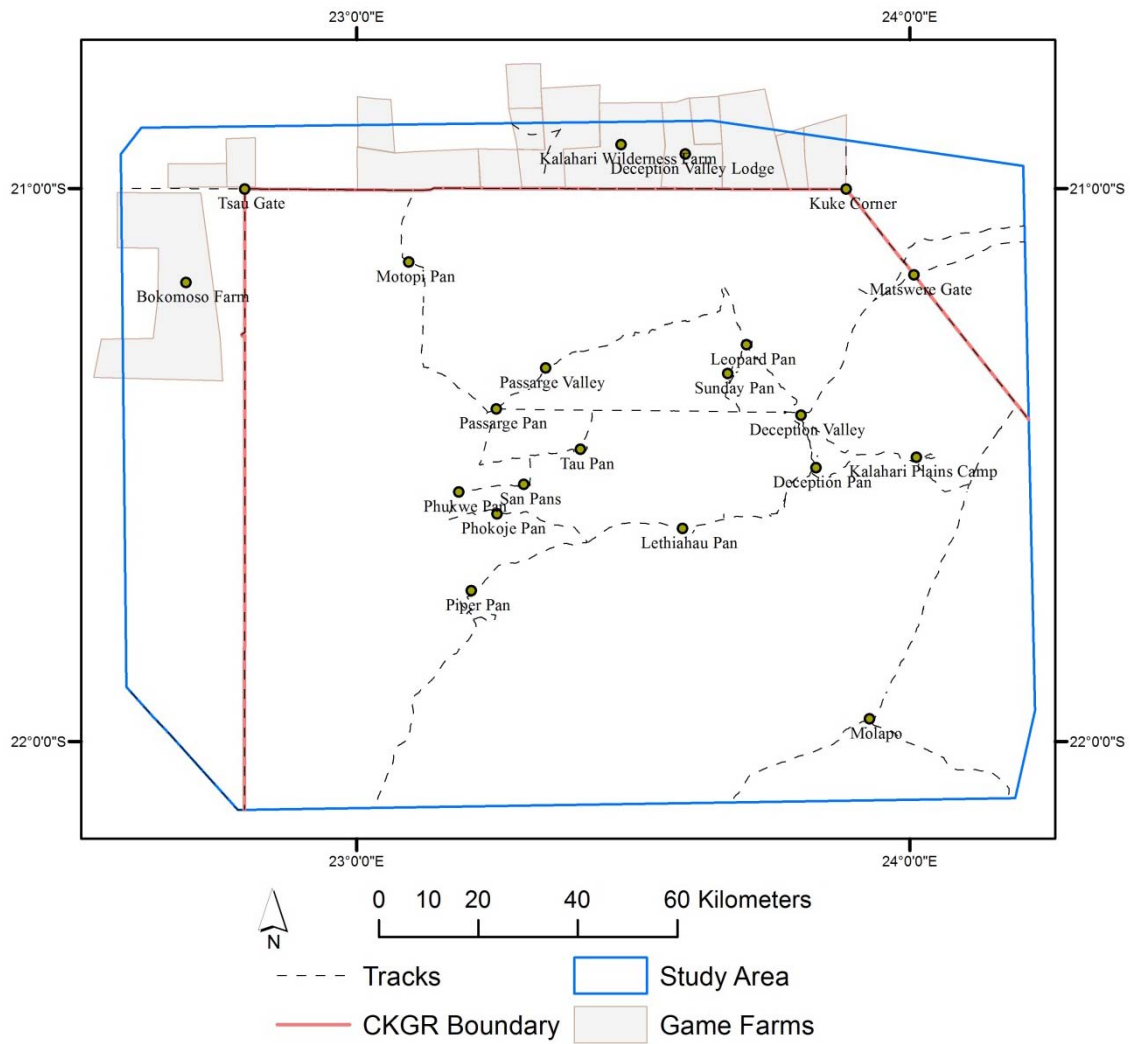
Figure 2.3: Enlarged portion of study area depicting the game reserve boundary and game farms outside the protected area, areas accessible by tracks and major pan systems.
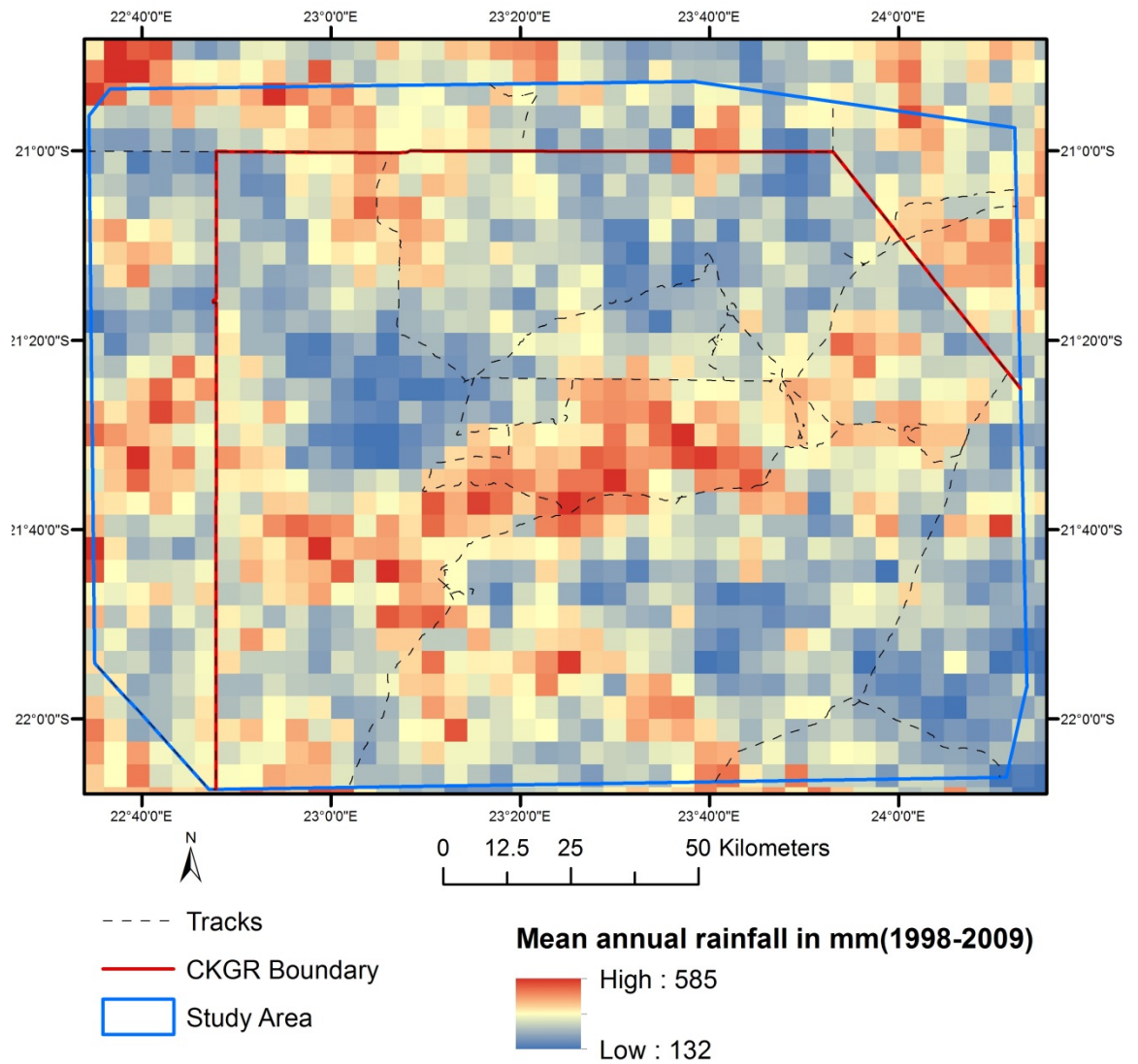
Figure 2.4: Mean of Monthly 12-year TRMM 2B31 rainfall time series (1998-2009) for the study area.
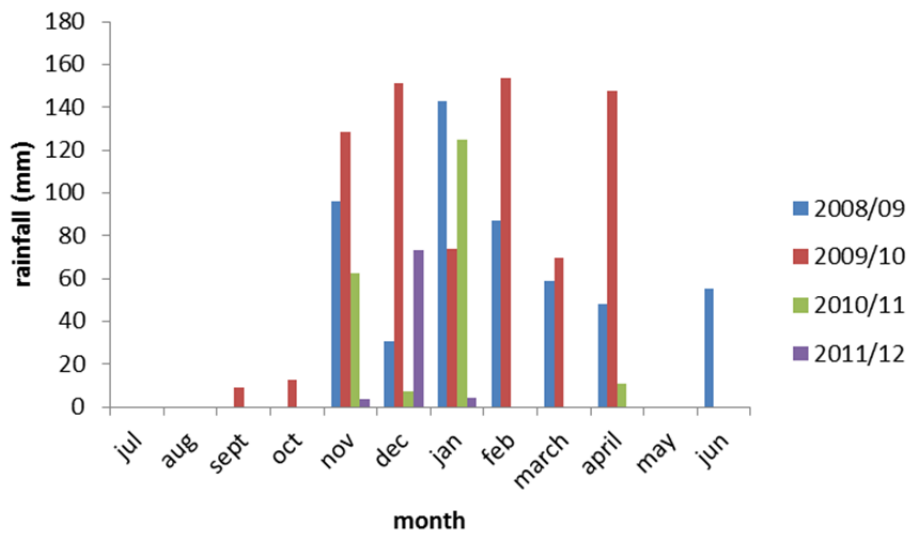
Figure 2.5: Mean monthly rainfall for Matsware (location shown in Figure 2.2)

(Source: Department of Wildlife and National Parks, Government of Botswana)
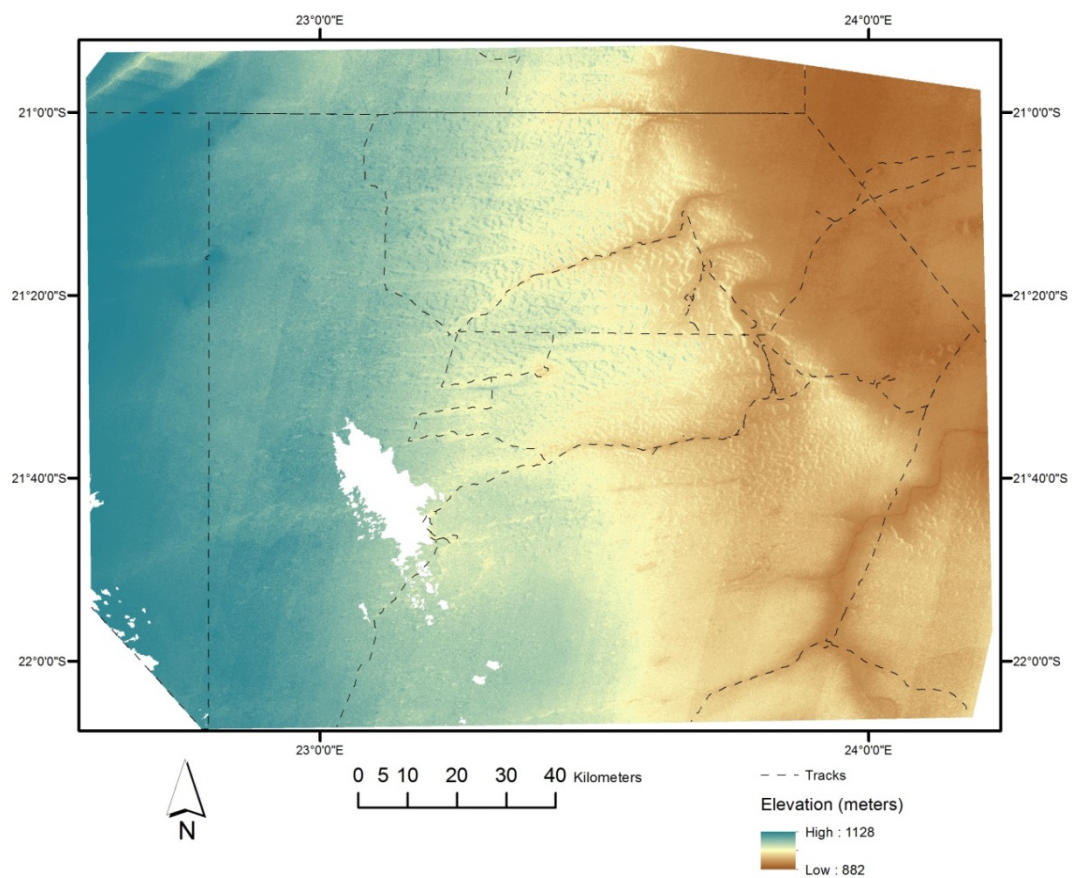
Figure 2.6: Elevation of the study area as depicted by ASTER GDEM2.
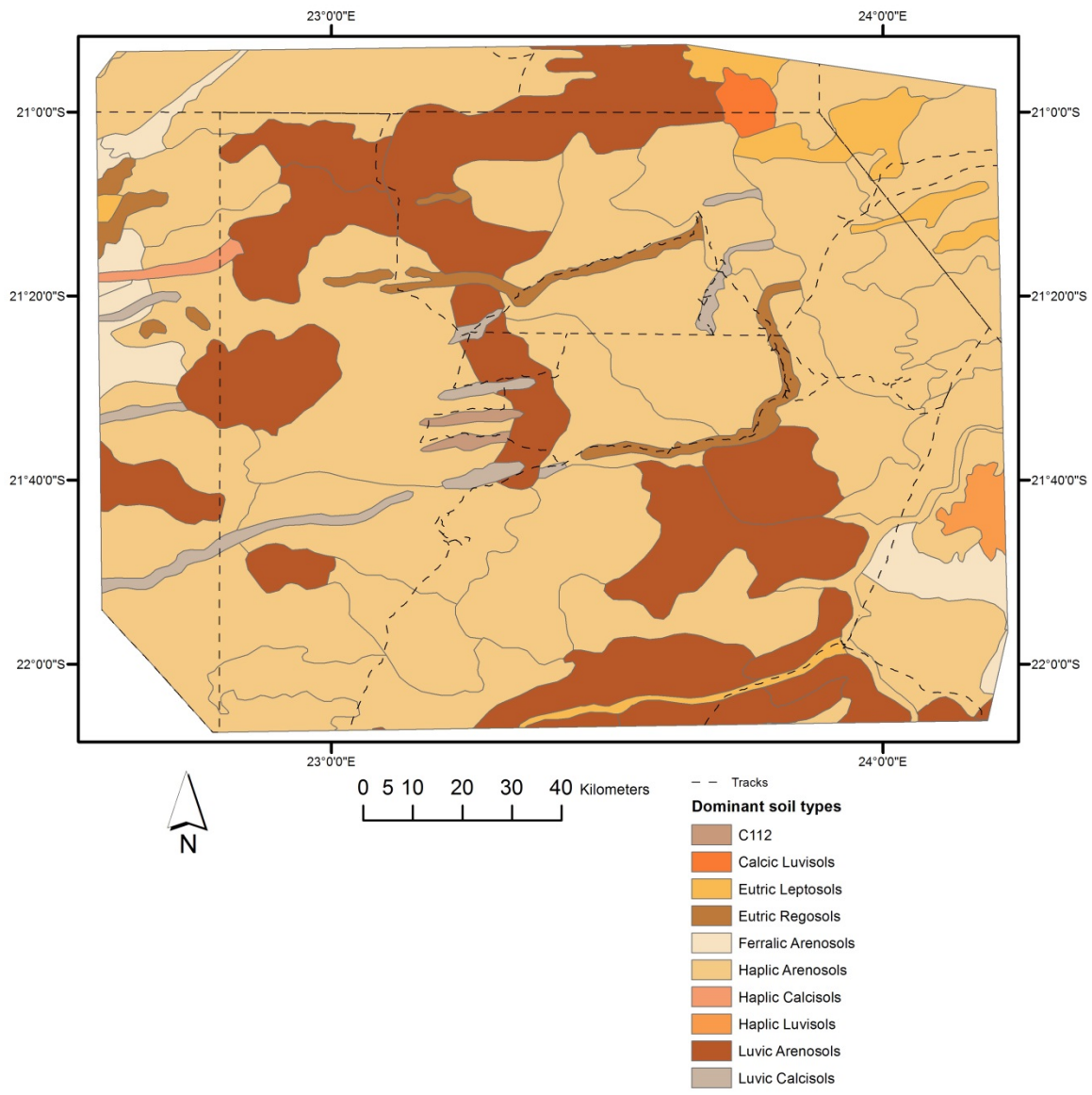
Figure 2.7: Major soil types of the study area (Sources: DWNP, 2003)
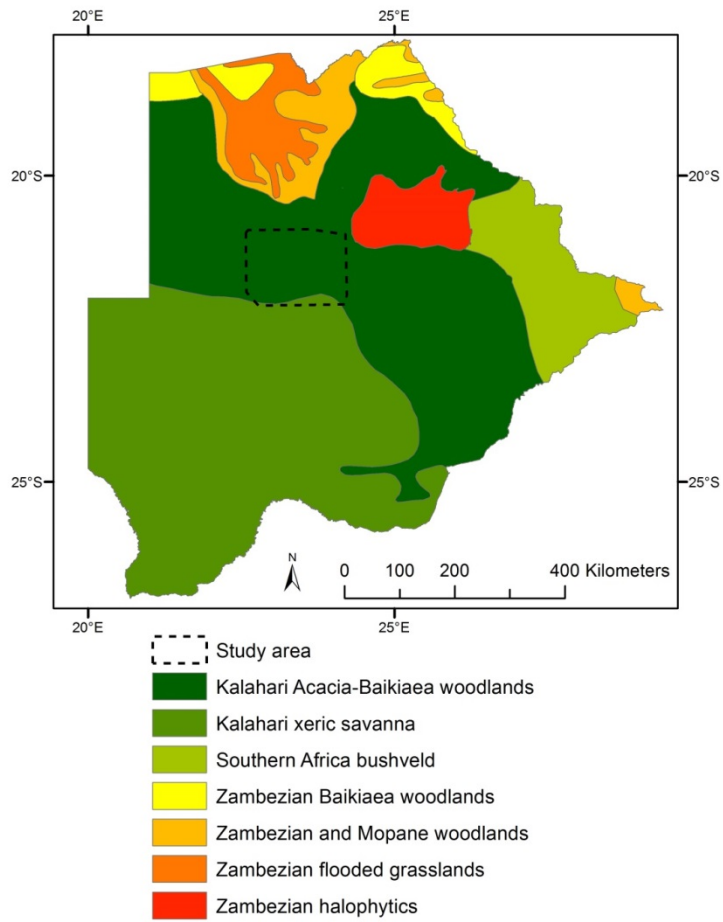
Figure 2.8: Eco-regions of Botswana (Olson et al. 2001) and the location of the study area in the central Kalahari of Botswana (highlighted as rectangle).
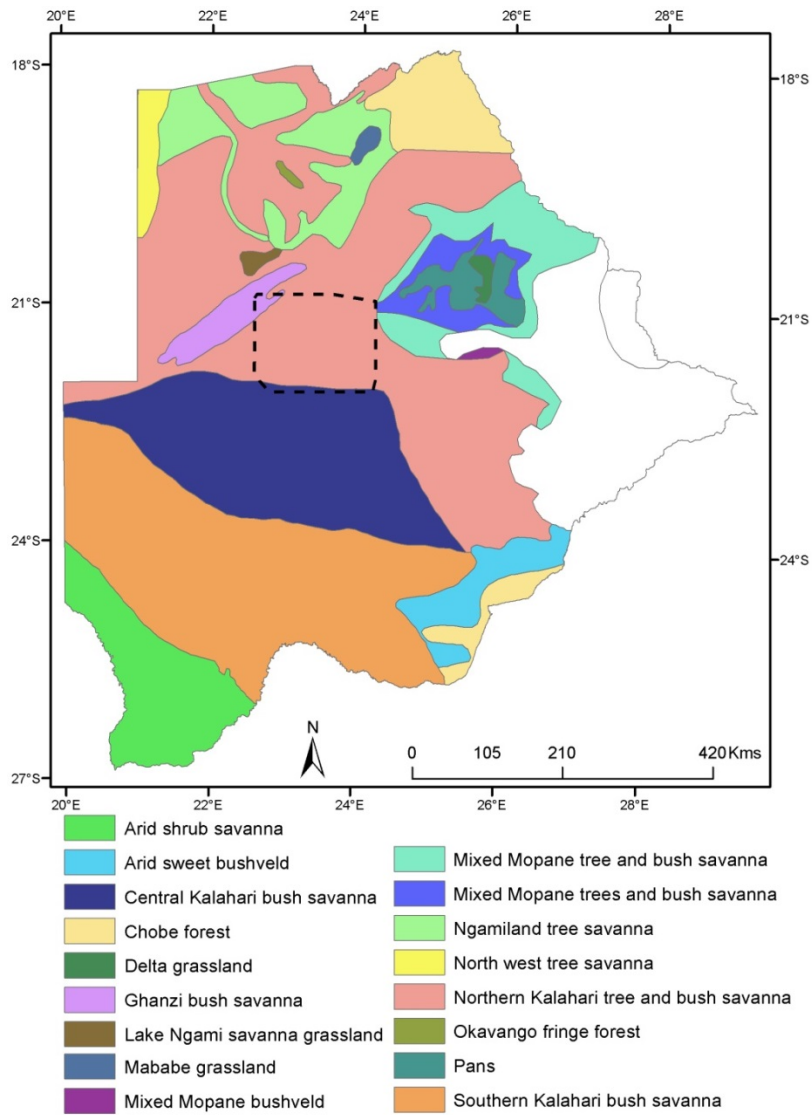
Figure 2.9: Vegetation communities in the Botswana Kalahari as presented by Weare and Yalala (1971). The study area is indicated as rectangle.

(a) Woodlands

(b) Open shrubland

(c) Very open shrubland

(d) Grassland

(e) Pans

Figure 2.10: Example of different vegetation physiognomic properties in the semi-arid central Kalahari at the start of dry season just after end of rainy season (The photos were taken by the author during field survey in May 2011).
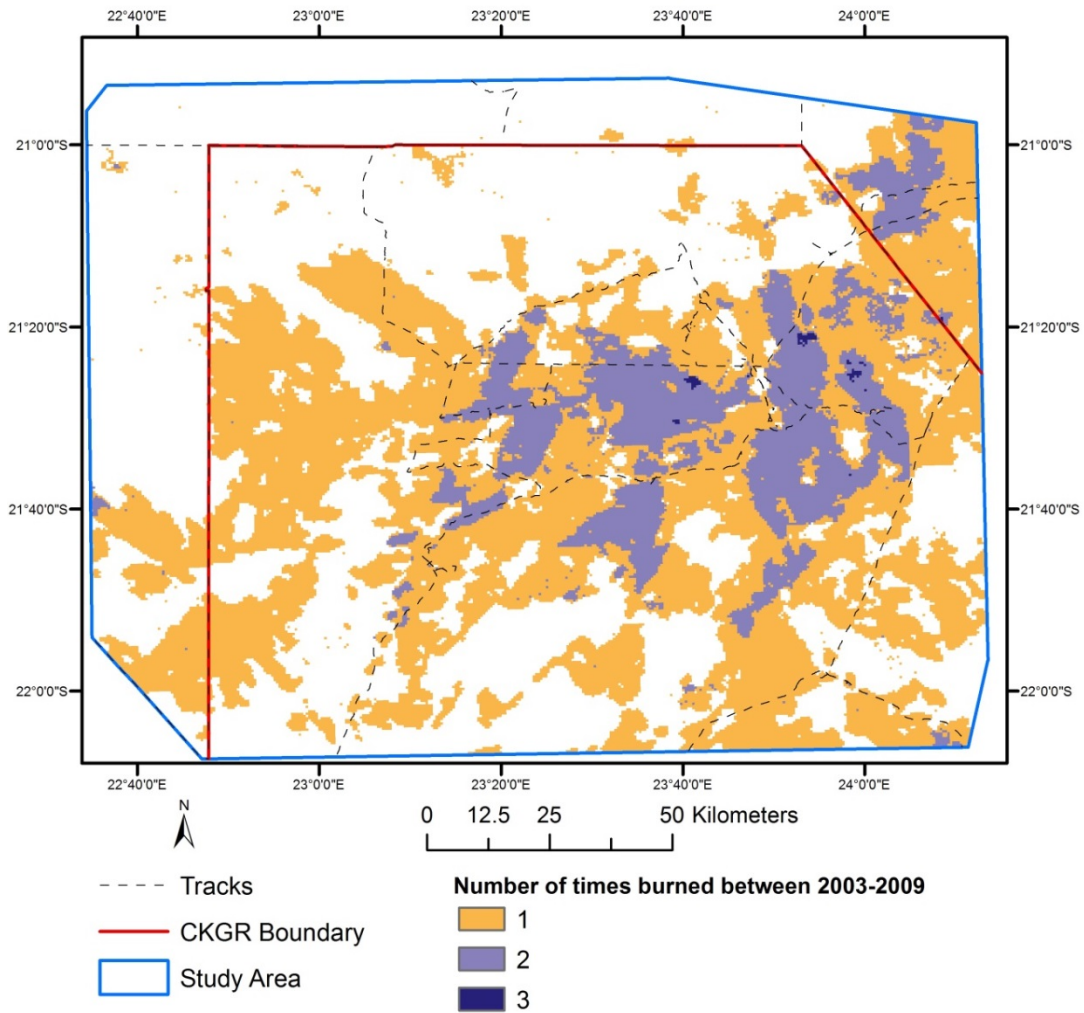
Figure 2.11: Fire history in the study area produced from the MODIS monthly burned area product (MCD45A1) for the period between January 1, 2003 and December 31, 2009.

Soil unit	General description
Arenosols	Soil excessively well drained, and have low water retention capacity. Fine sands are predominant (>75%) with minor clay or silt (<5%).
Regosols	Well drained to moderately well drained, but less drained than Arenosols; its sandy loam to clay loam with minor coarse sands.
Lixisols	Soil well drained. The sand content is about 20%, and high clay content (usually >20%).
Luvisols	Soil well drained. It consists of nearly equal proportions of coarse and fine sand. The sand content is about 20% to 30% with high clay content (usually >20% as a lixisols).
Vertisols	The soil unit is poor to perfectly drained. Soils are predominantly clay and fine silt. The clay content is generally in excess of 50%.

Table 2.1: General description of soil types found in the study area.

CHAPTER 3: Research Literature Review

Overview of savanna ecosystems

Savannas are geographically extensive biomes occupying nearly one eighth of Earth's terrestrial area (Mistry 2000; Scholes and Walker 1993). Tropical savannas are distributed in over 20 countries throughout Africa, South America, Australia and Asia (Sankaran et al. 2004) (Figure 3.1). Due to geographical extent, savannas play a major role in global land-atmosphere energy balance as well as carbon and nutrient cycles and account for almost 30% of global net primarily production (Lal 2004; Van Rooyen et al. 1990). Especially in southern Africa, savanna ecosystems are essential contributors to productivity and biodiversity as they contain some of the largest remaining wildlife habitats and offer the basis of economic activity by supporting high populations of domesticated livestock and wildlife-based tourism (Hemson 2003; Thomas and Sporton 1997; Tietjen and Jeltsch 2007).

Tree-grass interactions

Savanna ecosystems are characterized by a unique co-existence of herbaceous and woody life form compositions (ranging from high grasslands, continuous grasslands with scattered trees to closed canopy woodlands) following a climatic gradient with distinct rainy and dry seasons (Archer et al. 1995; Jeltsch et al. 1996; Lüttge 2008). The main factors that influence the interaction of life forms in savanna ecosystems are (i) spatio-temporal variability of resources (moisture and nutrient availability), (ii) physiological properties (canopy structure and root depth), (iii) photosynthetic pathway and

phenological difference (evergreen versus deciduous), (iv) fire intensity, (v) grazing pressure and (iv) edaphic factors.

To understand the interaction of these factors as determinant of key ecological processes and structure in savanna systems, different types of theoretical models have been proposed. Ecologists lack consensus and theorized several explanations for understanding the mechanism allowing tree-grass coexistence and the factors determining the relative proportion of each. Based on classical approach these models can be classified as either equilibrium model leading to stable coexistence or non-equilibrium models assuming no stability due to frequent disturbances that prevents the extinction of either competitor by restarting the race or by favoring any one of them (Scholes and Archer 1997). Shankaran et al. (2004) examined the assumptions and mechanisms of models explaining unique savanna structure by grouping them into two categories: theories highlighting the role of competitive interactions (i.e. competition based models) and those emphasizing the limiting role of demographic bottlenecks to tree establishment and persistence in savannas (i.e. demographic bottleneck models) (Figure 3.2).

Savanna structure, under *competition based models*, is the result of spatial and temporal niche separation in resource acquisition potential between trees and grasses and is the basic mechanism leading to tree-grass coexistence (Belsky 1990; Eagleson and Segarra 1985; Walker et al. 1981). Following competition based approach the primary determinant of savanna structure and function are water and nutrients, whereas impacts by fire and herbivore are considered as modifiers (Stott 1991). Majority of the

competition based models emphasize plant available moisture rather than plant available nutrient as exerting superior control on savanna structure (Caylor et al. 2003; Eagleson and Segarra 1985; Scholes et al. 2002; Walker et al. 1981). Four competition based models proposed by ecologists that currently dominates the savanna research are: *the root niche separation model, the phenological niche separation model, the balanced competition model* and *the hydrologically driven competition-colonization model*.

Proposed by Walter (1971), the *root niche separation model* of savannas considers water as the primary limiting factor for which trees and grasses compete in savannas (Figure 3.2). While grasses are rooted only in topsoil, trees have roots in both topsoil and subsoil with exclusive access to deeper water leading to stable coexistence of the two. Root niche separation theory predicts a characteristic tree-grass ratio for a given climatic and soil conditions as a function of vertical distribution of water in the soil profile with increasing tree biomass as water in the subsoil increases (Figure 3.2). However, variable rainfall patterns and grazing alter the ratio of subsoil to topsoil which causes the realized tree-grass ratio to be different from predictions which reduces theory's practical applications.

The *phenological niche separation model* is based on the altering warm and dry season, with hot wet season as a potential axis for niche separation between trees and grasses (House et al. 2003; Scholes and Archer 1997). Deciduous savanna trees achieve full leaf expansion early with the onset of rainy season, whereas peak leaf areas of grasses are achieved only after several months (Scholes and Walker 1993). In this

scenario, trees have exclusive access to resources during both early and late rainy season. However, the variability of total rainfall amount and the length of growing season in savannas hamper the prediction of phenological niche separation models.

Under *balanced competition model,* coexistence in savannas arises because trees being the superior competitor becomes self-limiting at a biomass insufficient to exclude grasses, which are inferior competitor (Scholes and Archer 1997). In absence of external perturbations, this model predicts a threshold with increasing rainfall above which woodlands dominate and below which grasses out compete trees. According to balanced competition model, the woodland savannas are the only stable savannas, whereas grass dominated savannas are unstable due to fire and grazing.

Contrary to the three models described above, the *hydrologically driven competition-colonization model* is a non-equilibrium competition-based model for describing savanna structure (Fernandez-Illescas and Rodriguez-Iturbe 2003). It emphasizes the tradeoffs between competitive ability and colonization potential of trees and grasses which changes in response to fluctuations in soil water stress caused by interannual rainfall variability. Model predictions on balance between trees and grasses are sensitive to the magnitude and variance of interannual rail fluctuations. The model predicts coexistence of trees and grasses in the long term and increasing tree cover with increasing mean growing season rainfall (Fernandez-Illescas and Rodriguez-Iturbe 2003).

For explaining savanna structure, *demographic bottleneck models* integrate effects of multiple drivers (e.g. fire, herbivore, climatic fluctuations) and rather than

emphasizing the post disturbance competitive interaction, they highlight the direct effect of these disturbances on germination, mortality and demographic transition of trees in savannas (Higgins et al. 2000; Holdo 2007; Jeltsch et al. 1996; Sankaran et al. 2004; Zimmermann et al. 2010). According to these models, tree-grass coexistence occurs in savanna because climatic variability and disturbances limit successful tree germination and mature tree establishment. There exist alternative view points within demographic bottleneck models, on control of savanna structure and functioning. The transitional "disequilibrium" system, consider disturbances, such as fire and grazing, as not only modifiers but also maintainers of the unique savanna structure by buffering the system against shifting to alternate states (Jeltsch et al. 1996). Alternatively, another view point is the non-equilibrium dynamics driven by variations in rainfall in arid regions (Higgins et al. 2000) and disequilibrium dynamics driven by variation in fire intensity in mesic savannas (Higgins et al. 2000). In arid and semi-arid savannas, due to spatio-temporal variability in rainfall, tree recruitment is pulsed in time on occasional good rainfall events, provided that the matured trees live long enough to bridge these events. However in mesic savannas, where trees can dominate canopy cover, frequent high intensity fires prevent the seeding to escape flame zone and thereby controlling the tree density (Higgins et al. 2000). Further, browsing prevents escaped seedlings' establishment as mature trees (Higgins et al. 2000; Jeltsch et al. 1996; Jeltsch et al. 2000). Recently, demographic models for characterizing savanna structure have gained favor over competition based models, which were found insufficient in explaining the long term

45

tree-grass coexistence in spatially explicit modeling of tree-grass interactions in savannas using field data (Jeltsch et al. 1997; Jeltsch et al. 1996; Jeltsch et al. 2000).

Although these different models have been supported by empirical evidence from different sites around the globe, no single model has been able to provide a generic mechanism that provides a single explanation for all cases (Hutley 2008). Furthermore, observational data collected during various studies in savanna ecosystems suggest that savanna structure and function results from the interaction of all the processes discussed above. In many savanna systems, root distribution of woody and herbaceous components is spatially separated as described in the niche separation model. Root partitioning favors tree growth in systems where rainfall occurs during periods when grass growth is dormant and rainfall can drain into deep layers supporting woody component. However in semi-arid savanna systems (e.g. central Kalahari) where growing season coincides with rainy season, reliance on deep root system could result in tree water stress due to high spatio-temporal variability in rainfall with little ground water recharge. In semi-arid savannas surface roots are more effective at exploiting moisture and finalized nutrients following discrete rainfall events. In mesic savannas, contrary to the predictions of niche separation models, root competition between both woody and herbaceous roots in the upper soil layers is apparent (Hanan and Lehmann 2010; Wigley et al. 2010).

Determinants of Savanna vegetation structure

Plant available moisture (PAM) and plant available nutrients (PAN)

At regional to continental scales, PAM is the most significant ecological determinant influencing woody versus herbaceous ratio in savanna systems. In general, increase in rainfall results in increase in woody cover and decrease in herbaceous

biomass. For quantifying PAM, different parameters exist that range from simple ones such as mean annual rainfall to those based on water balance parameter (e.g. rainfall as a fraction of potential or actual evapotranspiration). By systematic analysis of mean annual precipitation data coupled with remote sensing derived observations at continental scale Sankaran et al. (2005) showed that in African arid and semi-arid savannas woody cover is mainly a function of mean annual precipitation. Based on a piece-wise linear regression, mean annual precipitation of 650 ± 134 mm was estimated at which the maximum tree cover is attained and a minimum of 101 mm mean annual precipitation was required for the existence of trees (Figure 3.3). Another continental scale study by Bucini and Hanan (2007) found similar results by comparing mean annual precipitation with MODIS tree cover product developed by Hansen et al. (2006). According to Bucini and Hanan (2007) the comparison of MODIS and mean annual precipitation achieved best response with a sigmoid relationship. Based on this result, savanna were categorized as either arid (with less than 400 mm mean annual precipitation) that are less affected by perturbations and have little change in tree cover compared to semi-arid and mesic savannas (mean annual precipitation range: 400-1600 mm) where precipitation is the most important controlling factor.

Compared to plant available moisture (PAM) that influences woody versus herbaceous ratio at large spatial extents, plant available nutrients (PAN) and soil physiochemical properties have significant influence at more fine spatial scale. However, PAN is related to moisture availability and dry season nutrient uptake and nitrogen mineralization, in particular, is limited by low levels of PAM (Sankaran et al. 2004). Most significant growth in semi-arid savanna plants takes place during rainy season when nutrients are released via mineralization. Even within similar rainfall regime, fine scale changes in PAN (depending on soil type) can result in significantly different vegetation

structural and functional types. The long term savanna study site of Nylsvley in South Africa is an example for this case where broad-leafed *Burkea Africana* savanna on nutrient poor soil is surrounded by patches of fine leafed *Acacia tortilis* savanna on nutrient rich soil. Although both these vegetation types are under similar PAM regime, but availability of higher levels of soil available N and P in the fine leafed savanna makes its productivity approximately double compared to broad leafed savanna which attracts larger grazing and browsing animals (Attiwill 1994; Scholes and Walker 1993).

Fire

Fire in savannas is an important landscape-scale determinant that controls the distribution of woody life forms below the precipitation determined boundary (Sankaran et al. 2005). Fire activity, mainly during the dry seasons is the result of herbaceous production during the wet season followed by curing of this material in the dry season. While savanna fires impacts above ground plant parts, there is little or no impact on savanna seed bank or regenerative plant parts (Levick et al. 2009; van Langevelde et al. 2003). Early dry season fires (when fuel accumulation is low and curing incomplete) tend to be low-intensity, patchy, and limited in extent. Fires later in the season are of higher intensity and produce more extensive and homogeneous burning (Pike 1971). Determining direct effects of fire on savannas is often difficult due to confounding effects of grazing and browsing. Nevertheless, long-term burning experiments have shown that the higher-intensity, late dry-season fires are more damaging to woody species (Hamada et al. 2011).

Fire is the main ecological activity that links vegetation feedbacks (vegetation mortality, grass/forest cover) with climate feedbacks (regional precipitation, brought). Most savanna fires are surface fires that burn the flammable herbaceous layer and crown fires are rare due to general inflammability of savanna woody component. Fire activity

serves as a key ecological buffering mechanism which reduced and maintains the woody plant densities (Jeltsch et al. 2000). Recent studies have shown that in savannas decreased fire frequencies can lead to bush encroachment and increased fire frequencies can lead to grassland conversions (Gillson and Ekblom 2009; Hoffmann et al. 2002). The results of studies based on long term fire exclusion plots in southern Africa and Australian savanna support these findings (Levick et al. 2009). High frequency of fire in savannas can reduce tree seedling establishment and the ability of saplings to escape the flame zone via height growth. This in-turn enables grass persistence and growth, maintaining the fuel load. The aerial stems of small seedlings and suckers are often killed during fire but the individuals are able to resprout from lignotubers or from other underground and stem basal tissues.

Remote sensing based application for characterizing and monitoring fire regimes in tropical savannas has enhanced our understanding of fire severity and the distribution of burned area leading to their effective for their management (Roy et al. 2011). In this regard studies have utilized satellite data to access large scale fire patterns and analyzed the complex relationship of the fire frequency and timing with land cover properties, rainfall and land use designations, anthropogenic pressure in variety of savanna settings (Bolstad et al. 1998; Burke et al. 2002; Hill et al. 2011a; Justice et al. 2002; Parker and Bendix 1996). Combining savanna three dimensional vegetation structure derived from airborne LiDAR remote sensing with long term land management records in Kruger National Park, Levick et al. (2011) reported that (i) higher fire frequency areas covered much less canopy cover compared to their counterparts with lower fire frequency and (ii) woody cover reduction increased linearly with increasing difference in fire frequency.

Herbivore

Two different kinds of herbivores in savannas include large native angulates, domesticated cattle and more neglected relatively small invertebrates like grasshoppers, caterpillars, ants and termites. Herbivores impact savanna structure and function via consumption of biomass, seed predation, trampling of understory and destroying trees and shrubs (HilleRisLambers et al. 2001; Koppel et al. 2002; Ludwig et al. 2001). For example, in the Serengeti system, after the eradication of rinderpest in 1960s, the wildebeest population continued to increase until 1980s, which transformed part of it into woodland-dominated due to reduced burning and increased recruitment of plants (Sinclair 1995; Sinclair and Arcese 1995; Skarpe 1991). Large mammals, such as elephants, control tree-grass ratio in savannas by knocking down matured trees as well as feeding on seedlings and preventing regeneration. Woodlands in the Serengeti system declined throughout the 1960s due to elephant culling until the hunting of elephants by ivory poachers started to control their population in Serengeti in 1980s, but not in Mara. This human intervention helped woodland regeneration in 1980s in Serengeti, whereas the Mara system shifted to a grassland-dominated state. The influence of large mammals resulted in multiple ecological state within a single ecosystem (Dublin et al. 1990; Sinclair 1995). In African savanna, giraffes can also reduce woody seedling and sapling growth which can keep woody vegetation within fire sensitivity heights. Other significant impacts of herbivores in savanna structure and function includes changes in soil properties such as loss of crusts (important for nutrient cycling), compaction effects, soil erosion, nutrient loss and increased runoff (Hoogesteijn and Hoogesteijn 2010; Jones et al. 1996).

Researchers have utilized both *in situ* data and remotely sensed images to study the impact of herbivores on savanna vegetation structure. Using novel approach based on

airborne LiDAR remote sensing in Kruger National Park, South Africa, Asner et al (2009) demonstrated the extent to which herbivore can affect the three-dimensional structural diversity of vegetation. They found that areas under short-term (6 years) exclusion of herbivore contained 38%-80% less bare ground compared to those that were exposed to herbivore. Additionally, areas under long-term exclusion from herbivores (> 22 years) differed significantly in terms of three dimensional vegetation structure with up to 11-fold greater woody canopy cover in areas without herbivores.

In savanna systems, besides the large herbivores, insects are also critical to savanna due to their impact on productivity and ecosystem properties. However, there is lack of data and studies describing the detailed effects of small herbivores in savannas (Milton and Dean 2001). According to one study, in African savannas, a grasshopper biomass of 0.73 kg ha^{-1} can consume nearly 100 kg ha^{-1} of plants and can damage additional 36 kg ha^{-1} which is equivalent to a reduction of 16% in aboveground grass productivity (Weller et al. 1998). Small herbivores can account for up to half of the grass herbivore, although the rate and proportion varies significantly between years.

Land use / anthropogenic influence

Savannas are increasingly influenced by direct human activities and anthropogenic influence, which began with widespread Anglo-European expansion during 18th and 19th century. Anthropogenic clearing of forests led to fragmentation and creation of degraded savannas (Dougill et al. 1999; Gadgil and Meher-Homji 1985; Homewood 1996). In some areas, fire suppression, introduction of livestock and exotic trees, and overhunting resulted in large scale bush encroachment and herbaceous degradation (Dougill et al. 1999; Ludwig et al. 2001; Skarpe 1991; Wiegand et al. 2006).

Consequently, areas historically classified as savannas may now be considered as shrublands or woodlands and forest areas as savannas. Under increased CO_2 levels, global dynamic vegetation models (GDVM) predict further shrub and woody encroachment in tropical savannas because of greater response of C_3 trees to CO_2 enrichment (Polley et al. 1997). General circulation models (GCMs) predict clearing of tropical savannas will increase temperature, wind speed, decreased precipitation and relative humidity, and substantial increase in fire frequencies with warmer and drier climate (Hoffmann and Jackson 2000; Hoffmann et al. 2002). Thus, although animals and edaphic factors influence and determine savanna structure and mechanisms, humans are also modifying savannas significantly by their opportunistic management strategies to control its biotic and abiotic components for their own interest.

It should be noted that the effects of other determinants of savanna can be observed at short to periodic (rainfall) and medium to episodic (fire) timescales. On the other hand, the impact of land use on vegetation properties and land cover in savannas can be detected on much longer time periods (Booth and Tueller 2003; Lambin et al. 2001). For a large human population in developing countries of southern Africa, savanna systems are important source for fuelwood extraction, fodder and subsistence pastoral practices. The provision of biomass (fuel) by savanna woodlands is of considerable value to rural household of South Africa where approximately 54 % of households continue to use wood as their primary source of energy primarily for cooking and heating. The strong dependence on fuelwood has resulted in high levels of extraction which is not only modifying savanna structure significantly but also rising concerns of a fuelwood crisis in

near future (Blaschke 2010; Clinton et al. 2010). In a recent study investigating the impact of fuel wood extraction on ecosystem structure in South Africa, Wessels et al. (2004b) found that communal rangeland with open access for fuelwood extraction had an average of 12 ton/ha biomass which was less than half compared to the biomass in neighboring protected areas. Furthermore, this study predicted that under current rate of extraction biomass of the investigated communal area would deplete complete within twelve years.

Monitoring terrestrial vegetation based on field methods

In most natural landscapes of the Earth's terrestrial areas, vegetation is the most dominant land cover (covering over 70% of earth's land surface) and as one of the main interfaces between human societies and the Earth system it is one of the most critical components of terrestrial ecosystems (Goodwin and Fahrig 2002). Scientists have recognized the important role of vegetation and the knowledge about human transformation of vegetated areas as far back as Plato (Taylor 2003). Change in vegetation cover is considered one of the most important variables of global change affecting ecological systems (Vitousek 1994). Studies predict that vegetation cover change will be the most significant variable impacting biodiversity for next several decades (Hooper et al. 2005; Xie et al. 2008). Thus there is high demand for improved and accurate vegetation cover datasets. Monitoring terrestrial vegetation communities is important as ecologically significant information about species or communities can be

obtained by analyzing data acquired through monitoring. Monitoring is also essential for determine suitable adaptive management strategies (Goldsmith 1991; Stewart et al. 1989). Field based monitoring of vegetation properties can be very challenging task due to logistical issues related to data collection, changes in protocols and definitions over time, and constrains in time and budget (Bonham 1989; Goldsmith 1991). In many monitoring programs, follow-up and monitoring protocols are not adequately developed or implemented (Stewart et al. 1989).

To monitor the state of vegetation communities, it is critical to identify a set of variables that represent or indicate condition of the communities. For ecological monitoring in savanna systems, vegetation cover is considered an important variable and has been utilized in several studies for understanding ecological dynamics and sustainability. Mueller-Dombois and Ellenberg (1974) define cover as "the vertical projection of the crown or shoot area of a species to the ground surface expressed as a fraction or percent of a reference" (p.80). Along with species composition, cover is the most frequently utilized monitoring variable for many terrestrial ecosystems (Godinez-Alvarez et al., 2009). Cover would be a valuable measure for assessing species-specific habitat quality, which is the main objective for many conservation programs. Cover indicates the amount of canopy and bare ground exposure that may be key requirements for foraging and shelter for vertebrate species. Just as life-form cover is widely recognized as an important variable for quantifying productivity and soil stability in rangeland environments, resource managers and scientists have found that cover is a useful monitoring variable for biological conservation. The terms projected foliage cover

(PFC) (Coops and Culvenor 2000; Graetz 1990) and projected canopy cover (PCC) (Holmes 1990; Parker Williams and Hunt Jr 2002) are also found in literature. PFC or PCC is defined as the proportion of the cover of foliage or canopies that are projected to the surface per unit area (Steven et al. 1986). The difference between canopy and foliage cover is substantially greater for woody life-forms than herbaceous life-forms. Furthermore, in semi-arid savannas, even with woody life forms the total foliage and canopy cover can be substantially different between broadleaved species and microphyllous or fineleaved species. Hence measurements of cover based on PFC could be considerably less than those based on PCC. Vegetation cover is recognized to have greater ecological significance than vegetation density, which is obtained by total number of individuals divided by a unit area, because cover is correlated to biomass more strongly than the number of individuals (Ellenberg and Mueller-Dombois 1974). Cover is an unbiased quantitative measure regardless of plant size (Bauer, 1943) or life-forms (Ellenberg and Mueller-Dombois 1974), which is appropriate for monitoring semi-arid savannas consisting of multiple life-forms. Cover at the life-form level (e.g. trees/shrubs/grasses) can also serve as a proxy of vertical structure of a community (Graetz 1990).

Field sampling and remote sensing are the two main approaches that can be used to derive fractional vegetation/soil cover (proportional area occupied in a given unit area) in terrestrial ecosystems. Common field sampling methods used for estimating foliage cover are listed in table 3.1. Because of the unique characteristic of each method, the

resulting cover estimate may vary. Even though field sampling based on direct observation has the potential to provide accurate and precise cover estimates, frequent sampling of large number of plots is practically unfeasible in remote and logistically challenging areas.

Vegetation classification schemes in southern Africa savannas

Classification and nomenclature of vegetation classes can be achieved on the basis of many different characteristics e.g. dominant life form, floristic or species composition, physiognomic or structural properties (height/cover), seasonality (evergreen/deciduous), habitat characteristics or any combination of these features (Box 1996; Daubenmire 1968; Mucina 1997). Defining vegetation classes in semi-arid savanna systems is p challenging due to existence of multiple life-forms (e.g. grasses, shrubs and trees) and subtle but ecologically meaningful differences in vegetation physiognomy (i.e. height and density) (Fisher et al. 2013a; Hill et al. 2011a; Huttich et al. 2009; Thompson 1996). Despite the significance of vegetation cover as an important variable, the knowledge of land cover distribution and its dynamics, especially in remote and extensive ecosystems such as African savannas is limited (Hill et al. 2011a; Shugart et al. 2004). Previous studies have given special attention to how vegetation classes in these xeric ecosystems could be named.

Vegetation is such an important cover types in terrestrial ecosystems that many of the existing classifications systems are primarily vegetation classifications (Dansereau

1960; Eiten 1968; Fosberg 1967; Grossman and Conservancy 1998). Basic methods of field based assessment of vegetation characteristics involves stand methods such as transect based approach and the releve method proposed by Josias Braun-Blanquet (Westhoff and Van Der Maarel 1980) . The releve method is one of the quickest methods to obtain detail community information. This approach is qualitative in the sense that species cover is estimated instead of measured and it is also quantitative as it gives a complete list of species for the releve. However the releve method requires the precondition of homogeneous and representative vegetation stands (either in terms of species or physiognomic homogeneity).

Scale issue in determining savanna vegetation morphology types

Over the last few decades, mapping vegetation structural and functional properties and vegetation classification have greatly benefited from advances in satellite remote sensing, computer science and several other related disciplines (Thenkabail et al. 2012; Xie et al. 2008). Satellite and airborne remote sensing sensor systems are acquiring imagery at multiple spatial, temporal and spectral scales which has enabled characterization and mapping of important earth surface biophysical variables including vegetation. The thematic details of land cover produced by remote sensing sensor system depend on the spatial resolution of the imagery. Hence, depending on the scale of observation different classification systems have been proposed. The use of classification system and class nomenclature while classifying vegetation type is dependent on the scale of observation. While at species level classification system depends on the

individual ecological requirements of the observed biocenosis, at landscape to regional scales are distinguished by underlying class definitions (Hüttich et al. 2011a).

In recent years with increased availability of satellite images and derived products have been used extensively for land cover and vegetation mapping. However, satellite remote sensing derived land cover and other bio-physical attributes have shown high uncertainty in landscapes where vegetation is structurally heterogeneous and functionally diverse (e.g. savanna systems). For accurately characterizing these dynamic and diverse landscapes at regional scale, more recent studies have suggested integrated use of multi-scale land cover information is a prerequisite (Hüttich et al. 2011a). The field data derived *in-situ* represent the highest spatial and thematic detail where information such as plant life form, height, cover, density, species and soil characteristics could be derived following plot/transect based approach. However it is very challenging to collect in-situ vegetation and land cover information at landscape scale especially in southern Africa savanna systems due to limited infrastructure, accessibility and observation network. Compared to in-situ derived information, very high spatial resolution imagery (e.g. GeoEye, IKONOS) provides comparatively larger synoptic coverage with the potential to resolve individual tree and shrub stands, tree crown diameter, area under shade, proportion cover and density of life forms and fine scale vegetation patterns. However, use of very high spatial resolution datasets for landscape and regional scale assessment is hindered by small swath width, data volume and cost. At medium spatial resolution satellite data (e.g. Landsat) have the potential to provide ecological assessment at landscape scale but is limited in terms of spatial resolution and spectral sensitivity only

providing information on vegetation physiognomy, local scale patterns/ patchiness of woody and herbaceous vegetation.

The integration of land cover related thematic detail observed at different spatial scales (e.g. in-situ to high and medium spatial resolution) in a comparable manner is challenging but very important in context of inaccessible and logistically challenging savanna systems of southern Africa. In the Kalahari system, coupling in-situ data with variables derived from hierarchically nested multi-scale satellite images can detect and accurately characterize nuanced structural and functional properties of land cover that are ecologically more meaningful (e.g. relevant to habitat suitability, land degradation etc) (Huttich et al. 2009). Detail description of local soil and vegetation structural are critical for understanding remote sensing variables used for landscape to regional scale studies of ecosystem.

In general, use of the term savanna as an extension to names of vegetation types has caused confusions due to different interpretations of the term savanna (Harris 1980; Johnson and Tothill 1985). Further, many savanna vegetation types are classified and named based on floristic aspect or features of the sub canopy layer characteristics that are challenging to characterize from medium to coarse spatial resolution satellite images (Thompson 1996). From remote sensing perspective, structural and physiognomic characteristics are the most important criteria based on which semi-arid vegetation types could be distinguished (Groffman et al. 2005; Thompson 1996). Land cover and vegetation classes derived based on physiognomic characteristics can also be compared and harmonized with other classification schemes irrespective of species and ecosystems

or habitat characteristics (Hüttich et al. 2011a; Running et al. 1995). For classifying southern African savanna systems form remote sensing perspective, percent tree cover is an important criterion that has been utilized by various savanna vegetation classification schemes. Thomson (1996) presented a classification scheme that attempted to standardize class names based mainly on vegetation physiognomy and structural aspects. A schematic representation of the structural aspects, life forms, height and cover of the standard classification scheme after Thomson is shown in figure 3.5. Edwards (1992) presented another hierarchical and flexible classification scheme based on physiognomy-structural criteria that has been widely used due to its independence of geographic location or habitat characteristics.

Remote sensing of savanna ecosystems

Remote sensing serves as an effective tool to study savanna ecosystems over large spatio-temporal extents. The spectral reflectance data collected from remote sensing platforms have a linkage to plant physiological characteristics such as pigment concentration, plant mesophyll and leaf cell structures (Huete and Jackson 1988; Ustin et al. 2004; Wu and Marceau 2002) and biophysical attributes including cover, biomass, leaf area index (LAI) and photosynthetic active radiation (PAR) (Berry and Roderick 2002; Hufkens et al. 2008; Justice et al. 2002; Wu and Loucks 1995). Remote sensing based studies have been utilized for the management of savanna ecosystems for more than three decades. One of the most common applications of remote sensing in savanna

management is the estimation of vegetation properties including cover (Asner and Heidebrecht 2002; Elmore et al. 2000; Okin et al. 2001b; Paine et al. 1998), biomass and productivity (Chen et al. 1998; Van Rooyen et al. 1990; Wells et al. 1976; White et al. 1997; Wickham and Riitters 1995), vegetation density (Frost and Robertson 1987; Ringrose et al. 1998) and biophysical attributes such as Leaf Area Index (LAI), Fraction of Photosynthetically Active Radiation (fPAR) (Asner et al. 1998; Dupr and Ehrln 2002; Privette et al. 2004) and biogeochemical concentrations (Mutanga et al. 2004; Mutangao and Kumar 2007). A bottom-up approach is commonly used to correlate field observations and satellite signals and scale-up objects of interest to large spatial and/or longer temporal extents.

Remote sensing applications in semi-arid and arid savannas and rangelands started with the availability of multispectral products (e.g. Landsat MSS, TM) and many of the earlier studies used brightness and greenness indices to detect vegetation (Carlson and Ripley 1997; Elvidge and Chen 1995; Hurcom and Harrison 1998). However, these studies were susceptible to over or under estimation of arid vegetation cover as the methods used were primarily developed for assessing their humid counterparts characterized by large leaf area, fairly continuous canopies, high chlorophyll content, and thin, translucent leaves (Duncan et al. 1993; Escafadel and Huete 1991; Franklin et al. 1993; Huete and Jackson 1988; Huete et al. 1985; Pickup et al. 1993). To account for water and thermal stress, semi-arid vegetation has small vertically oriented leaves to avoid direct sunlight and open canopies that expose soil in canopy reflectance. Therefore, accurately characterizing semi-arid vegetation depended on methods that account for the

influence of soil background, atmospheric attenuation and solar position. Later studies suggested modified vegetation indices, either based on a soil line concept to account for the soil's contribution to the canopy reflectance or others that minimized atmospheric attenuation (Baugh and Groeneveld 2006). Perpendicular Vegetation Index (PVI) based on the soil line concept assumed that the perpendicular distance of the pixel from the soil line is linearly related to the vegetation cover (Richardson and Wiegand 1977). Huete (1988) suggested Soil Adjusted Vegetation Index (SAVI) based on the evidence that the iso-vegetation lines do not converge at a single point, and selected the L-factor in SAVI where lines of a specified vegetation density intersect the soil line. Huete (1988) suggested that SAVI takes on both the aspects of NDVI and PVI. The L- factor suggested for SAVI varied depending upon vegetation density. Transformed SAVI (TSAVI) was a further attempt to develop this concept that used a coefficient factor to adjust soil effects besides using the slope and intercept of the soil line (Baret et al. 1989). Some of the important atmospherically corrected vegetation indices included Atmospheric Resistant Vegetation Index (ARVI) (Kaufman and Tanre 1992) and Global Environmental Monitoring Index (GEMI) (Pinty and Verstraete 1992). Furthermore, due to seasonality of semi-arid savannas, plants typically manifest long periods of dormancy in which vegetation is in non-photosynthetic state, interspersed with brief periods of photosynthetic activity in response to seasonal rainfall. Thus separating the non-photosynthetic vegetation (NPV) from photosynthetic contribution is also important for which VI calculated using Short Wave Infra-Red (SWIR) wavelengths have been used. The Cellulose absorption Index (CAI) has been used to characterize non-photosynthetic

vegetation that is based on absorption features at 2100 nm and 2000 to 2200 nm regions due to cellulose and lignin in plant biomass. Absorption at these wavelengths is greatest in non-photosynthetic vegetation and absent from soil or green vegetation reflectance spectra (Guerschman et al. 2009; Nagler et al. 2003).

To find the best VI for use in sparsely vegetated regions, Baugh and Groeneveld (2006) compared the performance of fourteen VIs derived from Landsat TM data over San Luis Valley, Colorado. They found that although few VIs compensated for soil and atmospheric influence, those correcting for soil effects relied on arbitrary and potentially complex choices for establishing a soil line. Similarly, selecting scale factor to correct for atmospheric influence was arbitrary since data does not exist for the users to choose correct scaling. Furthermore, none of these studies based on multispectral wavebands were able to accurately and reliably discern shrubs from grasses which is probably the most important means by which to identify shrub encroachment and desertification in semi-arid savannas (Schlesinger et al. 1990; Warren and Hutchinson 1984). Due to limited spectral sensitivity of multispectral images even though the landscape components were found to be significantly different, the high variance in the results suggested that it is methodologically challenging to accurately retrieve the fractional contribution of PV, NPV and bare soil to spatially averaged measurements (Okin et al. 2001b; Okin et al. 1998). Therefore, future research in savanna ecosystems needs to develop methodologies to address this challenge by combining field derived information on vegetation functional properties and imagery acquired at multiple spatial scales (Gessner et al. 2013; Hüttich et al. 2011a).

Sub-pixel remote sensing for fractional cover estimation

The spatial characterization capability of earth observing spectral imaging sensors used in remote sensing is often limited by mixed pixel ('mixel') phenomena as these sensors frequently operate at spatial resolutions at which numerous distinct substances contribute to the spectrum of a single pixel (Goodchild 1997; Wu and Li 2009). As an alternative to physically derived pixel level VI, a more statistical probabilistic approach called Spectral Mixture Analysis (SMA) was adapted in studies that modeled the fractional cover within a pixel as linear combination of contributing pure spectra known as endmembers and allowed sub-pixel characterization (Adams and Adams 1984; Adams et al. 1995; Roberts et al. 1993; Twyman 2000). Following SMA, the best fit weighted coefficients of each endmember spectrum are interpreted as the relative area occupied by each endmember in a pixel (Adams and Adams 1984; Bateson and Curtiss 1996). Depending on the assumption on how the endmembers in a mixed pixel combine, SMA can be performed either as a linear mixing model or a non-linear mixing model. But for both linear and non-linear approaches, there is a perquisite of high quality endmembers. Therefore, the accuracy of SMA, most importantly depends on the purity of endmembers used (Borel and Gerstl 1994; Keshava 2003; Okin et al. 2001a). Following equation 1-3, linear SMA method models a mixed pixel as linear combination of endmembers spectra weighted by their percentage ground cover:

$$DN_b = \sum_{i=1}^{N} F_i DN_{i,b} + E_b \qquad (1)$$

$$\sum_{i=1}^{F_i} F_i = 1 \qquad\qquad (2)$$

$$RMSE = \sqrt{\sum_{i=1}^{B} \frac{(E_i)^2}{B}} \qquad\qquad (3)$$

Where, DN_b is the reflectance of a given pixel in a band at wavelength b, F_i is the fractional abundance of endmember I, $DN_{i,b}$ is the reflectance of endmember I at wavelength b, N is the number of endmembers, and E_b is the error of the fit for band b. Equation (2) imposes a non-negativity and equal unity constrain on the fractions within a pixel for the abundance estimates to be physically realizable. Equation (3) provides the total root mean square error for the solution where B is the total number of spectral bands.

Approaches for Endmember selection

Endmembers used in SMA can either be acquired in the field using a spectroradiometer (called "reference" endmembers) or can also be derived from the imagery itself (known as "image" endmembers). Figure 3.8 shows an example of reference endmember collection in the field and the resultant endmembers spectral plots for PV, NPV and soil. While reference endmembers are spectrally pure, their suitability is challenged by scale difference as the spectra of a given pixel represents average signal of much larger area. Image endmembers although provide the scalability, but are often not completely pure particularly for medium and low spatial resolution imagery acquired over spatially heterogeneous landscapes. From a mathematical perspective, selecting endmembers from imagery is similar to estimating a non-orthogonal subset of basis vectors whose weighted summations can be used to construct the mixing model (Howes

et al. 2004). In order to be physically realizable, these endmembers must have non-negative entries and they should also retain the physical characteristics of constituent substance (e.g. absorption, high or low reflectance). Essentially, endmembers are required to satisfy both mathematical constraints and physical imperatives, which make accurate endmember determination the most challenging part of SMA (Keshava 2003; Keshava et al. 2000). The type of endmember depends on the method of its determination, which is an active and interdisciplinary area of research. Various methods have been suggested for endmember selection for spectral unmixing. These methods can be grouped into three broad categories: manual selection, geometric approaches and statistical approaches.

In *manual approach,* most extreme data points (pixels) from the n-dimensional distribution are selected as endmember for which spectral libraries may be taken as a reference in the spatial context of the selected pixel. Since the choice of endmember selection using manual approach is restricted to actual data points, it is assumed that chosen endmember represents spectrally pure material. For manual approach, a study devised multidimensional visualization method (called manual endmember SMA) for interactively searching endmembers in the space of the principle component analysis (PCA) determined eigenvectors accounting for most of the variance (Bateson and Curtiss 1996). However, selecting endmembers manually can be time consuming and the purity of manually selected endmembers is highly dependent on the skill of the operator, limiting the suitability of the manual approach.

Geometric approaches of endmember determination are based on strong parallelism between linear mixing model and the theory of convex sets. It assumes that pixel spectra within a scene exists as vertices of n-dimensional simplex that encompass the data (Keshava 2003). The objective therefore, is to demarcate an enclosed surface having minimum volume, while still containing all the pixels. For computational efficiency the endmember selection process is typically preceded by dimensionality reduction (pixels are discarded and not bands). Since only the perimeter of the volume occupied by scene data is required to locate endmembers, the pixels within the convex hull of the data are discarded. In the second step, shrink-wrapping is performed where Minimum Volume Transformation (MVT) is applied iteratively to fit a multifaceted simplex around the convex hull (Craig 1994). A variant of MVT approach is also known as Dark Point Fixed Transformation (DPFT) that assumes knowledge of dark point of the sensor. This is a contrast to Fixed Point Free Transform (FPFT), which assumes unknown dark point (Chan et al. 2009; Craig 1994; Keshava 2003). In Pixel Purity Index (PPI) method of endmember selection, pixels are transformed and projected on to a random unit vector and most extreme pixels are determined for each projection. The pixels with higher number of extreme projections (higher PPI) are selected as endmembers (Boardman 1995). Geometric approach of endmember determination is non-parametric and non-statistical. They can be computationally heavy depending on the processing approach and are sensitive to outliers and bad pixels. However, they can expose rare objects that would otherwise go unnoticed using statistical approaches (Keshava 2003).

Since real data often displays clustered structure, endmembers have also been determined using iterative *statistical approaches* where endmembers are associated with data classes rather than data points. Variety of statistical endmember determination techniques exist, but majority of them arrive at estimate using second order statistics to define statistical classes for each endmember and by relating the fractional abundances of each pixel to partial membership in each class. Further, estimates of endmembers and abundances iteratively minimize a cost function which provides a maximum likelihood solution if the cost function arises from a probabilistic Gaussian distribution (Stocker and Schaum 1997; Tompkins et al. 1997). However, the solution can also be sought using non-parametric approach with statistical clustering techniques (e.g. fuzzy k-means clustering) which attempt to optimize a least square based cost function by finding best endmembers and abundances. The technique of nonlinear least squares for endmember determination and abundance estimation models the additive noise in the liner mixing model (LMM) as Gaussian and integrates a priori knowledge into least square formulation for unmixing. On the other hand, the Gaussian class estimation method does so without resumption of any additive noise. Instead, here endmembers are assumed Gaussian classes in an attempt to fuse the geometric interpretation of linear mixing with Gaussian mixture modeling and maximum likelihood estimation technique (Keshava 2003; Stocker and Schaum 1997).

Single endmember SMA versus multiple endmember SMA (MESMA)

SMA is a powerful approach and has advantage over competing approaches (e.g. vegetation indices), in that it provides physically meaningful measures of cover and

accounts for sub-pixel mixing. A single member SMA however fails to account for spectral degeneracy between materials, pixel-scale variability in spectral dimensionality and natural variation in spectra of most materials. Thus a single endmember SMA underutilizes the potential of most remote sensing data sets and could produce fractional errors due to incorrect type or number of endmembers used to unmix a given pixel. Multiple endmember SMA (MESMA) attempts to overcome these limitations by allowing both the number and type of endmembers to vary on a per pixel basis (Roberts et al. 1998). Thus MESMA overcomes limitations of SMA by testing multiple models for each image pixel while requiring a model to meet minimum fit, fraction and residual constraints. (Roberts et al. 1998; Roberts et al. 1997a).

Following MESMA approach, several endmember determination techniques are suggested and they essentially concentrate on selecting best representative endmembers to represent the spectral variation of material in an image. For example, a limited number of reference spectra or a priori knowledge was used by Painter et al., (1998) and Okin et al., (2001) to select endmembers for their analysis. Roberts et al., (1997) proposed a hierarchical endmember selection rule that classified endmembers as specialists or generalists based on their ability to model target spectra. Roberts et al. (2003) also proposed an approach called Count based endmember selection (CoB) as a means of selecting optimal endmembers as those members of a spectral library that model the greatest number of spectra within their class. Under CoB endmember selection approach the total number of spectra modeled within the class (in_CoB) and the total number of

69

models outside of the class (out_CoB) are recorded for each model. Finally, the optimum model is selected as the one that has the highest in_CoB value.

Another endmember selection approach known as Endmember Average RMSE (EAR) was proposed by Dennison and Roberts (2003). EAR is calculated as the average root mean square error (RMSE) produced by a spectrum when it is used to model all other members of the same class. EAR is calculated for each member of a class within the spectral library and the optimum endmember is the one that produces the lowest average RMSE. Proposed by Dennison et al. (2004), Minimum Average Spectral Angle (MASA) is another endmember selection method which is similar to EAR in that it is designed to select spectra with the best average fit within a class. It differs from EAR in that the measure of fit used is the spectral angle, not the RMSE. Using this approach each spectrum is used to calculate the spectral angle between itself and all other members of the spectral library. MASA within a class is calculated as the average spectral angle between the reference spectrum (candidate model) and all other spectra within the same class. The best MASA candidate is selected as the one that produces the lowest average spectral angle. Automatic Monte Carlo Unmixing (MCU) has been suggested an alternative to MESMA where endmembers are selected from 'bundles' of similar materials to generate a mean and standard deviation for each fraction (Asner and Lobell 2000). Although MCU approach automates the multiple endmember selection process, but is highly dependent on the library spectra and cannot account for target specific spectral variation as accounted by manual MESMA.

70

SMA/MESMA for fractional cover estimation in savanna systems

The availability of hyperspectral sensors or imaging spectroscopy (e.g. AVIRIS, HyMAP, CASI, Hyperion) characterized by fine spectral resolution (e.g. AVIRIS ~ 10 nm), high spectral sensitivity and signal to noise ratio required the development of advanced image analysis methods such as MESMA that could fully exploit the potential of these datasets. (Asner and Heidebrecht 2002; Goetz et al. 1985; Green et al. 1998; Roberts et al. 1997b; Vane et al. 1993). Several studies have utilized MESMA approach for environmental remote sensing applications in variety of ecosystems using both hyperspectral and multi-spectral images. Applying MESMA on AVIRIS data, Roberts et al (1993) could explain over 98 percent spectral variation using endmembers of green vegetation, soil and shade. Non-photosynthetic vegetation was explained as residuals in the SWIR wavelengths while the different types of green vegetation were distinguished by residuals due to non-linear mixing effects. Using MESMA on three AVIRIS images acquired in 1992 over Jasper Ridge, California, Roberts et al., (1997) also demonstrated the intra annual variation in the fractional cover of photosynthetic vegetation (PV), non-photosynthetic vegetation (NPV), soil and shade. Exploring endmember choices for MESMA analysis using AVIRIS data of Manix basin in the Mojave Desert, Okin et al. (1998) compared two, three and four endmember models. They found that while more than half of the image was well modeled with three endmembers, the four endmember models offered greater flexibility to account for inter and intra species spectral variability of endmembers expect for some instances where the model was overfit. This study also argued that RMSE is not an appropriate metric for comparing the fitness of

multiple endmember models as increasing the degree of freedom by adding more endmembers inflates the model fitness. As an alternative, they recommended considering the categorical changes and changes in relative magnitude of fractions in models of different degree. To test the potential of MESMA for retrieving vegetation characteristics using hyperspectral data in semi-arid areas, Okin et al. (2001) performed spectral simulations comprising a best case scenario in which many typical problems of remote sensing in low vegetation cover areas were minimized. Results showed that the soil type retrievals were more than 90 percent reliable and vegetation cover can also be estimated reliably. However, vegetation types could not be reliably estimated when the vegetation cover was below 30 percent. In another study in semi-arid shrubland ecosystem, Asner and Lobell (2000) tested auto MCU approach on AVIRIS images to map fractional cover of PV, NPV and soil. They utilized spectral derivative of SWIR2 (2100 nm to 2400 nm) spectra in which differential relation between PV and NPV was found to be consistent between different land cover types (Asner and Lobell 2000). Although the results were promising, but the fractional estimates derived were highly affected by the representative spectral library spectra and the results cannot account for species-specific differences in spectral response (Halligan 2008).

Studies utilizing MESMA in combination with airborne hyperspectral data could produce promising results because of the ideal bandwidth and high signal to noise ratio of these datasets. However, airborne hyperspectral datasets have limited swath coverage and also lack consistent multi-temporal image acquisition that is required for long term monitoring. The spaceborne hyperspectral instruments (e.g. EO-1 Hyperion) although

have much larger spatial swath and also provide high spectral resolution, but have much lower signal to noise ratio, reducing the reliability of its results. As an alternative, broadband multi-spectral sensors at medium spatial resolution (e.g. Landsat, ASTER, and SPOT) are characterized by much larger swath area and consistent revisit capability, making them more suitable for environmental remote sensing applications. These multispectral sensors have also been used with MESMA to determine bio-physical estimates, but, unlike hyperspectral sensors their accuracy have been limited due to lack of required high spectral sensitivity and ideal bandwidth especially in the shortwave infrared (SWIR) region where discrimination of soil and senescent vegetation is most effective (Asner, 1998; Asner et al., 2005; Asner and Heidebrecht, 2002). MESMA has also been used in studies to resolve vegetation fractional cover using broadband multispectral sensors with moderate results (Gill and Phinn 2008; Numata et al. 2007). In an attempt to overcome the issue of limited spectral dimensionality another study combined NDVI with the six reflectance bands of Landsat ETM+ image over semi-arid region of New Mexico to perform SMA using five endmembers and found improved separation of PV from NPV and soil (Xiao and Moody 2005).

Another approach for accurately mapping fractional cover of large areas followed by studies is to compare coincident hyperspectral and multispectral products in combination with high quality field spectra and use hyperspectral data to model and extend signatures to multispectral data. This has been achieved by developing an empirical relationship that was used to upscale the hyperspectral results to cover larger areas captured by multispectral product. In one such study in northern Death Valley,

73

spatially nested Hyperion and ASTER data were analyzed to determine spectral endmembers from the Hyperion image and the ASTER signatures were later modeled using Hyperion data and ASTER spectral response functions. The spatial distribution of predicted endmembers were later mapped using ASTER data and accuracy of mapping was accessed in both overlapping and non-overlapping image areas (Kruse 2007; Kruse and Perry 2009). For comparing hyperspectral (AVIRIS) and multispectral capabilities of determining fractional cover, Asner and Heidebrecht (2002) applied the auto MCU for a site in Chihuahua desert. The model tested five different hyperspectral sampling schemes available from the AVIRIS data as well as data convolved to Landsat TM, Terra MODIS and Terra ASTER optical wavelengths. Results of full range unmixing for both multispectral and hyperspectral images were found to overestimate bare soil and underestimate PV. However, the utilization of SWIR2 (2000 nm – 2300 nm) spectra with a procedure that normalizes all reflectance values to 2030 nm, the sub-pixel fractional covers were estimated much more accurately. For fractional cover mapping at large scale using AVHRR and MODIS products, a previous study decomposed the temporal variation of vegetation into a slow varying component (perennial trees) and rapidly varying component (herbaceous) (Berry and Roderick, 2002; Lu et al., 2003) but did not provide explicit measure of fractional covers. In another study using MODIS product, Okin (2007) found reflectance spectra of soil and NPV not dissimilar enough and proposed relative spectral mixture analysis where quantities were estimated relative to an initial date which could be selected arbitrarily. For mapping tillage practices in central Iowa, another study used Hyperion data to separate fractional PV (healthy crops) from

fractional NPV (dry crops and crop residues) using NDVI, while CAI was used to separate fractional NPV from fractional bare soil (Daughtry et al. 2006). Using Auto MCU method in combination with field spectra, Asner and Heidebrecht (2003) compared the performance of AVIRIS and Hyperion for quantifying fractional PV, NPV and bare soil for a monte desert biome in Argentina drylands. They found that AVIRIS data provided highly accurate measures of fractional cover of PV, NPV and bare soil, whereas Hyperion accurately estimated only fractional PV due to good red-edge performance. Comparatively lower S/N ratio of Hyperion in the SWIR wavelengths resulted in lower accuracies of NPV and soil fractions (Asner and Heidebrecht 2003). Based on the examination of NDVI and CAI plots derived from reference endmember spectra of PV, NPV and soil in tropical savanna of Australia, Guerschman et al., (2009) found that PV, NPV and bare soil occupied a triangular space when plotted against each other (Figure 3.11). Furthermore, the NDVI and CAI plots derived from multi-temporal Hyperion imagery of the same area also found to form a similar triangle. They used the corner most pixels of this NDVI-CAI triangular space as endmembers of PV, NPV and bare soil to unmix the Hyperion image and derive fractional cover. Leveraging the availability of this multi-temporal Hyperion imagery they also developed a scaling relation between Hyperion and MODIS that enabled endmember selection using NDVI-CAI approach and multi-temporal practical cover mapping for the entire tropical savannas in Northern Australia. Due to the lack of any spatio-temporally coincident hyperspectral imagery in the study area, this dissertation research builds upon these previous research strategies

and proposes an empirical multi-scale hierarchical approach for deriving endmembers at coarse spatial resolution imagery.

Pixel versus object based image analysis in savannas

Since savanna systems are often considered patch dynamic systems, analyses of remotely sensed images in savannas may benefit from object-based image analysis (OBIA) rather than the traditional per-pixel analysis approach (Laliberte et al. 2004; Soranno et al. 1999; Spies et al. 1994; Steffan-Dewenter et al. 2002). The OBIA approach is finding increasing popularity particularly when applied to high resolution satellite imagery (Lennartz and Congalton 2004). The range of resolutions of satellite imagery lends itself to mapping of land cover at a number of scales. High resolution images obviously contain more spatial information than low resolution. Therefore it is reasonable to suggest that coarser resolution data can be used to create small scale land cover maps while higher resolution data can map land cover in greater detail (Colombo et al. 2003). Pixels within a low resolution imagery may contain combined or integrated signals from a number of objects, whereas pixels within a high resolution image will more closely approximate these objects or their components (Hay et al. 2003). For the analysis of high spatial resolution imagery, the OBIA approach has been widely accepted by the remote sensing and GIScience community (Blaschke et al. 2008; Chen et al. 2012). Definiens GmbH introduced an image processing software called eCognition (eCognition is now owned by Trimble Inc.) and popularized object-based image analysis and object-based change detection in the field of remote sensing. OBIA applications, especially with high

and medium spatial resolution imagery have been demonstrated to alleviate some of the significant problems of per-pixel analysis approaches (Marpu et al. 2008; Whiteside et al. 2011). In savanna systems, important OBIA advantages includes (i) treatment of landscape to be consisting of relatively homogeneous patches (or 'objects') is ecologically more suitable than individual pixels (ii) landscape patches often depict scale dependency and following the OBIA approach landscape objects can be generated at multiple segmentation scales that can provide added insight into ecological processes (Strayer et al. 2003a) (iii) lower chances of 'salt-and-pepper' speckle which is often an issue with per-pixel analysis and (iv) OBIA offers the opportunity to add contextual, geometrical and texture related features (Strayer et al. 2003b).

Object Based Image Analysis (OBIA)

Primarily there are two steps to object-based image analysis, segmentation and classification (Blaschke and Hay 2001). Segmentation involves the partitioning of a remotely sensed image into objects that are homogeneous in nature (either spatially or spectrally). These segments correspond to objects or parts of objects detected within the imagery. Pixels within a segment or object have similar spectral values or belong to a similar pattern (as determined by segmentation parameters). Thus objects or segments are formed based on spatial correlation as well as high spectral autocorrelation (clustering in feature space) (Hay, 2002). Classification of these objects is then conducted using the mean band values and other statistical spectral information for these objects derived from the pixel values of the spectral bands of the imagery, shape features associated with the

objects, as well as the topological relationships between objects. Studies such Borsotti et al. (1998) and Pal and Pal (1993) provide in depth reviews of various segmentation techniques.

There are three main categories of image segmentation: edge-based segmentation, region-based segmentation and split and merge segmentation (Borsotti et al. 1998). In edge-based segmentation, an edge filter is applied to an image and pixels are either identified as edge or non-edge relevant to the objects displayed in the image. Chains of edge pixels are connected and segmentation can then be achieved by allocating to a single category all non-edge pixels which are not separated by an edge (Glasbey and Horgan 1995). Segmentation using edge detection uses pixel differences to create image objects whereas segmentation using region growing uses pixel similarities to create image objects. Region growing starts with a seed point or pixel and grows objects iteratively until a certain threshold is met (Sonka et al. 1996). Split and merge segmentation involves an initial image splitting phase (creating a quadtree segmentation) followed by an agglomerative clustering phase (Lucieer et al. 2005). In the splitting phase, the image is initially considered as one region. If a region has a degree of homogeneity it remains intact. If it lacks coherency it is split into four quadrants. These steps are applied recursively to each new region until all objects have a level of homogeneity. At this point, adjacent objects (regardless of size) may have similar spectral characteristics. Objects can then be merged into larger regions based on these characteristics.

Multi-resolution segmentation algorithm (MRSA) is one of the most popular region based image segmentation algorithm which is also available with commercial

OBIA software such as the eCognition (Baatz and Schäpe 2000a; Benz et al. 2004a). The following description of MRSA is based on the description by Benz el al. (2004). MRSA grows objects from individual pixels by automated merger decisions. Two growing objects are merged if the increase in heterogeneity (*f*) incurred by the merger is the smallest among all the candidate merges with adjacent objects (or pixels) and if it is less than a specified threshold (*f* < SP). The term 'scale parameter' is not prescriptive of the size (scale) of resulting objects, nor directly related to the dimension or resolution (scale) of the input data. It might be more intuitively called the 'object complexity limit', but the term 'scale parameter' is well established and so is retained. The change in the weighted heterogeneity (*f*) of a potential object merger is the sum of the change in color heterogeneity (Δh_{color}) and the change in shape heterogeneity (Δh_{shape}), multiplied by the color and shape weights (w_{color}, w_{shape}), respectively:

$$f = (w_{color}\, \Delta h_{color}) + (w_{shape}\, \Delta h_{shape}) \qquad (4)$$

The color and shape heterogeneity changes of a potential object merger are calculated as the heterogeneity score of the potential new larger object minus the sum of the scores of the original two smaller objects. The color heterogeneity of an object is its size in pixels (*n*) multiplied by the standard deviation of pixel values in each band (σ_b), summed over all bands. Bands are typically weighted equally ($w_b = 1$) but may be weighted individually:

$$\Delta h_{color} = \sum_{b} w_b \left(n_{new}\sigma_{new,b} - (n_{old1}\sigma_{old1,b} + n_{old2}\sigma_{old2,b}) \right) \qquad (5)$$

The shape heterogeneity of an object is the sum of the change in compactness heterogeneity (Δh_{comp}) and the change in smoothness heterogeneity (Δh_{smooth}) multiplied by the compactness and smoothness weights ($w_{comp.}$, $w_{smooth.}$), respectively:

$$\Delta h_{shape} = \left(w_{comp.} \Delta h_{comp.} \right) + \left(w_{smooth.} \Delta h_{smooth} \right) \quad (6)$$

The smoothness heterogeneity of an object is its size in pixels (n), multiplied by its perimeter (p), divided by the perimeter of a bounding box oriented parallel to the input raster (p_{box}):

$$\Delta h_{smooth.} = \frac{n_{new} p_{new}}{p_{new,box}} - \left(\frac{n_{old1} p_{old1}}{p_{old1,box}} + \frac{n_{old2} p_{old2}}{p_{old2,box}} \right) \quad (7)$$

The compactness heterogeneity of an object is its perimeter (p), multiplied by the square root of its size in pixels ($\sqrt{n}$):

$$\Delta h_{comp.} = \sqrt{n_{new}} p_{new} - \left(\sqrt{n_{old1}} p_{old1} + \sqrt{n_{old2}} p_{old2} \right) \quad (8)$$

In summary, the MRSA requires the user to supply the shape parameter, the color and shape weights (which must sum to 1), and the smoothness and compactness weights (which must sum to 1).

Within OBIA, the segmentation scale parameter used in segmentation controls the maximum allowable object level spectral heterogeneity and object size (Urban et al. 2002). Scale also affects the quality of segmented objects and which in turn affects the final classification accuracy (Keyghobadi et al. 1999; Yu et al. 2006). By manipulating segmentation scale factor, nested objects of different size can be created wherein smaller

80

objects (or sub-objects) are created with finer segmentation scale factor and larger objects (or super-objects) that consist of more than one sub-object are created with coarse segmentation scale values. These objects could be further hierarchically classified representing the output at multiple scales. Different studies have found such hierarchical classification of objects following approach especially appropriate for characterizing spatially heterogeneous natural systems such as wetlands (Dronova et al. 2012; Trzcinski et al. 1999) and arid rangelands (Laliberte et al. 2007; Laliberte et al. 2004).

Over the years the utilization of OBIA in environmental remote sensing related image analysis has increased considerably. The analysis of remote sensing datasets has evolved from predominantly per-pixel or sub-pixel based methods to the application of OBIA methods. Due to the relative homogeneity of objects used in OBIA, Hay et al. (2005) also stated that OBIA is a possible reduction of the MAUP problem in remote sensing. However, there are several challenges of OBIA that need to be addressed. A big challenge in OBIA is the concept and extraction of scale in an image, and its relative size. When pixels are linked to form image objects, ideally the visual interpretation of image objects and image objects derived from the software must match. This involves two dimensions of scale: (a) absolute scale when segmenting single objects such as individual trees or shrubs and (b) relative scale when considering the spatial resolution of different scale data (Blaschke, 2010). The OBIA software has too many parameters which do not produce consistent results across different studies. Furthermore, the OBIA approach requires iterative optimization of several segmentation and classification parameters that hinders automation and is a big challenge to overcome.

81

OBIA for Remotely Sensed Vegetation Mapping

Mapping and monitoring of vegetation properties is one of the most important objects in environmental remote sensing. More recently, OBIA has emerged as an important approach that has been utilized for mapping vegetation properties in different ecosystems using remotely sensed multi-spectral imagery at both high and medium spatial resolution (Blaschke 2010). Using high spatial resolution airborne imagery Yu et al. (2006) conducted comprehensive vegetation inventory and found OBIA to be superior to per-pixel approach as OBIA did not produce salt-and-pepper effect. For land cover mapping in a coal fire area in Mongolia, Yan et al. (2006) found improved classification accuracy using OBIA approach. To derive forest inventory parameters from high spatial resolution IKONOS imagery in Alberta, Canada, Chubey et al. (2006) used OBIA and achieve best relationship between field and image derived discrete land cover types, species composition and crown closure. To delineate vegetated polygons in a natural forest in northern Greece Mallinis et al. (2008) performed multi-scale OBIA classification and found the inclusion of texture important and the use of classification trees yielded higher accuracy compared to nearest neighbor classification.

Few studies have adopted the OBIA approach for characterizing vegetation properties in savannas and rangelands. For mapping rangeland vegetation in New Mexico, USA, Laliberte et al. (2007) segmented a Quickbird imagery at four different segmentation scales and used a non-parametric method (i.e. classification tree) for classifying objects. Results showed that different vegetation species attained the highest accuracy at different segmentation scales and both spectral and textural variables were

82

important for separating different vegetation types. In another study, for comparing the performance of per-pixel versus the OBIA approach for mapping selected vegetation classes in Australian tropical savanna, Whiteside et al. (2011) found a statistically significant higher overall accuracy of the OBIA results over the per-pixel classification. For characterizing the structural diversity of vegetation in South African savanna, Levick and Rogers (2006) integrated vegetation height derived from LiDAR and spectral information from aerial photos under an OBIA approach. The study found the OBIA approach important for fusing height data with imagery to derive multi-scale output. More recently, with the integration of vegetation height derived from LiDAR with multispectral and hyperspectral images under OBIA approach studies have been able to characterize both structural and functional diversity of savannas in three dimensions. For example, for understanding the influence of biophysical drivers on spatial pattern of 3-D structure of woody vegetation, Fisher et al. (2013b) mapped 3-D structural classes of vegetation (i.e. canopy cover, sub-canopy cover, canopy layers etc) in South African savannas using multi-threshold and multi-resolution segmentation techniques on volumetric pixel (voxel) data from Carnegie Airborne Observatory Alpha system.

Image classification using Classification trees

In remote sensing image analysis, classification refers to the process of reducing an image to information classes by assigning individual pixels in the imagery into classes of interest. Traditionally image classification has been conducted using parametric statistical methods such as maximum likelihood, minimum distance to mean and linear

83

discriminant analysis. These classifiers are generally characterized by having an explicit underlying probability model, which provides a probability of being in each class rather than simply a classification. The performance of such parametric classifiers depends on how well the actual distribution of data matches the pre-defined model (Lillesand and Kiefer 1994). However, these classifiers are not effective in dealing with complex and non-linear relationships that are often encountered in spatially heterogeneous and temporally dynamic natural systems. Non-parametric classification techniques (e.g. Artificial Neural Networks, Classification/decision trees, Support Vector Machines) have increasingly been used to overcome the statistical limitations encountered by parametric classifiers (Mather and Tso 2010). Classification tree is a tree based non-parametric method that has been widely utilized for the classification of remotely sensed data due to their simplicity, flexibility and computational efficiency in handling non-normal, non-homogeneous and noisy data (Friedl and Brodley 1997). Decision trees split the feature space into a set of sub-spaces using binary decisions. The class boundary is derived by asking a sequence of nested yes/no questions. For example, the first node (root) splits a variable *TI*. Cases larger than the value of five follow the left branch (Figure 3.14). The remaining values go to the right branch where further splits will be performed. Terminal nodes are reached when the data arriving at a node is of a single class. At the point where splitting is no longer possible, the class label is assigned corresponding to the majority class within the terminal node. Different splitting criterions (impurity functions) exist which are based on the probability of class assignments and can be derived using different statistical matrices measuring data heterogeneity, such as misclassification error,

Gini index and cross-entropy or deviance. The Random Forest classification method used in this dissertation used the Gini index method for splitting in which heterogeneity measurement values range from zero to one. In the Gini index, p_i is the probability at which an element of class I (element in a node), is chosen, s is the total number of classes, calculated as follows:

$$G = \sum_{i=1}^{s} p_i^2 \qquad (9)$$

When the value of $p_i=1$ (and $G=0$) is given at a maximum heterogeneity and the minimization of G results in maximum heterogeneity of the resulting split at a given node. Decision trees have emerged as one of the most commonly adapted method for classifying variety of multi-dimensional data. The main advantages of decision trees are: (i) decision trees are transparent in nature as they make explicit all possible alternatives and traces each alternative to its conclusion in a single view, allowing for easy comparison among the various alternatives, (ii) decision trees reduce ambiguity in decision making as it is able to assign specific values to problem, decisions and outcomes of each decision, (iii) decision trees are easy to use and interpret as they provide a graphic illustration of the problem and various alternative in a easy to understand manner, (iv) decision trees have the ability to deal with irrelevant data as trees naturally perform variable selection and nodes are divided from the best variables, (v) decision trees do not require any data pre-processing and can naturally handle binary, categorical and numerical data, (vi) missing data have little impact on the results of tree-based models (vii) decision trees are faster to generate in comparison to other iterate methods.

85

However, decision trees are not suitable for the prediction of linear relationships as they are discontinuous piecewise constant models. Also, the results of decision trees are very sensitive to the quality of training data as slight changes in training data can cause changes in modeling output (Cutler et al. 2007; Pal 2005).

Ensemble classification techniques: Random Forest

Ensemble classification methods construct a set of classifiers instead of one classifier, and then classify new data points by considering the majority vote of their predictions. The most commonly used ensemble classifiers are Bagging, Boosting and Random Forest. As shown in several studies, an ensemble of several decision trees generally improves the classification accuracy as it aims to reduce the variance of a single decision tree prediction. The Bagging algorithm draws many bootstrap samples from a training data set with replacement to train a classifier and for each bootstrapped sample a tree is constructed such that successive trees are independent from previous trees, and a majority vote is taken for the final prediction (Liaw and Wiener 2002). Unlike Bagging, the Boosting algorithm uses iterative re-training and as the iterations progress the weights of incorrectly classified samples are increased. In general, Boosting predictions are more accurate than the Bagging algorithm. Nevertheless is comparatively slow for large datasets and is very sensitive to noise in data (Camps-Valls and Bruzzone 2009). Random Forest is another ensemble tree-based classification technique and is an advanced version of the Bagging algorithm with added randomness (Breiman 2001). Instead of splitting each node using the best split among all variables, random forest splits each node using

the best among a subset of predictors randomly chosen at that node. A new training

dataset is created from the original dataset with replacement. Then, a tree is grown using

random feature selection. Grown trees are not pruned (Breiman 2001; Pal 2005). This

strategy makes RF highly accurate and a fast predictor that is also robust against

overfitting (Breiman and Cutler 1993).

The process of Random Forest classification is described below according to Hastie et al.

(2009):

a) For $b = 1$ to B:

1. The bootstrap sample Z^* of size N is drawn from the training data.

2. The random forest tree T_b is grown to the bootstrapped data. The following steps

    are recursively performed for each terminal node of the tree, until the minimum

    node size n_{min} is reached.

    2.1 M variables are selected at random from p variables.

    2.2 The best variable/split point among the m are picked.

    2.3 The node is split into two daughter nodes.

b) Output of the tree ensemble $\{T_b\}_1^B$

    The class prediction of each pixel in random forest class is based on:

$$C_{rf}^B(x) = majority\{C_b(x)\}_1^B \qquad (10)$$

$C_b(x)$ is the class prediction of the b_{th} random forest tree. The majority vote is applied

on the classification result C_b of the ensemble of B trees. The input data is classified with

an ensemble of decision trees ($DT_1 - DTn$). Classification result of the terminal nodes ($TN_1 - TNn$) of each tree are combined by majority voting.

To initialize Random Forest algorithm, the two parameters that need to be defined are the number of trees to grow and the number of variables used to split each node. Bootstrap samples are drawn from the 2/3 of the training data set. The remaining 1/3 of the training data, also called out-of-bag (OOB) data, are used to test the error of the predictions. Then, an un-pruned tree from each bootstrap sample is grown such that at each node certain number of predictors is randomly selected as a subset of predictor variables, and the best split from among those variables is chosen. It is crucial to select the number of variables that provides sufficiently low correlation with adequate predictive power (Horning 2010). Breiman (2002) suggests that setting the number of variables (m) equal to the square root of M (number of overall variable) gives generally near optimum results. Random Forest uses the Gini index as the splitting criteria (Beriman 2001). As Gini index increases class heterogeneity also increases; however, as the Gini index decreases, class homogeneity increases. If a child node of the Gini index is less than a parent node, then the split is successful. Tree splitting is terminated when the Gini index is zero, which means only one class is present at each terminal node (Cutler et al. 2007). Once all N trees are grown in the forest, the new data is predicted based on the outcome of the predictions of N trees (Liaw and Wiener 2002).

An important and informative feature of Random Forest algorithm is the calculation of variable importance score for the predictor variables used in class prediction. Random Forest provides two types of variable importance measures. The first

type of variable importance shows the improvement of split criterion (Gini index) which is attributed to the feature at each split of the tree and finally averaged over all the trees. The second type is based on the use of OOB samples. The prediction accuracy is calculated when the bth tree is grown. The accuracy is again calculated after the values of the jth feature are randomly permuted in the OOB samples. The result is a decrease of accuracy as a consequence of the permutation process. The decrease of accuracy is averaged over all trees. The second variable importance score indicates the prediction strength of each feature (Hastie et al. 2009; Liaw and Wiener 2002).
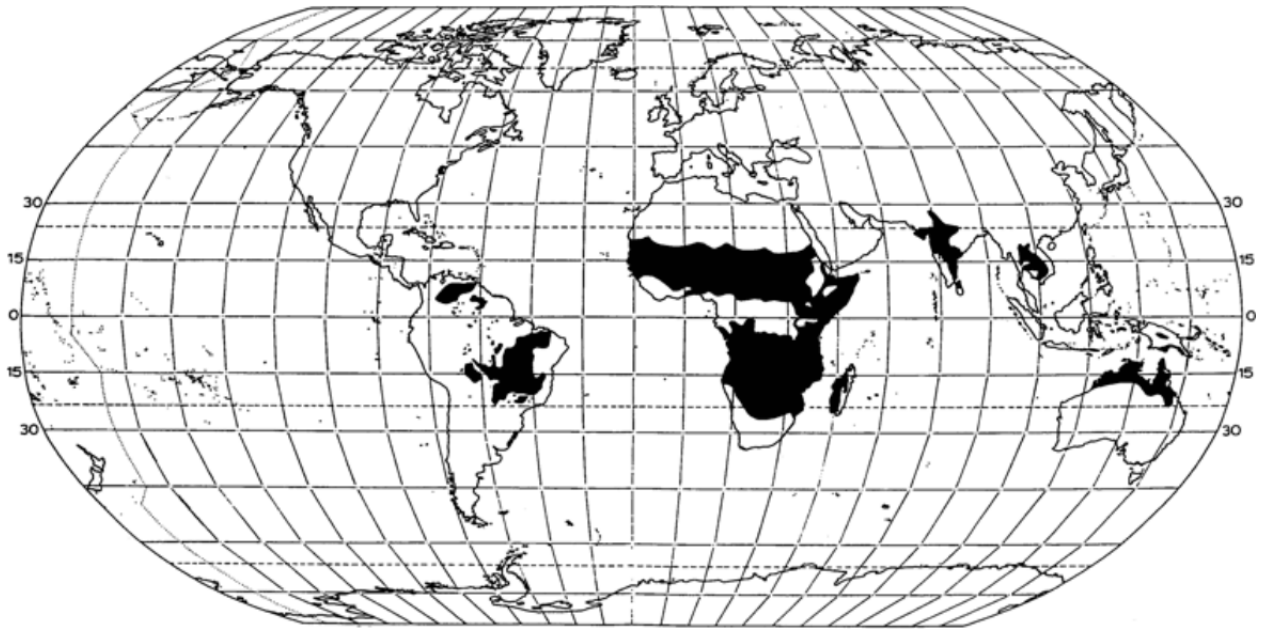
Figure 3.1: Global distribution of tropical savannas. Modified from Weller et al. (1998)

(a)

Grassland — Savanna — Forest

Max

Tree cover in absence of disturbance
Limited by
–water availability

Factors that can modify tree cover
e.g. fire, grazing, browsing

(b)

Max

Tree cover in absence of disturbance
Limited by
–Water availability
–Tree-on-tree
competition

Factors that can
decrease tree cover
e.g. fire, browsing

Tree cover %
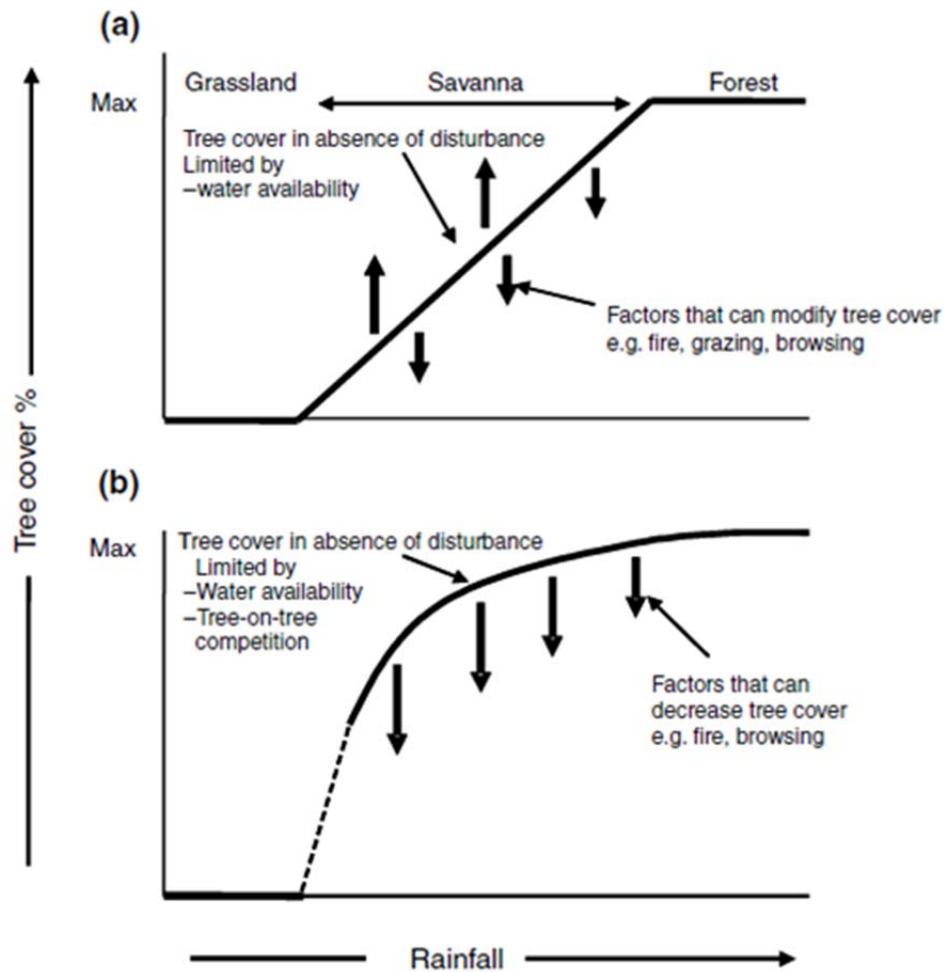
Rainfall

Figure 3.2: Predicted tree-grass ratios across rainfall gradients according to various competition based models: (a) root niche separation model and hydrologically-colonizing models, (b) balanced competition models. Solid line shows expected tree cover in absence of external perturbation and arrows indicate potential effect of disturbances on tree cover (Source: Shankaran et al., 2004, reproduced with permission from Wiley publication).
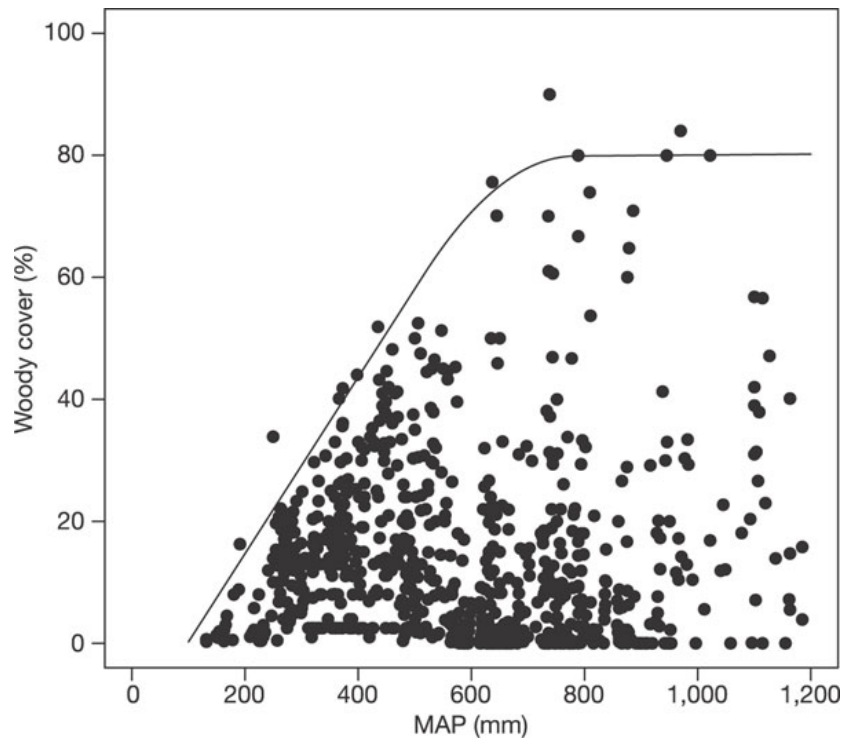
Figure 3.3: Results of a continental level study of changes in woody cover in African savannas as a function of mean annual precipitation. This plot shows the breakpoint of rainfall at which maximum tree cover is attained (Source: Shankaran et al., 2005, reproduced with permission from Nature publishing group).

Long-term exposure to herbivory and fire | Short-term protection from fire

Long-term exposure to herbivory and fire | Long-term protection from herbivory

Long-term exposure to herbivory and fire | Long-term protection from herbivory and short-term protection from fire
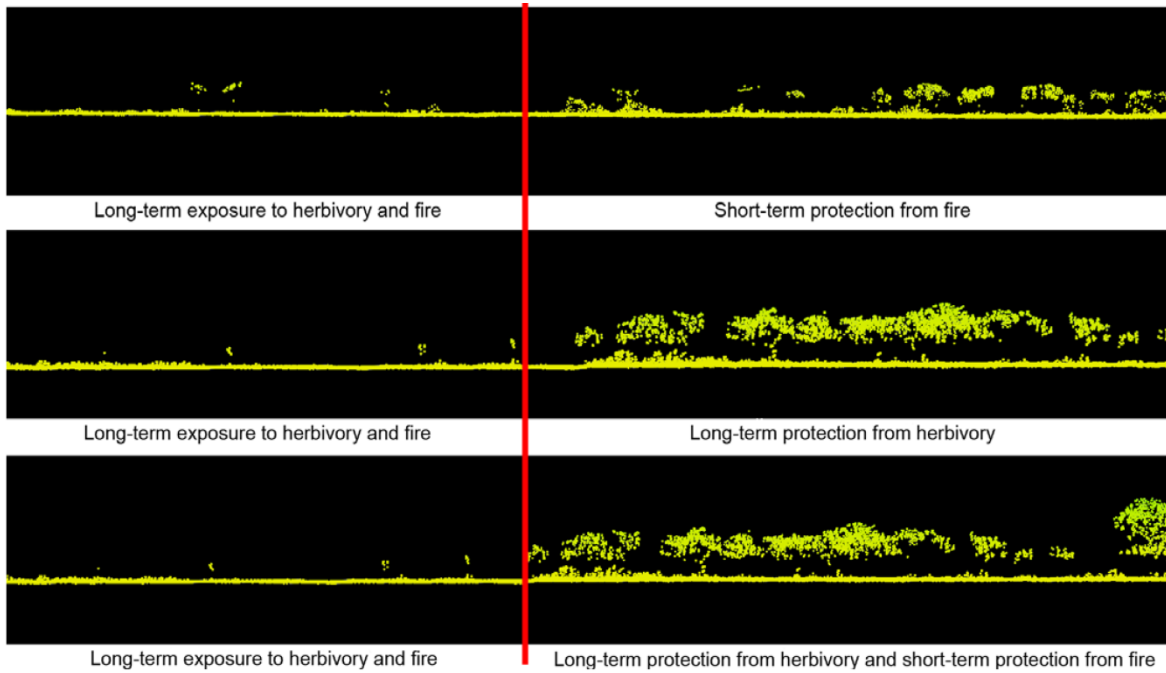
Figure 3.4: Cross-profile comparisons of the herbivore and fire experimental treatments and the control landscape. Profiles display the LiDAR point cloud of both ground surface and vegetation canopy returns. Solid redline marks the boundary between control and treatment sites (Source: Levick, et al. 2009, reproduced with permission from Elsevier Publishing).
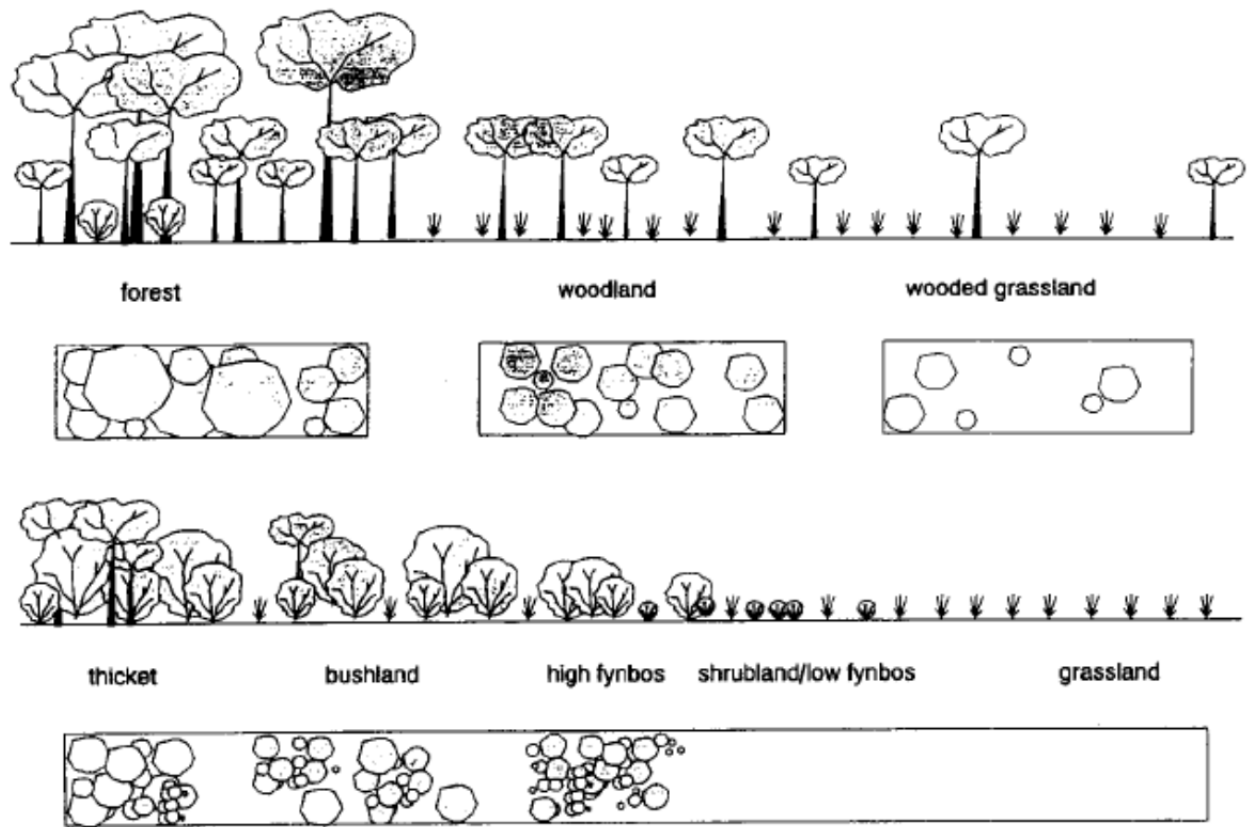
Figure 3.5: Schematic representation of physiognomic-structural components of land covers types in Southern African semi-arid savannas after Thomson (1996). The upper illustration shows the vertical layering system of the vegetation structure and the lower image visualizes the top view of different life forms, as measured by remotely sensed images. Reproduced with permission from the editor-in-chief, South African Journal of Science.
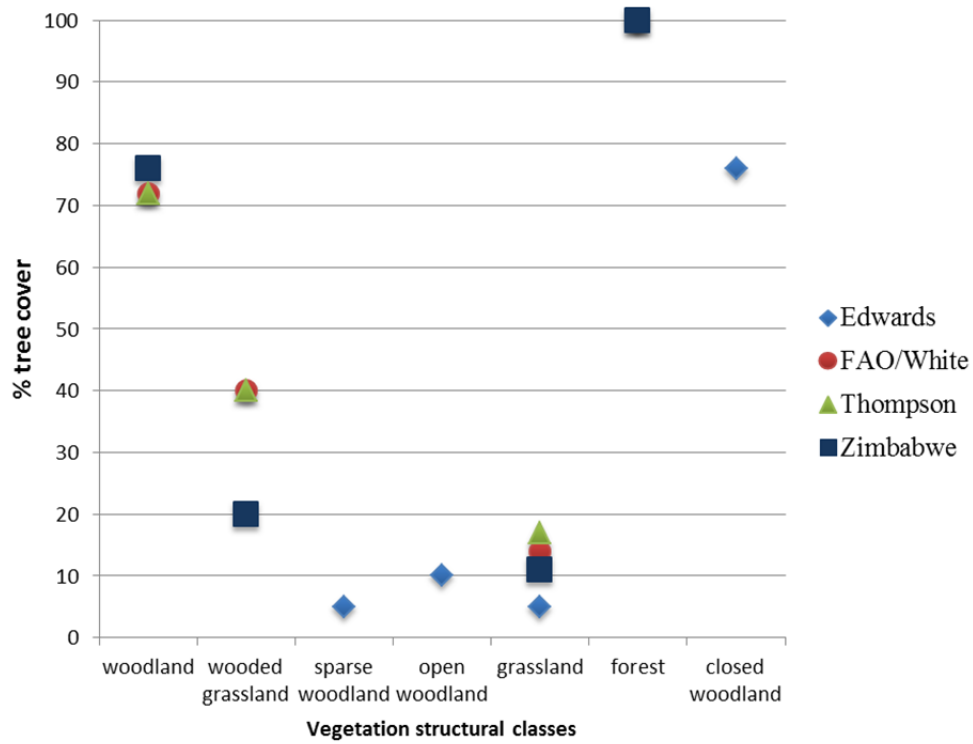
Figure 3.6: Comparison of four savanna vegetation classification schemes showing the class specific upper boundary definition of percent tree cover after Thompson (1996)

(a)
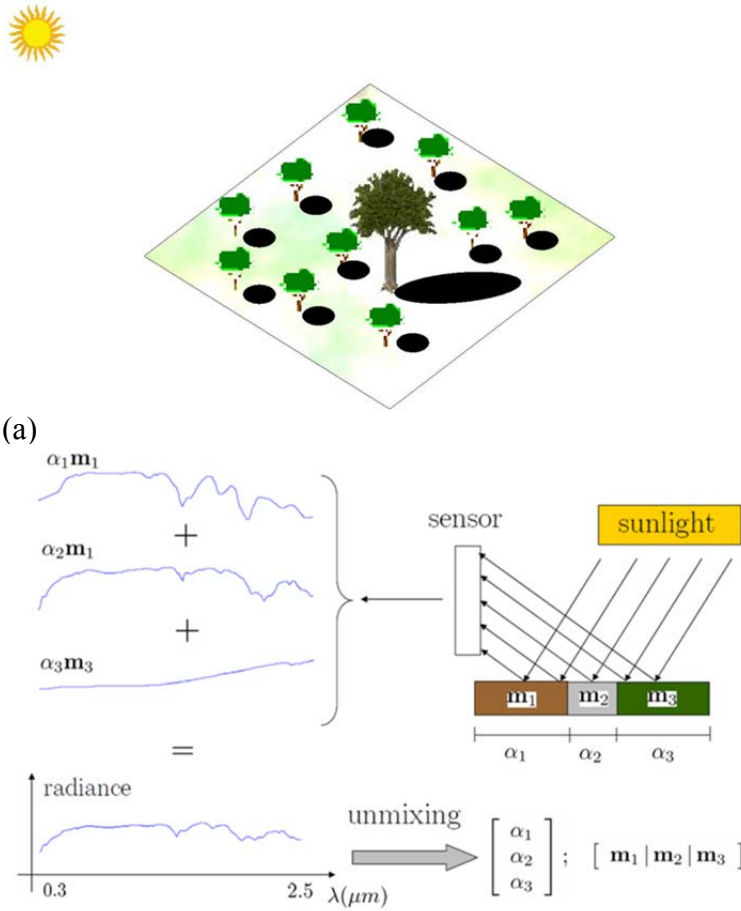
(b)

Figure 3.7: (a) Illustration depicting the solar illumination geometry used in remote sensing with sunlit and shaded parts of vegetation canopy as well as cast shadow, (b) a schematic representation where a pixels radiance is a linear mixture of three different endmembers and the processes of unmixing whereby this mixed spectrum is decomposed to drive endmember fractional cover estimate.
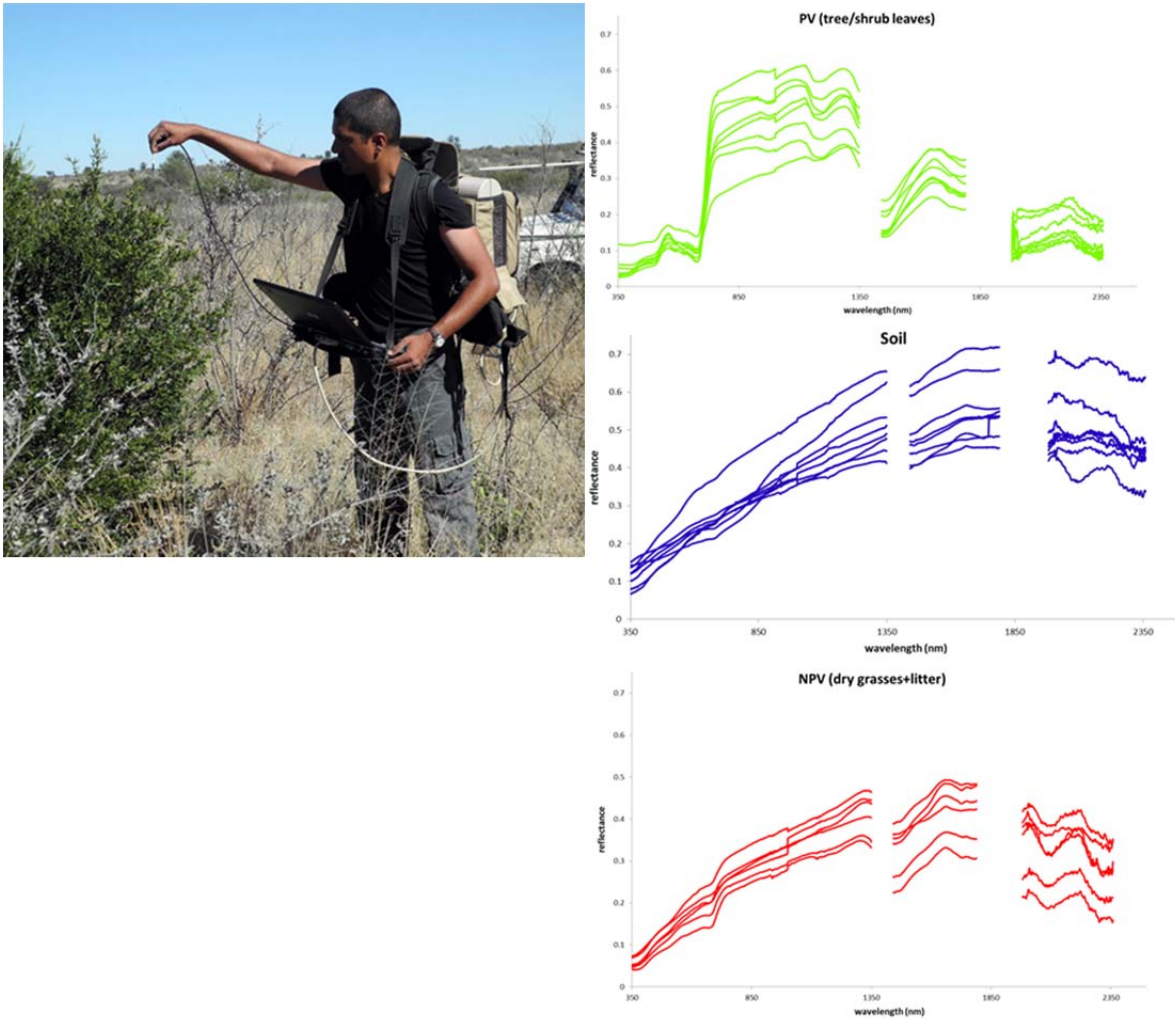
Figure 3.8: Collection of endmember spectra using a spectroradiometer in the field, also known as 'reference endmembers'. Some examples of resulting endmembers grouped according to plant/land cover functional properties are represented in the plots in the right column: green (photosynthetic vegetation), blue (soil) and red (non-photosynthetic vegetation).
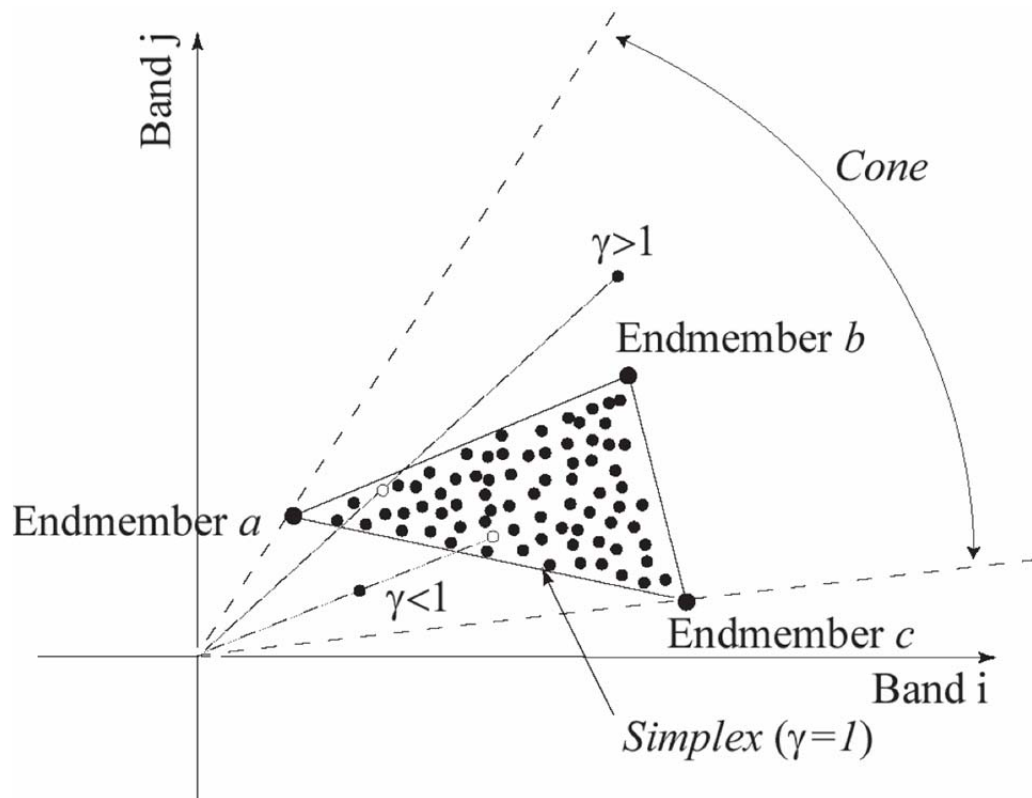
Figure 3.9: An example of geometrical approach of endmember section using a simplex. The illustration also shows the impact of topographic effects and resultant spectral variability due to which some outlier pixels can lie outside the simplex.
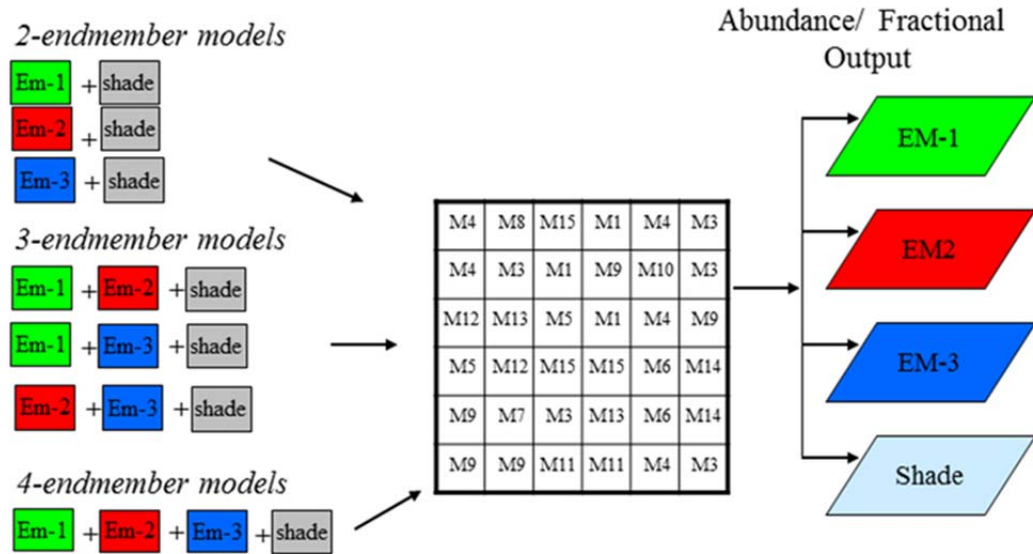
Figure 3.10: Schematic representation of the MESMA processes that allows both type and number of endmembers to vary on a per-pixel basis to produce sub-pixel abundance images (adapted from Rashed et al 2003).
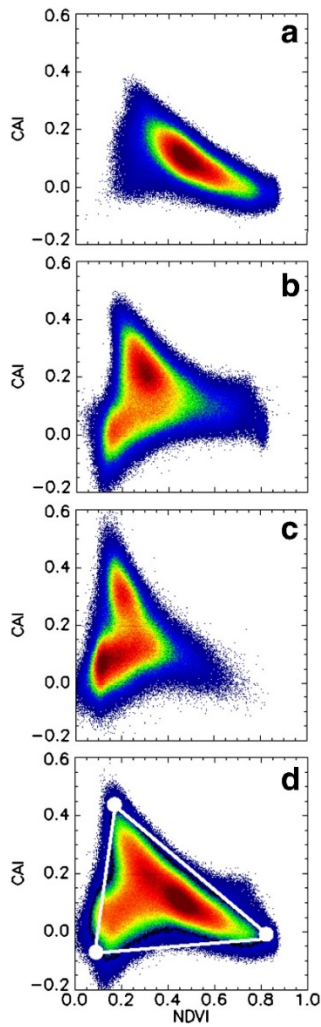
Figure 3.11: Selection of spectral endmembers for PV, NPV and soil using space defined by NDVI and CAI calculated from Hyperion images acquired at three different dates: (a) end of wet season, (b) middle of dry season (c) end of dry season and (d) all three dates combined. Color indicates density of samples and white dots indicates the position of endmembers in the NDVI-CAI space (source: Guerschman et al. 2009; reproduced with permission from Elsevier).
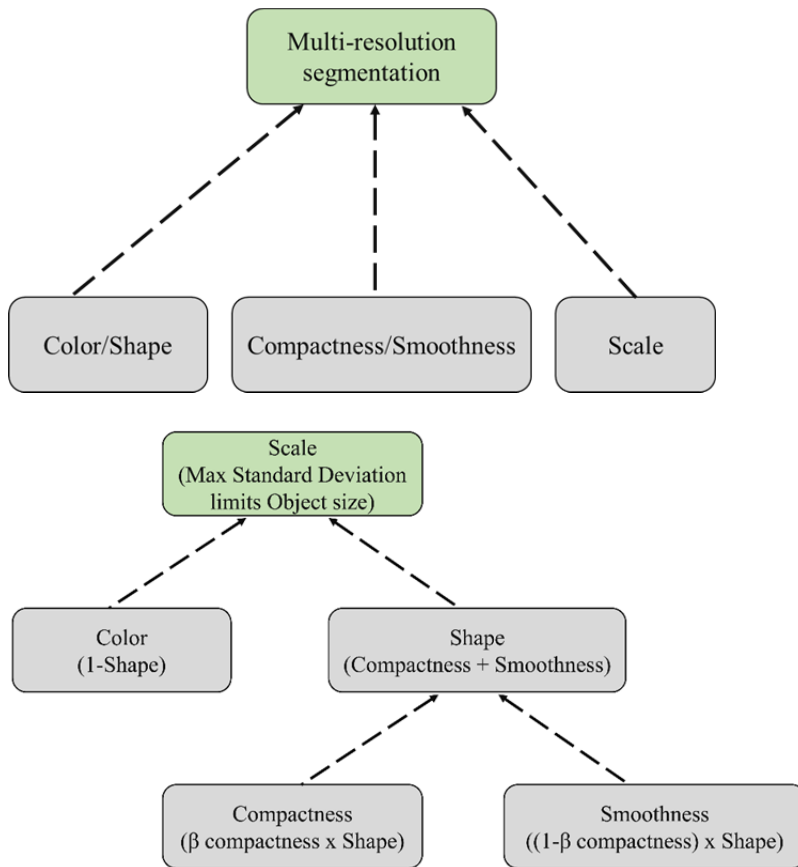
Figure3.12: Explanation of segmentation input parameters with eCognition Developer.
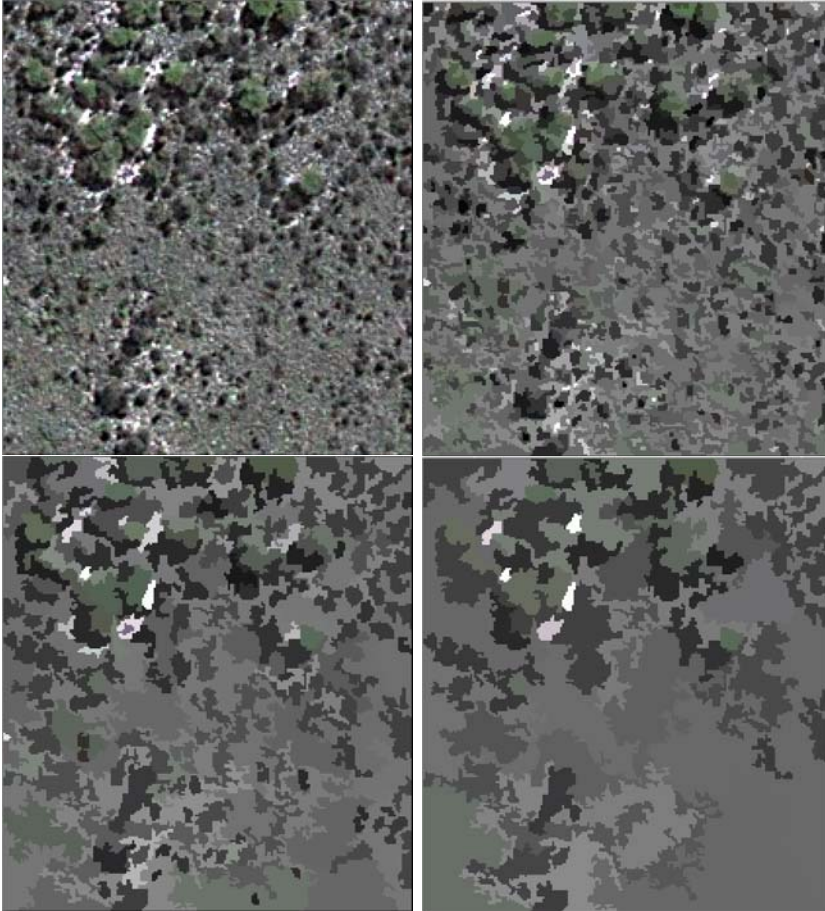
Figure 3.13: Illustration of changing object size with increasing scale factor in multiresolution segmentation output of a subset GeoEye-1 imagery from Central Kalahari in Botswana: a) original imagery true color subset b) segmentation scale:15 c) segmentation scale 30 and d) segmentation scale 50.
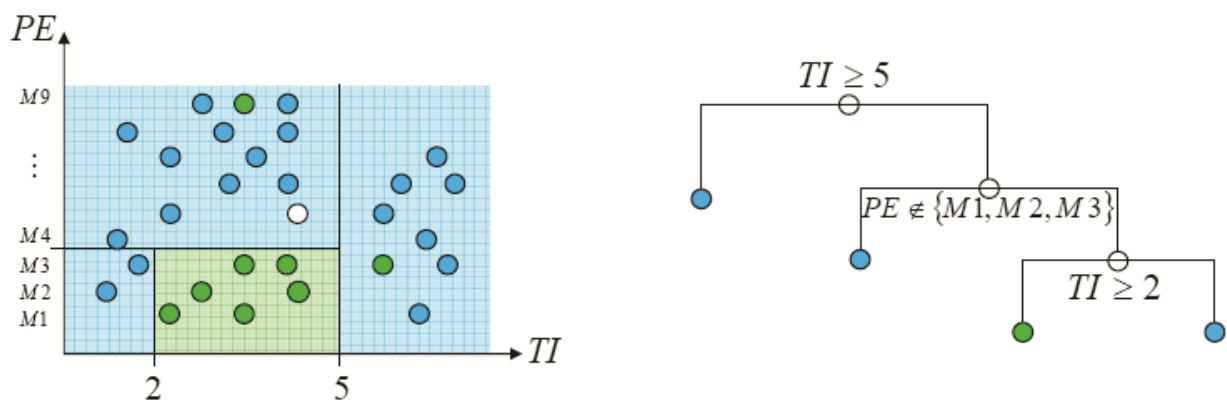
Figure 3.14: Example of a recursive decision tree showing the 'split' node and the 'terminal' node.

Method	Measurement basis	Reference
Visual estimate	Apparent area occupied by each cover type within a unit area.	Herrick et al. (2006) Bonham (1989)
Point intercept	The number of hits for each cover type at points along liner transect lines.	Herrick et al. (2006) Noss (1990)
Line intercept	The length/distance covered by each cover type along linear transect lines	Bonham (1989) Cottam and Curtis (1956)
Quadrat	Dominant cover within a quadrat or within each plot placed in the quadrat.	Bonham (1989)

Table 3.1: Different types of field sampling methods for characterizing vegetation properties used in previous studies.

Chapter 4: Estimating fractional land cover in semi-arid central Kalahari: The impact of mapping method (spectral unmixing versus object based image analysis) and vegetation morphology

Introduction

Savannas are geographically extensive ecosystems (nearly 40% of global terrestrial area and 50% of Africa) that are characterized by the unique coexistence of herbaceous and woody life forms (Hill et al. 2011a; Mistry 2000). In southern Africa, savanna ecosystems are both economically and ecologically significant containing large wildlife habitats and also provide the basis of economic activity by supporting livestock ranching and wildlife based tourism (Hill et al. 2011a; Lal 2004; Moore and Attwell 1999). Over the last few decades, due to increasing anthropogenic impact (e.g. changing land use, altered fire regime) coupled with climatic variability, vegetation structural and functional attributes in these xeric systems have been subject to large scale changes (Hill et al. 2011a; Scholes and Walker 1993). These changes are in turn affecting the ecological dynamics and availability of habitat related key structural properties (e.g. animal migration routes, solitary nesting trees and forging areas) (Blaum et al. 2007; Dougill et al. 1999; Tews et al. 2004).

Effective management of savanna ecosystems requires understanding the spatio-temporal variation in ecological processes. This understanding depends on our ability to accurately characterize and monitor the structural and functional attributes of savanna vegetation (e.g. vegetation cover, density, condition) (Mishra and Crews under review; Scholes and Walker 1993). In savanna ecosystems, vegetation cover is an important attribute that determines the ability of the system to capture rainfall. Thus, decreasing

104

vegetation cover is considered an important indicator of land degradation in savannas (Ludwig et al. 2007; Okin et al. 2009). Further, in these ecosystems the exchange of energy and water balance is controlled by transpiration and evaporation through the proportion of photosynthetically active vegetation (f_{PV}), non-photosynthetically active vegetation (f_{NPV}) and bare soil (f_{BS}) (Guerschman et al. 2009; Scanlon et al. 2005). Specially, in the semi-arid savannas, f_{NPV} is intimately related to fire frequency and intensity (Roy *et al.* 2011) and f_{BS} controls wind and water erosion (Okin et al. 2009). Field-based measurements of vegetation properties in savannas are limited in scope and scale, especially when considering systems that are vast, remote and wild. Remote sensing provides a tool for estimating fractional cover of vegetation as an indicator that can not only complement field measurements but also provide much larger spatial coverage (Asner et al. 2011; Elmore et al. 2000).

For estimating fractional land cover, linear spectral mixture analysis (SMA) is a popular technique that provides sub-pixel abundance estimates based on the assumption that the spectral signature of a pixel is a linear, proportion-weighted combination of endmembers (i.e., pure spectra of ground components) (Adams et al. 1995; Guerschman et al. 2009; Roberts et al. 1993). While the accuracy of SMA-derived fractional cover estimates depends highly on endmember purity, among other things, a single endmember model may fail to account for natural variability in the reflectance of endmembers. Multiple Endmember Spectral Mixture Analysis (MESMA) addresses this issue by allowing both the type and number of endmember models to vary on a per pixel basis (Asner and Lobell 2000; Roberts et al. 1998). MESMA has been widely utilized for

deriving fractional cover estimates in several ecosystems using medium spatial resolution (~20- 30 m) multispectral (e.g. Landsat/ASTER) and hyperspectral (AVIRIS/ EO-1 Hyperion) datasets (Asner and Lobell 2000; Elmore et al. 2000; Myint and Okin 2009; Powell et al. 2007; Roberts et al. 1998). Although MESMA of hyperspectral images has provided reliable estimates of fractional cover, it has produced modest results with multi-spectral imagery due to non-ideal bandwidth and spatial resolution (Asner and Heidebrecht 2002; Gill and Phinn 2008; Okin et al. 2001b). Besides spectral resolution, spatial resolution of imagery also impacts the accuracy of MESMA derived fractional estimates. This is especially important in the semi-arid savanna ecosystems marked by both high spatial heterogeneity and functional diversity in vegetation properties (Asner *et al.* 2011). Such heterogeneity can significantly limit the accuracy of bio-physical estimates derived from medium resolution multispectral imagery (e.g. Landsat) and may require data at a higher spatial resolution. More recently, the availability of high spatial resolution (i.e. < 2.5 m) multi-spectral datasets (e.g. GeoEye, Quickbird) presents new opportunities for testing their suitability for fractional land cover mapping in such heterogeneous areas. However, due to limited spectral dimensionality of high spatial resolution datasets very few studies have attempted such analysis (Hamada *et al.* 2011).

Since savanna ecosystems are considered patch dynamic systems (Meyer et al. 2009; Wiegand et al. 2006), mapping vegetation properties in savannas may benefit from Object Based Image Analysis (OBIA) (Blaschke 2010; Johansen et al. 2010; Laliberte et al. 2004). Based on OBIA, imagery is first segmented into objects representing relatively homogeneous group of pixels followed by sample selection and classification of

segments into classes of interest (Benz et al. 2004b; Blaschke 2010). Important OBIA advantages includes (i) treatment of landscape to be consisting of relatively homogeneous patches (or 'objects') is ecologically more suitable than arbitrarily imposed pixels (ii) landscape patches often depict scale dependency and based on OBIA, landscape objects can be generated at multiple segmentation scales that can provide added insight into ecological processes (Turner 2005) and (iii) OBIA approach offers the opportunity to add contextual, geometrical and texture related features (Kim *et al.* 2011). However, OBIA has not yet been extensively tested in natural landscapes where continuous variation in vegetation features makes it difficult to determine boundaries between 'objects'(Blaschke 2010; Yu et al. 2008). Further, in heterogeneous natural systems, landscape patches can vary in size, shape and structure that may require characterization at multiple spatial scales (Moustakas et al. 2009). Within the OBIA approach, 'segmentation scale' parameter used in segmentation controls the maximum allowable object level spectral heterogeneity and object size (Trimble 2011a). Segmentation scale is not prescriptive of the size (scale) of the resulting object, nor directly related to the resolution (scale) of the input data. It can more suitably be described as 'object complexity limit', but the term 'segmentation scale' is well established and so it is retained. Segmentation scale also affects the quality of segmented objects, which in turn, affects the classification accuracy (Addink et al. 2007; Yu et al. 2006). By manipulating the segmentation scale, nested objects of different size can be created that could be further hierarchically classified representing the output at multiple scales. While such hierarchical classification approach has been found suitable for characterizing spatially heterogeneous systems such as

107

wetlands (Dronova *et al.* 2012) and arid rangelands (Laliberte *et al.* 2004), its suitability for characterizing fractional cover in dry savanna systems merits further investigation. The objective of this study is to determine a better image analysis approach for estimating f_{PV}, f_{NPV} and f_{BS} in semi-arid savannas by comparing the suitability and limitations of MESMA and hierarchical OBIA approach against *in situ* obtained fractional cover estimates. The impact of vegetation structural and function heterogeneity on the accuracy of fractional cover derived using these two image analysis methods is also examined.

Study Area

This study was conducted in the semi-arid central Kalahari region of Botswana in southern Africa. The study area is approximately 17 km^2 and falls completely within a protected area (i.e. Central Kalahari Game Reserve) (Figure 4.1.a). The rainfall in the area is seasonal (between December-March) and the long-term annual average of precipitation amounts to 350 mm usually with high spatio-temporal variability (Makhabu et al. 2002; Scholes et al. 2002). Geologically, the area is dominated by Kalahari sand with sporadic outcrops of calcrete (Moore and Attwell 1999). Vegetation physiognomic properties in the study area is characterized by structurally heterogeneous mixture of woody and herbaceous species that exhibit temporally distinct phenological patterns (Figure 4.1.c). Notable broad-leafed species in the area includes *Lonchocarpus nelsii, Terminalia sericea, Bauhinia petersiana, Combretum hereroense, Croton gratissimu.* Important fine-leafed species are *A. erioloba, A. luederitzii, Ziziphus mucronata, Acacia mellifera, Acacia erubescens* (Moore and Attwell 1999). Vegetation boundaries based on plant species are often unclear since differences among vegetation communities is related

to changes in species dominance rather than occurrence of different species (Makhabu et al. 2002; Moore and Attwell 1999). Pan areas are geomorphologically different from other parts of the study area with flat topography and a high clay content soil. Pans are ecologically also important as they attract large herbivore and associated predators (Parris and Child 1973).

Data and methods

Field data collection and development of vegetation morphology classes

In situ data on fractional cover and vegetation morphological characteristics were acquired during the field campaign conducted in May 2012. Fractional cover of f_{PV}, f_{NPV} and f_{BS} were quantitatively estimated using a 30 m transect following the line intercept approach modified from Herrick et al. (2005). Each transect was divided into segments of 50 cm (total 60 segments within one transect) for which fractional cover of f_{PV}, f_{NPV} and f_{BS} was visually estimated and recorded. The fraction of each cover type was averaged from these 60 segments to get the f_{PV}, f_{NPV} and f_{BS} for every transect. Due to serious accessibility and safety issues (e.g. danger of predator attack), transects could not be established away from existing tracks. Field data were collected in 18 total transects spatially distributed across different vegetation morphology types. Geographic coordinates were recorded at the start and end points of each transect using global positioning system equipment. Additional information included visual estimation of dominant vegetation functional type (e.g. woody versus herbaceous), minimum, maximum and average vegetation height, dominant tree/shrub species, and pictures

acquired with a digital camera. Based on the analysis of field data, five vegetation morphology classes were developed mainly considering vegetation physiognomy, vertical and horizontal agreement, leaf type and phenology. These classes were (i) Mixed deciduous woodland with shrubs and herbaceous layer (Woodland), (ii) Mixed (70-40%) medium high shrubland with open short herbaceous layer (Open shrubland), (iii) Mixed (40-10%) medium high shrubland with open short herbaceous layer (Very open shrubland), (iv) Medium tall grassland with medium high shrubs (Grassland) and (v) Pans and bare areas (Pans) (Figure 4.1.c).

To avoid the influence of seasonality, field data on fractional cover were collected in the same month as image acquisition (i.e. May). In spite of the 2 year temporal difference between image acquisition and *in situ* data collection, this study could directly compare them because of the following evidence: (i) the study area lies completely inside a protected area and does not have any anthropogenic influence, (ii) due to low animal density the grazing impact from herbivores is very minimal. Although, spatio-temporal pattern of rainfall in the central Kalahari is highly variable, in this study there are no means to quantify this because the nearest meteorological station (i.e. Maun) is about 150 km north of the study area.

Remotely sensed imagery and pre-processing

This study utilized multispectral GeoEye-1 imagery consisting 2-m blue, green, red and near-infrared bands acquired on May 16, 2010 at 10:46 local time (08:46 UTC). In the central Kalahari, May represents the beginning of the dry season when trees and

shrubs are still green whereas herbaceous vegetation contained no observable green biomass. Surface reflectance was derived by radiometrically calibrating the imagery using ATCOR algorithm. ATCOR is an absolute atmospheric correction method that applies an atmospheric look-up table based on a large database containing the result of radiative transfer calculation from the MODTRAN-4 radiative transfer code (Richter and Schläpfer 2008). The optical depth of the atmospheric aerosols was calculated by comparing modeled at-sensor radiance with measured radiance in the red band of areas with dark dense vegetation. This correction was then applied on each pixel to derive surface reflectance. As an additional feature Normalized Difference Vegetation Index (NDVI) was derived from the calibrated imagery.

Multiple Endmember Spectral Mixture Analysis (MESMA)

The objective of MESMA analysis was to derive sub-pixel estimates of f_{PV}, f_{NPV} and f_{BS} from the GeoEye imagery. NDVI calculated from the GeoEye imagery was found to be weakly correlated with the red band ($R^2 = 0.41$) and very weakly correlated with the NIR band ($R^2 = 0.12$). Thus, the NDVI was considered as a nonlinear combination of red and NIR bands and was stacked with the existing GeoEye bands before endmember selection and MESMA analysis. Endmembers correspond to the spectra of spectrally pure materials and the goal of endmember selection process is to isolate such pure pixels by utilizing qualitative and/or quantitative purity measures. In this study endmember candidates were first selected based on: (i) pixel purity index (PPI) values, (ii) visualization of the multidimensional feature space plots and spectral indices values (Bateson and Curtiss 1996; Plaza et al. 2004). These candidate spectra were analyzed

quantitatively using three fit matrices: Endmember Average RMSE to select endmembers that produced the lowest RMSE within a class (Dennison and Roberts 2003), Minimum Average Spectral Angle that isolates endmembers with the lowest average spectral angle (Dennison *et al.* 2004) and Count Based endmember selection (Roberts *et al.* 2003). Finally, for PV, NPV and soil six, eight and six endmembers were selected respectively (Figure 4.2).

MESMA was performed using the VIPER tools (www.vipertools.org) program which is a free add-on to ENVI image processing software. Non-shade endmember fraction was calculated using singular value decomposition and shade was calculated as 1 minus the sum of all non-shade endmember fractions. Three model schemes (two-, three- and four- endmembers) were tested for each pixel (Table 4.1). MESMA was partially constrained with minimum and maximum allowable non-shade fractions and the $RMSE_S$ threshold set to -0.05, 1.05 and 0.025 respectively. Here $RMSE_S$ refers to the root mean square error or the model residual used to access the model fit. For choosing the best mixing model for each pixel, first, the model producing the lowest $RMSE_S$ was selected as the best model for each pixel at each model complexity level. In the second step, output composites of two-, three- and four- endmember models were compared. Since a three-endmember model will always produce a lower $RMSE_S$ than a two-endmember model (same for four versus three-endmember model results) the following criteria was adopted for their comparison: (i) if a three-endmember model had a lower $RMSE_S$ than a two-endmember model and the three-endmember model exceeded a predefined threshold of decreased $RMSE_S$ (0.007, determined empirically in this study similar to Powell and

112

Roberts 2008), then the three endmember model was considered superior; otherwise, the two-endmember model was selected as superior. (ii) if a four-endmember model had a lower $RMSE_S$ than the best three-endmember model and the four-endmember model exceeded the same threshold then the four-endmember model was selected; otherwise the three-endmember model was considered superior. MESMA obtained fractional cover estimates were shade normalized where the shade fraction from the results was taken out by dividing the fraction of each non-shade endmember by the sum of non-shade endmembers.

Object Based Image Analysis

The objective of object based analysis was to derive estimates of f_{PV}, f_{NPV} and f_{BS} from the GeoEye-1 imagery. To implement object based classification, first, the raster stack (4 GeoEye bands and NDVI) was segmented using the multiresolution segmentation algorithm in eCognition Developer 8 software (Trimble 2011b). Compared to other segmentation approaches, the multiresolution segmentation allows construction of objects of different sizes and enhances the response of object generation to landscape patch structure (Arbiol et al. 2006; Baatz and Schäpe 2000b). Due to spatial and structural heterogeneity in the study area, meaningful spectrally homogeneous objects can occur at different spatial scales (Arbiol *et al.* 2006). Additionally, it was expected that optimal patch size would vary depending on vegetation physiognomy. Hence, objects were generated at five segmentation levels at scale values 1, 2, 4, 6 and 8 (Figure 4.3). The other required segmentation parameters, shape and compactness were kept at a constant value of 0.2 and 0.4 respectively (Table 4.2). These values were selected as

113

optimal, based on visual comparison of the results of several iterative segmentation runs. The input imagery bands were given equal weight while the NDVI was given higher weight compared to other inputs. For classification at each segmentation scale, training objects were selected by visual interpretation.

For the selection of optimal classification features, initially 42 spectral, shape, texture and geometrical features were selected to include a sufficiently wide range. First, Spearman's rank correlation analysis was utilized to eliminate features with correlation coefficients above 0.9. Seventeen features were found to have correlations below this threshold value. The selection of the best features from these was based on Jeffrey's-Matusita distance (JM distance) calculated using the SEATH tool (Marpu et al. 2008; Nussbaum et al. 2006). This study calculated the largest average JM distance (the mean of all two class combinations) for every possible 12-17 feature combination. Combination with lesser number of features always had a lower JM distance compared to combinations with more features and selecting the lowest mean JM distance for the 11 candidates was deemed unsuitable. Hence, the feature combination that resulted in the largest JM distance for the least separable pair of classes was selected which is also an approach followed in previous studies (Laliberte et al. 2012; Swain and Davis 1978). This approach resulted in the final selection of 13-17 features depending on the segmentation scale factor (Table 4.3). Final classification at each of the segmentation scales was performed using these optimal features and object samples for each class using the nearest neighbor classification technique within eCognition.

Fractional cover validation/spatial association with vegetation morphology classes

In this study, *in situ* derived fractional cover estimates were first used to evaluate the accuracy of estimates derived from both MESMA and OBIA approaches. For this purpose, the fractional estimates of each 30 m transect were compared with the shade normalized mean f_{PV}, f_{NPV}, f_{BS} of spatially coincident 225 pixels (15 x 15 pixel window) equivalent to the transect length. Root mean square error ($RMSE_C$) was used as the error metric and was calculated based on considering *in situ* derived estimates as observed and MESMA and OBIA derived estimates as predicted estimates. The subscript "c" (as opposed to subscript "s" used above) refers to the root mean square error calculated in the comparison of cover estimates. However, due to the limited number of field transects (n=18) there was need for additional evaluation. Both qualitative and quantitative evaluation of results suggested that MESMA produced reliable fractional estimates than OBIA. Hence, as a second evaluation step, MESMA derived estimates were used to evaluate the OBIA derived fractional estimates obtained at the five different segmentation scales. For this purpose, a total of 214 grid cells each covering 30 x 30 m area (225 pixels) were created and their shade-normalized mean f_{PV}, f_{NPV}, f_{BS} derived from MESMA and OBIA were compared. Results were first evaluated by considering all 214 samples together to access overall agreement and then by grouping samples based on their vegetation morphology for examining their spatial association.

Results

Field versus MESMA and OBIA derived estimates

Fractional estimates derived *in situ* and those estimated for corresponding areas from MESMA and OBIA of imagery are plotted in figure 4.4. Comparison of *in situ* transect derived fractional estimates with those obtained from MESMA and the hierarchical OBIA approach depicted that MESMA produced a lower error for all ground cover component types compared to OBIA derived estimates (i.e. overall $RMSE_C$: 6.2%) (Table 4.4). Furthermore, based on the OBIA approach, the lowest error in fractional cover estimates were obtained at the finest segmentation scale (i.e. scale=1, overall $RMSE_C$ 8.6%) and with increasing segmentation scale, error increased consistently for all ground cover component types reaching the highest value at the segmentation scale value of 8 (i.e. overall $RMSE_C$: 22.9%) (Table 4.4). MESMA derived fractional cover estimates also showed cover specific differences in estimation accuracy as f_{PV} could be estimated with lower error (i.e. $RMSE_C$: 5.1%) compared to f_{NPV} and f_{BS} ($RMSE_C$: 7.1% and 7.4% respectively). Based on OBIA, similar cover specific differences in fractional cover estimation accuracy were observed at the finest segmentation scale (f_{PV} $RMSE_C$: 7.6% versus f_{BS} $RMSE_C$: 10.6%). However with the increasing segmentation scale in OBIA, these cover specific differences became indistinguishable as the estimation error increased consistently reaching a maximum value at the segmentation scale value 8 (Table 4.4).

116

MESMA versus OBIA derived fractional estimates: Agreement across vegetation morphology types

The results of fractional cover mapping based on the MESMA and hierarchical OBIA approach for the five different regions of the study area with different vegetation morphology types is shown in figure 4.5. Evaluation of OBIA derived fractional cover estimates considering MESMA results as observed estimates depicted several interesting results that are reported in Table 4.5. Based on OBIA, fractional estimates derived at the finest segmentation scale (i.e. value 1) produced the lowest overall error (i.e. $RMSE_C$ 7.7%) as well as the lowest cover specific error in fractional cover (Table 4.5.f). With increasing segmentation scale value, error in fractional cover estimation increased consistently. Furthermore, analysis of the results by grouping samples based on the vegetation morphology type showed that observed sensitivity of hierarchical OBIA results were also vegetation morphology specific. For all vegetation morphology classes, the lowest error in fractional cover estimates was achieved at the finest segmentation scale (segmentation scale =1). However, even at the finest segmentation scale, estimation accuracy varied depending on morphology type. For example, fractional estimates in areas representing vegetation morphology class 1 and class 2 were mapped with low error (overall $RMSE_C$ 4.2% and 5.1 % respectively) (Table 4.5.a and 4.5.b) compared to areas under morphology class 4 or 5 that showed higher error (overall $RMSE_C$ 10.4% and 11.6% respectively) (Table 4.5.d and 4.5.e). Furthermore, with increasing segmentation scale, different vegetation morphology types showed different responses in terms of fractional cover estimation accuracy. Areas under vegetation morphology class 1 were

117

less sensitive to changing segmentation scale and fractional cover estimation error was comparatively lower for these areas even at coarser segmentation scales (i.e. overall RMSE$_C$ at segmentation scale 8: 10.2%). On the contrary, areas under vegetation morphology class 4 and 5 were more sensitive to changing segmentation scale as the increase in the magnitude of estimation error was much higher at higher segmentation scale value (e.g. for class 4 and class 5 the overall RMSE$_C$ at segmentation scale 8: 32.1% and 21.3 respectively).

Discussion

Field versus MESMA and OBIA derived estimates

Results of this study suggest that when compared to *in situ* derived estimates, MESMA produced lower error than OBIA for fractional cover estimation in the semi-arid central Kalahari savanna. These results could be explained in light of how the image analysis approaches compared in this study (i.e. MESMA versus OBIA) represent and model the inherent structural and functional heterogeneity in semi-arid systems as captured by the GeoEye-1 imagery. Due to its high spatial resolution, GeoEye-1 imagery is able to distinguish individual tree/shrub canopies and also captures intra and inter canopy details e.g. sunlit versus shaded areas, green versus senescent foliage (Wulder et al. 2009). Given the high spatial heterogeneity in the study area, mixtures of different cover types (especially of NPV and soil) can exist even within a GeoEye-1 pixel. The MESMA approach attempts to account for this fine scale heterogeneity and provides sub-pixel abundance estimates by modeling a pixel's spectral response as a linear combination of considered endmember types. In heterogeneous savanna systems the

118

potential of non-linear mixing is higher at higher spatial resolution compared to lower spatial resolution. The endmembers used for MESMA analysis were thoroughly tested using both qualitative and quantitative purity measures. Using these pure and representative endmember spectra that were allowed to vary in number and type on a per-pixel basis, all pixels of the GeoEye-1 imagery could be modeled within 2.5 percent RMSEs and producing accurate fractional cover estimates. Qualitative assessments of MESMA derived fractional estimate against photo acquired at transect location showed good correspondence. Due to its high spatial resolution the input GeoEye imagery could be used for qualitative assessment which also depicted good agreement across all vegetation morphology types. Unlike MESMA, the OBIA approach considers the landscape to be consisting of relatively homogeneous objects. At the finest segmentation scale used in this study (i.e. scale value 1), an average object consists of nearly the size of a single GeoEye-1 pixel and with increasing segmentation scale the object size (and the number of pixels within an object) increases (as depicted in table 4.2). In this study, OBIA results at the finest segmentation scale produced a lower estimation error because it better represented the landscape heterogeneity compared to higher segmentation scale derived estimates. Increasing segmentation scale value under OBIA resulted in a larger object size (Figure 4.3) that is an oversimplified representation of landscape heterogeneity. Classification of these larger objects produced a much higher estimation error compared to both OBIA results at finer segmentation scale as well as MESMA derived estimates.

119

MESMA versus OBIA derived fractional estimates: Agreement across vegetation morphology types

The results of this study found that variations in savanna vegetation morphological properties impact fractional cover estimation accuracy. The varying sensitivity in the fractional cover estimation accuracy of different vegetation morphology types to OBIA segmentation scale could be explained by the varying patch sizes of savanna vegetation in the central Kalahari. Patch is the basic element of landscape structure and can be defined as an ecologically homogeneous unit. Patches are homogeneous at a particular scale and can become heterogeneous at increasingly coarser scales (Kotliar and Wiens 1990). Patch size in savanna systems has been found to be closely associated with vegetation physiognomic properties (Meyer *et al.* 2009). Area dominated and co-dominated by woody life forms (i.e. trees and/or shrubs) (e.g. woodlands and open shrublands) have larger patch sizes compared to areas that are dominated by herbaceous components (e.g. grasslands, very open shrublands) (Figure 4.1.c). Thus, due to their larger patch size, areas under woodlands and open shrublands (i.e. morphology class 1 and 2 respectively) produce homogeneous objects in terms of ground cover components at both small and large segmentation scale values and yield more accurate fractional estimates. On the contrary, grassland and very open shrubland areas (i.e. morphology class 4 and 3) have a much smaller patch size. In these areas, homogeneous objects are created only when image segmentation is performed at a fine segmentation scale resulting in small objects. At high segmentation scale values, image objects for these areas have more than one ground cover component (e.g. mixture of f_{NPV}

and f_{BS}). The classification result of these large and comparatively mixed objects results in a high error in fractional cover when compared to either *in situ* or MESMA derived estimates. These results underscore that besides the mapping method, the understanding of spatial and structural heterogeneity is also important in semi-arid savanna systems. To a certain extent, vegetation structure/land cover characteristics in the study area can be treated as representative of other naturally occurring semi-arid savanna systems found in southern Africa (Dougill *et al.* 1999) and tropical savannas in other parts of the world (e.g. Australia, South America). Thus, these results have several implications for future studies focusing on characterization and monitoring of semi-arid savanna systems using combined *in situ* data and high spatial resolution imagery. Future studies utilizing high resolution imagery for quantifying ecosystem related functional properties (e.g. fractional cover) in savannas should select the image analysis approach considering the structural/functional heterogeneity of the study area.

There are some sources of uncertainty in the data and method utilized in this study. The temporal difference between field data collection (i.e. May 2012) and image acquisition (i.e. May 2010) is likely to reduce the accuracy of imagery derived estimates to some extent as vegetation dynamics in central Kalahari is affected by spatio-temporal variability in rainfall (Scanlon et al. 2005; Scholes et al. 2002). Additionally, the visual separation of f_{PV} and f_{NPV} in the field was difficult and subjective to some extent. Thus, even with best efforts and careful interpretation, *in situ* derived fractional estimates contain some unquantifiable observer error. Furthermore, MESMA assumes linearity in the mixing of endmember spectra. However, in semi-arid systems complex vegetation

structure leads to non-linear mixing that may limit the accuracy of MESMA to a certain extent (Okin and Roberts 2004).

Conclusions

This study compared absolute estimates of f_{PV}, f_{NPV}, f_{BS} derived *in situ* and from GeoEye-1 imagery based on MESMA and OBIA approach to examine the comparative suitability of these methods. Comparison of analysis methods of remote sensing imagery is informative. Given the same input imagery comparison of results from different methods provides information on the inherent limitations among methods, regardless of *in situ* data. We also analyzed the association of results obtained from these methods with vegetation morphology types in the study area. Our results show that in the xeric central Kalahari, MESMA of GeoEye-1 imagery produced more accurate fractional cover estimates compared to hierarchical OBIA approach. Notably, OBIA results at the finest segmentation scale were close to field estimates as well as MESMA derived estimates. The sub-pixel analysis approach of MESMA was able to represent the spatial heterogeneity in semi-arid central Kalahari better than the OBIA approach. However, an important limitation of MESMA is the high computational time and computing resources required due to the large volume of high spatial resolution imagery making it less suitable for landscape or regional scale applications. Nonetheless, MESMA results for strategically selected representative sample areas could be used to validate results derived using coarse spatial resolution data that provide large spatio-temporal coverage but might be less accurate. While field data is critical for evaluating remote sensing methods, it also has inherent errors and its acquisition, especially in remote areas can be highly limited

122

due to logistical and safety issues. Due to the limited number of field transects, this study used MESMA derived fractions to validate OBIA results. The fine spatial detail provided by high spatial resolution imagery and its automated analysis using MESMA has the potential to substitute the requirement of field data to some extent and thus serve as a pragmatic approach for accurately characterizing savanna ecosystems.
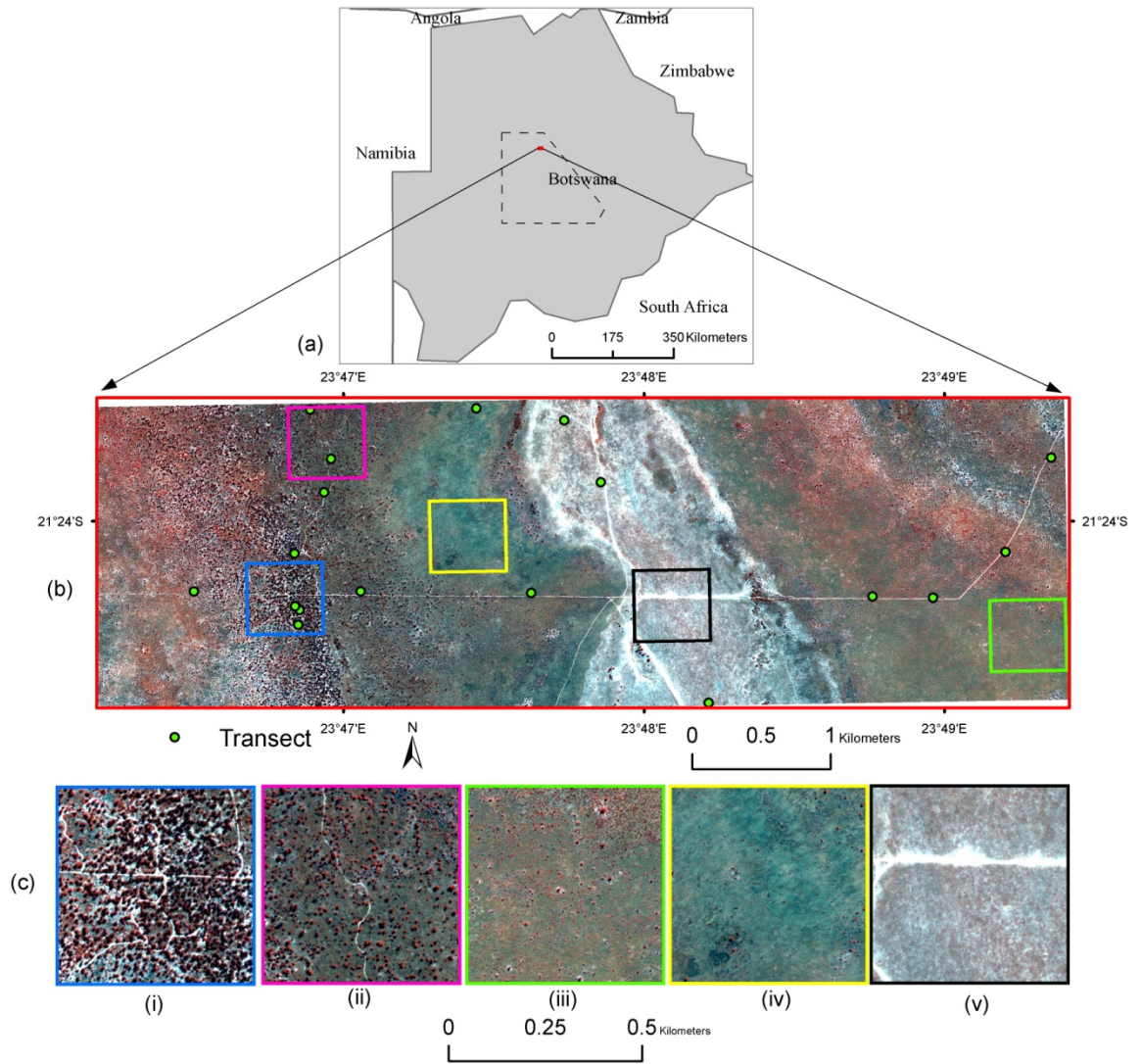
Figure 4.1: Location of study area within the central Kalahari of Botswana in Southern Africa, (b) study area as seen from GeoEye-1 imagery (RGB:421), (c) enlarged parts of the study area depicting different vegetation morphology types: (i) woodland, (ii) open shrubland, (iii) very open shrubland, (iv) grassland and (v) pan.
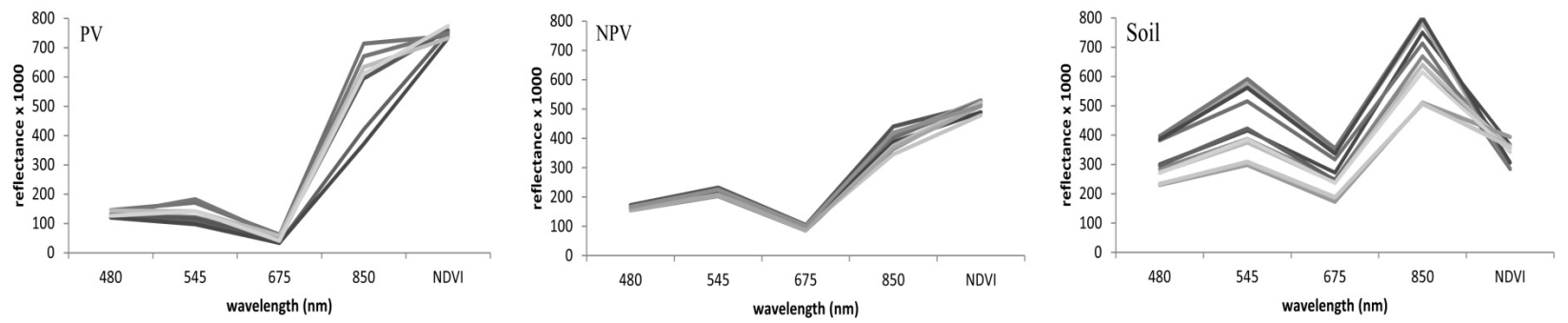
Figure 4.2: Spectral profile of endmembers used for MESMA analysis in this study.
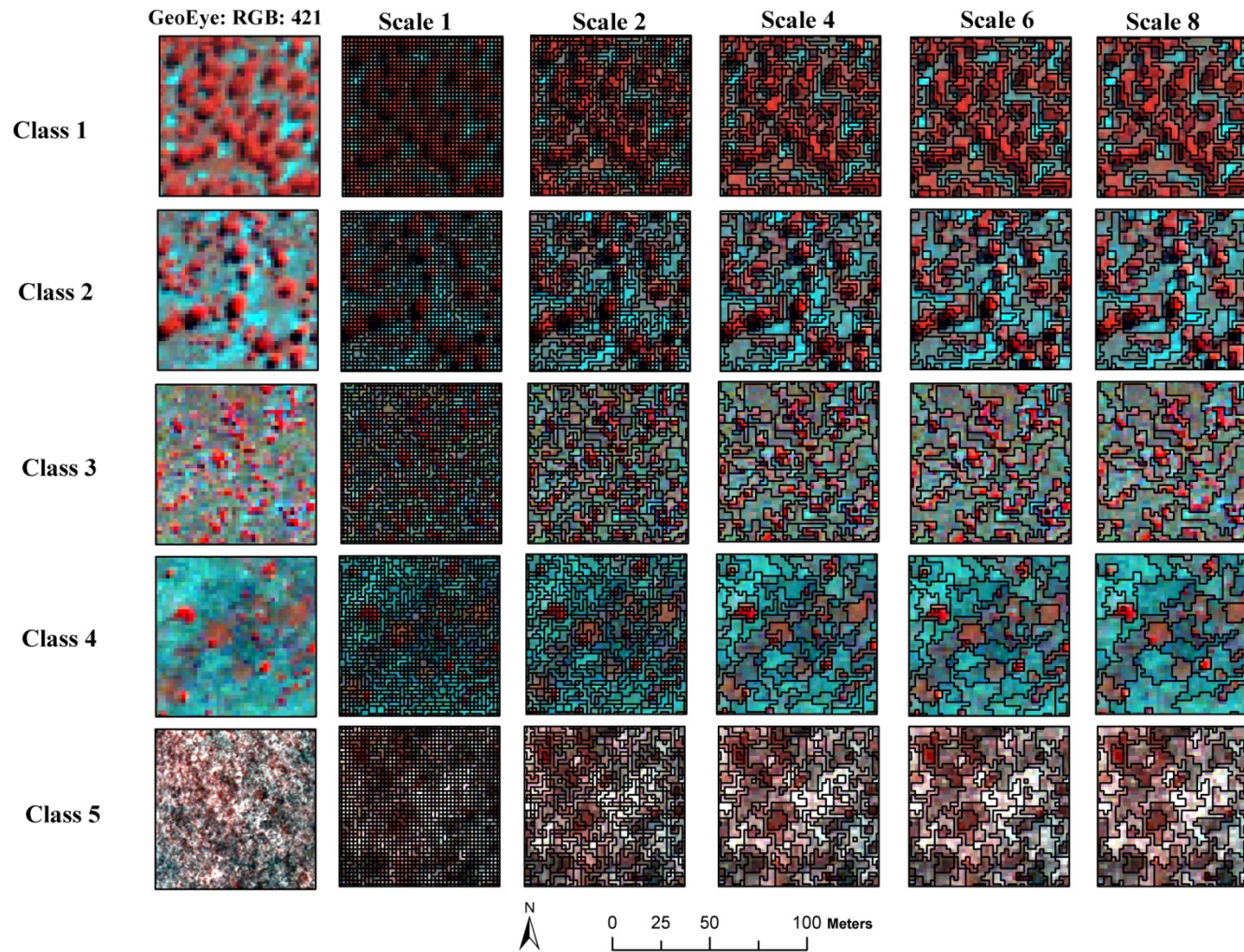
Figure 4.3: Illustration of how optimal segmentation scale following OBIA approach varies for different

vegetation morphology types in the semi-arid central Kalahari.

126
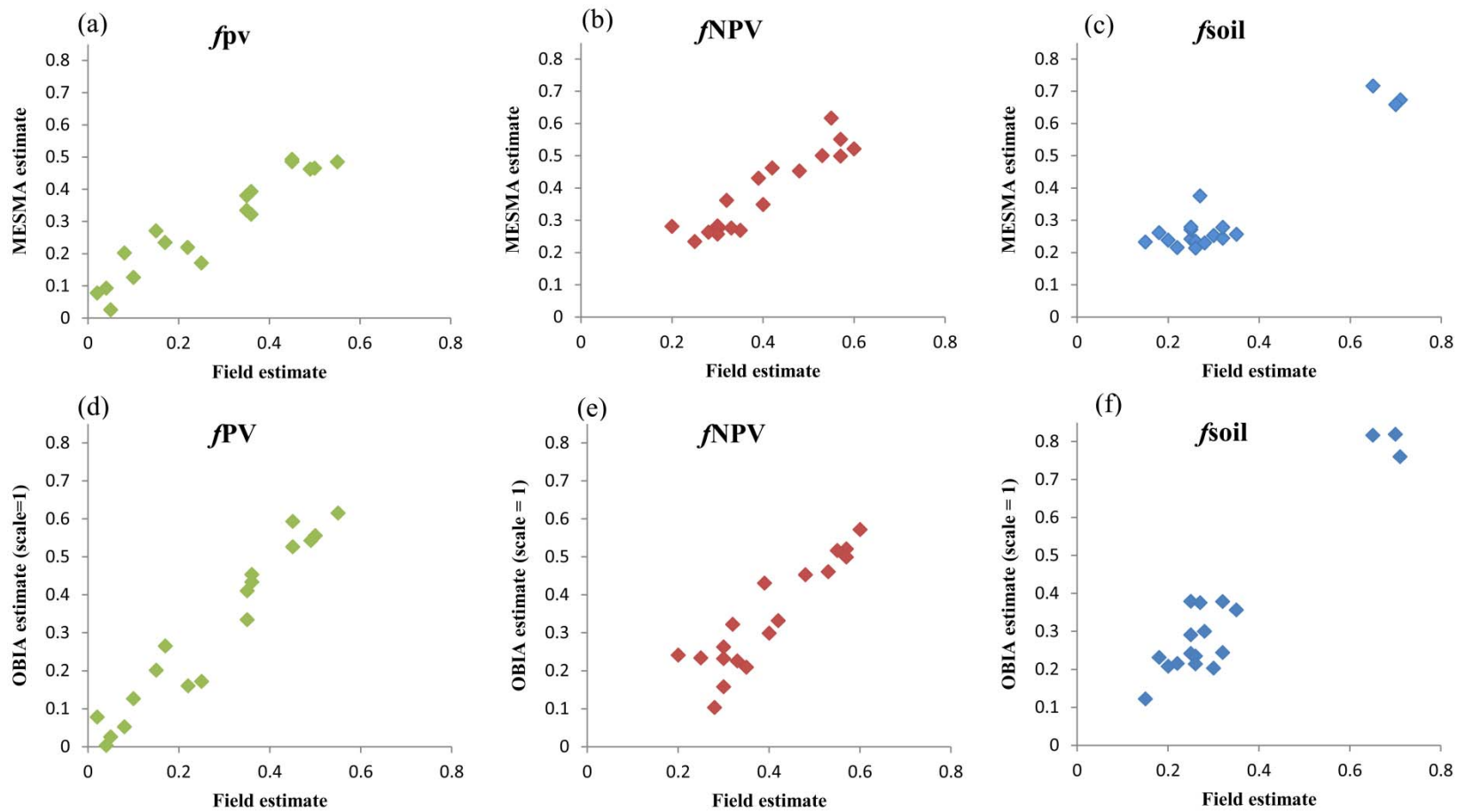
Figure 4.4: Comparison of field estimated fractional cover of *fPV*, *fNPV* and *fBS* against those estimated from MESMA and OBIA. The OBIA fractional estimates presented here were derived at segmentation scale value.
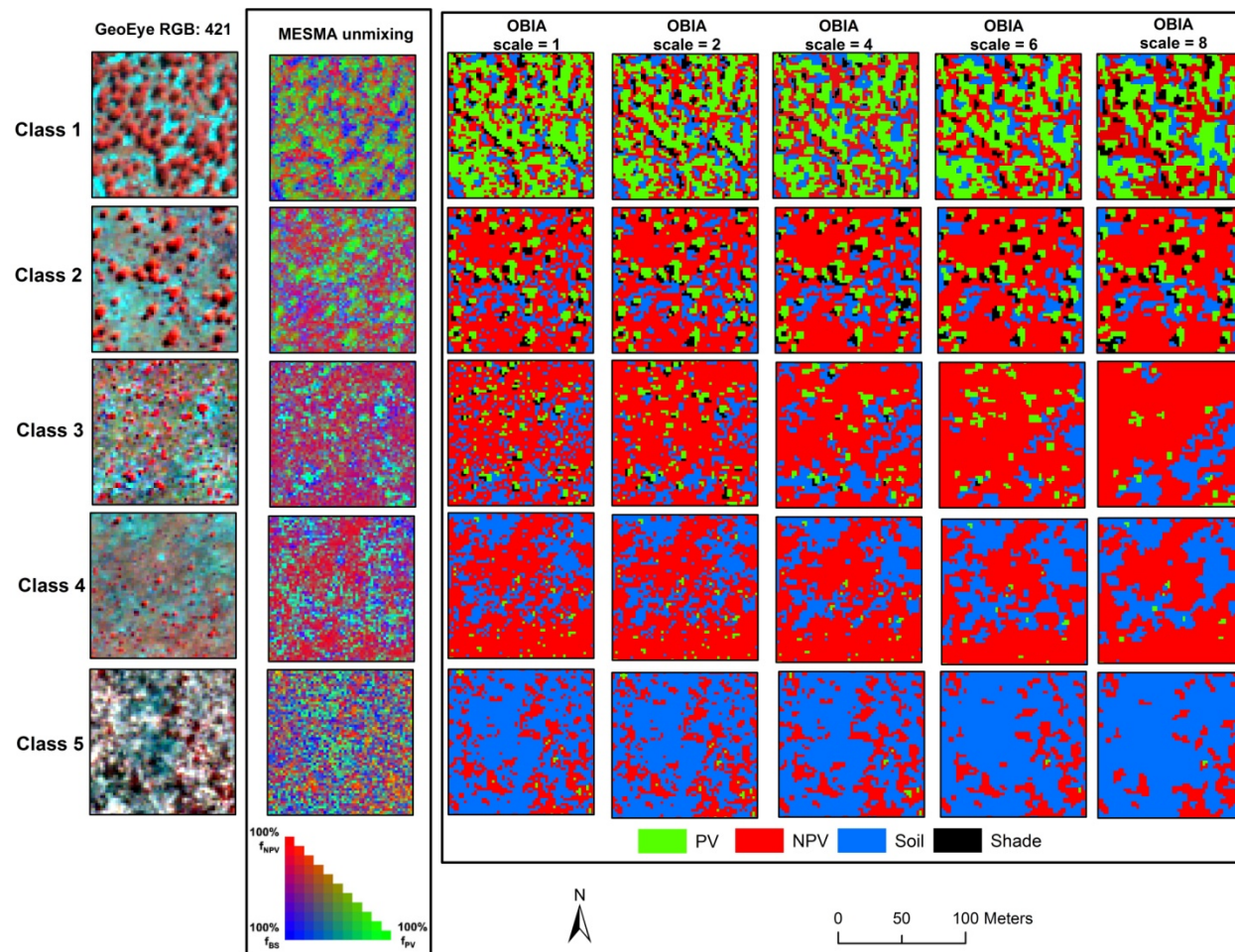
Figure 4.5: MESMA versus hierarchical OBIA classification results for areas fewer than five different vegetation morphology types in the central Kalahari.

Two Endmember models	Three Endmember models	Four Endmember models
PV + Shade (6)	PV + NPV + Shade (48)	PV + NPV + Soil + Shade (288)
NPV + Shade (8)	PV + Soil + Shade (36)	
Soil + Shade (6)	Soil+ NPV + Shade (48)	
Total models : 440		

Table 4.1: Different types and varying complexity of MESMA models used in this study. The number besides each model types represents the number of models tested at each model complexity level.

Level	Segmentation scale	Color/shape	Smoothness/compactness	Minimum/Mean/Maximum number of pixels in objects
1	1	0.8/0.2	0.6/0.4	1/1.4/8
2	2	0.8/0.2	0.6/0.4	1/2.1/25
3	4	0.8/0.2	0.6/0.4	1/3.37/164
4	6	0.8/0.2	0.6/0.4	1/7.53/400
5	8	0.8/0.2	0.6/0.4	2/16.7/1105

Table 4.2: Segmentation parameters and associated object statistics for the five segmentation scales considered in the study.

Features	Description
Mean layer value	The mean value represents the mean brightness of an image object within a single band; used feature: Mean NIR, Mean NDVI.
Ratios	The amount that a given band contributes to the total brightness; used feature: Ratio NDVI, Ratio Blue, Ratio Red.
Standard deviation	The standard deviation of all pixels which form an image object within a band; used feature: Standard Deviation Green, Standard Deviation NDVI, Standard Deviation Blue, Standard Deviation NIR., Standard Deviation GLCM (all bands).
Maximum difference	Minimum mean value of an object subtracted from its maximum value. The means of all bands belonging to an object are compared with each other and the result is divided by the brightness.
Texture after Haralick	GLCM (Grey Level Co-occurrence Matrix)calculated after Haralick et al. (1973): Describes how different combinations of pixel values occur within an object; used features (using the mean of all layers): GLCM Mean, GLCM Contrast, GLCM Dissimilarity, GLCM Standard Deviation, GLDV (Grey Level Difference Vector): The sum of the diagonals of the grey level co-occurrence matrix; used features (using the mean of all layers): GLDV entropy.

Table 4.3: Overview of the selected features used in image classification based on the OBIA approach.

Technique/segmentation scale	$RMSE_C$: All samples (n=18)			
	f_{PV}	f_{NPV}	f_{BS}	**Overall**
MESMA	5.1%	7.1%	7.4%	6.5%
OBIA (segmentation scale=1)	7.6%	7.8%	10.6%	8.6%
OBIA (segmentation scale=2)	10.4%	11.1%	13.8%	11.7%
OBIA (segmentation scale=4)	13.7%	16.6%	17.2%	15.8%
OBIA (segmentation scale=6)	19%	18.1%	18.8%	18.6%
OBIA (segmentation scale=8)	21.8%	22.3%	24.6%	22.9%

Table 4.4: Evaluation results of MESMA and hierarchical OBIA derived

fractional estimates against field derived estimates.

Scale	(a) RMSE$_C$: Class 1 (n=28)				Scale	(d) RMSE$_C$: Class 4 (n=43)			
	f_{PV}	f_{NPV}	f_{BS}	Overall		f_{PV}	f_{NPV}	f_{BS}	Overall
1	4.3%	3.6%	4.9%	4.2%	1	9.1%	11.8%	10.3%	10.4%
2	4.9%	4.3%	6.2%	5.1%	2	14.8%	13.2%	13.8%	13.9%
4	5.5%	5%	7.7%	6%	4	17.5%	14.1%	15.5%	15.7%
6	6.8%	8.1%	9.1%	8%	6	20.1%	18%	21.5%	19.8%
8	7.9%	10.4%	12.3%	10.2%	8	24.6%	20.3%	24.4%	23.1%

Scale	(b) RMSE$_C$: Class 2 (n=40)				Scale	(e) RMSE$_C$: Class 5 (n=55)			
	f_{PV}	f_{NPV}	f_{BS}	Overall		f_{PV}	f_{NPV}	f_{BS}	Overall
1	5.1%	4.8%	5.5%	5.1%	1	9.9%	13.8%	11.1%	11.6%
2	7.4%	6.8%	7.1%	7.1%	2	11%	14.3%	13.4%	12.9%
4	8.8%	8.1%	11.9%	9.6%	4	12.2%	17.8%	14.9%	14.9%
6	10.3%	10.1%	14.4%	11.6%	6	14.3%	21.4%	16.5%	17.4%
8	14.3%	14.4%	17%	15.2%	8	17.7%	24.8%	21.6%	21.3%

Scale	(c) RMSE$_C$: Class 3 (n=48)				Scale	(f) RMSE$_C$: All samples (n=214)			
	f_{PV}	f_{NPV}	f_{BS}	Overall		f_{PV}	f_{NPV}	f_{BS}	Overall
1	5.9%	7.1%	9.1%	7.3%	1	6.8%	8.3%	8.1%	7.7%
2	6.6%	8.8%	13.5%	9.6%	2	8.9%	9.4%	10.8%	9.7%
4	9.2%	11.3%	16.3%	12.2%	4	10.6%	11.1%	13.2%	11.6%
6	16.1%	13.4%	17.7%	15.7%	6	14.2%	14.2%	15.8%	14.7%
8	21%	18.4%	23.2%	20.8%	8	17.1%	17.6%	19.7%	18.1%

Table 4.5: Evaluation of hierarchical OBIA approach derived fractional estimates considering MESMA derived estimates as observed estimates. 5.a to 5.e represent results based on vegetation morphology type of samples where (a) Woodland, (b) Open shrubland, (c) Very open shrubland, (d) Grassland, (e) Pans and (f) represents the overall results considering all samples.

Chapter 5: Mapping vegetation morphology types in a dry savanna ecosystem: Integrating hierarchical object based image analysis with random forest

Introduction

Savanna ecosystems are mixed tree-grass systems that cover over 40% of global terrestrial area (50% of Africa) and play a significant role in global land-atmosphere energy balance as well as carbon and nutrient cycles (Hill et al. 2011a; Mistry 2000). Especially in southern Africa, savannas are essential contributors to productivity and biodiversity and also contain some of the largest remaining wildlife habitats (Scholes and Walker 1993). Vegetation structure and landscape composition in savanna systems is characterized as patchy, mainly the result of high spatio-temporal variability in rainfall and fire history (Turner et al. 2003; Wiegand et al. 2006). Besides providing ecosystem goods and services, southern Africa savannas are also economically significant as they offer the basis of economic activity by supporting high populations of livestock as well as wildlife-based tourism (Thomas and Sporton 1997; Werger 1973). Over the past two decade, many areas in the southern Africa savanna in general and the central Kalahari region in particular have become the focus of attention of stakeholders and government. These areas are perceived as large untapped grazing resources with potential of pastoral agriculture that can be a source of both people's livelihoods and government revenue (Dougill et al. 1999; Skarpe 1990; Thomas and Sporton 1997; Thomas and Twyman 2004). As a result, large parts of previously wild and undisturbed areas are experiencing structural and functional changes in vegetation characteristics mainly due to changing

land use, altered fire regimes exacerbated by climatic shifts (Dougill et al. 1999; Scholes et al. 2002; Turner et al. 1993; Werger 1973). These changes are in-turn affecting biogeochemical processes, availability of habitat-related key structural resources (e.g. solitary nesting trees, forging grounds and migration routes) and the overall ecological sustainability (Blaum et al. 2007; Dougill et al. 1999; Tews et al. 2004).

Sustainability of these fragile and dynamic systems need ecologically informed decision making by the land managers who require fundamental knowledge about the functional attributes of vegetation assemblages (e.g. vegetation structure, cover, density). These characteristics are also key variables in state and transition models used for modeling these systems (Scholes and Walker 1993; Van Rooyen et al. 1990). However, countries in southern Africa lack such geodata on vegetation and land cover at suitable spatial scales. Field-based assessment, though of high quality, is limited in scope and scale, especially considering systems that are extensive and wild. Further, vegetation dynamics is the result of processes interacting at multiple spatial scales that require monitoring at local to regional scales (Cramer et al. 2001; Xie et al. 2008). Remote sensing instruments provides valuable tool for this purpose and can not only complement field measurements but also provide much larger spatial coverage (Elmore et al. 2000; Wu and Marceau 2002). With the increasing number of remote sensing systems, images are available at multiple spatial scales, however with tradeoff between spatial resolution, temporal resolution and swath area. Systems providing low spatial resolution images (>250m e.g. MODIS) has high temporal revisit, large swath area making them more suitable for regional scale monitoring. While coarse resolution images have been able to

yield high accuracy in ecosystems with homogeneous cover, they have been found to produce much lower accuracy and high uncertainty in savanna systems mainly due to small patch sizes, heterogeneous classes with mixed vegetation (Giri et al. 2005; Latifovic and Olthof 2004; Mishra et al. 2014; Turner et al. 2004). Contrarily, very high spatial resolution imagery (< 10 m), though, provides the required spatial detail, is limited by small swath area, large data volume, low temporal frequency and high data cost. Medium spatial resolution imagery (20-30 m) (e.g. Landsat, ASTER) represents a good compromise in this regard and has been favored for landscape level applications in savanna systems (Davidson et al. 2008; Ringrose et al. 2003; Schwartz et al. 2003; Seagle 2003; Tangestani et al. 2008). Compared to low spatial resolution imagery, results obtained with medium resolution imagery are ecologically more meaningful as it allows inferring landscape patterns and related ecological processes (Newton et al. 2009; Opdam et al. 2002). However, in semi-arid savannas inferring vegetation properties form medium resolution   imagery is also methodologically challenging due to several reasons: e.g. expansive soil background leading to swamping out of spectral contribution of plants, lack of a strong red edge and reduced absorption in visible wavelengths due to evolutionary adaptations of semi-arid vegetation (Huete and Jackson 1988; Huete et al. 1985; Okin et al. 2001b; Wu and Marceau 2002).

Since savanna systems are often considered patch dynamic systems, mapping vegetation properties in savannas may benefit from object-based image analysis (OBIA) rather than traditional per-pixel analysis approach (Laliberte et al. 2004; Soranno et al. 1999; Spies et al. 1994; Steffan-Dewenter et al. 2002). Following OBIA approach,

imagery is first segmented into objects representing relatively homogeneous group of pixels by selecting desired scale, shape and compactness criteria. Segmentation is followed by sample selection and classification of segments into classes of interest (Benz et al. 2004b; Steffan-Dewenter et al. 2002). In savanna systems, important OBIA advantages includes (i) treatment of landscape to be consisting of relatively homogeneous patches (or 'objects') is ecologically more suitable than individual pixels, (ii) landscape patches often depict scale dependency and following OBIA approach landscape objects can be generated at multiple segmentation scales that can provide added insight into ecological processes (Strayer *et al.* 2003a), (iii) lower chances of 'salt-and-pepper' speckle which is often an issue with per-pixel analysis and (iv) OBIA offers the opportunity to add contextual, geometrical and texture related features (Strayer *et al.* 2003b). However, OBIA approach has not yet been extensively tested in natural landscapes where continuous variation in vegetation characteristics makes its challenging to define boundaries between 'objects' (Soranno et al. 1999; Tallmon et al. 2003).

Unlike human modified landscapes (e.g. urban areas), in heterogeneous natural systems, landscape patches can vary in size, shape and structure that may require characterization at multiple spatial scales (Mishra and Crews 2014a; Moustakas et al. 2009). Within OBIA, the segmentation scale parameter used in segmentation controls the maximum allowable object level spectral heterogeneity and object size (Urban *et al.* 2002). Scale also affects the quality of segmented objects and which in turn affects the final classification accuracy (Keyghobadi et al. 1999; Yu et al. 2006). By manipulating segmentation scale factor, nested objects of different size can be created that could be

further hierarchically classified representing the output at multiple scales. While such hierarchical classification approach has been found appropriate for characterizing spatially heterogeneous natural systems such as wetlands (Trzcinski *et al.* 1999) and arid rangelands (Gillon 1983), it's suitability for characterizing vegetation morphology in dry savanna systems at the landscape scale merits further investigation.

Determining suitable classification feature space is a crucial step before image classification which ensures that classes in question are discriminated effectively and with sufficiently high accuracy (Knight and Morris 1996). Following OBIA, the availability of hundreds of features (e.g. spectral, geometrical, textural, and contextual) makes it a time consuming and subjective process (Turner 1989). Specifically, the inclusion of textural features in OBIA increases the processing time significantly, thus limiting its suitability for landscape scale mapping (Soranno *et al.* 1999) . Very few previous studies have examined which classification features are more appropriate for characterizing vegetation morphology in xeric systems (Gillon 1983). Additionally, in low niche differentiation environments like the semi-arid savannas, separability of vegetation classes and classification accuracy may be enhanced by using more recently proposed non-parametric classification algorithms (e.g. classification trees). The application of ensemble of classification trees (i.e. Random Forest) as proposed by Breiman el al.(2000) has been proved to be effective for classifying remotely sensed data. Remote sensing studies utilizing Random Forest (RF) classification have focused on per pixel classification approach and regional to global scale studies. More recently, their application under OBIA approach has found to enhance thematic depth and classification

accuracies. Therefore, this study explored the utility of OBIA combined with RF classification for mapping vegetation morphology types in the semi-arid central Kalahari of Botswana. The study area is relatively understudied and lacks landscape scale environmental geodata due to accessibility and the dangers of wildlife. The primary objective of this study was to utilize *in situ* information on vegetation physiognomic characteristics to develop and map vegetation morphology types using OBIA by determining the optimal segmentation scale and classification features.

Site and situation

A part of southern African semi-arid savanna system, the central Kalahari (between $21°$-$24°$ S and $22°$-$26°$ E) occupies the north and central part of the larger Kalahari sand basin. The area follows the Kalahari rainfall gradient with its north and the west tip receiving up to 400 mm of rainfall whereas the rest of the area receives a mean annual precipitation of 350 mm. The rainy season is between October-April during which rainfall is spatially discontinuous and temporally variable (Makhabu et al. 2002; Scholes et al. 2002). The study area covers 22,292 sq. kms of which more than 70 percent falls under protected area (i.e. the Central Kalahari Game Reserve) and the rest is under private game farms and open-access commercial ranching (Figure 5.1). Geologically, the area is dominated by the spread of nutrient poor Kalahari sand with sporadic outcrops of calcrete, sandstone and schist of the Karoo sequence with an average altitude of 950 m (Fagan 2002). The topographical continuity is broken in the northern part of the study area due to the existence of longitudinal dune systems marked by comparatively much higher and denser vegetation. The natural water availability is limited to small, short-

138

lived accumulations in occasional pan depressions (Dougill and Trodd 1999). The vegetation is characterized by spatially complex and structurally heterogeneous mixture of woody and herbaceous species occurring on a scale of few meters and exhibit temporally distinct phenological patterns. Notable broad-leafed species in the area includes *Lonchocarpus nelsii, Terminalia sericea, Bauhinia petersiana, Combretum hereroense, Croton gratissimu.* Important fine-leafed species are *A. erioloba, A. luederitzii, Ziziphus mucronata, A. mellifera, A. erubescens* (Fagan 2002). Plant species diversity is relatively low for all plant communities and the difference among communities is related to changes in species dominance rather than occurrence of different species. Thus, vegetation boundaries based on plant species are often unclear (Fagan 2002; Makhabu et al. 2002). As in much of southern Africa's savannas, pans are geomorphologically distinct features with relatively flat topography and clay dominated soil. Pans are different from other bare areas as they are mostly contained in isolated sub circular to sub elliptical depressions that retain rain water for much longer duration. In the study area, many pans (e.g. Deception pan, Lethiahau pan) are remnants of ancient sand chocked drainage lines (also called fossil river valleys). Pans are ecologically important as they provide mineral licks, relatively nutrient-rich vegetation, attracting large herbivores and their associated predators and concomitant tourism (Turner 2005). Therefore, accurately mapping pan areas is important for the overall planning and management of the central Kalahari region.

139

5.3 Data and methods

5.3.1 Remotely sensed data and pre-processing

This study used terrain corrected (Level 1T) Landsat 5 TM imagery acquired at 10:16 local time (08:16 UTC) on May 9, 2010. In the central Kalahari, May represents the beginning of the dry season when trees and shrubs were still green whereas herbaceous vegetation contained no observable green biomass. Clouds in this imagery were manually masked and surface reflectance was derived by radiometrically calibrating the imagery using ATCOR algorithm. ATCOR is an absolute atmospheric correction method that applies an atmospheric look-up table based on a large database containing the result of radiative transfer calculation from the MODTRAN-4 radiative transfer code (Pearson *et al.* 1999). The optical depth of the atmospheric aerosols was calculated by comparing modeled at-sensor radiance with measured radiance in the red band of areas with dark dense vegetation. This correction was then applied on each pixel to derive surface reflectance. As an additional feature, Normalized Difference Vegetation Index (NDVI) was derived after calibrating Landsat TM imagery. An ASTER GDEM (Version 2) representing the study area was also used to derive slope and aspect. At high spatial resolution, GeoEye-1 and SPOT-5 images were available covering 1,353sq.kms. (6%) and 15,821 sq. kms. (70%) of the study area respectively.

5.3.2 Field data processing and development of vegetation morphology classes

Field data related to vegetation physiognomy (i.e. structure and density) and species composition was acquired following transect based approach during two field

campaigns conducted during 18 May- 2 June 2011 and 11-28 May 2012 (coincident to the calendar month of image acquisition). The location of these transects were determined based on knowledge gained during May 2010 reconnaissance trip and visual interpretation of high spatial resolution imagery (i.e. GeoEye/SPOT). Transect locations were spatially distributed with an aim to sample all important vegetation morphology types in the study area. Due to serious accessibility and safety issues (e.g. danger of predator attack), these transects could not be established away from tracks except in the pan and more open areas. Combining the fieldwork conducted during 2011 and 2012, data were collected in 148 transects (figure 5.1). At each of these transects, geographic coordinates were recorded at the start and end points using a standard global positioning system. Additional information included visual interpretation of the dominant vegetation functional type (e.g. woody versus herbaceous), minimum, maximum and average vegetation height, dominant tree/shrub species and pictures acquired with a digital camera. These characteristics were also interpreted and recorded at 143 more locations where setting up transect was not possible due to high vegetation density and serious safety issues (figure 5.1).

In southern Africa savanna systems, at the spatial/spectral resolution of Landsat TM imagery, vegetation physiognomic-structural aspects are the most important determinants of a pixels reflectance (Groffman *et al.* 2005). Hence, the development of vegetation morphology classes was based on (i) vegetation physiognomy, (ii) vertical and horizontal agreement, (iii) leaf type and (iv) phenology. The accurate representation of the typical co-existence of tree, shrubs and grasses in savanna ecosystem requires

141

consideration of the layering system of vegetation structure. An important advantage of considering layering system in heterogeneous systems such as savannas is the independence of geographic scale (Groffman *et al.* 1992). Thus, considering the layering system of vegetation and above mentioned physiognomic characteristics recorded in field transects, the following five vegetation morphology classes were defined: (i) Mixed deciduous woodland with shrubs and herbaceous layer, (ii) Mixed (70-40%) medium high shrubland with open short herbaceous layer, (iii) Mixed (40-10%) medium high shrubland with open short herbaceous layer, (iv) Medium tall grassland with medium high shrubs and (v) Pans and bare areas (Table 5.1).

Object based image analysis

Image segmentation and training/testing object selection

The workflow of the methodology followed in this study is outlined in figure 5.2. To implement object based classification, first, image segmentation was carried out in eCognition Developer 8 software (Loreau *et al.* 2003). The raster stack (6 landsat bands excluding thermal band, NDVI, DEM, slope and aspect) was segmented using multiresolution segmentation algorithm. Multiresolution segmentation approach allows construction of objects of different sizes and enhances the response of object generation to landscape patch structure compared to other approaches (Jules et al. 2002; Naiman and Rogers 1997). Due to high structural heterogeneity in savanna systems meaningful spectrally homogeneous objects can occur at different spatial scales (Naiman and Rogers 1997). Additionally, based on field information on landscape heterogeneity it was

142

expected that optimal patch size would vary depending on vegetation morphological characteristics. Hence, in this study objects were generated at six segmentation levels with scale values ranging from 15 to 60 resulting in average object size of 20358-408625 m^2 (Table 5.2).

Figure 5.3 shows segmentation results for a subset area at the six considered segmentation scales depicting how increasing segmentation scale value also increased the resulting object size. Visual inspection of segmentation results confirmed that beyond the scale value of 60, it was no longer possible to find representative homogeneous objects as the chance of class mixture inside the object increased with object size (Liu and Xia 2010). Hence, segmentation was not conducted beyond the scale value of 60. The other required segmentation parameters, shape and compactness were kept at a constant value of 0.2 and 0.4 respectively (Table 5.2). These values were selected as optimal based on visual comparison of the results of several iterative segmentation runs. While conducting segmentation, the input Landsat bands, DEM, slope and aspect were given equal weight while the NDVI layer was given higher weight compared to all other input layers.

For each segmentation scale training and test objects for classification were selected by (i) intersecting surrounding Landsat segment with specific field transect and (ii) more objects in the neighborhood of field transect locations were selected as samples by interpreting and confirming their homogeneity in terms of vegetation physiognomy by overlying them on high resolution imagery (GeoEye/SPOT) (figure 5.4.a). To ensure systematic geographic distribution of training/testing data, objects were divided between calibration and validation datasets based on the object ID created systematically across

the image during segmentation. In most cases, sample objects derived with lower scale values were nested within objects derived from higher factor values. In semi-arid savannas, the spatio-temporal pattern of rainfall determines the temporal dynamics of vegetation (Hill et al. 2011a). Hence, the suitability of the selected training/testing objects was also validated by spatially overlaying them on the mean Enhanced Vegetation Index (EVI) value calculated from 6 years (2005-2011) of MODIS data (MOD13Q1 product) (figure 5.4.b). Further, to avoid the inclusion of any burned area in training/test data MODIS burned area product (MOD45A1) (Foster *et al.* 1999) was used. Finally, for each scale 843-1638 training/test objects with 68-631 objects per class were selected. Compared to other classes the number of samples selected for pan areas was higher because (i) much of the field tracks in central Kalahari follow the pan systems (figure 5.1) that allowed easier access and (ii) due to their high albedo it was relatively easier to visually distinguish pans on the high spatial resolution imagery. Thus, while pans and bare area represent relatively small percentage of the total study area, the number of validation and training samples selected for them was higher (Table 5.1).

Feature space selection for classification

For selection of optimal features to be used in classification, initially 41 spectral, shape, texture, pattern and contextual features were selected to include sufficiently wide range of features. To reduce the data dimensionality Spearman's rank correlation analysis (Spearman 1904) was utilized to eliminate features with correlation coefficients above 0.9. Seventeen features were found to have correlations below this threshold value. The

144

selection of best features from these remaining features was based on Jeffrey's-Matusita distance (JM distance) which is a pairwise measure of class separability based on the probability distribution of two classes. JM distance has a finite dynamic range that allows easier comparison of class separability. For calculating JM distance the SEATH tool was used (Marpu et al. 2008; Nussbaum et al. 2006). Using the sample data for each class, a probability distribution is estimated based on mean and variance value. Thresholds are determined by fitting a Gaussian probability mixture model to the frequency distribution of a feature for the two classes. SEATH calculates class separability and threshold for every two class combination. This study calculated the largest average JM distance (the mean of all two class combinations) for every possible 9-17 feature combination. Combination with lesser number of features always had lower JM distance compared to combinations with more features and selecting the lowest mean JM distance for the 9 candidates was deemed unsuitable. Hence, the feature combination that resulted in the largest JM distance for the least separable pair of classes were selected which is also an approach followed in previous studies (Swain and Davis 1978; Turner 1989). This approach resulted in the final selection of 13 features (Table 5.3) out of which 4 were textural features calculated after Haralick et al. (2003). The appropriateness of these features was also confirmed by comparing them with results of feature space optimization (FSO), a feature selection tool available within eCognition (Loreau *et al.* 2003).

Image classification and accuracy assessment

In this study, vegetation morphology types were mapped using a non-parametric classifier called Random Forest (RF). The RF classifier builds multiple decision trees from bootstrap samples of the reference data. Decision tree classifiers have advantages over traditional classifiers in that they make no assumptions about data distribution (e.g. normality) and can adapt to non-liner relationships inherent in the data (Friedl and Brodley 1997). RF classification has been employed in environmental remote sensing for variety of applications including land cover mapping (Pal 2005; Sesnie et al. 2008), forest structural parameters and biomass estimation (Baccini et al. 2004; Hudak et al. 2008) and mapping invasive species (Lawrence et al. 2006). In land cover mapping studies, RF classification has been found to yield overall accuracies that are either comparable to or better than other state of the art classifiers such as neural networks and support vector machines (Pal 2005). In RF classification, each decision tree uses a random subset of training data and a random subset of input predictor variables which reduces the correlation between decision trees as well as the overall computational complexity. Roughly 2/3 of the data is sampled with replacement while 1/3 of the sample data is withheld from tree construction (also called "out-of-the-bag" or OOB samples). OOB samples are used to calculate the difference between predicted versus observed samples based on which unbiased error matrix is calculated. Final class prediction is determined by majority voting based on the ensemble of trees. RF also calculates the measure of variable importance for individual classes and the classification as a whole. Variable

146

importance measure allows determining which of the input features contribute most to the class separation. Predictor variable importance plots are generated based on a random permutation of the input variables and the effect of the permutation is quantified for each variable by the change in the OOB error (Breiman 2001). Variables those are important for separating classes show significant change in the OOB error.

RF classification was implemented in the statistical package R using the "random Forest" package (Liaw and Weiener 2002). The selected predictor objects were converted to ESRI shapefile and the associated attribute table was exported for RF classification in R. The parameters used for classification included: number of trees *(ntree=500)*, minimum samples in terminal node *(nodesize=10)* and *sqrt(p)* as the number of variables randomly sampled as candidates at each split, where *p* is the number of variables. After classification, the RF class predictions were written back to the attribute table. The classification accuracy was accessed using independent sample objects reserved for each class at each segmentation scale. Error matrices were calculated based on number of objects per class without considering object size. Accuracy matrices reported include class-wise user's and producer's accuracy, overall accuracy and kappa statistic at each segmentation scale.

Results and Discussion

Vegetation Morphology type mapping

The vegetation morphology type mapping in this study was based on vegetation survey in the northern part of the Central Kalahari Game Reserve. In general, vegetation in the study area represents a transition zone between tree savanna with mixed broad

147

leafed and microphyllous (fine leafed) species in the northern part that gradually changes into microphyllous species dominated areas in the south and south-west. The mapped vegetation types for the whole study area are shown in figure 5.5(a). Results depict that vegetation morphology class 3 (i.e. mixed (40%-10%) medium high shrubland with open short herbaceous layer) was the spatially most dominant (covering about 60 % area) whereas vegetation morphology class 1 (i.e. mixed deciduous woodland with shrubs and herbaceous layer) was least dominant (less than 1 % of the total area).Vegetation morphology class 2, 4 and 5 covered 20.32%, 13.76% and 3.03% areas respectively. The spatial distribution of the different vegetation morphology types in the study area is a reflection of the spatial heterogeneities in the ecological mechanisms (e.g. soil characteristics, rainfall pattern, fire history) that influence savanna vegetation structure and composition. Vegetation morphology class 1 was present in the north, north-east and south -east parts of the study area (figure 5.5.a). During the field campaign, it was noted that the patches of vegetation morphology class 1 in the northern part of study area were dominated by *Terminalia prunioides* mixed with *Croton gratissimus* and *Acacia erioloba*. On the other hand, those in the south-eastern part of the study area were dominated by *Colophospermum mopane*, co-dominant *Lonchocarpus nelsii* and *Acacia luederitzii*.

Vegetation morphology class 1 and class 2 generally dominate areas known as northern Kalahari sandveld that are topographically characterized by immobile longitudinal sand dunes. Vegetation morphology class 3 dominates areas that are topographically characterized as inter-dunal and plains with relatively shallow depth of

148

sand. It also marks the transition zone between relatively densely vegetated areas and more open areas with predominantly herbaceous vegetation. Areas under vegetation morphology class 4 are mostly plains with shallow sand making the top layer. Pan areas (vegetation morphology class 5) have dominant clay content and are found in the study area as either forming the ancient fossil river valley systems or others that are randomly scattered throughout the study area. Pan areas are characterized by occasional occurrence of clump of trees also called "tree islands", a result of the complex interaction of longer water availability, fire history and soil characteristics.

Class separability

Class spectral separability analysis was conducted on the training samples of considered vegetation morphology classes using the finally selected 13 feature space variables. The separability metric used was JM distance that indicates a relative measure of how reliably one class can be statistically separated compared to the remaining classes. The results of this separability analysis are reported in table 5.4. Class pair-wise JM distance separability value is reported between 0-2, with 2 indicating complete separability. The result of pairwise separability analysis suggested high separability for most class pairs. The smallest JM distance value was reported for the pair of morphology class 2 and 3 (i.e. JM distance: 1.61). This could be attributed to the fact that the differentiation between these two classes was established considering the percent cover or density of shrubs as observed in the field and high resolution imagery. However in feature space the two classes were relatively similar even after using the optimally

149

selected classification features. The highest inter class separability values were reported for morphology class 5 and all other classes. This could be attributed to very high surface albedo of pans and bare areas and also due to significant delay of the growing season period and late green up caused by a typical flooding situation at the end of the rainy season. On the other hand, low class separability between morphology class 2 and class 3 could be attributed to the comparative similarity in vegetation physiognomic characteristics between the two classes.

Segmentation scale versus classification accuracy

Results suggest that classification accuracy was sensitive to image segmentation scale and various important outcomes could be noticed in this response. Among the six considered segmentation scales, the overall accuracy consistently increased from scale 15 to coarser scale values, attaining the highest overall accuracy at segmentation scale of 40 (i.e. overall user's and producer's accuracy 87.05% and 83.69% respectively, kappa=0.82). However, at segmentation scale higher than 40, the classification accuracy again decreased (Table 5.5). Furthermore, the observed sensitivity of classification accuracy to changing segmentation scale was also class specific as highest classification accuracies for different vegetation morphology classes was observed at different segmentation scales (Table 5.5). For example, areas with comparatively dense vegetation (e.g. morphology class 1) attained highest classification accuracy at the segmentation scale value of 15. Contrarily, in areas dominated by relatively open herbaceous vegetation (e.g. morphology class 4), highest classification accuracy was observed at

150

coarse segmentation scale value (i.e. 60). Unlike other classes, the classification accuracy of vegetation morphology class 5 (representing pans and bare areas) showed least variation and was not as much affected by the changing segmentation scale (Table 5.5).

These results could be interpreted in the light of the spatial variability in structural and functional properties of the different vegetation morphology types in the central Kalahari. Hierarchical segmentation approach used in this study is well suited for this purpose. Results indicate that the highest overall classification accuracy was not found at smaller segmentation scale value but at coarser segmentation scale. This could be attributed to the fact that at coarser scale value integration of spectral signature across large number of pixels increased the contrast among vegetation morphology types due to the reduction in within class spectral variation (Strayer *et al.* 2003b). However, at further coarse segmentation scale (i.e. scale value greater than 40) the classification accuracy started decreasing apparently due to reduction in the spectral contrast between classes due to class mixtures. Savannas are often considered patch dynamic systems as the vegetation spatial distribution resembles patchy shapes due to the influence of determinants such as (e.g. high spatio-temporal variability in rainfall pattern and fire history) (Moustakas et al. 2009). For accurately characterizing vegetation morphology in savannas, it is important that segmentation output matches the patch size and structure for different classes of interest prior to classification (Gustafson 1998; Tallmon et al. 2003). This study compared segmentation output with 6 different scale values. Although the highest overall classification accuracy was achieved at the scale value of 40, however for different classes highest class specific accuracies were achieved at different segmentation scale

151

values. Thus, no single scale values could be suggested optimal for all classes. Optimal segmentation scale (for which a given class attains highest classification accuracy) for vegetation morphology class 1 was smaller (i.e. 15) compared to morphology class 4 that attained highest classification accuracy at larger segmentation scale (i.e. 50). These results could be attributed to the fact that while patches of vegetation morphology class 1 are relatively small and woody dominated that occupy topographically and pedologically different longitudinal dune systems, vegetation morphology class 4 has predominant herbaceous life forms that occupy inter-dunal areas as well as plains that cover larger areas and have bigger patch size. Contrarily, the classification accuracy of vegetation morphology class 5 (i.e. pans and bare areas) was not sensitive to the changing segmentation scale and was mapped with high accuracy across all tested segmentation scales (table 5.5). These results highlight that segmented objects for pan and bare areas have low within class spectral variability compared to other classes and are relatively homogeneous.

Variable importance in RF classification

Due to the availability of hundreds of feature space variables under OBIA approach, the analysis can be very time consuming in terms of image processing and memory allocation. Hence, selecting suitable feature space variables is critical for conducting OBIA based analysis over large geographical areas. This study highlights the most useful feature space variables for mapping vegetation morphology types in dry savanna systems. Many of the initial geometrical and contextual features were found to

be highly correlated with each other and were subsequently omitted. Based on the feature selection criteria explained in section 3, finally 13 features were selected for classification. Figure 5.6 depicts the class specific as well as the overall importance score of 13 variables for the classification obtained at segmentation scale value of 40 (for which highest overall classification accuracy was observed).The variable importance plot depicts these 13 features in order of decreasing importance for discriminating vegetation morphology types. Figure 5.6(a)-(e) shows class specific variable importance while the overall variable importance is depicted in figure 5.6(f). Standard deviation of mid infrared was the most important feature variable underscoring the distinguishability of savanna vegetation morphology types in pedological context. This result confirms the findings of previous studies based mainly on field observation emphasizing the subjacent soil properties as an important determinant of savanna structure in the central Kalahari (Fagan 2002; van Rooyen and van Rooyen 1998). The presence of two texture associated variables (i.e. GLCM contrast and GLCM standard deviation) among the top five variables (and total 4 texture related variables among the 13 selected variables) shows the importance of textural features in discriminating savanna vegetation morphology. These results suggest that in semi-arid systems where different vegetation morphology types have subtle difference in physiognomic characteristics may exhibit similar spectral response and require inclusion of textural characteristics for effective discrimination. The class specific variable importance indicates the suitability of each feature for an increase in accuracy in the random forest ensemble. For all classes the most significant classification feature was a spectral feature (i.e. mean NDVI or Ratio NDVI) except for

153

vegetation morphology class 4 for which textural feature was most significant (i.e. GLCM standard deviation).

Conclusions

This study represents an application of OBIA for mapping vegetation morphology types at landscape scale in an extensive and structurally heterogeneous semi-arid savanna ecosystem. The objective was to accurately map the vegetation morphology types in the central Kalahari by determining the optimal segmentation scale and best features for classification. Results depicted that highest overall classification accuracy was recorded not at the finest segmentation scale but at coarser segmentation scale. Further, for different classes highest class-specific accuracy was achieved at different segmentation scale highlighting the fact that spatial heterogeneity in savanna systems requires multi-scale characterization. The hierarchical OBIA approach adapted in this study was found suitable for this purpose. OBIA approach treats landscapes as relatively homogeneous mosaic of patches that allow smoothing of local variability and enhances class separability. This approach is especially relevant in the semi-arid savanna systems with low niche differentiation and where the complex interaction of biotic and abiotic determinants often results in landscapes that should be treated as patches. Further, the multi-scale hierarchical approach was deemed suitable because in natural landscapes such as savanna the optimal patch size for different morphology types is often unknown and expected to depict a multi-scale character. Besides the spectral features, object level texture features were also found to be important for distinguishing savanna vegetation

morphology types. This could be attributed to the fact that vegetation morphology types in semi-arid systems are often marked by subtle difference in vegetation physiognomy and species composition has relatively similar spectral characteristics. Texture information is based on second order statistics and provides dimensionality needed for distinguishing these subtle differences between classes.

The RF classification technique used in this study proved to be effective in terms of classification error, overfitting and variable importance measures. The bottom up approach of using *in situ* derived vegetation physiognomic properties to derive classification samples that could be coupled with advance classification techniques holds promise for remote sensing applications in savanna systems. The highest overall classification accuracy of 85.59% obtained at segmentation scale 40 was satisfactory for mapping vegetation morphology types in semi-arid savanna given subtle physiognomic difference for few classes. This study showed that *in situ* information combined with OBIA-RF classification of multispectral imagery can be an effective method for mapping vegetation morphology classes in the semi-arid savanna systems at the landscape scale. The approach allowed the evaluation and selection of several spectral, geometrical, contextual and textural features and finally determining the suitable analysis scale. The vegetation morphology map created in this study is significant and provides the necessity environmental geodata for the study area. It is expected to support variety of ecological studies such as understanding spatio temporal dynamics of habitat use by the wildlife, plat function and biogeochemical fluxes and overall management of the area. The mapped spatial distribution of vegetation morphology types may also serve as useful

input to the models of climate and land use change in the study area. This study could map vegetation morphology types defined based on vegetation physiognomic characteristics rather than floristic/species aspects. Therefore, future related research would focus on applying this technique to distinguish floristic classes in semi-arid savannas using both medium resolution (e.g. Landsat) as well as high resolution imagery (e.g. GeoEye).

(a)

(b)

N

0   255   510 Kms

⬚ Study Area
⬚ Central Kalahari Game Reserve
⬚ Botswana Country Boundary

(c)

N

0   15   30   60 Kilometers

• Photo
• Photo + Transect
- - - Tracks

—— CKGR Boundary   ⬚ Game Farm Boundary
⬚ Study Area

157
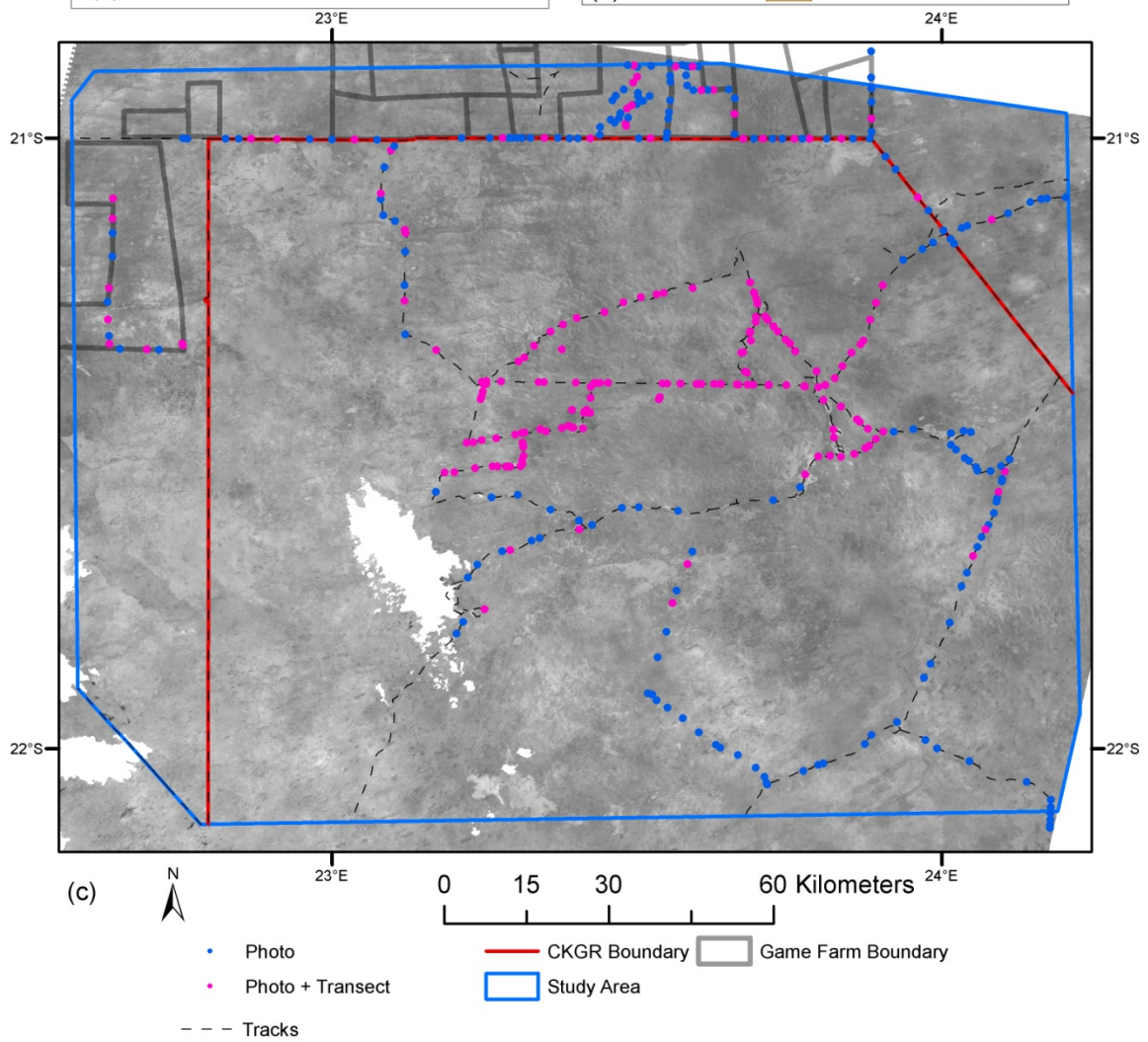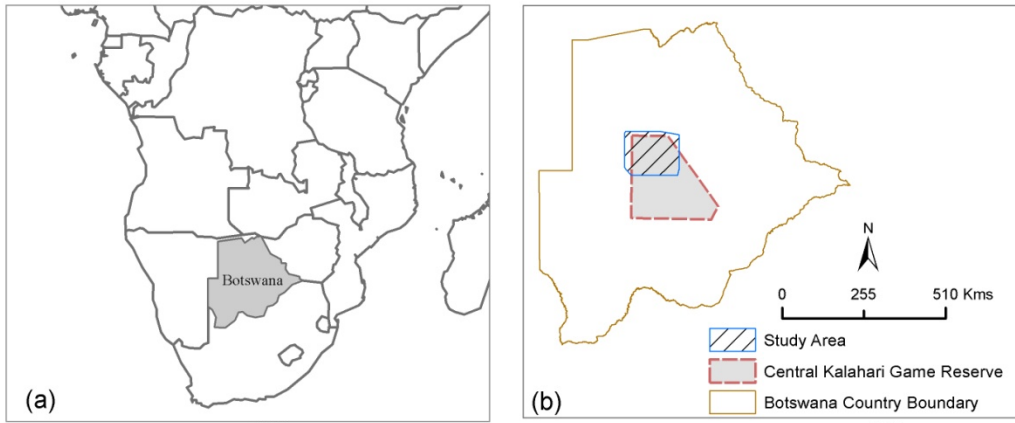
Figure 5.1: (a) Location of Botswana in southern Africa (b) Location of study area in the central Kalahari of Botswana and (c) enlarged portion of study area depicting the game reserve boundary and game farms outside the protected area, and the points were field data was collected. Background image is cloud masked Landsat TM (band 4) used in this study.
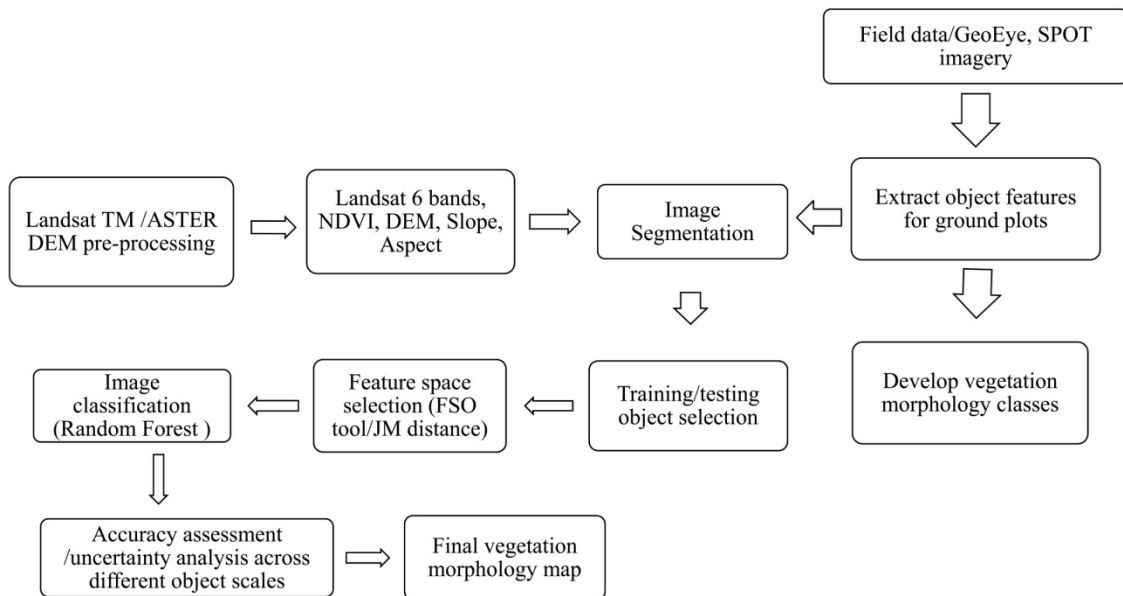
Figure 5.2: Schematic workflow of the study procedures.
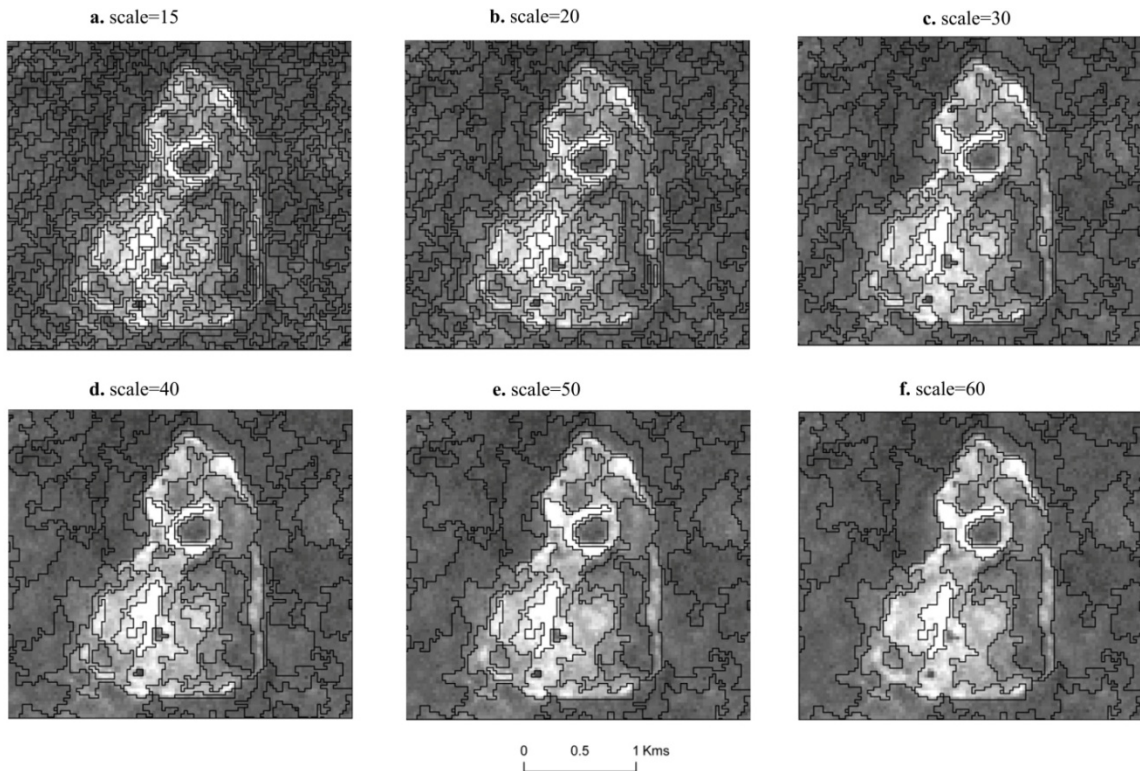
Figure 5.3: Illustration of changing object size with increasing scale factor in multiresolution segmentation output.
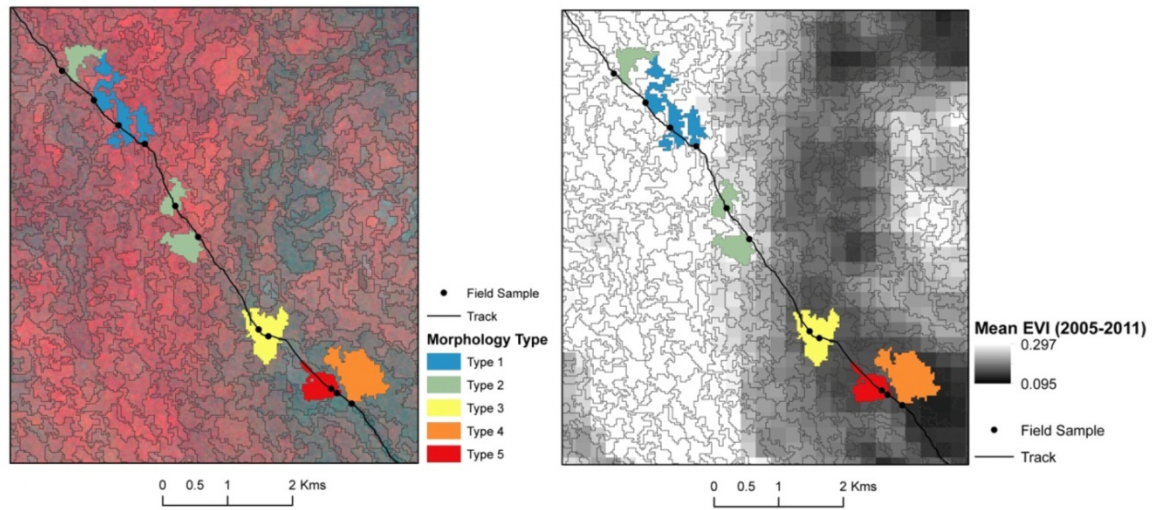
Figure 5.4: Example for the selection of training objects for different classes by intersecting location of field samples with homogeneous objects retrieved from segmentation (a) represents sample objects with Landsat false color composite in the background, (b) background shows mean EVI values (2005-2011) derived from MODIS time-series images.

(i) Landsat RGB: 421   **(ii) Classification output (iii) Inset GeoEye RGB: 421**

Class 1: Mixed deciduous woodland with shrubs and herbaceous layer
Class 2: Mixed (70-40%) medium high shrubland with open short herbaceous layer
Class 3: Mixed (40-10%) medium to high shrubland with open short herbaceous layer
Class 4: Medium tall grassland with medium-high shrubs
Class 5: Pans and bare areas

Figure 5.5: Vegetation morphology type classification derived from Random Forest classification on objects generated at segmentation scale value 40. Figure 5.5(a)

161

represents the map of whole study area. Figure 5.5(b) and 5.5(c) show two subset areas with different morphology types and are compared to Landsat and GeoEye images.
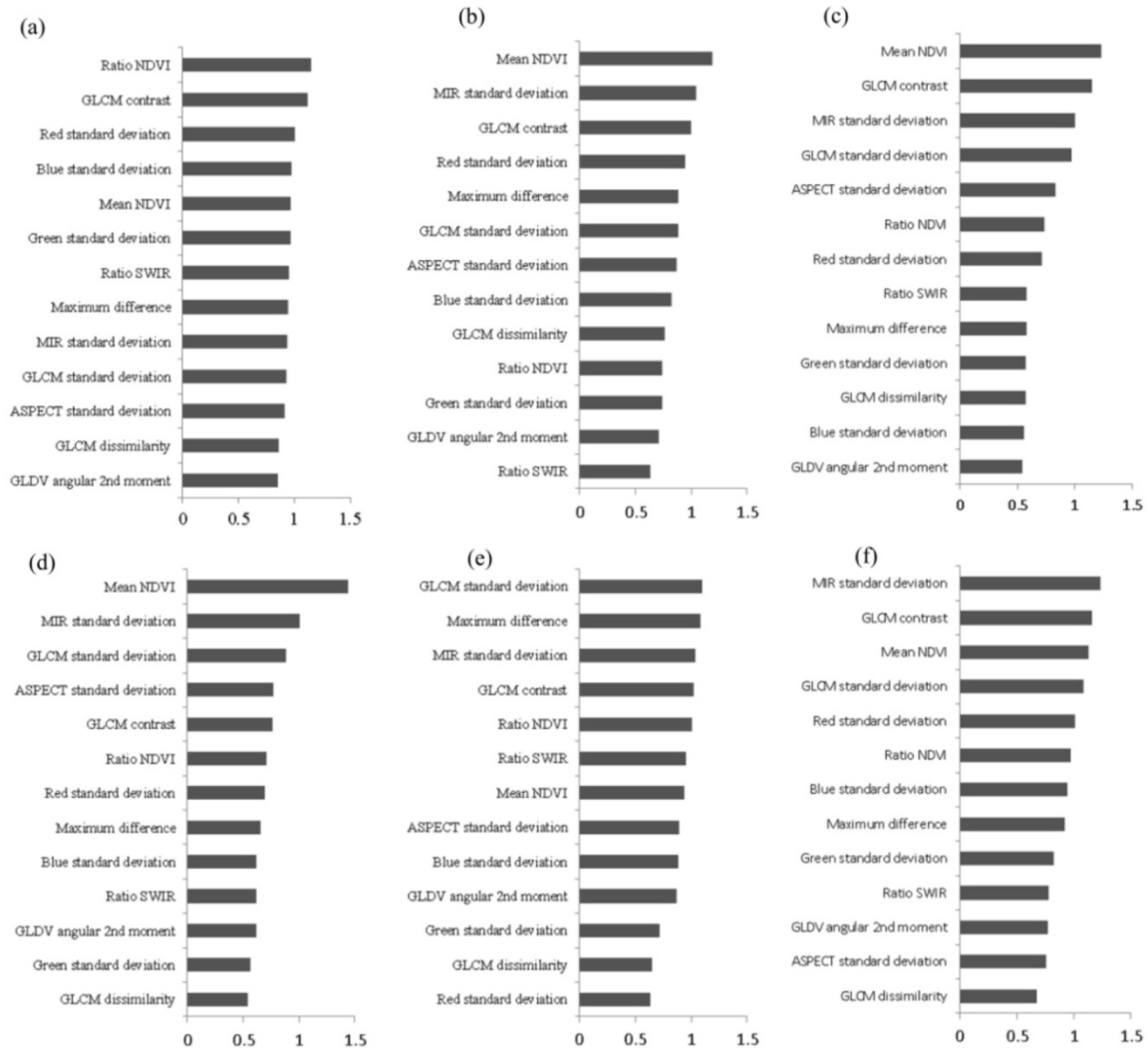
Figure 5.6: Variable importance reported as mean decrease in class specific and overall producer's accuracy from 500 trees in random forest classification. Those variables with higher mean decrease in accuracy are considered to be more important for overall or class level classification. Figure (a)-(e) represents class specific variable

importance for morphology classes 1-5 respectively and (f) depicts variable importance for overall classification. All results are for classification conducted at objects generated at segmentation scale 40. In each figure x-axis represents the variable name and y-axis represents the percent decrease in accuracy.

Field Photo	Class name(main woody or herbaceous species)	No. of field transect/ photo locations	Vegetation structure	Average # of objects (training/valida tion)
	Class 1: Mixed deciduous woodland with shrubs and herbaceous layer (species: Terminalia prunioides, C. mopane, Acacia erioloba, Croton gratissimus)	27/14	First layer: • Life form: trees • Mean percent cover: 13.4% • Mean height: 20m Second layer: • Life form: shrubs • Mean percent cover: 41.6% • Mean height: 6m Third layer: • Life form: herbaceous vegetation • Mean percent cover: 32% • Mean height: 0.8m	218/87
	Class 2: Mixed (70-40%) medium high shrubland with open short herbaceous layer (species: Acacia mellifera, Croton gratissimus, Acacia erubescens)	59/38	First layer: • Life form: shrubs • Mean percent cover: 36.4% • Mean height: 5.5m Second layer: • Life form: herbaceous vegetation • Mean percent cover: 46.8% • Mean height: 0.7m	446/178
	Class 3: Mixed (40-10%) medium high shrubland with open short herbaceous layer (species: L. nelssi, C. alexandri, Bauhinia petersiana, G. Flava)	91/54	First layer: • Life form: shrubs • Mean percent cover: 24.08% • Mean height: 3.4m Second layer: • Life form: herbaceous vegetation • Mean percent cover: 48.05% • Mean height: 0.5m	1097/439
	Class 4: Medium tall grassland with medium high shrubs (species: Stipagrostis spp, Aristida spp , L. nelssi)	55/32	First layer: • Life form: shrubs • Mean percent cover: 14.11% • Mean height: 2.6m Second layer: • Life form: herbaceous vegetation • Mean percent cover: 55.36% • Mean height: 2m	520/208
	Class 5: Pans and bare areas (species: Enneapogon desvauxii, Sporobolus ioclados)	56/23	First layer: • Life form: herbaceous vegetation • Mean percent cover: <15% • Mean height: 0.1m	1188/683

Table 5.1: Different vegetation morphology types and their physiognomic characteristics considered in this study as derived from field measurements.

Level	Scale parameter	Color/ shape	Smoothness/ compactness	No. of Objects	Mean area of object (sqm)
1	15	0.8/0.2	0.6/0.4	1091547	20358
2	20	0.8/0.2	0.6/0.4	541281	41068
3	30	0.8/0.2	0.6/0.4	217984	102048
4	40	0.8/0.2	0.6/0.4	119868	185609
5	50	0.8/0.2	0.6/0.4	77161	288408
6	60	0.8/0.2	0.6/0.4	54470	408625

Table 5.2: Segmentation parameters and associated object statistics for the six segmentation scales considered in the study.

Features	Description
Mean layer value	The mean value represents the mean brightness of an image object within a single band; used feature: Mean NDVI.
Ratios	The amount that a given band contributes to the total brightness; used feature: Ratio SWIR (Landsat TM band 6), Ratio NDVI.
Standard deviation	The standard deviation of all pixels which form an image object within a band; used feature: Standard Deviation Aspect, Standard Deviation Red, Standard Deviation Green, Standard Deviation Blue, Standard Deviation NIR., Standard Deviation GLCM (all bands).
Maximum difference	Minimum mean value of an object subtracted from its maximum value. The means of all bands belonging to an object are compared with each other and the result is divided by the brightness.
Texture after Haralick	GLCM (Grey Level Co-occurrence Matrix)calculated after Haralick et al. (1973): Describes how different combinations of pixel values occur within an object; used features (using the mean of all layers): GLCM Contrast, GLCM Dissimilarity, GLCM Standard Deviation, GLDV (Grey Level Difference Vector): The sum of the diagonals of the grey level co-occurrence matrix; used features (using the mean of all layers):GLDV Angular 2nd moment.

Table 5.3: Overview of the selected features that were used in final image classification.

	Class 1	Class 2	Class 3	Class 4	Class 5
Class 1	-	1.71	1.96	1.99	1.99
Class 2		-	1.61	1.82	1.99
Class 3			-	1.68	1.99
Class 4				-	1.98
Class 5					-

Table 5.4: Jeffrey's-Matusita distance class separability calculated on samples for the five vegetation morphology classes using the thirteen features used in final classification.

Scale	15		20		30		40		50		60	
Class	users	prod	users	Prod	users	prod	users	prod	users	prod	users	prod
Class 1	86.31	83.65	87.65	83.71	86.9	80.88	83.67	79.07	83.01	75	79.71	71.07
Class 2	85.55	83.21	82.06	80.44	79.43	78.53	85.08	77.16	74.55	70.29	70.99	69.7
Class 3	80.43	76.81	84.13	81.03	85.78	90.45	88.33	89.58	85.13	87.93	84.77	86.58
Class 4	70	66.52	70.84	71.74	74.64	75.37	83.16	80.41	84.1	84.88	86.01	76.39
Class 5	93.01	90.7	94.51	90.59	95.29	88.51	95.03	92.24	95.94	92.2	91.8	89.44
Overall accuracy	83.06	80.17	83.83	81.50	84.40	82.74	87.05	83.69	84.54	82.0	82.65	78.63
Kappa	0.76		0.79		0.81		0.82		0.81		0.79	

Table 5.5: User's-, producer's- and average accuracies calculated on independent samples at six segmentation scale outputs.

165

Chapter 6: Relating spatial patterns of fractional land cover to savanna vegetation morphology using multi-scale remote sensing in the central Kalahari

Introduction

Savannas are composed of a dynamic mixture of woody and herbaceous life forms with considerable variation in plant composition, biomass and net primary productivity (Hill et al. 2011a; Mistry 2000). At the global scale, tropical savannas play a major role in land-atmosphere energy balance; in southern Africa, arid and semi-arid savanna systems are important contributors to productivity and biodiversity, contain some of the largest wildlife habitats and offer the basis of economic activity (Furley 2004; Lal 2004; Stott 1991). Southern Africa's semi-arid savannas are xeric systems in which ecosystem and carbon dynamics are primarily controlled by seasonal rainfall and vegetation structure. They are often characterized as patchy, mainly the result of spatio-temporal variability in rainfall as well as fire history. Patch-level vegetation structure and composition determines water balance and ecohydrology in these systems (Caylor et al. 2003; Furley 2010; Privette et al. 2004). As a result of increasing anthropogenic pressure, changing land use, altered fire regimes and climatic shifts, vegetation in savannas in general and southern Africa semi-arid savanna systems in particular are undergoing large scale structural and functional changes (Adeel et al. 2005; Dougill et al. 1999; Scholes et al. 2002). These changes are in turn affecting biogeochemical processes and availability

166

of habitat-related key structural resources (e.g. solitary nesting trees, foraging grounds and migration routes) (Blaum et al. 2007; Dougill et al. 1999; Tews et al. 2004).

Long-term sustainability of these fragile and dynamic systems needs informed decision-making that requires the understanding of spatio-temporal variation in savanna ecological processes. This understanding depends on the ability to quantitatively characterize and monitor attributes of savanna vegetation (e.g. vegetation cover, density, condition) (Guerschman et al. 2009; Scholes and Walker 1993). While vegetation cover is treated as an important indicator in semi-arid systems, it is also a determinant of landscape function as it is related to the ability of the landscape to capture rainfall or lose it through surface runoff (Caylor et al. 2003; Ludwig et al. 2007). Further, in these ecosystems the exchange of energy and water balance is controlled by transpiration and evaporation through the proportion of photosynthetically active vegetation (f_{PV}), non-photosynthetically active vegetation (f_{NPV}) and bare soil (f_{BS}) (Asner et al. 2011; Scanlon et al. 2002). In semi-arid savannas, f_{NPV} is intimately related to fire frequency and intensity (Roy et al. 2011) and f_{BS} controls wind and water erosion (Okin et al. 2009).

Field-based measurements of fractional cover in savannas are limited in scope and scale, especially when considering systems that are vast, remote and wild. Remote sensing provides an important tool for estimating fractional cover of vegetation as an indicator that can not only complement field measurements but also provide much larger spatial coverage (Asner et al. 2011; Hill et al. 2011b). However, remote sensing-based characterization of fractional vegetation cover in semi-arid systems is challenging for

167

several reasons: high soil background leading to minimization of spectral contribution of plants, lack of a strong red edge and reduced absorption in visible wavelengths due to evolutionary adaptations of semi-arid vegetation, potential of non-linear mixing in arid and semi-arid areas due to multiple scattering and high spectral variability within individuals of similar species (Asner 1998; Huete and Jackson 1988; Okin et al. 2001b). In remote sensing, green vegetation traditionally has been quantified based on vegetation indices (VIs) such as Normalized Difference Vegetation Index (NDVI) while Cellulose Absorption Index (CAI) has been used to differentiate non-photosynthetic vegetation from green vegetation and soils (Daughtry et al. 2006; Guerschman et al. 2009; Nagler et al. 2003). Unlike NDVI, calculating CAI requires high spectral resolution in SWIR wavelengths that is only available with hyperspectral sensors (e.g. AVIRIS, EO-1 Hyperion). Although VIs have been used widely in the remote sensing of vegetation, they have been critiqued for only being able to provide an indirect surrogate of vegetation cover and not being able to estimate total vegetation cover (especially non-photosynthetic vegetation) (Elmore et al. 2000; Okin 2007b; Yang et al. 2012). Improving upon the limitations of VIs, and also addressing the issue of sub-pixel heterogeneity, some studies have adopted a promising alternative called linear spectral mixture analysis (SMA). SMA is less affected by soil background effects (Garcia-Haro et al. 1996) and provides sub-pixel abundance estimates based on the assumption that spectral signature of a pixel is a linear, proportion-weighted combination of endmembers (i.e., pure spectra of ground components) (Adams et al. 1995; Asner and Lobell 2000; Roberts et al. 1993). While the accuracy of SMA-derived fractional cover estimates depends highly on endmember

168

purity, among other things, a single endmember model may fail to account for natural variability in the reflectance of endmembers. Multiple Endmember Spectral Mixture Analysis (MESMA) addresses this issue by allowing both the type and number of endmember models to vary on per pixel basis (Okin et al. 2013; Somers et al. 2011). MESMA has been widely utilized with hyperspectral images (e.g. AVIRIS) for deriving fractional cover estimates in several ecosystems including xeric systems(Asner and Heidebrecht 2002; Mishra and Chaudhuri 2013; Okin et al. 2001b; Ustin et al. 2004). Although hyperspectral images provide detailed reflectance information for fractional cover mapping using MESMA, their utility is largely restricted due to limited spatial coverage and data, especially over Southern African savannas. In contrast, multi-spectral remote sensing products at both medium (e.g. Landsat, ASTER) and coarse (e.g. MODIS) spatial resolutions provide synoptic spatial extent and repeated coverage, but lack spectral sensitivity and ideal bands in the SWIR, where discrimination of non-photosynthetic vegetation and soil is most effective (Asner and Lobell 2000). Hence, MESMA of Landsat/ASTER imagery has provided modest results for fractional cover estimation compared to hyperspectral estimates (Asner and Heidebrecht 2002; Gill and Phinn 2008; Theseira et al. 2002). Imagery at coarse spatial resolution (e.g. MODIS) provides regional scale coverage but has lower spectral resolution and therefore endmember determination and reliable fractional cover estimation are even more challenging. In a more recent study for mapping $f_{PV,}$ f_{NPV} and f_{BS} with MODIS imagery over Australian tropical savanna, Guerschman et al. (2009) leveraged the availability of spatially and temporally coincident hyperspectral images (i.e. EO-1 Hyperion) to develop

169

a MODIS-based fractional cover mapping product. In the present work, no hyperspectral image is available close to the date of fieldwork, and therefore we employ an empirical approach to derive endmembers for coarse scale images by using spatially and temporally coincident high and medium spatial resolution images.

Recent availability of high spatial resolution (i.e. < 2.5 m) multi-spectral datasets (e.g. GeoEye-1, Quickbird) presents new opportunities for testing their suitability for fractional land cover mapping. For analyzing high spatial resolution imagery most of the previous studies have adopted either a per pixel classifier (Dennison et al. 2010; Wang et al. 2004) or an object based approach (Laliberte et al. 2004; Mallinis et al. 2008; Mishra and Crews 2014a); but very few have considered using spectral unmixing for sub-pixel abundance estimation in natural landscapes. In a recent study, Hamada et al.(2011) successfully utilized MESMA of Quickbird imagery to characterize conditions of sage scrub community in Southern California.

Since savannas are structurally heterogeneous and functionally diverse systems, vegetation morphology ranges from dense shrubland and woodland to medium dense shrubland with grasses and open grassland with little shrub cover (Sankaran et al. 2005). In these heterogeneous systems it is not only important but ecologically more meaningful to examine how the magnitude of fraction of cover types (i.e. PV, NPV and bare soil) and estimation error is dependent on vegetation morphology class. Very few previous studies (Gessner *et al.* 2013) have considered systematic investigation of this spatial association. Furthermore, with increasing availability of remotely sensed data at multiple spatial

scales, it is essential to examine how changing spatial resolution impacts the characterization of both fractional cover estimates and its spatial association with vegetation morphology. This study investigates these important research questions by adopting a multi-scale hierarchical nested approach that combines fractional cover estimates and vegetation morphology characteristics derived *in situ* with those estimated using spatially and temporally coincident multispectral images at high (GeoEye-1), medium (Landsat TM) and coarse (MODIS) spatial resolutions in the central Kalahari.

Site and situation

Located between 21º-24º S and 22º-26º E, the Central Kalahari occupies the central part of the larger Kalahari sand basin and is part of the southern African semi-arid savanna system (Makhabu et al. 2002). The study area covers 22,607 km^2 of which more than 70 percent falls under protected area (i.e. the Central Kalahari Game Reserve) and the rest is under private game farms and open-access commercial ranching (Figure 6.1). The climate is continental and the long-term average of mean annual precipitation (MAP) is 350-400 mm with high variability that increases with decreasing precipitation. Geologically, the area is dominated by the Kalahari sands with sporadic outcrops of calcrete, sandstone and schist of the Karoo sequence in the Ghanzi Ridge. The area is mostly flat with a mean altitude of 950 m (Moore and Attwell 1999). Water availability is limited to small, short-lived accumulations in occasional pan depressions (Dougill and Trodd 1999). The vegetation is characterized by spatially complex and structurally heterogeneous mixture of woody and herbaceous species and exhibits temporally distinct

phenological patterns. Following the rainfall gradient in general, the study area represents an ecotone with north and central part dominated by broad-leafed species (e.g. *Lonchocarpus nelsii, Terminalia sericea, Bauhinia petersiana*) which is gradually replaced by fine-leafed species (e.g. *Acacia erioloba, A. luederitzii, Ziziphus mucronata*) in the southern part (Moore and Attwell 1999). Plant species diversity is relatively low for all plant communities in the study area. The difference among communities is related to changes in species dominance rather than occurrence of different species and thus vegetation boundaries based on plant species are often unclear (Makhabu et al. 2002; Shugart et al. 2004). Fire during the late dry season is an important determinant of vegetation dynamics. Based on land use, the study area is comprised of protected area (i.e. Central Kalahari Game Reserve), community areas, and game and cattle farms. Based on geomorphic attributes, the study area can be categorized into four broad landscape types i.e. the fossil river valleys and pans, dunes, inter-dunal areas and plains (Makhabu et al. 2002). As in much of southern Africa's savannas, pans are geomorphologically distinct features in the study area and are important as they provide mineral licks (Parris 1971; Parris and Child 1973) and relatively nutrient-rich vegetation, attracting large herbivores and their associated predators and concomitant tourism (Thouless 1998).

Data and Methods

Field data collection

In situ data on fractional cover and vegetation morphological characteristics were acquired during two field campaigns. Fractional cover of f_{PV}, f_{NPV} and f_{BS} were quantitatively estimated in the field using 30 m transects following the line intercept approach modified from Herrick et al. (2005). Each transect was divided into segments of 50 cm (total 60 segments within one transect) for which fractional cover of f_{PV}, f_{NPV} and f_{BS} was visually interpreted and recorded. The fraction of each cover type was averaged from these 60 segments to get the f_{PV}, f_{NPV} and f_{BS} for the whole transect. Transect locations were spatially distributed to capture all important vegetation morphology classes in the study area. Due to serious accessibility and safety issues (e.g., danger of predator attack), these transects could not be established away from tracks except in pan and more open areas. Combining the fieldwork conducted during 18 May- 2 June 2011 and 11-28 May 2012 fractional cover was estimated for over 148 transects. At each of these transects, geographic coordinates were recorded at the start and end points using consumer-grade global positioning system (GPS) equipment. Additional information included visual interpretation of dominant vegetation functional type (e.g. woody versus herbaceous), minimum, maximum and average vegetation height, dominant tree/shrub species, and pictures acquired with a digital camera. These characteristics were also interpreted and recorded at 143 more locations where setting up transects were not possible due to high vegetation density and safety issues.

To avoid the influence of seasonality, field data on fractional cover were collected in the same month as image acquisition (i.e. May). In spite of the temporal difference between image acquisition and *in situ* data collection, this study could directly compare

173

them because of the following evidence: (i) the study area lies completely inside a protected area and does not have any anthropogenic influence, (ii) due to low animal density the grazing impact from herbivores is very minimal. Although, spatio-temporal pattern of rainfall in the central Kalahari is highly variable, in this study there are no means to quantify this because the nearest meteorological station (i.e. Maun) is about 150 km north of the study area.

Remotely sensed data

Three types of remotely sensed images were used in this study: GeoEye-1/SPOT, Landsat TM and MODIS NBAR (Table 6.1). The study area covered a total area of approximately 22,607 km^2, with 100% MODIS coverage and 98.6% Landsat TM coverage (22,291 km^2) after masking clouds. The eight tiles of GeoEye-1 imagery and six SPOT-5 scenes covered 1,353 km^2 (6 %) and 15,821 km^2 (70%) of the study area respectively. The GeoEye-1 multispectral image data consisted of 2-m blue, green, red and near-infrared bands and a 0.5-m panchromatic band acquired on May 16, 2010 at 10:46 local time (08:46 UTC). The spatial resolution of the SPOT data was 2.5 m and was temporally not coincident with other datasets (Table 6.1). At medium spatial resolution (30 m), the six reflective bands (excluding thermal band) of the Landsat TM imagery acquired at 10:16 local time (08:16 UTC) on May 9, 2010 were used. At the coarsest spatial scale this study used a MODIS product (MCD43A4) developed by combining the highest quality pixels from both Terra and Aqua. MCD43A4 is a nadir BRDF-adjusted reflectance (NBAR) product that provides a 16-day, 463.3 m reflectance

174

corrected for bidirectional reflectance distribution function (BRDF) and atmospheric effects creating an apparent surface reflectance that is not affected by the locations of the sensor relative to the pixel at the time of data acquisition (Cescatti et al. 2012; Román et al. 2009). Since the SPOT images used in this study were temporally not coincident with the other three datasets (i.e. GeoEye-1, Landsat TM and MODIS data), it was only used for interpreting vegetation morphological properties and not for estimating fractional cover (Table 6.1).

Image pre-processing

While all the GeoEye-1 scenes were cloud-free, clouds and cloud shadows in the Landsat TM imagery were manually digitized and masked prior to radiometric calibration. Both GeoEye-1 and Landsat TM images were atmospherically corrected using ATCOR algorithm. ATCOR is an absolute atmospheric correction method that applies an atmospheric look-up table based on a large database containing the result of radiative transfer calculation from the MODTRAN-4 radiative transfer code (Richter and Schläpfer 2008). The optical depth of the atmospheric aerosols was calculated by comparing modeled at-sensor radiance with measured radiance in the red band of areas with dark dense vegetation. This correction was then applied on each pixel to derive surface reflectance. Radiometric calibration of the MODIS product (MCD43A4) was not required since it is a surface reflectance product. The original MODIS pixel size of 463.3 m was resampled to 450 m using nearest neighbor approach in order to make comparison with Landsat TM (1 MODIS pixel=15x15 Landsat TM pixels). For consistent

comparison of fractional cover results across multi-scale datasets it was very important that all images have minimal registration mismatch. Thus, considering the Landsat TM as the base image, the GeoEye-1 imagery was co-registered using 34 carefully selected ground control points with RMSE value of 6.1 m. In the second step, MODIS imagery was co-registered considering the Landsat TM as base image using 16 ground control points resulting in RMSE value of 92.4 m.

Endmembers selection and MESMA

MESMA was applied to GeoEye-1, Landsat TM and MODIS imagery for estimating fractional cover. All the images were acquired in the month of May, the beginning of dry season when trees and shrubs were still green whereas herbaceous vegetation was dry and contained no observable green foliage. For the GeoEye-1 imagery Normalized Difference Vegetation Index (NDVI) was calculated which was found to be weakly correlated with the red band ($R^2 = 0.39$) and very weakly correlated with the NIR band ($R^2 = 0.09$). Thus the NDVI was considered as a non-linear combination of red and NIR bands and was stacked with the existing GeoEye-1 bands before endmember selection and MESMA analysis. For both GeoEye-1 and Landsat TM imagery, endmembers were selected based on: (i) pixel purity index (PPI) values, obtained from the minimum noise fraction transformed spectral bands, (ii) visualization and interpretation of the multi-dimensional feature space plots and spectral indices values, and (iii) spatially overlaying the candidate pixels on very high resolution imagery to examine their purity (Urban et al. 1987; Vos et al. 2001). The candidate spectra were finally analyzed quantitatively using three fit matrices available in the VIPER tools

software program (www.vipertools.org): Endmember Average RMSE to select endmembers that produced the lowest RMSE within a class (Dennison and Roberts 2003), Minimum Average Spectral Angle that isolates endmembers with the lowest average spectral angle (Dennison et al. 2004) and Count Based endmember selection (Roberts et al. 2003). Utilizing these purity measures, finally, seven, eight and ten endmembers for the GeoEye-1 image and thirteen, nine and nine endmembers for the Landsat TM image were selected for PV, NPV and soil respectively.

Selecting endmembers for the MODIS imagery was the most challenging, since at this spatial resolution in semi-arid savanna systems pixels with a single homogeneous cover of PV, NPV or soil does not exist. Hence a multi-scale empirical approach was adopted for addressing this challenge. First, PPI values were calculated for the MODIS imagery and the pixels below an empirically determined threshold PPI value were masked. The remaining pixels (n=112) were considered endmember candidates and were converted into vector polygons that were used for clipping their corresponding area of the shade-normalized fractional cover output from MESMA of the Landsat TM imagery (15x15=225 pixels, area equivalent to 1 MODIS pixel). Mean f_{PV}, f_{NPV} and f_{BS} content were calculated for each of these clipped outputs and were ordered into decreasing content. Finally, pixels with at least 75 % mean f_{PV}, f_{NPV} and f_{BS} content were selected for visual determination of purity by overlaying on the GeoEye-1 and SPOT images. This empirical approach resulted in the selection of two PV, three NPV and two bare soil endmembers for MODIS (Figure 6.2).

177

MESMA was performed on all images using the VIPER tools program. Non-shade endmember fractions are calculated in VIPER tools using singular value decomposition and shade is calculated as 1 minus the sum of all non-shade endmember fractions. Since MESMA allows both type and number of endmembers to vary on a per-pixel basis, in this study three endmember model schemes (two-, three- and four-endmembers) were tested on each pixel for GeoEye-1 and Landsat images, while MODIS was unmixed with only four-endmember models. Shade was always present in all models to account for variation in illumination within scene. All possible permutations of spectra described in table 6.2 were tested for each pixel.

MESMA analysis was partially constrained with minimum and maximum allowable fractions and the $RMSE_S$ threshold set to -0.05, 1.05 and 0.025 respectively ($RMSE_S$ is the root mean squared error of the modeled vs pixel spectra). A pixel was left unmodeled when no model met the constraints. Finally, the best mixing model for each GeoEye-1 and Landsat TM pixel was selected in two steps: first, the model producing the lowest $RMSE_S$ was selected as the best model for each pixel at each model complexity level. In the second step, output composites of two-, three- and four- endmember models were compared. Since a three-endmember model will always produce a lower $RMSE_S$ than a two-endmember model (same for four versus three-endmember model results) the following criteria were adopted for their comparison: (i) if a three-endmember model had a lower $RMSE_S$ than a two-endmember model and the three-endmember model exceeded a predefined threshold of decreased $RMSE_S$ (0.007, determined empirically in this study similar to Powell and Roberts 2008), then the three endmember model was considered

178

superior for that pixel; otherwise, the two-endmember model was selected as superior. (ii) if a four-endmember model had a lower RMSE$_S$ than the best three-endmember model and the four- endmember model exceeded a same threshold then the four-endmember model was selected; otherwise the three-endmember model was considered better.

Mapping vegetation morphology classes

Using field data in combination with GeoEye-1 images, five vegetation morphology classes were developed (based on vegetation physiognomy and structure). These classes were: (i) Mixed deciduous woodland with shrubs and herbaceous layer, (ii) Mixed (70-40%) medium high shrubland with open short herbaceous layer, (iii) Mixed (40-10%) medium to high shrubland with open short herbaceous layer, (iv) Medium tall grassland with medium-high shrubs and (v) Pans and bare areas. These classes were mapped in a separate study (Mishra and Crews under review) by combining hierarchical object-based image analysis of the Landsat TM imagery with random forest classification.

Fractional cover validation/association with vegetation morphology classes

In this study, *in situ* fractional cover estimates were first used to evaluate fractional cover estimates obtained from MESMA of GeoEye-1. *In situ* transect-derived estimates were compared to the mean $f_{PV,}$ f_{NPV} and f_{BS} of spatially coincident 225 GeoEye-1 pixels (15x15 pixel window equivalent to the 30 m transect length). However, direct comparison of *in situ* fractional cover estimates with those derived at Landsat TM and MODIS spatial resolutions was deemed inappropriate given the high degree of spatial

heterogeneity recorded in the field and visible in the GeoEye-1 imagery as well as the limited transect length (30 m). Hence, fractional estimates derived at coarser resolution were evaluated against the GeoEye-1 fractional cover estimates. For this purpose, sample pixels equivalent to the size of MODIS were selected from part of the study area where all three satellite products were spatially coincident. An important criterion for selecting these samples was their homogeneity in terms of vegetation morphology with at least 70% area of each sample covered by a single vegetation morphology type. This approach resulted in the selection of total 273 MODIS pixels. Before fractional cover validation, shade fraction from all the fractional cover products was taken out by dividing the fraction of each non-shade endmember by the sum of non-shade endmembers. For each of the 273 MODIS pixels, the shade-normalized f_{PV}, f_{NPV}, f_{BS} and MESMA-derived $RMSE_S$ value were recorded. Further, their corresponding pixels from the shade-normalized fractional cover product derived from Landsat TM (225 pixels) and GeoEye-1 (50625 pixels) were cropped and mean f_{PV}, f_{NPV}, f_{BS} and $RMSE_S$ were calculated. Finally, Landsat TM and MODIS-derived fractional estimates and $RMSE_S$ were evaluated by comparing them with mean f_{PV}, f_{NPV}, f_{BS} and $RMSE_S$ derived from GeoEye-1.

Accuracy of fractional cover estimates were accessed using the following statistical measures: (i) mean error (ME_C), which preserves the sign of error and provides overall bias in error, (ii) mean absolute error (MAE_C), the average absolute difference between observed and predicted values which is less affected by outliers (iii) $RMSE_C$, the square root of the mean squared difference between observed and predicted values, which puts relatively high weights to large errors, and, finally (iv) correlation between observed

and predicted fractional cover. The subscript "$_C$" (as opposed to the subscript "$_S$" used above) refers to mean error, mean absolute error, and root mean squared error calculated in the comparison of cover estimates. Validation was conducted first by considering all 273 samples to assess overall agreement and then by grouping samples based on five vegetation morphology classes for examining the spatial association of vegetation physiognomy with fractional cover magnitude and modeling error.

Results

Overall agreement

Comparison of $RMSE_S$ values obtained for the satellite datasets showed that highest $RMSE_S$ and variance in $RMSE_S$ was observed for unmixing of the GeoEye-1 imagery while Landsat TM produced the lowest $RMSE_S$ values (Figure 6.4). $RMSE_S$ obtained with GeoEye-1 was nearly three times higher compared to those obtained with Landsat TM and MODIS. Comparison of the multi-scale fractional cover estimates indicates that with increasing pixel size the magnitude of overall error (i.e. MAE_C and $RMSE_C$) increased consistently for all fraction cover types (Table 6.3). Among the three satellite datasets, the lowest overall error is observed with GeoEye-1 (e.g. MAE_C 5.3% and $RMSE_C$ 6.5%, fractional cover units) and highest overall error was observed with MODIS (e.g. MAE_C 12.9% and $RMSE_C$ 15.9%, fractional cover units) for all cover types (Table 6.3). Box plots reveal that increasing pixel size results in increasing variance in the fractional estimates for all cover types, but the magnitude of increase in variance of f_{NPV} and f_{BS} is much higher compared to f_{PV}. Additionally, with increasing pixel size f_{NPV}

is consistently overestimated with a corresponding underestimation of f_{BS}. On the contrary, f_{PV} estimates are comparatively unbiased even at coarse spatial resolution (Figure 6.5.f) and indeed f_{PV} exhibited the lower error compared to f_{NPV} and f_{BS} across all spatial scales (Table 6.3). Comparison of field-derived versus GeoEye-1-derived fractions indicates good agreement, producing low overall MAE_C and $RMSE_C$ for all ground cover components and high (positive) correlation with f_{PV} (r^2= 0.76) , f_{BS} (r^2= 0.67) and f_{NPV} (r^2= 0.70) estimates. GeoEye-1 imagery estimated f_{PV} with higher accuracy compared to f_{NPV} and $f_{BS,}$ possibly due to the lack of spectral bands in the SWIR bands in which f_{NPV} and f_{BS} are most easily separated (Asner and Lobell 2000; Guerschman et al. 2009; Nagler et al. 2003; Okin 2007b). Furthermore, GeoEye-1-derived fractional cover estimates indicate lower variance than those estimated with Landsat TM and MODIS (Figure 6.5.f).

Both overall (MEA_C: 8.9%, $RMSE_C$: 10.8%) and cover specific (i.e. PV, NPV and soil) fractional cover errors in Landsat TM are lower than those derived from MODIS (overall MEA_C: 12.9%, $RMSE_C$: 15.9%) (Table 6.3). With Landsat TM, the variance in estimated f_{PV} is smaller than the variance of f_{NPV} and f_{BS} (Figure 6.5.f). MODIS produced the highest $RMSE_C$ among the tree satellite dataset, and, cover specific difference in $RMSE_C$ are apparent as f_{PV} showed lower $RMSE_C$ (i.e. 12.9%) than f_{NPV} and f_{BS} (i.e. 18.3 % and 16% respectively) (Table 6.3).

Spatial association with vegetation morphology

Analysis of RMSE$_S$ values considering vegetation morphology classes indicate that medium-tall grassland with medium-high shrubs (i.e. class 4) produce lowest RMSE$_S$ values among all the vegetation morphology classes across the three considered spatial resolutions (Figure 6.4). A likely explanation for this pertains to the comparative structural and functional homogeneity of the vegetation morphology class 4 with predominant grass cover and low shrubs covering large areas that are spatially homogeneous even if observed at coarse spatial resolutions. In contrast, vegetation morphology class 1 and 2 produce higher mean RMSE$_S$ due to inherent structural and functional heterogeneity. Pan areas (morphology class 5) do not produce the lowest mean RMSE$_S$ since these areas often contain encroached patches of small to medium high shrubs, tree islands and variation in soil reflectance.

In the central Kalahari, fractional cover of ground cover components varies considerably among the five vegetation morphology classes. As expected, f_{PV} is dominant (i.e. highest of all cover types) and co-dominant in areas with vegetation morphology class 1 (Mixed deciduous woodland with shrubs and herbaceous layer) and class 2 (Mixed (70-40%) medium high shrubland with open short herbaceous layer) respectively (Figure 6.4.a and 6.3.b). On the contrary, f_{NPV} is dominant ground cover component in both vegetation morphology class 3 (Mixed (40-10%) medium to high shrubland with open short herbaceous layer) and class 4 (Medium tall grassland with medium-high shrubs) (Figure 6.4.c and 6.4.d) across all three spatial resolutions. In vegetation morphology class 5 (Pans and bare areas), f_{BS} is the dominant cover type across all spatial resolutions (Figure 6.5.e). Comparison of results across spatial resolutions also indicate

183

that at coarser resolution, fractional estimates are biased but the amount of bias and the ground cover component for which the estimates are biased, depends on the vegetation morphology class as well as spatial resolution of imagery. In general, in areas with vegetation morphology class 1 and 2, as the pixel size increases, f_{PV} was overestimated at the cost of mainly underestimating f_{BS} (Figure 6.5.b and 6.5.c). In morphology class 3 and 4, at coarser spatial resolution, f_{NPV} is overestimated with a corresponding underestimation of both f_{PV} and f_{BS} (Figure 6.5.d and 6.5.e) whereas in areas of morphology class 5, f_{NPV} is overestimated at the cost of underestimating f_{BS} (Figure 6.5.f). For all vegetation morphology classes, the error in fractional cover is lower for Landsat TM compared to MODIS. Further, comparison of fractional cover error among five vegetation morphology classes reveals class-specific differences in error. For example, $RMSE_C$ obtained for MODIS shows that for morphology class 1 the highest $RMSE_C$ was recorded for f_{PV}, compared to morphology class 4 and 5 for which highest $RMSE_C$ is observed for f_{NPV} (Table 6.3).

Discussion

Overall agreement across image spatial resolution/ground cover components

In this study, we compare absolute estimates of f_{PV}, f_{NPV} and f_{BS} derived from MESMA of three datasets to examine the impact of changing spatial resolution as well as vegetation morphology on fractional cover estimation accuracy. Comparison of results among datasets at different spatial resolution is important since trade-off between spatial resolution and swath width of spaceborne platforms constrains potential strategies of

observation. Given the same mapping method (i.e. MESMA), comparison among results from different datasets provides information on the inherent limitation of these datasets. High magnitude as well as high variance in $RMSE_S$ values for GeoEye-1 could be attributed to the high variability in the reflectance that could be captured with GeoEye-1 in structurally heterogeneous semi-arid savanna. At high spatial resolution, GeoEye-1 imagery was able to distinguish individual tree/shrub canopies and also capture intra- and inter-canopy details e.g. sunlit versus shaded areas, green versus senescent foliage (Schmitz et al. 2000). Moreover, besides high spectral variability, at the high spatial resolution of GeoEye-1, the impact of non-linear mixing of spectra is also high. Such non-linear mixing is not modeled with MESMA as it assumes linear mixing of endmember spectra at pixel level and thus likely results in high residual error when non-linear unmixing is important. Unlike GeoEye-1, at medium spatial resolution, Landsat TM imagery is unable to capture the both intra- and inter-canopy details and pixels reflectance is the sum of the spectral properties of sub-constituents of 900 m^2 area. At even coarser spatial resolution (i.e. MODIS), the increasingly larger pixel footprint averages the spatial variability even more and thus resulting in lower $RMSE_S$.

Contrary to high $RMSE_S$ values GeoEye-1 results depicted good agreement with the *in situ* derived fractional estimates and produced low $RMSE_C$ values. This result could be attributed to high spatial resolution of GeoEye-1 that is similar to the average size of individual shrub canopies in the study area, which minimizes the spectral confusion between ground cover components. Lower $RMSE_C$ for GeoEye-1 estimated f_{PV} in comparison to f_{NPV} and f_{BS} could be attributed to lack of spectral bands in short wave

infrared (SWIR) which is required for the separation of to f_{NPV} and f_{BS} (Asner and Lobell 2000; Nagler et al. 2003; Okin 2007b).

In spite of better spectral coverage than GeoEye-1, both Landsat TM and MODIS produce comparatively high error in estimation of fractional cover due to much lower spatial resolution. Although spectral mixing occurs across spatial scales, in heterogeneous semi-arid savanna systems, with increasing pixel size (i.e. decreasing spatial resolution), pixels reflectance become an increasingly more complex mixture of functionally and structurally different vegetation (e.g. woody versus herbaceous) types and soil. Thus, in contrast to high spatial resolution (e.g. GeoEye-1) where most pixels are likely dominated by a single cover type, at increasingly coarse spatial resolution most pixels are mixed and have more than one cover type. The mean f_{PV}, f_{NPV} and f_{BS} calculated from 50,625 GeoEye-1 pixels (equivalent to 1 MODIS pixel), thus produces accurate and representative fractional cover estimate. On the contrary, pixels at coarse spatial resolution (MODIS) have high level of mixed cover and it is more difficult to accurately derive the fractions of larger mixed pixel. This results in high fractional cover error compared to high spatial resolution estimates. Additionally, both bias and error in the fractional cover estimates derived with MODIS may also be attributed to the likely spectral impurity of MODIS endmembers. In heterogeneous ecosystems such as savanna, decreasing spatial resolution imposes significant limitation on the ability to select endmember spectra from images (i.e. "image endmembers") with commonly available multispectral sensors especially for NPV and soil (Okin and Roberts 2004). While dominant spectral features such as "red edge" provide a physical basis for identifying PV

endmember, locating and distinguishing NPV and soil endmember spectra is particularly challenging since their spectrum could be statistically similar in VNIR and requires high spectral resolution in SWIR wavelengths for separation (Nagler et al. 2003; Okin et al. 2001b). To determine endmembers at coarse spatial scale (i.e. MODIS), this study leveraged the availability of spatio-temporally coincident multi-scale images and employed a multi-scale hierarchical approach. Although final MODIS endmembers used here were the best that this approach combined with our field knowledge could produce, they were not absolutely pure and likely contained small fraction of bare soil and NPV. Nevertheless, at coarse scales, this spectral contamination is unavoidable when image endmembers are used.

Spatial association of fractional cover/estimation error with vegetation morphology types

Our results indicate that besides spatial resolution, vegetation morphology also exerts control on the accuracy of fractional cover estimates in the central Kalahari. The vegetation morphology classes found in the study area vary considerably in terms of vegetation physiognomic characteristics impacting error in a manner dependent on vegetation morphology as well as levels of fractional cover of PV, NPV and bare soil. Field data combined with GeoEye-1 imagery confirmed that areas with vegetation morphology class 1 and 2 represent landscapes where woody life forms (i.e. trees and shrubs) were dominant or co-dominant with average height of woody component reaching over 8m and 5m respectively (Figure 6.3). In contrast, herbaceous life-forms were co-dominant and dominant in vegetation morphology class 3 and 4 respectively

with main distinguishing factor being the difference in the relative shrub density. Soil was the dominant cover type in areas classified as vegetation morphology class 5 (Figure 6.3).

This study was conducted in an area with low anthropogenic pressure and where natural processes (e.g. rainfall, fire) are the most important determinants of savannas structure and function. To a certain extent, vegetation structure/land cover characteristics in the study area can be treated as representative of other naturally occurring semi-arid savanna systems found not only in southern Africa but also in other parts of the world (e.g. northern Africa, Australia, and South America). Therefore, this study has several implications for estimating f_{PV}, f_{NPV} and f_{BS} in semi-arid systems using MESMA of commonly available multispectral images at high, medium and low spatial resolution. GeoEye-1-derived fractional cover estimates indicated good agreement with field-derived estimates. Although the accuracy of GeoEye-1-derived fractional estimates also varied depending on the vegetation morphology class, the magnitude of error (i.e. over/under estimation) was much lower compared to those obtained from coarser-scale data. Although MESMA of GeoEye-1 produced the most accurate fractional estimates, it has limited applicability for landscape- or regional-scale fractional cover assessment due to smaller spatial coverage and high cost. Moreover, because of high spectral variability associated with high spatial resolution of GeoEye-1 data, deriving estimates within acceptable $RMSE_S$ (generally within 2.5% of reflectance) requires multiple endmembers for each endmember type. This combined with large data volume increases the computing time for MESMA significantly making its applicability over large areas

188

difficult. Conversely, MESMA of medium spatial resolution imagery (e.g. Landsat TM) is both cost/time effective, providing landscape scale coverage with acceptable accuracy except in areas with high structural heterogeneity within semi-arid systems. While MODIS can provide regional-scale coverage, in semi-arid central Kalahari this study found that compared to results obtained with higher spatial resolution images, MODIS-derived fractional cover estimates had high $RMSE_C$ particularly for f_{NPV} and f_{BS}. In heterogeneous ecosystems, using high-resolution imagery to evaluate coarse-resolution fractional cover results is a more robust validation approach compared to previous studies (e.g. Guerschman et al. 2009) that utilized field transects with length much smaller than a single pixel. Furthermore, results of this study present a more realistic sensitivity analysis compared to previous studies. For example, in examining the impact of reduced spectral resolution, Asner and Heidebrecht (2002) convolved AVIRIS to spectral bands of commonly available multi-spectral sensors (e.g. Landsat TM, ASTER, MODIS) without changing the original spatial resolution of AVIRIS data (i.e. 19 m). However, this study utilizes original images (instead of spectrally convolved), thus, allowing both the spatial and spectral resolution to vary, representing the actual suitability of these data sets for fractional cover estimation.

There are some sources of uncertainty inherent in the data and method used in this study. Due to the fine-scale spatial heterogeneity in the study area, the separation of f_{PV} and f_{NPV} in the field using visual interpretation was difficult and subjective to some extent. Thus, even with best efforts and careful interpretation, *in situ* derived fractional estimates may have some unquantifiable observer error. The use of GeoEye-1 imagery

189

circumvent this limitation and provide means to 'ground-truth' Landsat TM and MODIS-derived fractional estimates produced over greater spatial extents. Admittedly, however, this evaluation depends on whether one accepts that the accuracy of the MESMA-derived fractional cover estimates from GeoEye-1 is acceptable, especially in light of potential error in the field discrimination of f_{PV} and f_{NPV}. Additionally, temporal differences between collection of *in situ* data (i.e. May 2011, 2012) and image acquisition (i.e. May 2010) also likely reduces the accuracy of GeoEye-1-derived fractions to some extent as vegetation dynamics in central Kalahari are rainfall-driven and rainfall is in-turn characterized by high spatio-temporal variability (Scanlon et al. 2005; Scholes et al. 2002). Furthermore, although MESMA addresses the issue of variability in the endmember spectra, it still assumes linearity in the mixing of endmember spectra. However, in semi-arid systems complex vegetation structure leads to non-linear mixing which may limit the accuracy of MESMA to certain extent (Okin and Roberts 2004).

Summary

In this study, we employed MESMA to quantitatively estimate $f_{PV,}$ f_{NPV} and f_{BS} using images at high, medium and low spatial resolutions to examine the comparative suitability and limitations of the three datasets. We also assessed the spatial association of fractional cover and mapping error with vegetation morphology classes at three spatial resolutions in the semi-arid central Kalahari. Results indicate that even with limited spectral dimensionality, MESMA of high spatial resolution imagery (i.e. GeoEye-1) could estimate fractional cover with high accuracy. Validation of fractional cover obtained from medium (Landsat) and low (MODIS) spatial resolution datasets against the

GeoEye-1-derived estimates indicated that error in fractional estimates increased with decreasing spatial resolution. With increasing pixel size, variance in fractional cover also increased depending on cover type. Overall, at reduced spatial resolution, while f_{PV} could be estimated with comparatively smaller error across scales, f_{NPV} was overestimated whereas f_{BS} was underestimated. Further analysis considering vegetation morphology indicated that observed error in fraction cover magnitude also depended on ecosystem structure. At reduced spatial resolutions, in areas with dominant woody vegetation (morphology types 1 and 2) at a time when woody canopies were mostly green, f_{PV} was overestimated at the cost of mainly underestimating f_{BS}; in contrast, in areas with dominant herbaceous vegetation (morphology types 4 and 3) at a time when herbaceous vegetation was mostly senescent, f_{NPV} was overestimated with a corresponding underestimation of both f_{PV} and f_{BS}. Few previous studies in semi-arid systems (Elmore et al. 2000; Smith et al. 1990) have only indirectly attributed the impact of spatial heterogeneity in vegetation community structure on the accuracy of remotely derived biophysical attributes. This study furthers our understanding in this regard by mapping fractional cover and systematically analyzing its relationship with vegetation morphology across spatial scales.

Our results have broader significance for studies utilizing commonly available multispectral imagery at different spatial scales, particularly for characterizing structurally heterogeneous and logistically challenging semi-arid savanna systems. Although coarse resolution imagery provides suitable spatial extent for regional-scale monitoring in semi-arid systems, their fractional cover estimates are biased with low

accuracy especially for f_{NPV} and f_{BS}. A multi-scale approach would be essential in developing new methods to address this challenge. While previous studies have evaluated fractional estimates derived with coarse resolution imagery against *in situ* data (Guerschman et al. 2009; Okin et al. 2013), this approach remains problematic in heterogeneous semi-arid systems due to (i) limited number and distribution of field transects and (ii) transect length that is often much smaller than a single pixel size (i.e. < 500 m). High spatial resolution imagery can be helpful in not only model calibration (e.g. endmember selection, understanding spatial heterogeneity), but can also circumvent these limitations by enabling accurate and spatially comprehensive fractional estimates that can be used for ground-truthing coarser scale results. Although, in this study, GeoEye-1 imagery provided acceptable levels of fractional cover error, a limitation of this approach is the computational time and computing resources required for large volume of data. A possible solution to this issue could be either implementing MESMA in a parallel processing environment (Okin et al. 1998) or unmixing only selected subset/sample areas of high resolution imagery with comparable *in situ* data or known vegetation morphology. Further, considering factors such as data availability/cost, spatial coverage, MESMA processing/computing time and fractional cover accuracy, Landsat TM is a good compromise compared to GeoEye-1 and MODIS for landscape scale fractional cover mapping in semi-arid savanna systems. However, the use of Landsat data also poses problems (e.g. sensor drift, scan line corrector striping problems in Landsat 7 ETM+, insufficient bands for complete atmospheric correction, long repeat intervals allowing only seasonal-scale mapping) that need careful attention during the image

processing stage. More importantly, besides data-specific issues, researchers should be aware of the structural and functional heterogeneity in the study area and should assess accuracy by sampling all vegetation morphology classes.
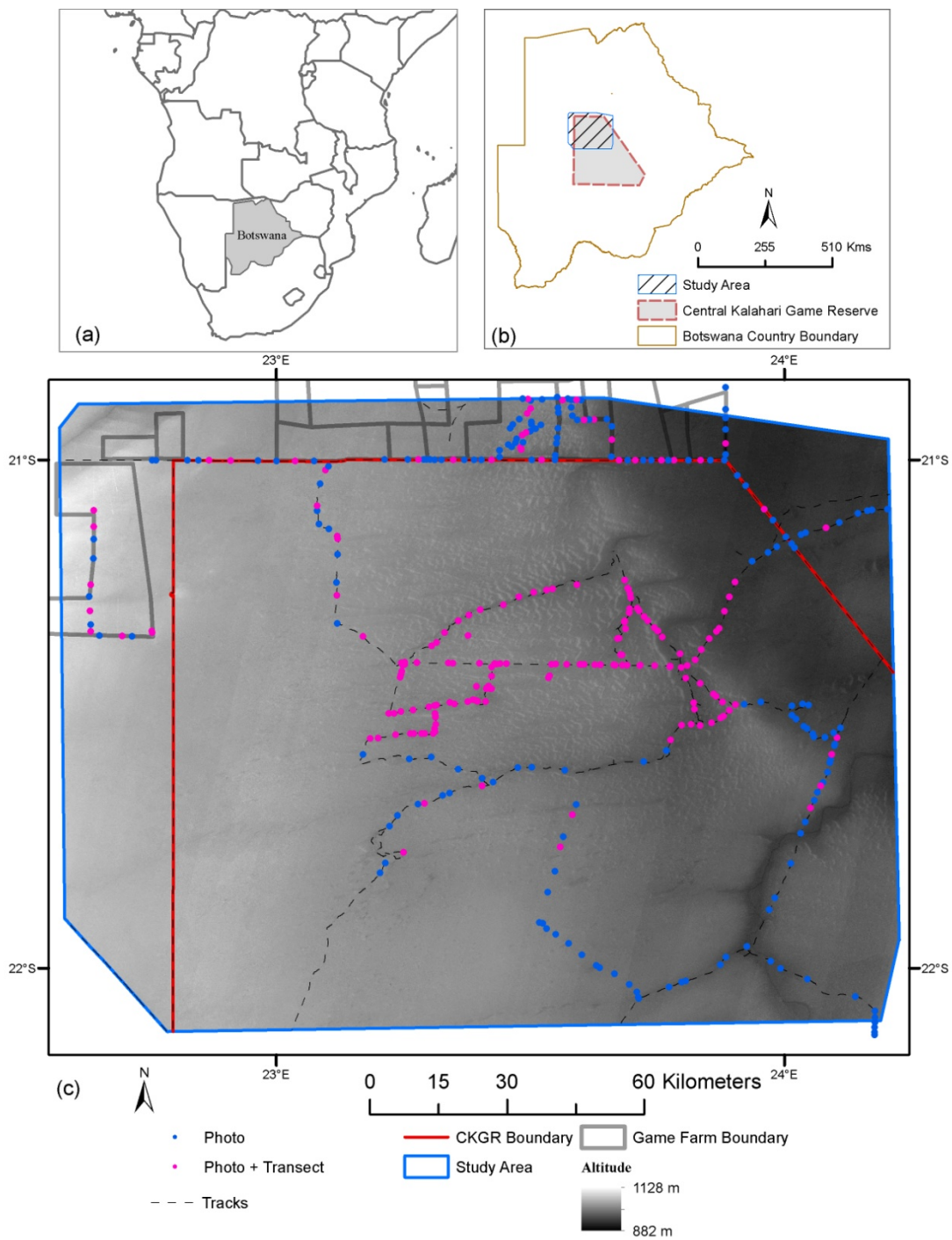
Figure 6.1: (a) Location of Botswana in southern Africa, (b) Location of study

area in the central Kalahari of Botswana and (c) enlarged portion of study area depicting

the game reserve boundary and game farms outside the protected area, areas accessible by tracks in the study are, major pan systems and points of interest. Background image is altitude of the study area represented by ASTER GDEM2.

| (a) GeoEye | (b) Landsat TM | (c) MODIS |
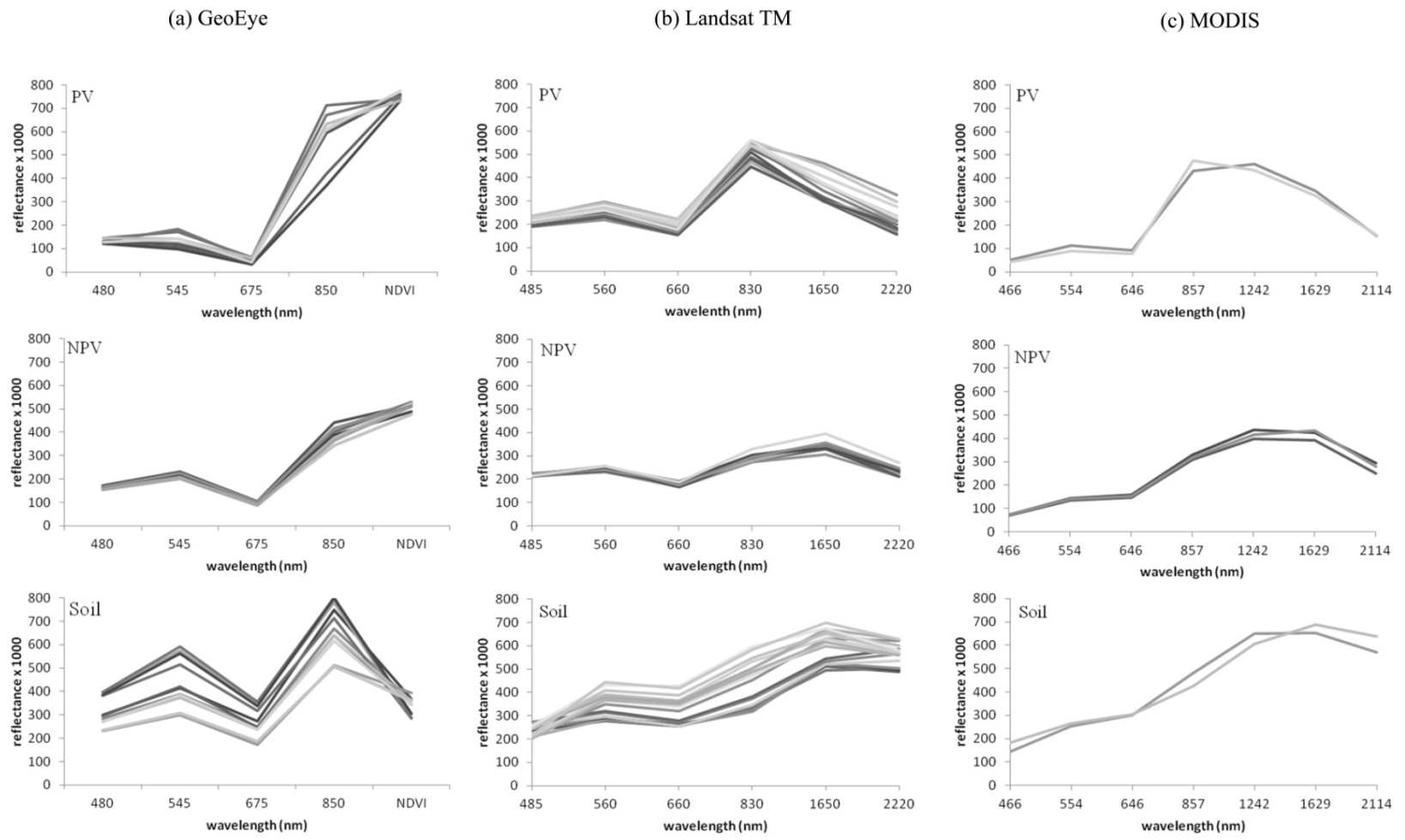
Figure 6.2: Endmembers of PV, NPV and soil used for MESMA analysis with GeoEye, Landsat TM and MODIS.

196

Field Photo	GeoEye RGB:421 Pixel size:2m	GeoEye MESMA (1MODIS pixel=50625 GeoEye pixels)	Landsat MESMA (1MODIS pixel=225 Landsat pixels)
Class 1: Mixed deciduous woodland with shrubs and herbaceous layer	Class 1	Class 1 $f_{PV}:0.46 f_{NPV}:0.28 f_{BS}:26$	Class 1 $f_{PV}:0.52 f_{NPV}:0.35 f_{BS}:0.13$
Class 2: Mixed (70-40%) medium high shrubland with open short herbaceous layer	Class 2	Class 2 $f_{PV}:0.33 f_{NPV}: 0.37 f_{BS}:0.30$	Class 2 $f_{PV}:0.39 f_{NPV}:0.41 f_{BS}:0.20$
Class 3: Mixed (40-10%) medium high shrubland with open short herbaceous layer	Class 3	Class 3 $f_{PV}: 0.24 f_{NPV}:0.51 f_{BS}:0.25$	Class 3 $f_{PV}:0.22 f_{NPV}: 0.55 f_{BS}:23$
Class 4: Medium tall grassland with medium high shrubs	Class 4	Class 4 $f_{PV}:0.14 f_{NPV}:0.66 f_{BS}:0.20$	Class 4 $f_{PV}:0.10 f_{NPV}:0.71 f_{BS}:0.19$
Class 5: Pans	Class 5	Class 5 $f_{PV}:0.09 f_{NPV}:0.17 f_{BS}: 0.74$	Class 5 $f_{PV}:0.05 f_{NPV}: 0.26 f_{BS}:0. 69$
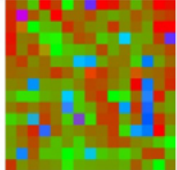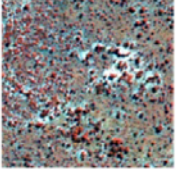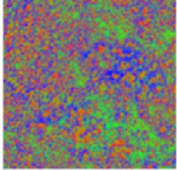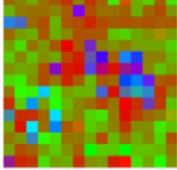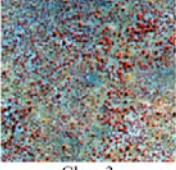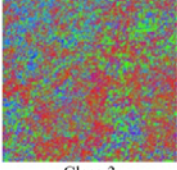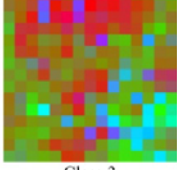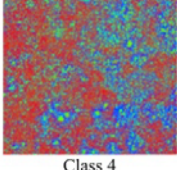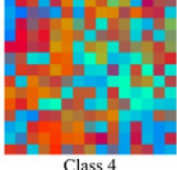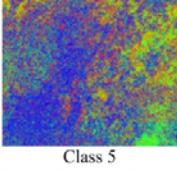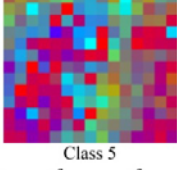
Figure 6.3: Spatial association of multi-scale fractional cover with vegetation morphology types for five prototype MODIS pixels in the central Kalahari.

197
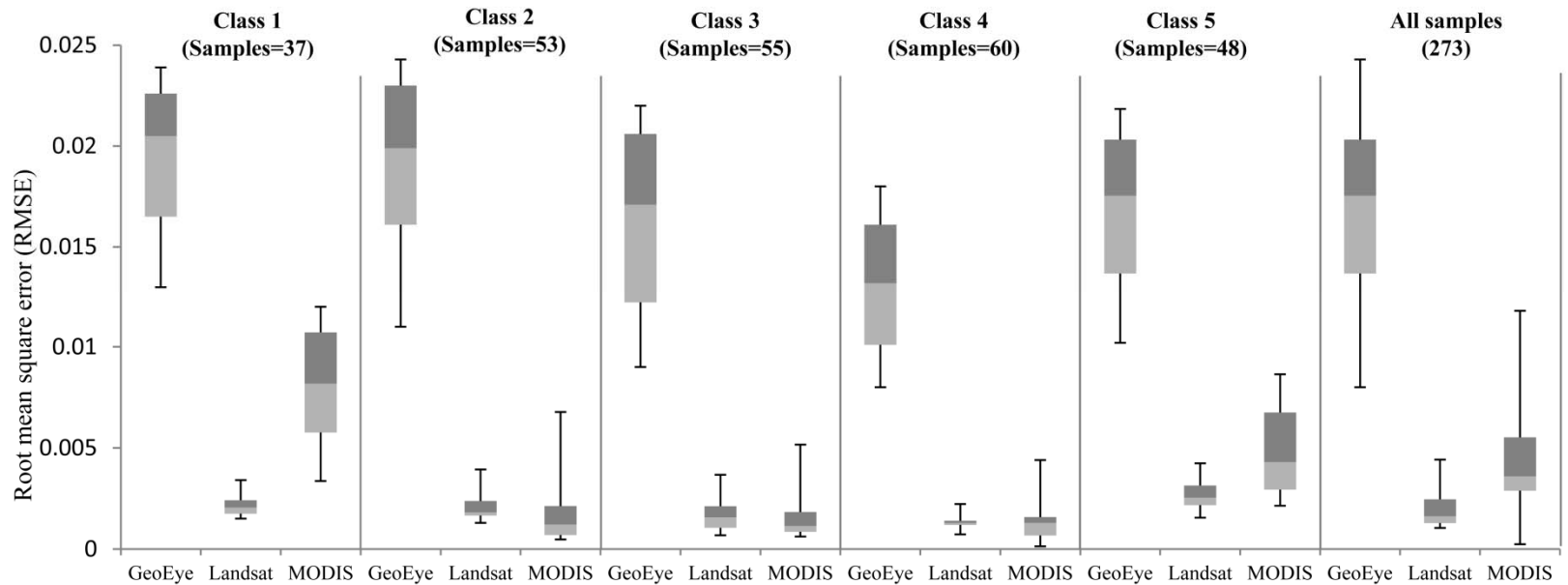
Figure 6.4: RMSE$_S$ for different vegetation morphology types obtained from MESMA of GeoEye, Landsat TM and MODIS imagery. Class 1: Mixed deciduous woodland with shrubs and herbaceous layer, Class 2: Mixed (70-40%) medium high shrubland with open short herbaceous layer, Class 3: Mixed (40-10%) medium to high shrubland with open short herbaceous layer, Class 4: Medium tall grassland with medium-high shrubs and Class 5: Pans and bare areas.
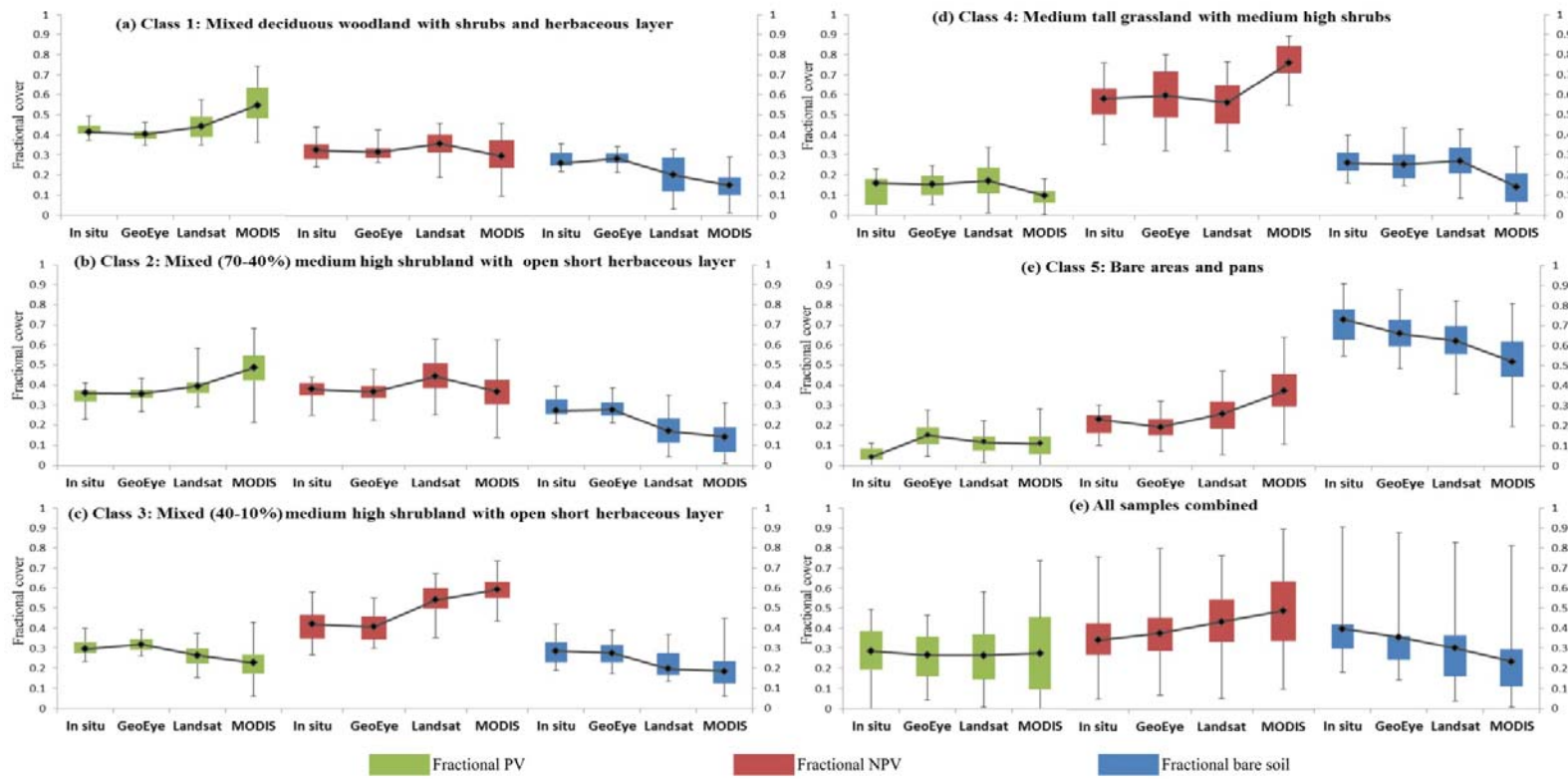
Figure 6.5: Variability in fractional cover estimates in the central Kalahari; in every figure, ƒPV, ƒNPV and ƒBS is represented by four box plots that denote the distribution of fractional cover obtained at in situ, GeoEye, Landsat and MODIS scales respectively (In situ estimates represent fractional cover obtained in 30 m transects while rest were calculated for area equivalent to one MODIS pixel).

Image type	Spatial Resolution (m)	Spectral range (nm)	Radiometric quantization (bit)	Data acquisition date
GeoEye-1	0.5 (panchromatic) 2 (multispectral)	Pan:450-800 B: 450-510 G:510-580 R:655-690 NIR:780-920	11	16 May 2010
SPOT-5	2.5 (multispectral)	G:500-590 R:610-680 NIR:790-890	8	8 April 2006 (2 scenes) 21 May 2011 (2 scenes) 25 March 2006 17 March 2011
Landsat 5 TM Path: 174 Row: 075	30	B:450-520 G:520-600 R:630-690 NIR:760-900 SWIR:1550-1750 SWIR:2080-2350	8	9 May 2010
MODIS (MCD43A4) Tile:H20V11 Composite no: 129	463.2	B:459-479 G:545-565 R: 620-670 NIR:841-876 SWIR:1230-1250 SWIR:1628-1652 SWIR:2105-2155	16	Compositing period: 9-24 May 2010

Table 6.1: Image data specification

GeoEye Endmembers	Landsat Endmembers	MODIS Endmembers
PV+Shade (7)	PV+Shade (13)	
NPV+Sahde (8)	NPV+Sahde (9)	
Soil+Shade (10)	Soil+Shade (9)	
PV+NPV+Shade (56)	PV+NPV+Shade (117)	
PV+Soil+Shade (70)	PV+Soil+Shade (117)	
NPV+Soil+Shade (80)	NPV+Soil+Shade (81)	
PV+NPV+Soil+Shade (560)	PV+NPV+Soil+Shade (1053)	PV+NPV+Soil+Shade (12)
Total models:791	Total models: 1399	Total models: 12

Table 6.2: Different Type and varying complexity of MESMA models used in this study.

Morphology Class	Imagery type	f_{PV}			f_{NPV}			f_{BS}			Overall	
		ME	MAE	RMSE	ME	MAE	RMSE	ME	MAE	RMSE	MAE	RMSE
1. (n=37)	GeoEye	4.2%	5.6%	5%	4%	6.8%	7.1%	-3.3%	4.9%	5.1%	5.7%	5.9%
	Landsat	3.8%	4.7%	5.7%	4.3%	9.5%	10.4%	-8%	10.7%	12.2%	8.3%	9.4%
	MODIS	14.4%	14.7	17.5%	-0.01%	8.8%	10.2%	-0.1%	13.2%	14.2%	12.2%	14.0%
2. (n=53)	GeoEye	0.9%	4.2%	4.1%	3%	5.6%	5.8%	-3.3%	4%	5.9%	4.7%	5.2%
	Landsat	3.7%	5.1%	7.1%	7.6%	10.1%	12.6%	-10.8%	11.2%	13.6%	8.8%	11.1%
	MODIS	12.8%	14.1%	16.4%	0.02%	8.4%	11.3%	-13.5%	13.9%	16.1%	12.1%	14.6%
3. (n=55)	GeoEye	-3%	4.8%	6.1%	2.6%	6.8%	6%	-2.7%	4.9%	8.1%	5.5%	6.7%
	Landsat	-5.5%	6.2%	7.3%	13.4%	13.4%	14.4%	-7.7%	8%	9.8%	9.2%	10.5%
	MODIS	-9.1%	10.3%	11.8%	18.5%	18.5%	20.2%	-9%	10.3%	12.86	13%	14.9%
4. (n=60)	GeoEye	1.8%	4.1%	4.7%	-2.2%	6.2%	7.5%	1.1%	4.3%	5.4%	4.8%	5%
	Landsat	1.7%	7.3%	8.7%	-3.3%	13.8%	16.6%	1.7%	10.4%	12%	10.5%	12.4%
	MODIS	-5.9%	8.3%	9.8%	17.4%	19.3%	22.7%	-11.6%	13.9%	16.7%	13.8%	15.4%
5. (n=48)	GeoEye	0.9%	4%	6.1%	6.2%	7.8%	8.3%	-2.8%	6.4%	6.9%	6%	7.1%
	Landsat	-3.3%	6.9%	8.6%	6.8%	9.2%	11%	-3.6%	8.4%	10%	8.1%	10.1%
	MODIS	-4.1%	6.7%	8.5%	18%	18.8%	21.8%	14%	15.9%	18.9%	13.8%	16.4%
All (n=273)	GeoEye	-2.9%	4.3%	4.9%	4.5%	6.1%	6.9%	-5.1%	6.7%	8.8%	5.3%	6.5%
	Landsat	-0.1%	6.1%	7.6%	5.7%	11.2%	13.3%	-5.5%	9.6%	11.5%	8.9%	10.8%
	MODIS	0.8%	10.4%	12.9%	11%	15%	18.3%	12.7%	13.4%	16%	12.9%	15.9%

ME: mean error; MEA: mean absolute error; RMSE: root mean square error

Table 6.3: Overall and vegetation morphology specific fractional cover accuracy of GeoEye, Landsat TM and MODIS derived fractional cover estimates. Field derived fractional estimates (in 30 m transect) were compared with GeoEye predicted fractions (mean of 225 GeoEye) while Landsat TM and MODIS were validated against mean fractions derived from 50625

GeoEye pixels (equivalent to 1 MODIS pixel size).

Chapter 7: Conclusions

In 2007, the National Research Council identified "understanding shifts in ecosystem structure and function" as "an emerging global challenge" (p 1) (NRC 2007). The objective of this dissertation was to examine the effectiveness and suitability of earth observation datasets and selected methodologies for characterizing the structural and functional properties in savanna ecosystems by reviewing and synthesizing information from existing literature and methods pertaining to arid and semi-arid savanna ecosystems (Chapter 3). The key focus was to examine and improve the characterization and monitoring ability of relevant and informative variables of ecosystem structural and functional dynamics. For this purpose this research utilized *in situ* derived data on vegetation and land cover structural and functional properties and compared them with those derived from remotely sensed imagery at multiple spatial/spectral resolution using two different methodological approaches (i.e. spectral mixture analysis versus object based image analysis). The structural and functional properties of savanna vegetation types in Botswana in general and the central Kalahari region in particular require further monitoring and are still a long-term research issue. Because of its low anthropogenic pressure Botswana's central Kalahari provided a 'natural laboratory' for examining some methodological and conceptual issues related to savanna structural and functional properties by combining in situ data with earth observation data. Although this research was conducted in the central Kalahari, the methodologies tested in this study are generalizable and could be implemented in other xeric savanna areas.

The semi-arid savanna of the central Kalahari region and throughout southern Africa is an important natural resource for pastoral agriculture, grazing, tourism and rangeland management. Their existence, ecological integrity and sustainability is a pre-

condition for the maintenance of biodiversity in southern Africa. These xeric ecosystems provide a number of important ecosystem services to the local population in this region. Vegetation type maps and field based data such as morphological properties/ details are primary and essential data sources for monitoring plant communities in southern Africa savanna systems. Vegetation morphology maps at the landscape to regional scales provide ecologically valuable information but only represent information from the structural perspective. In savanna systems including details regarding the relative proportions of PV, NPV and soil in a unit area is meaningful from the ecosystem functional perspective. Combining information of both structural and functional perspective provides a comprehensive understanding and should improve the value and efficiency of habitat and vegetation community conservation and related adaptive management strategies.

Remote sensing techniques combined with field data can play an important role in monitoring vegetation and land cover properties in the remote and inaccessible areas. Several challenges for remote sensing based monitoring in savanna systems include (i) high structural and functional diversity as depicted by the complex configuration of vegetation, (ii) phenological differences in different vegetation life forms that are also temporally influenced by spatio-temporal variability in moisture availability and (iii) the impact of other non-linear processes such as fire and grazing pressure. The complex interaction of these processes and their impact on ecosystem structure and function is not well understood yet. Future ecological research in savanna ecosystems has to evaluate these complex interactions effects on remotely derived properties of vegetation and land cover and develop new methods that allow their treatment/consideration in remote sensing based applications in savannas. In the following section, the main conclusions of this dissertation are presented resulting in a number of rising tasks and questions for

future research. As a results of the integrated use of *in situ* data and multi-scale remote sensing imagery for cross scalar analysis using selected methodologies and paradigms, some final remarks are proposed in order to make a contribution towards future development of concepts and methodologies for continued monitoring and assessment of semi-arid savanna systems.

Contributions of this dissertation research

High spatial resolution multi-spectral imagery for quantifying functional cover in savanna ecosystem: Suitability of Multiple Endmember Spectral Mixture Analysis (MESMA) versus Hierarchical Object Based Image Analysis (OBIA)

Savanna ecologists and biogeographers have been using remotely sensed imagery and methods for characterizing functional properties of savanna vegetation as a more efficient approach to address the challenge of the lack of field data and due to the difficulty of conducting field campaigns (Hanan and Lehmann 2010; Hill et al. 2011a). In this respect the comparison of existing image analysis methods is warranted to examine their relative suitability especially on comparatively recent and underutilized remotely sensed datasets. Several previous studies and current monitoring and management programs in savanna ecosystems suggest that fractional cover of PV, NPV and soil are suitable proxy measures of ecosystem functional properties and vegetation conditions as they relate to aboveground carbon dynamics, fire potential and wind erosion potential. Combining field derived fractional cover with a high spatial resolution multispectral imagery (i.e. GeoEye-1) this dissertation research tested the suitability of two image analysis approaches (i.e. MESMA versus hierarchical OBIA) for estimating fractional land cover for part of the central Kalahari with diverse vegetation morphological properties. The analysis and results presented in chapter 4 specifically test hypothesis 1 whether both MESMA and hierarchical OBIA can map fractional cover with equal

accuracy. The results indicate that hypothesis 3 is refuted since the MESMA approach was found to produce more accurate fractional estimates compared to the hierarchical OBIA approach. As the first study to compare the suitability of MESMA and OBIA approaches for mapping fractional land cover in savannas, the findings of this dissertation informs future studies planning to utilize high spatial resolution multi-spectral imagery.

The fractional estimates and vegetation morphological properties derived in the field were important and served as a critical reference that not only allowed to determine the superior method but also in understanding the impact of vegetation morphological properties on the accuracy of fractional cover mapping results. Spectral mixing occurs at all spatial scales and in savanna ecosystems, even a pixel of high spatial resolution imagery (e.g. 2 m) in functionally diverse savanna systems is highly likely to be a mixture of more than one cover type. The sub-pixel analysis approach of MESMA is able to represent the spatial heterogeneity in semi-arid central Kalahari better than the OBIA approach which treats landscape to be consisting of patches that are represented in OBIA approach as objects (formed by grouping homogeneous pixels). However, some limiting factors of MESMA approach for deriving fractional cover from high spatial resolution multi-spectral imagery includes (i) high potential of non-linear mixing at high spatial resolutions which makes it challenging to unmixing a pixel with $RMSE_S$ that are below 2.5% of reflectance and (ii) high computational time required for analysis largely due to large data volume. These challenges limit the applicability of MESMA for analysis of high spatial resolution imagery (e.g. GeoEye, SPOT, IKONOS) for landscape to regional scale applications of fractional cover estimation. Also, while field data is critical for evaluating remote sensing methods and results even at high spatial resolution data, it also has inherent errors and its acquisition, especially in remote areas can be highly limited due to logistical and safety issues. Given these trades-offs, a more pragmatic strategy for

future research in savanna ecosystems would be to use MESMA results for strategically selected representative sample areas for validating the results derived from coarse spatial resolution data that provide large spatio-temporal coverage but might be less accurate.

Mapping vegetation morphological properties in semi-arid savannas: Suitability of Hierarchical Object Based Image Analysis (OBIA)

Very few vegetation surveys have been conducted in Botswana in general and the central Kalahari region in particular. The most recent map of landscape ecological vegetation types of the central Kalahari is from 1980 and was created by the DHV consulting engineers and is a highly simplistic and unscientific illustration of the vegetation structural properties of this area. Hence there is a general lack of consistent and area wide geo-information on vegetation morphology type distribution. Evaluations of existing land cover products in savanna systems have revealed that high landscape heterogeneity and variable patch sizes are the main reasons for low mapping accuracies in savanna systems. The objective of this part of this dissertation research (i.e. chapter 5) was to examine ways in which remote sensing data classification techniques can be adapted to semi-arid savanna environments in order to account for the low niche differentiation in mapping savanna vegetation morphology types. Given the task of distinguishing and mapping these vegetation morphology types at the landscape scale using commonly/freely available single date medium spatial resolution satellite imagery, an *in situ* database was generated that contained details collected at several point/transect locations and included information of vegetation average density and height, dominant/co-dominant vegetation life forms. For relating and upscaling this field data to medium spatial resolution satellite imagery, (i) the OBIA approach was adopted to segment the imagery at multiple segmentation scales creating image objects of different sizes, (ii) selected spatially homogeneous objects by confirming their purity against high

spatial resolution imagery and (iii) confirming the temporal consistency of these objects by comparing their mean vegetation indices values calculated from MODIS time-series products. The analysis of results presented in chapter 5 explicitly tested hypothesis two (presented in chapter 1) which indicates that classification accuracy for different vegetation morphology types in the central Kalahari varies according to the segmentation scale parameter. Results of classification and accuracy assessment conducted at six different segmentation scales confirm the validity of this hypothesis.

The integration of *in situ* data to a multi-scale OBIA framework proved to be a conceptual and methodological advancement that is leading to improved knowledge about the fine scale structural heterogeneity of vegetation in the central Kalahari. For spatially explicit vegetation type mapping in heterogeneous savanna systems, pixel based analysis can pose significant challenges as pixels impose arbitrary sampling boundaries and are unable to address the patchy vegetation patterns in savanna landscapes. These issues have been confirmed by the limited mapping accuracies and major cartographic errors found in previous mapping exercises conducted in semi-arid savannas in Namibia (Hüttich et al. 2011b; Strohbach et al. 2004) and in Australia (Blaschke 2010). The use of hierarchical OBIA proved to be advantageous for distinguishing patches with subtle but ecologically important structural differences in vegetation morphology types in the semi-arid central Kalahari savanna. Segmentation of the imagery at six different segmentation scales allowed for the creation of objects of different sizes and their classification results showed how this methodology suitably works in savannas as the optimal patch size varies with vegetation morphological properties requiring different representative object sizes. Previous studies (Hamada et al. 2011; Laliberte et al. 2007; Lucieer et al. 2005) have argued that a single multi-spectral image (e.g. Landsat TM) may not have enough spectral dimensionality to distinguish savanna vegetation morphology types requiring

phenological variables derived from time-series imagery. The results of this study shows that savanna vegetation morphology types can be distinguished and mapped with sufficiently acceptable accuracy using single date imagery. Further analysis of the predictor variable importance depicted that textural measure derived using the grey level co-occurrence matrix (GLCM) were most important variables followed by spectral measures for distinguishing and mapping considered vegetation morphology types. Image analysis based on the OBIA approach offers the possibility of the inclusion of spectral, textural, contextual, neighborhood etc variables as predictors in a classification problem. The integrated use of machine learning techniques (e.g. Random Forest) along with these predictor variables holds significant potential for multi-dimensional data analysis. Using variable important functionalities (such as offered by the Random Forest classifier) while classifying satellite imagery would lead to an increased understanding of the relative bio-physical relevance of each predictor variable. In future research in savannas, this approach will lead to increased classification accuracy by choosing the most appropriate variable and thus reduction in computation time. The resulting variables could also be used to access environmental cues for the classification of semi-arid vegetation types. Other advantages of using the hierarchical OBIA approach combined with Random Forest classifier in context of semi-arid central Kalahari savanna as found in the research includes (i) an accurate and realistic spatial distribution of fine scale spatial patterns of semi-arid vegetation types and (ii) the detection of transition zones between different vegetation types which are closely associated to soil properties as observed in the field.

Impact of savanna vegetation morphological properties and imagery spatial/spectral resolutions on characterization/estimation accuracy of fractional cover of PV, NPV and soil in savanna systems

With the aim to improve mapping of functional properties in heterogeneous landscapes, the objective of this part of the dissertation research (i.e. chapter 6) was to apply a multi-resolution approach for deriving fractional land cover and examine (i) how changing spatial/spectral resolution of imagery impacts mapping results and (ii) how does vegetation morphological properties influence the result accuracy across the considered spatial/spectral resolution of imagery? Results found that with increasing pixel size the magnitude of overall error increased consistently for all fraction cover types. Also, even with low spectral dimensionality high spatial resolution imagery (i.e. GeoEye-1) could map fractional cover with low error (overall RMSE: 6.5 %) and estimation error increased with coarsening pixel size (overall RMSE Landsat TM: 10.8% and MODIS: 15.9%). Furthermore, the savanna vegetation morphological properties were also found to impact estimation accuracy as in areas with dominant woody vegetation (morphology types 1 and 2) at a time when woody canopies were mostly green, f_{PV} was overestimated at the cost of mainly underestimating f_{BS}; in contrast, in areas with dominant herbaceous vegetation (morphology types 4 and 3) at a time when herbaceous vegetation was mostly senescent, f_{NPV} was overestimated with a corresponding underestimation of both f_{PV} and f_{BS}. Analysis and results presented in chapter 6 examined the validity of hypothesis three and four (presented in chapter 1). Based on the results, both hypothesis three and four were found to be valid as coarse spatial resolution imagery (i.e. MODIS) produced lower estimation accuracy than medium spatial resolution imagery (i.e. Landsat TM) which in turn produced lower accuracy than high spatial resolution imagery (i.e. GeoEye-1). Also vegetation morphological properties were found to influence the fractional cover

estimation and different vegetation morphology types have also comparatively different fractional cover types that were mapped with different mapping accuracies at different spatial/spectral resolutions.

For mapping functional properties of vegetation in savanna systems 'hard' classification schemes have been found unsuitable largely due to the co-existence of woody and herbaceous life forms with markedly different phenological cycles (Gessner et al. 2013; Hill et al. 2011a). Climatic gradient of occurrence and mixtures of life-forms are suitably represented following sub-pixel abundance estimation approach. At coarse spatial resolution (>500 m) the occurrence of pure pixel (endmember) of a single cover type (e.g. PV, NPV, soil) is highly unlikely in savanna ecosystems. Nevertheless, for regional to continental scale monitoring applications using remotely sensed imagery, coarse spatial resolution imagery (e.g. MODIS) will continue to be preferred by scientists due to large swath area and higher temporal frequency. However the results of this dissertation research found that in spatially heterogeneous and temporally dynamic ecosystems such as savannas, the estimation accuracy of ecologically relevant variables (e. g. fractional cover of PV, NPV and soil) derived from coarse spatial resolution multi-spectral imagery can be limited. Several factors can contribute to these limitations including problems in model parameterization (e.g. due to challenges in selecting endmembers, non-optimal bandwidth of imagery, overgeneralized representation of savanna spatial heterogeneity due to coarse spatial resolution). These results are consistent with findings of studies conducted in other semi-arid savannas such as in Australia (Guerschman et al. 2009; Guerschman et al. 2012) and South America (Asner and Heidebrecht 2003; Numata et al. 2007). On the contrary, high and medium spatial resolution imagery provides a limited swath area but has the potential to map fractional cover with a much higher accuracy. Thus future studies in savanna ecosystems using

coarse spatial resolution imagery should utilize any spatio-temporally coincident imagery available at higher spatial resolution to strategically calibrate and validate the performance of adopted modeling/mapping technique.

The findings of this dissertation research have several implications for future studies aiming to combine field derived measurements with earth observation data for characterizing spatial patterns in structural and functional properties of savanna vegetation and understanding underlying ecological processes. The key issue of this dissertation was to examine and improve mapping applications related to vegetation structural and functional properties in savanna ecosystems with integrated use of field and earth observation data. The characterization of vegetation morphology types and fractional cover across multiple spatial scales using multi-scale remotely sensed imagery contributes not only to the ecology of savannas but also informs the remote sensing science about the potentials/limitations of considered datasets and techniques for investigating the scale dependency of these relevant ecosystem properties. The availability of spatio-temporally coincident satellite dataset at multiple spatial scales close to the *in situ* data collection dates facilitated the exploration of ecological and methodological questions regarding the characterization sensitivity of savanna functional (i.e. fractional cover) and structural properties (i.e. morphology classes) to changing spatial/spectral resolution of input imagery. The problem of relating similar measurements conducted at different spatial resolutions (keeping the extent constant) is a central problem studied in many different scientific disciplines. Existing literature on ecological upscaling suggests that measurements made at fine grain sizes depicts high spatial variance and at increasingly larger grain sizes the spatial variance is lost resulting in low spatial variance at coarse grain size. Furthermore, the observed sensitivity of spatial variance in measurements to changing grain size has reportedly shown much

213

different pattern/response in structurally/functionally heterogeneous ecosystems versus homogeneous ecosystems. In homogeneous landscapes (e.g. boreal forests, tropical rain forests) in terms of vegetation structural and functional properties, the coarsening grain size has been observed to depict highly linear negative correlation between spatial variance and grain size (Wu and Li 2009; Wu and Marceau 2002). In contrast, in structurally and functionally heterogeneous landscapes (e.g. tropical savannas) a non-linear negative correlation between coarsening grain size and spatial variance (Turner 2005; Wu and Li 2009).

Future research directions and needs

This dissertation faces various issues on cross scalar comparison and integration of ecologically relevant variables derived at multiple scales and methodological concepts in the field of multivariate data analysis for applications in characterization of ecological patterns in savanna ecosystems. Even though the major objectives of the research were achieved, a number of issues stand that require attention in future research. Given the importance and relevance of fractional cover of PV, NPV and soil as reflective of functional properties of ecosystem, in future research the fractional cover mapping needs to be geographically extended to cover larger extents (e.g. at the country level or for whole southern Africa) using MODIS imagery. Such projects have already been conducted in other savanna areas such as Australia (Guerschman et al. 2012) but are lacking in southern Africa savanna systems. Increasing the geographical extent of fractional cover mapping would hugely increase the structural and floristic diversity of vegetation as well differences in soil properties. Furthermore, due to the lack of field measurements or other secondary data that can provide some understanding about the magnitude of variability of these parameters, it would be challenging to calibrate the

unmixing model (i.e. finding representative endmembers) and assess the influence of changing vegetation properties on modeling results. A multi-scale strategy that leverages the availability of any higher spatial resolution multi or hyperspectral imagery would thus be essential for understanding the uncertainty in regional scale estimates and such results may be pivotal in developing more effective methodologies. A possible way to quantitatively measure heterogeneity for monitoring and modeling over large and logistically challenging areas could be to use the variability of NDVI measured by Landsat imagery in an area equivalent to a MODIS pixel which could be used as a proxy of the degree of heterogeneity. Using this approach it would also be possible to further test if the unmixing modelling error is positively associated with the measure of variability. For this purpose existing soil and vegetation type maps and secondary data could also be suitably used wherever available.

Another important long term research goal in the central Kalahari region is the creation of vegetation morphology maps for the entire central Kalahari region. Remote sensing will be an indispensable tool for such regional scale mapping exercises. This dissertation research considered vegetation types/classes defined considering the vegetation morphological properties (height, density and life form composition). However from the perspective of characterizing and monitoring biodiversity status in the southern Africa savanna, it is also necessary to consider the floristic composition and define classes based on dominant/co-dominant species of existing life forms. However such datasets are currently non-existent for the central Kalahari region as well as large parts of Botswana and essentially require intensive and time consuming field work in logistically challenging areas. The results of this dissertation found that the inclusion of textural, spectral and other variables following OBIA approach allowed the discrimination and mapping of vegetation morphology types that were not distinguishable

based on spectral features alone. Thus it would be a logical next step for future researchers to investigate the suitability of these features for distinguishing and mapping vegetation types defined considering the floristic composition of savannas. While some recent studies have suggested that floristic classes in savannas can be distinguished based on the differences in their phenological properties derived from MODIS time series (Colditz et al. 2007; Huttich et al. 2009), an important limitation of using coarse spatial resolution imagery is the oversimplified representation of fine scale variability as observed in savanna patches. Thus testing the suitability of the features available following the OBIA approach using medium spatial resolution imagery in future research in savannas is warranted.

The savannas in Botswana are of important economic value since they provide the main source of ecosystem services e.g. food production by large scale livestock farming and eco-tourism. But a basic issue faced by savanna researchers lies in deciding the class definitions of savanna vegetation. This challenge is mainly due to the high variability that is encountered in southern Africa savanna vegetation in terms of vegetation height, density and the variability in the existence of a given life form (e.g. trees, shrubs, grasses) within a given area (Thomas 2002; Thompson 1996). As a result national vegetation maps in southern Africa differ significantly in terms of class nomenclature, thematic detail, minimum mapping unit and the classification system applied (Dougill et al. 2010; Strohbach et al. 2004) and there are frequent instances where similar vegetation types in similar landscapes were assigned different names across international borders (Hüttich et al. 2011a). Following the previous works of Edwards (1983) and Thompson (1996), in this dissertation class nomenclature to vegetation classes were assigned based on a layering system of the life forms and important physiognomic properties (height and density) that provide independence of geographic scale for cross-scalar comparisons and

are also more relevant from remote sensing perspective. Although the assigned class names gives the reader a good understanding of the dominant/co-dominant life forms and their height and density but it is not consistent with the FAO and UNEP Land Cover Classification System (LCCS) which will soon become the global standard for land cover and has its own requirements to classify any land cover type. Therefore future research needs to be carried out to better integrate and harmonize class names developed using *in situ* obtained vegetation types descriptions with those in the existing LCCS. While research on these issues has very recently started for land cover types in southern African countries such as Namibia (Hüttich et al. 2011a), there is a need for such studies in countries such as Botswana, Zimbabwe etc with variation in vegetation properties.

Over the last few decades great progress has been made in remote sensing based land cover characterization and monitoring mechanisms including calibration and validation strategies, class definitions and classification techniques. Environmental remote sensing still faces several issues particularly in structurally heterogeneous and functionally dynamics landscapes (e.g. savannas, wetlands) because there are high uncertainties in remote sensing derived variables in these areas. Within this dissertation some suggestions and margins of improvements were provided for remote sensing based characterization of structural and functional properties in savanna ecosystems (e.g. dependence/association of vegetation structural properties with modeling results, impact of spatial/spectral resolution, potential and limitations of hierarchical OBIA and spectral unmixing). Further methodological and conceptual research in savanna ecosystems needs to be conducted that will allow ecologically informed decision making and their sustainable management under impending threats from increasing anthropogenic pressure and climatic variability.

217

Appendix-A

In situ observation of vegetation functional and structural properties in the central Kalahari:

Location no.	Latitude/ Longitude (decimal degrees)	Fractional cover measured	Absolute fractional cover			Spectral measurements conducted	Dominant woody species	Average woody species height (m)	Vegetation morphology type
			f_{PV}	f_{NPV}	f_{BS}				
1	21.400143S 23.377821E	yes	0.13	0.58	0.29	yes	G. Flava, A. erubescens	1	4
2	21.401891S 23.384386E	yes	0.05	0.59	0.26	yes	A. luederiziit, G. Flava	1.5	4
3	21.400602S 23.399622E	yes	0.10	0.65	0.25	yes	A. luederiziit, G. Flava	1.2	4
4	21.346151S 23.377037E	yes	0.02	0.56	0.42	yes	A. luederiziit, L. nelsii	1	4
5	21.399826S 23.338818E	yes	0.12	0.51	0.37	yes	C. alexandrii, Bauhinia petersiana	1.2	4
6	21.395226S 23.335412E	yes	0.28	0.55	0.27	yes	A. mellifera, C. alexandrii	2	3
7	21.403442S 23.267342E	yes	0.27	0.51	0.22	yes	L. nelsii, Boscia albitrunca	1.7	3
8	21.398838S 23.276995E	yes	0.02	0.42	0.66	yes	Bauhinia petersiana L. nelsii	0.9	4
9	21.398227S 23.253073E	yes	0.01	0.62	0.27	yes	A. mellifera, C. alexandrii	1.9	4
10	21.399161S 23.245842E	yes	0.22	0.46	0.32	yes	C. alexandrii L. nelsii	2.5	3
11	21.402731S	yes	0.20	0.48	0.32	yes	C. alexandrii ,	2.1	3

218

	23.252732**E**						*A. hebeclada*		
12	21.407901**S** 23.423788**E**	yes	0.12	0.51	0.37	yes	*A. erioloba A. luederiziit*	1	4
13	21.425361**S** 23.423985**E**	yes	0.31	0.56	0.13	yes	*A. erubescens L. nelsii*	2.5	3
14	21.538098**S** 23.308772**E**	yes	0.02	0.14	0.84	yes	*none*	0	5
15	21.538376S 23.285244E	yes	0.11	0.43	0.46	yes	*C. alexandrii*	1.1	4
16	21.537961S 23.263755E	yes	0.12	0.58	0.3	yes	*G. Flava*	0.4	4
17	21.540652S 23.235018E	yes	0.04	0.07	0.89	yes	*none*	0	5
18	21.547547S 23.200752E	yes	0.06	0.51	0.43	yes	*G. Flava, A. mellifera*	1	4
19	21.548095S 23.184821E	yes	0.08	0.48	0.44	yes	*G. Flava*	0.4	4
20	21.538548S 23.292214E	yes	0.11	0.52	0.37	yes	*C. alexandrii Boscia albitrunca*	1	4
21	21.520661S 23.313896E	yes	0.12	0.63	0.25	yes	*L. nelsii Terminalia sericea*	1.4	4
22	21.503297S 23.313312E	yes	0.25	0.36	0.29	yes	*Croton gratissimus L. nelsii*	1.5	3
23	21.483016S 23.311423E	yes	0.08	0.47	0.45	yes	*L. nelsii*	1.5	4
24	21.499023S 23.221201E	yes	0.14	0.39	0.47	yes	*C. alexandrii Combretum hereroense*	1	4
25	21.498617S	yes	0	0.08	0.92	yes	*none*	0	5

	23.231568E								
26	21.445617S 32.393518E	yes	0.1	0.53	0.37	yes	*Combretum hereroense A. erubescens*	1	4
27	21.445115S 23.417472E	yes	0.33	0.35	0.32	yes	*G. Flava, A. erubescens, Combretum hereroense*	2	3
28	21.482336S 23.315718E	yes	0.09	0.66	0.25	yes	*Boscia albitrunca, L. nelsii*	1	4
29	21.477246S 23.341522E	yes	0.28	0.39	0.33	no	*C. alexandrii A. Robusta*	2	3
30	21.480383S 23.350489E	yes	0.24	0.43	0.33	no	*Boscia albitrunca, C. alexandrii*	1.5	3
31	21.475361S 23.376585E	yes	0.16	0.52	0.32	no	*L. nelsii*	1.5	4
32	21.471616S 23.387378E	yes	0.29	0.33	0.38	no	*C. alexandrii*	1	3
33	21.473748S 23.393308E	no	-	-	-	no	*none*	0	5
34	21.474674S 32.396149E	yes	0.05	0.1	0.85	no	*none*	0	5
35	21.475567S 23.411658E	yes	0.06	0.18	0.76	yes	*A. tortilis*	5	5
36	21.450357S 23.413002E	yes	0.22	0.38	0.4	no	*L. nelsii, A. erioloba*	2	3
37	21.448566S 23.413649E	yes	0.33	0.26	0.31	yes	*A. tortilis, Boscia albitrunca*	7	2
38	21.401295S 23.439771E	yes	0.33	0.29	0.28	no	*A. Mellifera, A. luederiziit*	4	2

39	21.401328S 23.452906E	no	-	-	-	no	*Boscia albitrunca, L. nelsii*	2	3
40	21.449979S 23.421082E	yes	0.26	0.42	0.32	yes	*Dichrostachyas cinerea, Commiphira africana*	2	2
41	21.450013S 23.422147E	yes	0.27	0.44	0.29	yes	*Croton gratissimus Dichrostachyas cinerea*	2.5	2
42	21.45019S 23.42338E	yes	0.34	0.31	0.35	yes	*Croton gratissimus Boscia albitrunca*	2.5	2
43	21.402116S 23.549681E	no	0.08	0.49	0.43	no	*Combretum hereroense L. nelsii*	1	4
44	21.402406S 23.571103E	yes	0.22	0.41	0.38	no	*L. nelsii, Ziziphus mucronata*	1.5	3
45	21.402714S 23.597299E	yes	0.29	0.36	0.35	no	*Croton gratissimus L. nelsii*	2	3
46	21.402813S 23.605464E	yes	0.11	0.46	0.43	no	*C. alexandrii*	1	4
47	21.403015S 23.626493E	yes	0.32	0.25	0.43	no	*Croton gratissimus L. nelsii*	2.2	2
48	21.403174S 23.637992E	yes	0.38	0.29	0.23	no	*A. erubescens, Albizia anthelmintica*	3	2
49	21.403563S 23.663607E	no	-	-	-	no	*A. erubescens, Croton gratissimus*	3.5	2
50	21.404015S 23.690284E	yes	0.22	0.46	0.32	no	*C. alexandrii Albizia anthelmintica*	1.5	3
51	21.404371S 23.715983E	yes	0.36	0.43	0.21	no	*A. luederiziit Croton gratissimus*	3.5	2
52	21.404628S	yes	0.32	0.40	0.26	no	A. erubescens	2.4	2

							L. nelsii		
	23.744867E						*L. nelsii*		
53	21.408383S 23.797139E	yes	0.1	0.35	0.55	no	none	0	5
54	21.382823S 23.677355E	yes	0.24	0.38		no	*A. luederiziit Combretum hereroense*	2	3
55	21.350707S 23.674152E	yes	0.12	0.57		yes	*C. alexandrii A. erubescens*	1	4
56	21.315828S 23.671299E	yes	0.26	0.48		yes	*A. luederiziit A. erioloba*	3	3
57	21.316833S 23.685841E	no	-	-	-	yes	*A. Mellifera, Boscia albitrunca*	2.5	3
58	21.252791S 23.691835E	yes	0.41	0.35	0.24	no	*A. luederiziit A. Mellifera, Boscia albitrunca*	6	1
59	21.236724S 23.686005E	yes	0.46	0.39	0.15	no	*Croton gratissimus Terminalia prunioides*	6.5	1
60	21.384122S 23.680029E	yes	0.27	0.38	0.35	no	*A. erubescens L. nelsii Albizia anthelmintica*	3.5	2
61	21.403875S 23.666762E	no	-	-	-	no	*L. nelsii A. erioloba Dichrostachyas cinerea,*	3	2
62	21.402711S 23.600125E	yes	0.29	0.42	0.29	yes	*Croton gratissimus A. Mellifera*	2.5	2
63	21.293061S 23.695394E	yes	0.26	0.43	0.31	yes	*Albizia anthelmintica A. luederiziit*	2.2	3
64	21.254839S 23.692985E	yes	0.23	0.45	0.32	no	*A. Mellifera, A. erubescens*	3.3	3

65	21.245795S 23.591498E	yes	0.36	0.37	0.27	yes	*Boscia albitrunca* *Terminalia prunioides*	3.5	2
							G. Flava		
66	21.253626S 23.543932E	yes	0.05	0.58	0.37	no	*A. robusta* *C. alexandrii*	1.5	4
67	21.256198S 23.532053E	no	-	-	-	no	*none*	0	5
68	21.285182S 23.446748E	yes	0.32	0.40	0.28	no	*C. alexandrii* *L. nelsii*	1.4	3
69	21.340075S 23.331254E	yes	0.13	0.56	0.31	no	*C. alexandrii* *A. Mellifera*	1.3	4
70	21.429238S 23.805586E	yes	0.05	0.13	0.82	no	*none*	0	5
71	21.520518S 23.816315E	yes	0.11	0.61	0.28	yes	*A. Robusta* *Commifora Africana*	1	4
72	21.610831S 23.567414E	yes	0.32	0.52	0.16	yes	*C. alexandrii* *Albizia anthelmintica*	1.5	3
73	21.626752S 23.404928E	yes	0.14	0.47	0.39	no	*C. alexandrii* *A. Mellifera*	1.2	4
74	21.608747S 23.358044E	yes	0.18	0.44	0.38	no	*A. Mellifera* *G. Flava*	1.5	4
75	21.584322S 23.304873E	yes	0.03	0.13	0.84	no	*none*	0	5
76	21.588414S 23.261819E	no	-	-	-	no	*none*	0	5
77	21.579735S 23.170336E	no	-	-	-	no	*none*	0	5
78	21.425177S 23.537752E	yes	0.30	0.34		yes	*A. luederiziit* *A. Mellifera*	2.5	3

79	21.428265S 23.535741E	yes	0.21	0.53		yes	*A. Mellifera* *A. Tortilis*	3.5	3
80	21.405012S 23.808525N	yes	0.29	0.39	0.22	no	*A. Mellifera* *C. alexandrii*	3	2
81	21.393496S 23.824409E	yes	0.23	0.28	0.49	no	*A. luederiziit* *A. erubescens*	2.4	3
82	21.373378S 23.824401E	yes	0.39	0.34	0.27	no	*A. Senegal* *Terminalia prunioides* *Croton gratissimus*	3.5	2
83	21.351596S 23.851805E	yes	0.02	0.60	0.38	no	*A. erubescens* *Albizia anthelmintica*	1	4
84	21.337776S 23.866377E	no	-	-	-	no	*A. erubescens* *Albizia anthelmintica*	1	4
85	21.331852S 23.871143E	yes	0.04	0.55	0.41	no	*A. luederiziit*	1	4
86	21.297761S 23.882201E	yes	0.23	0.50	0.27	no	*A. Mellifera*	2.5	3
87	21.26976S 23.891787E	yes	0.1	0.45	0.45	no	*A. Mellifera* *L. nelsii*	1.2	4
88	21.240908S 23.902972E	yes	0.03	0.52	0.45	no	*A. Tortilis* *Ziziphus mucronata*	1.2	4
89	21.199714S 23.936311E	yes	0.29	0.48	0.23	no	*A. luederiziit* *Boscia albitrunca*	2	3
90	21.604852S 23.50290E	yes	0.12	0.41		no	*A. Robusta* *A. Mellifera*	1.8	4
91	21.605719S 23.475293E	no	-	-	-	no	*C. alexandrii* *A. Robusta*	2	4
92	21.593677S 23.723131E	no	-	-	-	no	*none*	0	5

93	21.521702S 23.797539E	yes	0.07	0.14	0.79	no	*none*	0	5
94	21.551146S 23.775651E	no	-	-	-	no	*none*	0	5
95	21.572199S 23.767685E	yes	0.1	0.58	0.32	no	*A. Tortilis*	1.1	4
96	21.477841S 23.821808E	yes	0.08	0.08	0.84	no	*none*	0	5
97	21.490599S 23.822981E	no	-	-	-	no	*A. Mellifera A. Tortilis*	3.1	3
98	21.359301S 23.315352E	no	-	-	-	no	*A. hebeclada A. luederiziit*	3	3
99	21.365988S 23.306001E	yes	0.31	0.37	0.32	no	*Bauhinia petersiana A. hebeclada*	2.2	3
100	21.316772S 23.358049E	no	-	-	-	no	*A. Robusta C. alexandrii*	2	4
101	21.294711S 23.401156E	yes	0.14	0.48	0.38	no	*C. alexandrii A. Robusta*	0.8	4
102	21.305397S 23.378731E	yes	0	0.22	0.78	no	*none*	0	5
103	21.260975S 23.506733E	yes	0.02	0.15	0.83	no	*none*	0	5
104	21.269403S 23.477638E	no	-	-	-	no	*none*	0	5
105	21.481266S 23.329691E	yes	0.09	0.52	0.39	no	*C. alexandrii*	1.2	4
106	21.481114S 23.336042E	yes	0.15	0.44	0.41	no	*C. alexandrii Combretum hereroense*	2	4

107	21.427805S 23.243473E	yes	0.06	0.50	0.44	no	*L. nelsii* *A. Senegal*	1	4
108	21.415586S 23.245442E	no	-	-	-	no	*Boscia albitrunca* *A. Senegal*	1.2	4
109	21.422991S 23.245448E	yes	0.24	0.46	0.3	no	*A. Mellifera* *Boscia albitrunca*	2.5	3
110	21.482771S 23.322461E	no	-	-	-	no	*C. alexandrii* *A. Robusta*	1.3	4
111	21.486144S 23.300384E	no	-	-	-	no	*G. Flava* *C. alexandrii*	1	4
112	21.506249S 23.313562E	no	-	-	-	no	*L. nelsii*	0.8	4
113	21.498932S 23.312166E	no	-	-	-	no	*A. Senegal* *Boscia albitrunca*	3	4
114	21.534591S 23.312468E	no	-	-	-	no	*C. alexandrii*	0.6	4

115	21.528308S 23.311645E	no	-	-	-	no	*A. Mellifera* *L. nelsii*	2	4
116	21.538098S 23.287146E	no	-	-	-	no	*C. alexandrii*	1.5	4
117	21.537976S 23.270955E	no	-	-	-	no	*none*	0	4
118	20.777238S 23.884031E	yes	0.22	0.39	0.39	no	*A. Mellifera* *Boscia albitrunca*	1.4	3
119	20.80568503S 23.88405296E	no	-	-	-	no	*A. Mellifera* *Boscia albitrunca*	1.6	3
120	20.83059001S 23.88408104E	no	-	-	-	no	*A. Mellifera* *Boscia albitrunca*	1.4	3

121	20.85743699S 23.88411297E	no	-	-	-	no	*A. Mellifera*	1.7	3
122	20.90061503S 23.88416201E	no	-	-	-	no	*A. Mellifera* *C. alexandrii*	1.5	3
123	20.91847803S 23.88417399E	yes	0.23	0.41	0.36	no	*A. Mellifera* *Boscia albitrunca*	1.5	3
124	20.940676S 23.88420501E	no	-	-	-	no	*L. nelsii* *A. Mellifera*	1.5	4
125	20.96822396S 23.884232E	yes	0.12	0.42	0.46	no	*L. nelsii* *A. Mellifera*	1.4	4
126	20.989631S 23.88425396E	no	-	-	-	no	*L. nelsii* *A. Mellifera*	1.4	4
127	21.00095697S 23.881643E	no	-	-	-	no	*L. nelsii* *A. Mellifera*	1.5	3
128	21.000948S 23.85408497E	yes	0.08	0.48	0.44	no	*L. nelsii*	1.5	4
129	21.00094297S 23.85408799E	yes	0.1	0.40	0.5	no	*L. nelsii* *A. Mellifera*	1.5	4

130	21.00093098S 23.83475698E	no	-	-	-	no	*A. Mellifera* *L. nelsii*	2	4
131	21.00090299S 23.78273704E	yes	0.25	0.44	0.31	no	*A. Mellifera* *Boscia albitrunca* *C. alexandrii*	3.5	3
132	21.000877S 23.75797296E	yes	0.33	0.41	0.26	no	*Boscia albitrunca* *A. Mellifera* *Terminalia prunioides*	4.6	2
133	21.00082898S 23.72195198E	yes	0.43	0.37	0.20	no	*A. Mellifera* *Terminalia prunioides*	9	1

134	21.00077701S 23.69158803E	yes	0.29	0.36	0.35	no	*A. Mellifera* *Boscia albitrunca*	5	2
135	20.99398498S 23.65986002E	yes	0.26	0.25	0.49	no	*Croton gratissimus* *A. Mellifera*	5	2
136	20.934794S 23.66047399E	yes	0.45	0.37	0.18	no	*A. Mellifera* *L. nelsii* *Terminalia prunioides*	8	1
137	20.92093703S 23.62533999E	yes	0.39	0.35	0.26	no	*A. Robusta* *Croton gratissimus*	5	2
138	20.92150801S 23.60584896E	yes	0.28	0.33	0.39	no	*Boscia albitrunca* *Croton gratissimus*	5	2
139	20.91380797S 23.58243604E	yes	0.48	0.29	0.23	no	*A. Robusta* *A. Mellifera* *Boscia albitrunca*	6	1
140	20.88235497S 23.58026002E	yes	0.48	0.37	0.15	no	*A. luederiziit* *A. Mellifera* *Boscia albitrunca*	8	1
141	20.88250299S 23.58600003E	yes	0.44	0.36	0.24	no	*Boscia albitrunca* *Terminalia prunioides* *Croton gratissimus*	9	1
142	20.88264297S 23.59096798E	yes	0.28	0.37	0.35	no	*Boscia albitrunca* *A. hebeclada*	4.2	2
143	20.88299702S 23.56340703E	yes	0.25	0.43	0.32	no	*A. hebeclada* *Boscia albitrunca*	5.5	2
144	20.89788797S 23.55422599E	no	-	-	-	no	*A. Mellifera* *Croton gratissimus*	3.5	3
145	20.93806797S 23.55425902E	no	-	-	-	no	*Croton gratissimus* *Combretum hereroense*	3	2

146	20.96829797S 23.55138704E	yes	0.31	0.27	0.42	no	*Croton gratissimus* *A. hebeclada*	4.5	2
147	20.99991803S 23.54843401E	no	-	-	-	no	*A. Mellifera* *Croton gratissimus*	5	3
148	21.00045104S 23.50290804E	yes	0.32	0.35	0.33	no	*Croton gratissimus* *A. hebeclada* *A. Mellifera*	6.5	2
149	20.98191001S 23.43932301E	no	-	-	-	no	*Boscia albitrunca* *L. nelsii*	2.5	3
150	20.97576499S 23.48114099E	no	-	-	-	no	*Boscia albitrunca* *A. hebeclada*	2.8	3
151	20.93846804S 23.46005799E	no	-	-	-	no	*Croton gratissimus* *A. Mellifera*	2	4
152	20.92036799S 23.478151E	no	-	-	-	no	*L. nelsii* *A. Mellifera*	1.5	4
153	20.89948297S 23.50060704E	no	-	-	-	no	*A. hebeclada* *L. nelsii*	2.5	3
154	20.88112903S 23.49518697E	yes	0.37	0.40	0.23	no	*A. hebeclada* *Terminalia prunioides*	6	2
155	20.88127999S 23.52314204E	no	-	-	-	no	*A. Mellifera* *L. nelsii*	2	4
156	20.93107704S 23.50193004E	no	-	-	-	no	*Croton gratissimus* *A. Mellifera*	3.5	3
157	20.93141902S 23.52055899E	yes	0.37	0.36	0.27	no	*A. luederiziit* *Croton gratissimus*	4.5	2
158	20.94414602S 23.500025E	no	-	-	-	no	*Boscia albitrunca* *L. nelsii*	2	4
159	20.95145797S 23.48384902E	no	-	-	-	no	*Croton gratissimus* *G. Flava*	3.5	3

229

160	20.96673299S 23.47087098E	no	-	-	-	no	*A. Robusta A. Mellifera*	3	3
161	20.97006102S 23.45671202E	no	-	-	-	no	*A. Robusta A. Mellifera*	4	3
162	21.00018902S 23.403325E	yes	0.30	0.41	0.29	no	*Croton gratissimus Boscia albitrunca*	5	2
163	21.00007704S 23.370076E	yes	0.22	0.58	0.2	no	*Croton gratissimus G. Flava*	3	3
164	20.99993203S 23.32548302E	no	-	-	-	no	*A. Robusta Boscia albitrunca*	3	4
165	20.99985198S 23.30305103E	no	-	-	-	no	*Croton gratissimus G. Flava*	2.5	3
166	20.99980496S 23.29022001E	no	-	-	-	no	*A. Robusta G. Flava*	4	3
167	20.99970203S 23.25858403E	no	-	-	-	no	*A. Mellifera G. Flava*	3.5	3
168	21.00279202S 23.07432398E	no	-	-	-	no	*L. nelsii*	2	4
169	21.00216304S 23.000178E	no	-	-	-	no	*Combretum hereroense Croton gratissimus A. Mellifera*	6	2
170	21.00143298S 22.90993399E	no	-	-	-	no	*Croton gratissimus A. Mellifera*	3.5	3
171	21.00092797S 22.84696201E	no	-	-	-	no	*A. Robusta C. alexandrii*	3	3
172	21.00072504S 22.76303703E	no	-	-	-	no	*Croton gratissimus A. Robusta*	6.5	2
173	21.33691798S	no	-	-	-	no	*Comberetum*	5	2

	22.75482E						*Apiculutam*		
174	21.346945S 22.71644304E	no	-	-	-	no	*none*	0	5
175	21.34543098S 22.65221402E	no	-	-	-	no	*L. nelsii* *C. alexandrii*	2.5	3
176	21.32417698S 22.63441999E	yes	0.26	0.41	0.33	no	*Boscia albitrunca* *A. hebeclada*	3	3
177	21.26879197S 22.63201397E	no	-	-	-	no	*A. hebeclada* *Boscia albitrunca* *Ziziphus mucronata*	4	2
178	21.19406504S 22.64010703E	no	-	-	-	no	*A. hebeclada* *Ziziphus mucronata*	4	2
179	21.13156797S 22.64078898E	no	-	-	-	no	*A. Robusta* *A. hebeclada* *Boscia albitrunca*	3.5	3
180	20.99996103S 22.42857797E	no	-	-	-	no	*L. nelsii* *A. Robusta*	2	4
181	21.40683596S 23.77498998E	yes	0.38	0.35	0.27	no	*A. luederiziit* *A. hebeclada* *Terminalia prunioides*	6	1
182	21.40659498S 23.77455102E	yes	0.45	0.40	0.15	no	*A. luederiziit* *Terminalia prunioides* *A. Robusta*	7	1
183	21.40662801S 23.77412296E	yes	0.39	0.31	0.30	no	*A. luederiziit* *Terminalia prunioides* *Boscia albitrunca*	6	1
184	21.38182302S 23.79441898E	yes	0.34	0.39	0.27	no	*A. erubescens*	5	2
185	21.34913997S 23.75918398E	no	-	-	-	no	*A. erubescens* *Boscia albitrunca*	2	3

186	21.33662797S 23.75082999E	no	-	-	-	no	*A. erubescens* *Croton gratissimus*	5.5	2
187	21.32988196S 23.74349196E	yes	0.47	0.26	0.27	no	*A. erubescens* *Croton gratissimus* *A. hebeclada*	7	1
188	21.30872503S 23.723925E	no	-	-	-	no	*A. erubescens* *Boscia albitrunca*	5	2
189	21.29234402S 23.71008203E	yes	0.26	0.35	0.39	no	*A. hebeclada* *L. nelsii*	3.5	3
188	21.30872503S 23.723925E	no	-	-	-	no	*A. erubescens* *Boscia albitrunca*	5	2
189	21.29234402S 23.71008203E	no	-	-	-	no	*G. Flava* *A. erubescens*	3.5	3
190	21.26367297S 23.696012E	no	-	-	-	no	*A. erubescens* *Boscia albitrunca*	5.5	2
191	21.31862397S 23.68509097E	no	-	-	-	no	*L. nelsii* *A. Robusta*	2.5	3
192	21.33210702S 23.68679401E	yes	0.42	0.37	0.21	no	*Croton gratissimus* *A. hebeclada* *A. Mellifera*	5.5	1
193	21.40223103S 23.54172296E	no	-	-	-	no	*L. nelsii* *G. Flava*	1.5	4
194	21.402716S 23.59761701E	no	-	-	-	no	*Croton gratissimus* *L. nelsii*	2.5	2
195	21.40351798S 23.66364E	no	-	-	-	no	*Croton gratissimus* *L. nelsii*	4	2
196	21.40443496S 23.71524503E	yes	0.47	0.30	0.23	no	*Croton gratissimus* *L. nelsii* *Terminalia prunioides*	6	1
197	21.69810098S	no	-	-	-	no	*L. nelsii*	2	3

	23.58284801E						*A. Mellifera*		
198	21.76164804S 23.55868198E	no	-	-	-	no	*L. nelsii*	1	4
199	21.85061197S 23.53397196E	no	-	-	-	no	*Boscia albitrunca* *L. nelsii*	1.5	4
200	21.90984503S 23.51776304E	no	-	-	-	no	*G. Flava* *L. nelsii*	2	4
201	21.932965S 23.54999498E	no	-	-	-	no	*L. nelsii* *A. Mellifera*	2.5	3
202	21.97364599S 23.60112299E	no	-	-	-	no	*L. nelsii* *Boscia albitrunca*	1.5	4
203	21.99892304S 23.636646E	no	-	-	-	no	*A. erubescens* *Croton gratissimus* *L. nelsii*	2.5	3
204	22.03182997S 23.69449002E	no	-	-	-	no	*Croton gratissimus* *L. nelsii*	3	3

205	22.05709001S 23.71234196E	no	-	-	-	no	*Croton gratissimus*	1.8	4
206	22.03687898S 23.77290498E	no	-	-	-	no	*none*	0	5
207	22.024831S 23.80575802E	no	-	-	-	no	*none*	0	5
208	21.97804498S 23.88455596E	no	-	-	-	no	*L. nelsii* *A. mellifera*	2	4
209	21.73442597S 24.03196799E	yes	0.35	0.39	0.26	no	*C. Mopane* *A. erubescens*	8	2
210	21.64129799S 24.07156401E	yes	0.40	0.33	0.27	no	*C. Mopane*	8	2
211	21.65390798S 24.06502898E	yes	0.38	0.31	0.31	no	*C. Mopane*	10	1
212	21.68459002S 24.05100597E	yes	0.33	0.38	0.29	no	*Croton gratissimus* *G. Flava* *C. alexandrii*	7	2
213	21.88430504S 23.97032504E	no	-	-	-	no	*A. erubescens* *Croton gratissimus*	5	2
214	21.99999902S 23.99226098E	no	-	-	-	no	*none*	0	5
215	21.00088899S 23.77128996E	no	-	-	-	no	*A. Mellifera* *Terminalia prunioides*	9	1
216	21.00084499S 23.73791699E	no	-	-	-	no	*A. Mellifera* *Boscia albitrunca*	5	2
217	21.000776S 23.70660103E	no	-	-	-	no	*Croton gratissimus* *A. Mellifera*	4.5	2
218	21.00076402S 23.67411696E	no	-	-	-	no	*A. Robusta* *Croton gratissimus*	5	2
219	20.96037397S 23.660216E	no	-	-	-	no	*A. Mellifera* *L. nelsii*	4	3

220	20.92017302S 23.65017003E	no	-	-	-	no	*A. Robusta* *Croton gratissimus*	3.5	3
221	20.92122998S 23.61572301E	no	-	-	-	no	*Croton gratissimus* *A. hebeclada*	5	2
222	20.92182702S 23.59243498E	no	-	-	-	no	*Croton gratissimus* *L. nelsii*	3	3
223	20.89695004S 23.580344E	no	-	-	-	no	*A. erubescens* *Croton gratissimus*	5	2
224	20.88249997S 23.58600497E	no	-	-	-	no	*A. erubescens* *Croton gratissimus*	5	2
225	20.88287104S 23.59999001E	yes	0.46	0.30	0.24	no	*A. erubescens* *Terminalia prunioides*	6	1
226	20.88030299S 23.57379204E	no	-	-	-	no	*A. erubescens* *Croton gratissimus*	2	4
227	20.87726397S 23.55280803E	no	-	-	-	no	*A. Mellifera* *Croton gratissimus*	3.5	3
228	20.90762297S 23.554875E	no	-	-	-	no	*Boscia albitrunca* *A. Mellifera*	4.5	2
229	20.95713504S 23.55245003E	no	-	-	-	no	*A. Mellifera* *Croton gratissimus*	3	3
230	20.99139196S 23.54923096E	no	-	-	-	no	*L. nelsii*	1.5	4
231	21.000502S 23.522129E	no	-	-	-	no	*A. hebeclada* *Croton gratissimus*	5	2
232	20.99494304S 23.43911598E	no	-	-	-	no	none	0	5
233	20.98009701S 23.48180903E	no	-	-	-	no	*Croton gratissimus* *A. erubescens*	4	3
234	20.96618397S 23.485601E	no	-	-	-	no	*Boscia albitrunca* *Croton gratissimus*	4.5	3

Bibliography

Adams, J.B., & Adams, J.D. (1984). Geologic mapping using Landsat MSS and TM images - Removing vegetation by modeling spectral mixtures. In, *Third Thematic Conference on Remote Sensing for Exploration Geology*. Colorado Springs

Adams, J.B., Sabol, D.E., Kapos, V., Almeida, R., Roberts, D.A., Smith, M.O., & Gillespie, A.R. (1995). Classification of Multispectral Images Based on Fractions of Endmembers: Application to Land-Cover Change in the Brazilian Amazon. *Remote Sensing of Environment, 52*, 137-154

Addicott, J.F., Aho, J.M., Antolin, M.F., Padilla, D.K., Richardson, J.S., & Soluk, D.A. (1987). Ecological neighborhoods: scaling environmental patterns. In (p. 340)

Addink, E.A., de Jong, S.M., & Pebesma, E.J. (2007). The importance of scale in object-based mapping of vegetation parameters with hyperspectral imagery. *Photogrammetric Engineering and Remote Sensing, 73*, 905

Adeel, Z., de Kalbermatten, G., & Assessment, M.E. (2005). *Ecosystems and human well-being: desertification synthesis*: Island Press

Andrews, A. (1990). Fragmentation of Habitat by Roads and Utility Corridors a Review. *Australian Zoologist, 26*, 130-141

Aplin, P. (2005). Remote sensing: ecology. *Progress in Physical Geography, 29*, 104-113

Arbiol, R., Zhang, Y., & Palá, V. (2006). Advanced classification techniques: A review. In, *ISPRS Commission VII Mid-term Symposium "From Pixel to Processes"*. Enschede, NL

Archer, S., Schimel, D.S., & Holland, E.A. (1995). Mechanisms of Shrub land Expansion-Land-use, Climate or CO2. *Climatic Change, 29*, 91-99

Archer, S., Scifres, C., Bassham, C.R., & Maggio, R. (1988). Autogenic Succession in a Sub-Tropical Savanna - Conversion of Grassland to Thorn Woodland. *Ecological Monographs, 58*, 111-127

Archer, S., Vavra, M., Laycock, W., & Pieper, R. (1994). Woody plant encroachment into southwestern grasslands and savannas: rates, patterns and proximate causes. In, *Ecological implications of livestock herbivory in the west.* (pp. 13-68): Society for Range Management.

Archibald, S., Scholes, R., Roy, D., Roberts, G., & Boschetti, L. (2010). Southern African fire regimes as revealed by remote sensing. *International Journal of Wildland Fire, 19*, 861-878

Asner, G.P. (1998). Biophysical and biochemical sources of variability in canopy reflectance. *Remote Sensing of Environment, 64*, 234-253

Asner, G.P., & Heidebrecht, K.B. (2002). Spectral unmixing of vegetation, soil and dry carbon cover in arid regions: comparing multispectral and hyperspectral observations. *International Journal of Remote Sensing, 23*, 3939-3958

Asner, G.P., & Heidebrecht, K.B. (2003). Imaging spectroscopy for desertification studies: comparing AVIRIS and EO-1 Hyperion in Argentina drylands. *Geoscience and Remote Sensing, IEEE Transactions on, 41*, 1283-1296

Asner, G.P., Levick, S.R., & Smith, P.J. (2011). Remote Sensing of Fractional Cover and Biochemistry in Savannas. In M.J. Hill & N.P. Hanan (Eds.), *Ecosystem Function in Savannas: Measurement and Modeling at Landscape to Global Scales*: CRC Press

Asner, G.P., & Lobell, D.B. (2000). A Biogeophysical Approach for Automated SWIR Unmixing of Soils and Vegetation. *Remote Sensing of Environment, 74*, 99-112

Asner, G.P., Wessman, C.A., & Schimel, D.S. (1998). Heterogeneity of Savanna Canopy Structure and Function from Imaging Spectrometry and Inverse Modeling. In (pp. 1022-1036)

Attiwill, P.M. (1994). The disturbance of forest ecosystems: the ecological basis for conservative management. In (p. 247)

Avon, C., Berges, L., Dumas, Y., & Dupouey, J.L. Does the effect of forest roads extend a few meters or more into the adjacent forest? A study on understory plant diversity in managed oak stands. *Forest Ecology and Management, 259*, 1546-1555

Baatz, M., & Schäpe, A. (2000a). Multiresolution segmentation: an optimization approach for high quality multi-scale image segmentation. *Angewandte geographische informationsverarbeitung, 12*, 12-23

Baatz, M., & Schäpe, M. (2000b). Multiresolution segmentation—An optimization approach for high-quality multi-scale image segmentation. In J. Strobl, T. Blaschke & G. Griesebner (Eds.), *Angewandte Geographische Informations-Verarbeitung* (pp. 12-23). Wichmann Verlag, Karlsruhe

Baccini, A., Friedl, M.A., Woodcock, C.E., & Warbington, R. (2004). Forest biomass estimation over regional scales using multisource data. *Geophysical Research Letters, 31*

Baillieul, T.A. (1975). A reconnaissance survey of the cover sands in the Republic of Botswana. *Journal of Sedimentary Research, 45*, 494-503

Baret, F., Guyot, G., & Major, D.J. (1989). TSAVI: A Vegetation Index Which Minimizes Soil Brightness Effects On LAI And APAR Estimation. In, *Geoscience and Remote Sensing Symposium, 1989. IGARSS'89. 12th Canadian Symposium on Remote Sensing., 1989 International* (pp. 1355-1358)

Barker, J.F. (1982). Towards a biogeography of the Kalahari. Part I . To which region does the Kalahari belong? *Botswana Notes and Records, 15*, 85-91

Bateson, A., & Curtiss, B. (1996). A method for manual endmember selection and spectral unmixing. *Remote Sensing of Environment, 55*, 229-243

Baugh, W.M., & Groeneveld, D.P. (2006). Broadband vegetation index performance evaluated for a low-cover environment. *International Journal of Remote Sensing, 27*, 4715-4730

Belsky, A.J. (1990). Tree Grass Ratios in East-African Savannas - a Comparison of Existing Models. *Journal of Biogeography, 17*, 483-489

Benz, U.C., Hofmann, P., Willhauck, G., Lingenfelder, I., & Heynen, M. (2004a). Multi-resolution, object-oriented fuzzy analysis of remote sensing data for GIS-ready information. *Isprs Journal of Photogrammetry and Remote Sensing, 58*, 239-258

Benz, U.C., Hofmann, P., Willhauck, G., Lingenfelder, I., & Heynen, M. (2004b). Multi-resolution, object-oriented fuzzy analysis of remote sensing data for GIS-ready information. *Isprs Journal of Photogrammetry and Remote Sensing, 58*, 239-258

Berry, S.L., & Roderick, M.L. (2002). Estimating mixtures of leaf functional types using continental-scale satellite and climatic data. *Global Ecology and Biogeography, 11*, 23-39

Bhattacharya, M., Primack, R.B., & Gerwein, J. (2003). Are roads and railroads barriers to bumblebee movement in a temperate suburban conservation area? *Biological Conservation, 109*, 37-45

Blaschke, T. (2010). Object based image analysis for remote sensing. *Isprs Journal of Photogrammetry and Remote Sensing, 65*, 2-16

Blaschke, T., & Hay, G.J. (2001). Object-oriented image analysis and scale-space: theory and methods for modeling and evaluating multiscale landscape structure. *International Archives of Photogrammetry and Remote Sensing, 34*, 22-29

Blaschke, T., Lang, S., & Hay, G.J. (2008). *Object-based image analysis: spatial concepts for knowledge-driven remote sensing applications*: Springer Verlag

Blaum, N., Rossmanith, E., & Jeltsch, F. (2007). Land use affects rodent communities in Kalahari savannah rangelands. *African Journal of Ecology, 45*, 189-195

Boardman, J.W., Kruse, F.A., and Green, R.O., (1995). Mapping target signatures via partial unmixing of AVIRIS data. In, *Summaries of the Fifth Annual JPL Airborne Geoscience Workshop* (pp. 23-26): Jet Propulsion Laboratory, Pasadena, CA

Bolstad, P.V., Swank, W., & Vose, J. (1998). Predicting Southern Appalachian overstory vegetation with digital terrain data. In (p. 271)

Bonham, C.D. (1989). *Measurements for terrestrial vegetation*: Wiley New York etc.

Booth, D.T., & Tueller, P.T. (2003). Rangeland monitoring using remote sensing. *Arid Land Research and Management, 17*, 455-467

Borel, C.C., & Gerstl, S.A.W. (1994). Nonlinear spectral mixing models for vegetative and soil surfaces. *Remote Sensing of Environment, 47*, 403-416

Borsotti, M., Campadelli, P., & Schettini, R. (1998). Quantitative evaluation of color image segmentation results. *Pattern Recognition Letters, 19*, 741-747

Box, E.O. (1996). Plant functional types and climate at the global scale. *Journal of Vegetation Science, 7*, 309-320

Boyce, M.S., Mao, J.S., Merrill, E.H., Fortin, D., & Turner, M.G. (2003). Scale and heterogeneity in habitat selection by elk in Yellowstone National Park. In (p. 421)

Breiman, L. (2001). Random forests. *Machine Learning, 45*, 5-32

Breiman, L., & Cutler, A. (1993). A deterministic algorithm for global optimization. *Mathematical Programming, 58*, 179-199

Brock, R.E., & Kelt, D.A. (2004). Influence of roads on the endangered Stephens' kangaroo rat (Dipodomys stephensi): are dirt and gravel roads different? *Biological Conservation, 118*, 633-640

Bucini, G., & Hanan, N.P. (2007). A continental-scale analysis of tree cover in African savannas. *Global Ecology and Biogeography, 16*, 593-605

Burke, I.C., Lauenroth, W.K., Cunfer, G., Barrett, J.E., & Mosier, A. (2002). Nitrogen in the central grasslands region of the United States. In (p. 813)

Camps-Valls, G., & Bruzzone, L. (2009). *Kernel methods for remote sensing data analysis*: Wiley Online Library

Carlson, T.N., & Ripley, D.A. (1997). On the relation between NDVI, fractional vegetation cover, and leaf area index. *Remote Sensing of Environment, 62*, 241-252

Caylor, K.K., Shugart, H.H., Dowty, P.R., & Smith, T.M. (2003). Tree spacing along the Kalahari transect in southern Africa. *Journal of Arid Environments, 54*, 281-296

Cescatti, A., Marcolla, B., Santhana Vannan, S.K., Pan, J.Y., Román, M.O., Yang, X., Ciais, P., Cook, R.B., Law, B.E., & Matteucci, G. (2012). Intercomparison of MODIS albedo retrievals and in situ measurements across the global FLUXNET network. *Remote Sensing of Environment, 121*, 323-334

Chamaille-Jammes, S., & Fritz, H. (2009). Precipitation-NDVI relationships in eastern and southern African savannas vary along a precipitation gradient. *International Journal of Remote Sensing, 30*, 3409-3422

Chan, T.H., Chi, C.Y., Huang, Y.M., & Ma, W.K. (2009). A Convex Analysis-Based Minimum-Volume Enclosing Simplex Algorithm for Hyperspectral Unmixing. *Ieee Transactions on Signal Processing, 57*, 4418-4432

Chen, G., Hay, G.J., Carvalho, L.M., & Wulder, M.A. (2012). Object-based change detection. *International Journal of Remote Sensing, 33*, 4434-4457

Chen, Z.K., Elvidge, C.D., & Groeneveld, D.P. (1998). Monitoring seasonal dynamics of arid land vegetation using AVIRIS data. *Remote Sensing of Environment, 65*, 255-266

Chubey, M.S., Franklin, S.E., & Wulder, M.A. (2006). Object-based analysis of Ikonos-2 imagery for extraction of forest inventory parameters. *Photogrammetric Engineering and Remote Sensing, 72*, 383-394

Clinton, N., Holt, A., Scarborough, J., Yan, L., & Gong, P. (2010). Accuracy Assessment Measures for Object-based Image Segmentation Goodness. *Photogrammetric Engineering and Remote Sensing, 76*, 289-299

Colditz, R., Gessner, U., Conrad, C., van Zyl, D., Malherbe, J., Nevvby, T., Landmann, T., Schmidt, M., & Dech, S. (2007). Dynamics of MODIS time series for ecological applications in southern África. In, *Analysis of Multi-temporal Remote Sensing Images, 2007. MultiTemp 2007. International Workshop on the* (pp. 1-6): IEEE

Colombo, R., Bellingeri, D., Fasolini, D., & Marino, C.M. (2003). Retrieval of leaf area index in different vegetation types using high resolution satellite data. *Remote Sensing of Environment, 86*, 120-131

Coops, N., & Culvenor, D. (2000). Utilizing local variance of simulated high spatial resolution imagery to predict spatial pattern of forest stands. *Remote Sensing of Environment, 71*, 248-260

Cottam, G., & Curtis, J.T. (1956). The use of distance measures in phytosociological sampling. *Ecology, 37*, 451-460

Craig, M.D. (1994). Minimum-Volume Transforms for Remotely-Sensed Data. *Ieee Transactions on Geoscience and Remote Sensing, 32*, 542-552

Cramer, W., Bondeau, A., Woodward, F.I., Prentice, I.C., Betts, R.A., Brovkin, V., Cox, P.M., Fisher, V., Foley, J.A., Friend, A.D., Kucharik, C., Lomas, M.R., Ramankutty, N., Sitch, S., Smith, B., White, A., & Young-Molling, C. (2001). Global response of terrestrial ecosystem structure and function to CO2 and climate change: results from six dynamic global vegetation models. *Global Change Biology, 7*, 357-373

Cui, X., Gibbes, C., Southworth, J., & Waylen, P. (2013). Using Remote Sensing to Quantify Vegetation Change and Ecological Resilience in a Semi-Arid System. *Land, 2*, 108-130

Cutler, D.R., Edwards Jr, T.C., Beard, K.H., Cutler, A., Hess, K.T., Gibson, J., & Lawler, J.J. (2007). Random forests for classification in ecology. *Ecology, 88*, 2783-2792

Dahlberg, A.C. (2000). Vegetation diversity and change in relation to land use, soil and rainfall—a case study from North-East District, Botswana. *Journal of Arid Environments, 44*, 19-40

Dansereau, P. (1960). Essai di représentation cartographique des éléments structuraux de la végétation. *Méthodes de la cartographie de la végétation. Toulouse*

Daubenmire, R. (1968). Plant communities. A textbook of plant synecology. *Plant communities. A textbook of plant synecology*

Daughtry, C.S.T., Doraiswamy, P.C., Hunt, E.R., Stern, A.J., McMurtrey, J.E., & Prueger, J.H. (2006). Remote sensing of crop residue cover and soil tillage intensity. *Soil & Tillage Research, 91*, 101-108

Davidson, E.A., Asner, G.P., Stone, T.A., Neill, C., & Figueiredo, R.O. (2008). Objective indicators of pasture degradation from spectral mixture analysis of Landsat imagery. *Journal of Geophysical Research-Biogeosciences, 113*, 7

Dennison, P.E., Brunelle, A.R., & Carter, V.A. (2010). Assessing canopy mortality during a mountain pine beetle outbreak using GeoEye-1 high spatial resolution satellite data. *Remote Sensing of Environment, 114*, 2431-2435

Dennison, P.E., Halligan, K.Q., & Roberts, D.A. (2004). A comparison of error metrics and constraints for multiple endmember spectral mixture analysis and spectral angle mapper. *Remote Sensing of Environment, 93*, 359-367

Dennison, P.E., & Roberts, D.A. (2003). Endmember selection for multiple endmember spectral mixture analysis using endmember average RMSE. *Remote Sensing of Environment, 87*, 123-135

Develey, P.F., & Stouffer, P.C. (2001). Effects of Roads on Movements by Understory Birds in Mixed-Species Flocks in Central Amazonian Brazil. *Conservation Biology, 15*, 1416-1422

DHV (1980). Country Wide Animal and Range Assessment Project: DHV Consulting Engineers Final report to the Department of Wildlife, National Parks and Tourism, Government of Botswana. In

Dougill, A., & Trodd, N. (1999). Monitoring and modelling open savannas using multisource information: analyses of Kalahari studies. *Global Ecology and Biogeography, 8*, 211-221

Dougill, A.J., Fraser, E.D.G., & Reed, M.S. (2010). Anticipating Vulnerability to Climate Change in Dryland Pastoral Systems: Using Dynamic Systems Models for the Kalahari. *Ecology and Society, 15*

Dougill, A.J., Thomas, D.S.G., & Heathwaite, A.L. (1999). Environmental Change in the Kalahari: Integrated Land Degradation Studies for Nonequilibrium Dryland Environments. *Annals of the Association of American Geographers, 89*, 420-442

Dronova, I., Gong, P., Clinton, N.E., Wang, L., Fu, W., Qi, S., & Liu, Y. (2012). Landscape analysis of wetland plant functional types: The effects of image segmentation scale, vegetation classes and classification methods. *Remote Sensing of Environment, 127*, 357-369

Dublin, H.T., Sinclair, A.R.E., & McGlade, J. (1990). Elephants and Fire as Causes of Multiple Stable States in the Serengeti Mara Woodlands. *Journal of Animal Ecology, 59*, 1147-1164

Duncan, J., Stow, D., Franklin, J., & Hope, A. (1993). Assessing the Relationship between Spectral Vegetation Indexes and Shrub Cover in the Jornada Basin, New-Mexico. *International Journal of Remote Sensing, 14*, 3395-3416

Dupr, C., & Ehrln, J. (2002). Habitat configuration, species trains and plant distributions. In (p. 796)

DWNP (2003). Central Kalahari and Kutse Game Reserve Management Plan. In: Deaprtment of Wildlife and National Park, Government of Botswana, Gaborone

Dyer, T., & Tyson, P. (1977). Estimating Above and Below Normal Rainfall Periods over South Africa, 1972-2000. *Journal of Applied Meteorology, 16*, 145-147

Eagleson, P.S., & Segarra, R.I. (1985). Water-Limited Equilibrium of Savanna Vegetation Systems. *Water Resources Research, 21*, 1483-1493

Edwards, A.C., Maier, S.W., Hutley, L.B., Williams, R.J., & Russell-Smith, J. (2013). Spectral analysis of fire severity in north Australian tropical savannas. *Remote Sensing of Environment, 136*, 56-65

Edwards, D. (1983). A broad-scale structural classification of vegetation for practical purposes. *Bothalia, 14*

Eigenbrod, F., Hecnar, S.J., & Fahrig, L. (2008). Accessible habitat: an improved measure of the effects of habitat loss and roads on wildlife populations. *Landscape Ecology, 23*, 159-168

Eiten, G. (1968). *Vegetation Forms: A Classification of Stands Vegetation Based on Structure, Growth Form of the Components, and Vegetative Periodicity*: Instituto de Botanica

Ellenberg, D., & Mueller-Dombois, D. (1974). *Aims and methods of vegetation ecology*: Wiley New York, NY

Elmore, A.J., Mustard, J.F., Manning, S.J., & Lobell, D.B. (2000). Quantifying Vegetation Change in Semiarid Environments: Precision and Accuracy of

Spectral Mixture Analysis and the Normalized Difference Vegetation Index. *Remote Sensing of Environment, 73*, 87-102

Elvidge, C.D., & Chen, Z.K. (1995). Comparison of Broad-Band and Narrow-Band Red and near-Infrared Vegetation Indexes. *Remote Sensing of Environment, 54*, 38-48

Escafadel, R., & Huete, A.R. (1991). Improvement in remote sensing of low vegetation cover in arid regions by correcting vegetation indices for soil "noise". *Comptes Rendus de l'Academie des Sciences de Paris, 312*, 1385–1391

Fagan, W.F. (2002). Connectivity, fragmentation, and extinction risk in dendritic metapopulations. In (p. 3243)

Fahrig, L., & Rytwinski, T. (2009). Effects of Roads on Animal Abundance: an Empirical Review and Synthesis. *Ecology and Society, 14*, 20

Fernandez-Illescas, C.P., & Rodriguez-Iturbe, I. (2003). Hydrologically driven hierarchical competition-colonization models: The impact of interannual climate fluctuations. *Ecological Monographs, 73*, 207-222

Fisher, J.T., Erasmus, B.F., Witkowski, E.T., Aardt, J., Wessels, K.J., & Asner, G.P. (2013a). Savanna woody vegetation classification–now in 3-D. *Applied Vegetation Science*

Fisher, J.T., Erasmus, B.F.N., Witkowski, E.T.F., van Aardt, J., Wessels, K.J., & Asner, G.P. (2013b). Savanna woody vegetation classification – now in 3-D. *Applied Vegetation Science*, n/a-n/a

Flather, C.H., & Bevers, M. (2002). Patchy reaction-diffusion and population abundance: the relative importance of habitat amount and arrangement. In (p. 40)

Flory, S.L., & Clay, K. (2006). Invasive shrub distribution varies with distance to roads and stand age in eastern deciduous forests in Indiana, USA. *Plant Ecology, 184*, 131-141

Forman, R.T.T., & Alexander, L.E. (1998). Roads and their major ecological effects. *Annual Review of Ecology and Systematics* (pp. 207-231): Annual Reviews Inc. {a}

Forman, R.T.T., Reineking, B., & Hersperger, A.M. (2002). Road traffic and nearby grassland bird patterns in a suburbanizing landscape. *Environmental Management, 29*, 782-800

Fortin, M.J., Boots, B., Csillag, F., & Remmel, T.K. (2003). On the role of spatial stochastic models in understanding landscape indices. In (p. 203)

Fosberg, F.R. (1967). *A classification of vegetation for general purposes*: Section IPB/CT, International Biological Programme

Foster, D.R., Fluet, M., & Boose, E.R. (1999). Human or natural disturbance: landscape-scale dynamics of the tropical forests of Puerto Rico. In (p. 555)

Franklin, J., Duncan, J., & Turner, D.L. (1993). Reflectance of Vegetation and Soil in Chihuahuan Desert Plant-Communities from Ground Radiometry Using Spot Wavebands. *Remote Sensing of Environment, 46*, 291-304

Friedl, M.A., & Brodley, C.E. (1997). Decision tree classification of land cover from remotely sensed data. *Remote Sensing of Environment, 61*, 399-409

Frost, P.G.H., & Robertson, F. (1987). Fire: The Ecological Effects of Fire in Savannas. In B.H. Walker (Ed.), *Determinants of Tropical Savannas.* (pp. 93–140): Oxford.

Furley, P. (2004). Tropical savannas. *Progress in Physical Geography, 28*, 581-598

Furley, P. (2010). Tropical savannas: Biomass, plant ecology, and the role of fire and soil on vegetation. *Progress in Physical Geography, 34*, 563-585

Gadgil, M., & Meher-Homji, V.M. (1985). Land Use and Productive Potential of Indian Savannas. *Tothill, J. C. and J. J. Mott* (pp. 107-113)

Garcia-Haro, F., Gilabert, M., & Melia, J. (1996). Linear spectral mixture modelling to estimate vegetation amount from optical spectral data. *International Journal of Remote Sensing, 17*, 3373-3400

Gelbard, J.L., & Belnap, J. (2003). Roads as conduits for exotic plant invasions in a semiarid landscape. *Conservation Biology, 17*, 420-432

Gessner, U., Machwitz, M., Conrad, C., & Dech, S. (2013). Estimating the fractional cover of growth forms and bare surface in savannas. A multi-resolution approach based on regression tree ensembles. *Remote Sensing of Environment, 129*, 90-102

Gill, T., & Phinn, S. (2008). Estimates of bare ground and vegetation cover from Advanced Spaceborne Thermal Emission and Reflection Radiometer (ASTER) short-wave-infrared reflectance imagery. *Journal of Applied Remote Sensing, 2*, 023511-023519

Gillon, G. (1983). The Fire Problem in Tropical Savannas. In F. Bourlière (Ed.), *Tropical Savannas: Ecosystems of the World, 13.* Amsterdam: Elsevier

Gillson, L., & Ekblom, A. (2009). Resilience and Thresholds in Savannas: Nitrogen and Fire as Drivers and Responders of Vegetation Transition. *Ecosystems, 12*, 1189-1203

Giri, C., Zhu, Z.L., & Reed, B. (2005). A comparative analysis of the Global Land Cover 2000 and MODIS land cover data sets. *Remote Sensing of Environment, 94*, 123-132

Glasbey, C.A., & Horgan, G.W. (1995). *Image analysis for the biological sciences*: Wiley Chichester

Goetz, A.F.H., Vane, G., Solomon, J.E., & Rock, B.N. (1985). Imaging Spectrometry for Earth Remote-Sensing. *Science, 228*, 1147-1153

Goldsmith, B. (1991). *Monitoring for conservation and ecology*: Chapman and Hall Ltd

Goodchild, M.F., Quattrochi, D.A. (1997). Introduction: Scale, Multiscaling, Remote Sensing, and GIS. In D.A.G. Quattrochi, M.F., (Ed.), *Scale in remote sensing and GIS*: Lewis Publishers: Boca Raton, Fla.

Goodwin, B.J., & Fahrig, L. (2002). How does landscape structure influence landscape connectivity. In (p. 552)

Graetz, R.D. (1990). Remote sensing of terrestrial ecosystem structure: an ecologist's pragmatic view. *Remote sensing of biosphere functioning* (pp. 5-30): Springer

Green, R.O., Eastwood, M.L., Sarture, C.M., Chrien, T.G., Aronsson, M., Chippendale, B.J., Faust, J.A., Pavri, B.E., Chovit, C.J., Solis, M.S., Olah, M.R., & Williams,

O. (1998). Imaging spectroscopy and the Airborne Visible Infrared Imaging Spectrometer (AVIRIS). *Remote Sensing of Environment, 65*, 227-248

Groffman, P.M., Baron, J.S., Blett, T., Gold, A.J., & Goodman, I. (2005). Ecological thresholds: the key to successful environmental management or an important concept with no practical application. In

Groffman, P.M., Tiedje, T.M., Mokma, D.L., & Simkins, S. (1992). Regional-scale analysis of denitrification in north temperate forest soils. In (p. 45)

Grossman, D.H., & Conservancy, N. (1998). *International classification of ecological communities: terrestrial vegetation of the United States*: Nature Conservancy

Guerschman, J.P., Hill, M.J., Renzullo, L.J., Barrett, D.J., Marks, A.S., & Botha, E.J. (2009). Estimating fractional cover of photosynthetic vegetation, non-photosynthetic vegetation and bare soil in the Australian tropical savanna region upscaling the EO-1 Hyperion and MODIS sensors. *Remote Sensing of Environment, 113*, 928-945

Guerschman, J.P., Oyarzabal, M., Malthus, T., McVicar, T., Byrne, G., Randall, L., & Stewart, J. (2012). Evaluation of the MODIS-based vegetation fractional cover product. In: CSIRO, Australia

Gustafson, E.J. (1998). Quantifying landscape spatial pattern: What is the state of the art. In (p. 143)

Gutman, G. (2004). *Land Change Science: Observing, Monitoring and Undeerstanding Trajectories of Change on the Earth's Surface*: Springer

Halligan, K. (2008). Introduction to MESMA. In

Hamada, Y., Stow, D.A., & Roberts, D.A. (2011). Estimating life-form cover fractions in California sage scrub communities using multispectral remote sensing. *Remote Sensing of Environment, 115*, 3056-3068

Hanan, N.P., & Lehmann, C.E. (2010). Tree–Grass Interactions in Savannas: Paradigms, Contradictions, and Conceptual Models. *Ecosystem Function in Savannas: Measurement and Modeling at Landscape to Global Scales*, 39

Harris, D.R. (1980). Tropical savanna environments: definition, distribution, diversity, and development. *Human ecology in savanna environments.*, 3-27

Hastie, T., Tibshirani, R., & Friedman, J. (2009). Linear Methods for Regression. *The elements of statistical learning* (pp. 43-99): Springer New York

Hay, G.J., Blaschke, T., Marceau, D.J., & Bouchard, A. (2003). A comparison of three image-object methods for the multiscale analysis of landscape structure. *Isprs Journal of Photogrammetry and Remote Sensing, 57*, 327-345

Heilman, G.E., Strittholt, J.R., Slosser, N.C., & Dellasala, D.A. (2002). Forest fragmentation of the conterminous United States: Assessing forest intactness through road density and spatial characteristics. *Bioscience, 52*, 411-422

Hemson, G. (2003). The Ecology and Conservation of Lions: Human-Wildlife Conflict in semi-arid Botswana. In (p. 213): University of Oxford

Herold, M., Woodcock, C.E., Loveland, T.R., Townshend, J., Brady, M., Steenmans, C., & Schmullius, C.C. (2008). Land-cover observations as part of a global earth

observation system of systems (GEOSS): progress, activities, and prospects. *Systems Journal, IEEE, 2*, 414-423

Herremans, M. (1998). Conservation status of birds in Botswana in relation to land use. *Biological Conservation, 86*, 139-160

Herrick, J., Bestelmeyer, B., Archer, S., Tugel, A., & Brown, J. (2006). An integrated framework for science-based arid land management. *Journal of Arid Environments, 65*, 319-335

Herrick, J.E., Van Zee, J.W., Havstad, K.M., Burkett, L.M., & Whitford, W.G. (2005). Monitoring Manual for Grassland, Shrubland and Savanna Ecosystems. In: Las Cruces, NM,: USDA-ARS Jornada Experimental Range

Higgins, S.I., Bond, W.J., & Trollope, W.S.W. (2000). Fire, resprouting and variability: a recipe for grass-tree coexistence in savanna. *Journal of Ecology, 88*, 213-229

Hill, M.J. (2013). Vegetation index suites as indicators of vegetation state in grassland and savanna: An analysis with simulated SENTINEL 2 data for a North American transect. *Remote Sensing of Environment, 137*, 94-111

Hill, M.J., Roman, M.O., & Schaaf, C.B. (2011a). Biogeography and Dynamis of Global Tropical and Subtropical Savannas: A Spatiotemporal View. In M.J. Hill & N.P. Hanan (Eds.), *Ecosystem Function in Savannas: Measurement and Modeling at Landscape to Global Scales*: CRC Press

Hill, M.J., Román, M.O., & Schaaf, C.B. (2011b). Dynamics of vegetation indices in tropical and subtropical savannas defined by ecoregions and Moderate Resolution Imaging Spectroradiometer (MODIS) land cover. *Geocarto International, 27*, 153-191

Hill, M.J., Román, M.O., & Schaaf, C.B. (2012). Dynamics of vegetation indices in tropical and subtropical savannas defined by ecoregions and Moderate Resolution Imaging Spectroradiometer (MODIS) land cover. *Geocarto International, 27*, 153-191

HilleRisLambers, R., Rietkerk, M., van den Bosch, F., Prins, H.H.T., & de Kroon, H. (2001). Vegetation pattern formation in semi-arid grazing systems. *Ecology, 82*, 50-61

Hoffmann, W.A., & Jackson, R.B. (2000). Vegetation-climate feedbacks in the conversion of tropical savanna to grassland. *Journal of Climate, 13*, 1593-1602

Hoffmann, W.A., Schroeder, W., & Jackson, R.B. (2002). Positive feedbacks of fire, climate, and vegetation and the conversion of tropical savanna. *Geophysical Research Letters, 29*, 4

Holdo, R.M. (2007). Elephants, fire, and frost can determine community structure and composition in Kalahari woodlands. *Ecological Applications, 17*, 558-568

Holmes, P. (1990). Dispersal and predation in alien Acacia. *Oecologia, 83*, 288-290

Homewood, K. (1996). The World's Savannas: Economic driving forces, ecological constraints and policy options for sustainable land use - Young,MD, Solbrig,OT. *Disasters, 20*, 83-84

Hoogesteijn, A., & Hoogesteijn, R. (2010). Cattle Ranching and Biodiversity Conservation as Allies in South America's Flooded Savannas. *Great Plains Research, 20*, 37-50

Hooper, D., Chapin Iii, F., Ewel, J., Hector, A., Inchausti, P., Lavorel, S., Lawton, J., Lodge, D., Loreau, M., & Naeem, S. (2005). Effects of biodiversity on ecosystem functioning: a consensus of current knowledge. *Ecological Monographs, 75*, 3-35

House, J.I., Archer, S., Breshears, D.D., & Scholes, R.J. (2003). Conundrums in mixed woody-herbaceous plant systems. *Journal of Biogeography, 30*, 1763-1777

Howes, D., Clare, P., Oxford, W., & Murphy, S. (2004). Endmember selection techniques for improved spectral unmixing. In S.S. Shen & P.E. Lewis (Eds.), *Algorithms and Technologies for Multispectral, Hyperspectral, and Ultraspectral Imagery X* (pp. 65-76). Bellingham: Spie-Int Soc Optical Engineering

Hudak, A.T., Crookston, N.L., Evans, J.S., Hall, D.E., & Falkowski, M.J. (2008). Nearest neighbor imputation of species-level, plot-scale forest structure attributes from LiDAR data. *Remote Sensing of Environment, 112*, 2232-2245

Hudak, A.T., & Wessman, C.A. (1998). Textural analysis of historical aerial photography to characterize woody plant encroachment in South African savanna. *Remote Sensing of Environment, 66*, 317-330

Huete, A.R., & Jackson, R.D. (1988). Soil and Atmosphere Influences on the Spectra of Partial Canopies. *Remote Sensing of Environment, 25*, 89-105

Huete, A.R., Jackson, R.D., & Post, D.F. (1985). Spectral Response of a Plant Canopy with Different Soil Backgrounds. *Remote Sensing of Environment, 17*, 37-53

Huete, A.R., Miura, T., & Gao, X. (2003). Land cover conversion and degradation analyses through coupled soil-plant biophysical parameters derived from hyperspectral EO-1 Hyperion. *Ieee Transactions on Geoscience and Remote Sensing, 41*, 1268-1276

Hufkens, K., Bogaert, J., Dong, Q.H., Lu, L., Huang, C.L., Ma, M.G., Che, T., Li, X., Veroustraete, F., & Ceulemans, R. (2008). Impacts and uncertainties of upscaling of remote-sensing data validation for a semi-arid woodland. *Journal of Arid Environments, 72*, 1490-1505

Hulme, M., & Arntzen, J.W. (1996). *Climate change and Southern Africa: an exploration of some potential impacts and implications for the SADC region*: Climatic Research Unit, University of East Anglia Norwich, UK

Hulme, M., Doherty, R., Ngara, T., New, M., & Low, P. (2005). Global warming and African climate change: a reassessment. *Climate change and Africa*, 29-40

Huntley, B. (1982). Southern African savannas. *Ecology of tropical savannas* (pp. 101-119): Springer

Hurcom, S.J., & Harrison, A.R. (1998). The NDVI and spectral decomposition for semi-arid vegetation abundance estimation. *International Journal of Remote Sensing, 19*, 3109-3125

Hutley, L.B. (2008). Savanna. In (pp. 3143-3154)

Huttich, C., Gessner, U., Herold, M., Strohbach, B.J., Schmidt, M., Keil, M., & Dech, S. (2009). On the Suitability of MODIS Time Series Metrics to Map Vegetation

Types in Dry Savanna Ecosystems: A Case Study in the Kalahari of NE Namibia. *Remote Sensing, 1*, 620-643

Hüttich, C., Herold, M., Strohbach, B.J., & Dech, S. (2011a). Integrating in-situ, Landsat, and MODIS data for mapping in Southern African savannas: experiences of LCCS-based land-cover mapping in the Kalahari in Namibia. *Environmental Monitoring and Assessment, 176*, 531-547

Hüttich, C., Herold, M., Wegmann, M., Cord, A., Strohbach, B., Schmullius, C., & Dech, S. (2011b). Assessing effects of temporal compositing and varying observation periods for large-area land-cover mapping in semi-arid ecosystems: Implications for global monitoring. *Remote Sensing of Environment, 115*, 2445-2459

Jaeger, J.A.G., Bowman, J., Brennan, J., Fahrig, L., Bert, D., Bouchard, J., Charbonneau, N., Frank, K., Gruber, B., & von Toschanowitz, K.T. (2005). Predicting when animal populations are at risk from roads: an interactive model of road avoidance behavior. *Ecological Modelling, 185*, 329-348

Jane, S., Graeme, S.C., Matt, M., & Michael, W.B. (2006). Linking Spatial and Temporal Variation at Multiple Scales in a Heterogeneous Landscape[*]. In (pp. 406-420)

Jeltsch, F., Milton, S.J., Dean, W.R.J., & Rooyen, N.v. (1997). Simulated Pattern Formation around Artificial Waterholes in the Semi-Arid Kalahari. *Journal of Vegetation Science, 8*, 177-188

Jeltsch, F., Milton, S.J., Dean, W.R.J., & VanRooyen, N. (1996). Tree spacing and coexistence in semiarid savannas. *Journal of Ecology, 84*, 583-595

Jeltsch, F., Weber, G.E., & Grimm, V. (2000). Ecological buffering mechanisms in savannas: A unifying theory of long-term tree-grass coexistence. *Plant Ecology, 150*, 161-171

Jin, C., Xiao, X., Merbold, L., Arneth, A., Veenendaal, E., & Kutsch, W.L. (2013). Phenology and gross primary production of two dominant savanna woodland ecosystems in Southern Africa. *Remote Sensing of Environment, 135*, 189-201

Johansen, K., Arroyo, L.A., Armston, J., Phinn, S., & Witte, C. (2010). Mapping riparian condition indicators in a sub-tropical savanna environment from discrete return LiDAR data using object-based image analysis. *Ecological Indicators, 10*, 796-807

Johnson, R., & Tothill, J. (1985). Definition and broad geographic outline of savanna lands. *Ecology and Management of the World's Savannas. Australian Academy of Sciences, Canberra, ACT*, 1-13

Jones, C.G., Lawton, J.H., & Shachak, M. (1996). Organisms as ecosystem engineers. (Reprinted from Oikos vol. 69, pp. 373-386, 1994). *Ecosystem management: Selected readings* (pp. 130-147): Springer-Verlag New York, Inc.; Springer-Verlag

Jules, E.S., Kauffman, M.J., Ritts, W.D., & Carroll, A.L. (2002). Spread of an invasive pathogen over a variable landscape: a nonnative root rot on Port Orford cedar. In (p. 3167)

Justice, C., Kendall, J., Dowty, P., & Scholes, R. (1996). Satellite remote sensing of fires during the SAFARI campaign using NOAA advanced very high resolution radiometer data. *Journal of Geophysical Research: Atmospheres (1984–2012), 101*, 23851-23863

Justice, C.O., Giglio, L., Korontzi, S., Owens, J., Morisette, J.T., Roy, D., Descloitres, J., Alleaume, S., Petitcolin, F., & Kaufman, Y. (2002). The MODIS fire products. *Remote Sensing of Environment, 83*, 244-262

Kaufman, Y.J., & Tanre, D. (1992). Atmospherically Resistant Vegetation Index (Arvi) for Eos-Modis. *Ieee Transactions on Geoscience and Remote Sensing, 30*, 261-270

Keshava, N. (2003). A Survey of Spectral Unmixing Algorithms. *Lincoln Laboratory Journal, 14*

Keshava, N., Kerekes, J., Manolakis, D., & Shaw, G. (2000). An algorithm taxonomy for hyperspectral unmixing. In S.S. Shen & M.R. Descour (Eds.), *Algorithms for Multispectral, Hyperspectral, and Ultraspectral Imagery Vi* (pp. 42-63). Bellingham: Spie-Int Soc Optical Engineering

Keyghobadi, N., Roland, J., & Strobeck, C. (1999). Influence of landscape on the population genetic structure of the alpine butterfly Parnassius smintheus (Papilionidae). In (p. 1481)

Kim, M., Warner, T.A., Madden, M., & Atkinson, D.S. (2011). Multi-scale GEOBIA with very high spatial resolution digital aerial imagery: scale, texture and image objects. *International Journal of Remote Sensing, 32*, 2825-2850

Knight, T.W., & Morris, D.W. (1996). How many habitats do landscapes contain. In (p. 1756)

Koppel, J.v.d., Rietkerk, M., Langevelde, F.v., Kumar, L., Klausmeier, C.A., Fryxell, J.M., Hearne, J.W., Andel, J.v., Ridder, N.d., Skidmore, A., Stroosnijder, L., & Prins, H.H.T. (2002). Spatial Heterogeneity and Irreversible Vegetation Change in Semiarid Grazing Systems. *The American Naturalist, 159*, 209-218

Kotliar, N.B., & Wiens, J.A. (1990). Multiple Scales of Patchiness and Patch Structure: A Hierarchical Framework for the Study of Heterogeneity. *Oikos, 59*, 253-260

Krug, C., Esler, K., Hoffman, M., Henschel, J., Schmiedel, U., & Jürgens, N. (2006). North-South cooperation through BIOTA: an interdisciplinary monitoring programme in arid and semi-arid southern Africa. *South African Journal of Science, 102*, 187-190

Kruse, F.A. (2007). Improving multispectral mapping by spectral modeling with hyperspectral signatures. In S.S. Shen & P.E. Lewis (Eds.), *Algorithms and Technologies for Multispectral, Hyperspectral, and Ultraspectral Imagery XIII* (pp. U365-U376). Bellingham: Spie-Int Soc Optical Engineering

Kruse, F.A., & Perry, S.L. (2009). Improving multispectral mapping by spectral modeling with hyperspectral signatures. *Journal of Applied Remote Sensing, 3*, 22

Lal, R. (2004). Carbon Sequestration in Dryland Ecosystems. *Environmental Management, 33*, 528-544

Laliberte, A., Browning, D., & Rango, A. (2012). A comparison of three feature selection methods for object-based classification of sub-decimeter resolution UltraCam-L imagery. *International Journal of Applied Earth Observation and Geoinformation, 15*, 70-78

Laliberte, A.S., Fredrickson, E.L., & Rango, A. (2007). Combining decision trees with hierarchical object-oriented image analysis for mapping arid rangelands. *Photogrammetric Engineering and Remote Sensing, 73*, 197

Laliberte, A.S., Rango, A., Havstad, K.M., Paris, J.F., Beck, R.F., McNeely, R., & Gonzalez, A.L. (2004). Object-oriented image analysis for mapping shrub encroachment from 1937 to 2003 in southern New Mexico. *Remote Sensing of Environment, 93*, 198-210

Lambin, E.F., & Geist, H.J. (2006). *Land use and land cover change: local processes and global impacts*: Springer

Lambin, E.F., Turner, B.L., Geist, H.J., Agbola, S.B., Angelsen, A., Bruce, J.W., Coomes, O.T., Dirzo, R., Fischer, G., Folke, C., George, P.S., Homewood, K., Imbernon, J., Leemans, R., Li, X.B., Moran, E.F., Mortimore, M., Ramakrishnan, P.S., Richards, J.F., Skanes, H., Steffen, W., Stone, G.D., Svedin, U., Veldkamp, T.A., Vogel, C., & Xu, J.C. (2001). The causes of land-use and land-cover change: moving beyond the myths. *Global Environmental Change-Human and Policy Dimensions, 11*, 261-269

Latifovic, R., & Olthof, I. (2004). Accuracy assessment using sub-pixel fractional error matrices of global land cover products derived from satellite data. *Remote Sensing of Environment, 90*, 153-165

Lawrence, R.L., Wood, S.D., & Sheley, R.L. (2006). Mapping invasive plants using hyperspectral imagery and Breiman Cutler classifications (RandomForest). *Remote Sensing of Environment, 100*, 356-362

Lennartz, S.P., & Congalton, R.G. (2004). Classifying and mapping forest cover types using Ikonos imagery in the northeastern United States. In, *Proceedings of the ASPRS 2004 Annual Conference* (pp. 23-28)

Levick, S., & Rogers, K. (2006). LiDAR and object-based image analysis as tools for monitoring the structural diversity of savanna vegetation. *The International Archives of the Photogrammetry, Remote Sensing nad Spatial Information Sciences, 34*

Levick, S.R., Asner, G.P., Kennedy-Bowdoin, T., & Knapp, D.E. (2009). The relative influence of fire and herbivory on savanna three-dimensional vegetation structure. *Biological Conservation, 142*, 1693-1700

Li, S.-G., Liu, Q., & Afshari, S. (2006). An object-oriented hierarchical patch dynamics paradigm (HPDP) for modeling complex groundwater systems across multiple-scales. *Environmental Modelling & Software, 21*, 744-749

Liaw, A., & Weiener, M. (2002). Classification and regression by randomForest. *R News, 2*, 18-22

Liaw, A., & Wiener, M. (2002). Classification and Regression by randomForest. *R News, 2*, 18-22

Lillesand, T.M., & Kiefer, R.W. (1994). *Remote sensing and image interpretation / Thomas M. Lillesand, Ralph W. Kiefer*. New York :: Wiley & Sons

Liu, D.S., & Xia, F. (2010). Assessing object-based classification: advantages and limitations. *Remote Sensing Letters, 1*, 187-194

Loreau, M., Mouquet, N., & Holt, R.D. (2003). Meta-ecosystems: a theoretical framework for a spatial ecosystem ecology. In (p. 673)

Low, P.S. (2005). *Climate change and Africa*: Cambridge University Press

Lucieer, A., Stein, A., & Fisher, P. (2005). Multivariate texture segmentation of high-resolution remotely sensed imagery for identification of fuzzy objects. *International Journal of Remote Sensing, 26*, 2917-2936

Ludwig, J.A., Bastin, G.N., Chewings, V.H., Eager, R.W., & Liedloff, A.C. (2007). Leakiness: A new index for monitoring the health of arid and semiarid landscapes using remotely sensed vegetation cover and elevation data. *Ecological Indicators, 7*, 442-454

Ludwig, J.A., Coughenour, M.B., Liedloff, A.C., & Dyer, R. (2001). Modelling the resilience of Australian savanna systems to grazing impacts. *Environment International, 27*, 167-172

Ludwig, J.A., Tongway, D.J., Bastin, G.N., & James, C.D. (2004). Monitoring ecological indicators of rangeland functional integrity and their relation to biodiversity at local to regional scales. *Austral Ecology, 29*, 108-120

Lüttge, U. (2008). Savannas. I. Physiognomy, Terminology and Ecotones: Why Do Savannas Exist? , *Physiological Ecology of Tropical Plants* (pp. 293-312): Springer Berlin Heidelberg

Makhabu, S.W., Marotsi, B., & Perkins, J. (2002). Vegetation gradients around artificial water points in the Central Kalahari Game Reserve of Botswana. *African Journal of Ecology, 40*, 103-109

Mallinis, G., Koutsias, N., Tsakiri-Strati, M., & Karteris, M. (2008). Object-based classification using Quickbird imagery for delineating forest vegetation polygons in a Mediterranean test site. *Isprs Journal of Photogrammetry and Remote Sensing, 63*, 237-250

Manel, S., Schwartz, M.K., Luikart, G., & Taberlet, P. (2003). Landscape genetics: combining landscape ecology and population genetics. In (p. 189)

Marpu, P.R., Nussbaum, S., Niemeyer, I., & Gloaguen, R. (2008). A Procedure for Automatic Object-based Classification. In: (Eds.) (2008). In T. Blaschke, S. Lang & G. Hay (Eds.), *Object-Based Image Analysis Spatial Concepts for Knowledge-Driven Remote Sensing Applications. Series: Lecture Notes in Geoinformation and Cartography* (pp. 169-184). Berlin: Springer

Mather, P., & Tso, B. (2010). *Classification methods for remotely sensed data*: CRC press

McCown, R., & Williams, J. (1990). The water environment and implications for productivity. *Journal of Biogeography*, 513-520

McDermid, G.J., Franklin, S.E., & LeDrew, E.F. (2005). Remote sensing for large-area habitat mapping. *Progress in Physical Geography, 29*, 449-474

McGlynn, I.O., & Okin, G.S. (2006). Characterization of shrub distribution using high spatial resolution remote sensing: Ecosystem implications for a former Chihuahuan Desert grassland. *Remote Sensing of Environment, 101*, 554-566

Meyer, K.M., Wiegand, K., & Ward, D. (2009). Patch dynamics integrate mechanisms for savanna tree-grass coexistence. *Basic and Applied Ecology, 10*, 491-499

Milton, S.J., & Dean, W.R.J. (1998). Alien Plant Assemblages near Roads in Arid and Semi-Arid South Africa. *Diversity and Distributions, 4*, 175-187

Milton, S.J., & Dean, W.R.J. (2001). Seeds dispersed in dung of insectivores and herbivores in semi-arid southern Africa. *Journal of Arid Environments, 47*, 465-483

Mishra, N.B., & Chaudhuri, G. (2013). Characterizing the Physical Environment of Kolkata by Spectral Unmixing of Landsat TM. In, *NASA LCLUC Regional Science Meeting in South Asia*

Mishra, N.B., & Crews, K.A. (2014a). Estimating fractional land cover in semi-arid central Kalahari: The impact of mapping method (spectral unmixing versus object based image analysis) and vegetation morphology. *Geocart International*

Mishra, N.B., & Crews, K.A. (2014b). Mapping vegetation morphology types in a dry savanna ecosystem: integrating hierarchical object-based image analysis with Random Forest. *International Journal of Remote Sensing, 35*, 1175-1198

Mishra, N.B., & Crews, K.A. (under review). Mapping vegetation morphology types in a dry savanna ecosystem: Integrating hierarchical object based image analysis with random forest

Mishra, N.B., Crews, K.A., & Okin, G.S. (2014). Relating Spatial Patterns of Fractional Land Cover to Savanna Vegetation Morphology using Multi-scale Remote Sensing in the Central Kalahari. *International Journal of Remote Sensing, 35*, 2082-2104

Mistry, J. (2000). Savannas. *Progress in Physical Geography, 24*, 601-608

Moleele, N., Ringrose, S., Matheson, W., & Vanderpost, C. (2002). More woody plants? The status of bush encroachment in Botswana's grazing areas. *Journal of Environmental Management, 64*, 3-11

Moore, A., & Attwell, C. (1999). Geological controls on the distribution of woody vegetation in the central Kalahari, Botswana. *South African Journal of Geology, 102*, 350-362

Moustakas, A., Sakkos, K., Wiegand, K., Ward, D., Meyer, K.M., & Eisinger, D. (2009). Are savannas patch-dynamic systems? A landscape model. *Ecological Modelling, 220*, 3576-3588

Mucina, L. (1997). Classification of vegetation: Past, present and future. *Journal of Vegetation Science, 8*, 751-760

Mutanga, O., Skidmore, A.K., & Prins, H.H.T. (2004). Predicting in situ pasture quality in the Kruger National Park, South Africa, using continuum-removed absorption features. *Remote Sensing of Environment, 89*, 393-408

Mutangao, O., & Kumar, L. (2007). Estimating and mapping grass phosphorus concentration in an African savanna using hyperspectral image data. *International Journal of Remote Sensing, 28*, 4897-4911

Myint, S.W., & Okin, G.S. (2009). Modelling land-cover types using multiple endmember spectral mixture analysis in a desert city. *International Journal of Remote Sensing, 30*, 2237-2257

Nagler, P.L., Inoue, Y., Glenn, E.P., Russ, A.L., & Daughtry, C.S.T. (2003). Cellulose absorption index (CAI) to quantify mixed soil-plant litter scenes. *Remote Sensing of Environment, 87*, 310-325

Naiman, R.J., & Rogers, K.H. (1997). Large animals and system level characteristics in river corridors. In (p. 521)

Newton, A.C., Hill, R.A., Echeverria, C., Golicher, D., Benayas, J.M.R., Cayuela, L., & Hinsley, S.A. (2009). Remote sensing and the future of landscape ecology. *Progress in Physical Geography, 33*, 528-546

Noss, R.F. (1990). Indicators for monitoring biodiversity: a hierarchical approach. *Conservation Biology, 4*, 355-364

NRC (2007). *Earth Science and Applications from Space: National Imperatives for the next Decade and Beyond*: National Academic Press

Numata, I., Roberts, D.A., Chadwick, O.A., Schimel, J., Sampaio, F.R., Leonidas, F.C., & Soares, J.V. (2007). Characterization of pasture biophysical properties and the impact of grazing intensity using remotely sensed data. *Remote Sensing of Environment, 109*, 314-327

Nussbaum, S., Niemeyer, I., & Canty, M.J. (2006). SEaTH - A new tool for automated feature extraction in the context of object-oriented image analysis. . In, *Proc. AGIT - Obia,* . Salzburg: ISPRS

Okin, G.S. (2007a). Relative spectral mixture analysis -- A multitemporal index of total vegetation cover. *Remote Sensing of Environment, 106*, 467-479

Okin, G.S. (2007b). Relative spectral mixture analysis - A multitemporal index of total vegetation cover. *Remote Sensing of Environment, 106*, 467-479

Okin, G.S., Clarke, K.D., & Lewis, M.M. (2013). Comparison of methods for estimation of absolute vegetation and soil fractional cover using MODIS normalized BRDF-adjusted reflectance data. *Remote Sensing of Environment, 130*, 266-279

Okin, G.S., Murray, B., & Schlesinger, W.H. (2001a). Degradation of sandy arid shrubland environments: observations, process modelling, and management implications. *Journal of Arid Environments, 47*, 123-144

Okin, G.S., Parsons, A.J., Wainwright, J., Herrick, J.E., Bestelmeyer, B.T., Peters, D.C., & Fredrickson, E.L. (2009). Do Changes in Connectivity Explain Desertification? *Bioscience, 59*, 237-244

Okin, G.S., & Roberts, D.A. (2004). Remote sensing in arid regions: challenges and opportunities. *Manual of Remote Sensing, 4*, 111-146

Okin, G.S., Roberts, D.A., Murray, B., & Okin, W.J. (2001b). Practical limits on hyperspectral vegetation discrimination in arid and semiarid environments. *Remote Sensing of Environment, 77*, 212-225

Okin, W.J., Okin, G.S., Roberts, D.A., & Murray, B. (1998). Multiple endmember spectral mixture analysis: Endmember choice in an arid shrubland In, *Proceedings of the 5th AVIRIS Airborne Geosciences Workshop.* . JPL, CA

Olson, D.M., Dinerstein, E., Wikramanayake, E.D., Burgess, N.D., Powell, G.V.N., Underwood, E.C., D'Amico, J.A., Itoua, I., Strand, H.E., Morrison, J.C., Loucks, C.J., Allnutt, T.F., Ricketts, T.H., Kura, Y., Lamoreux, J.F., Wettengel, W.W., Hedao, P., & Kassem, K.R. (2001). Terrestrial ecoregions of the worlds: A new map of life on Earth. *Bioscience, 51*, 933-938

Opdam, P., Foppen, R., & Vos, C. (2002). Bridging the gap between ecology and spatial planning in landscape ecology. In (p. 767)

Paine, R.T., Tegner, M.J., & Johnson, E.A. (1998). Compounded perturbations yield ecological surprises. In (p. 535)

Pal, M. (2005). Random forest classifier for remote sensing classification. *International Journal of Remote Sensing, 26*, 217-222

Pal, N.R., & Pal, S.K. (1993). A review on image segmentation techniques. *Pattern recognition, 26*, 1277-1294

Parker, K.C., & Bendix, J. (1996). Landscape-scale geomorphic influences on vegetation patterns in four environments. In (p. 113)

Parker Williams, A., & Hunt Jr, E.R. (2002). Estimation of leafy spurge cover from hyperspectral imagery using mixture tuned matched filtering. *Remote Sensing of Environment, 82*, 446-456

Parris, R. (1971). The ecology and behaviour of wildlife in the Kalahari. *Botswana Notes and Records, 1*, 96-107

Parris, R., & Child, G. (1973). The importance of pans to wildlife in the Kalahari and the effect of human settlements on these areas. *Journal of South African Wildlife Management Association, 3*, 1-8

Pearson, S.M., Turner, M.G., & Drake, J.B. (1999). Landscape change and habitat availability in the southern Appalachian highlands and the Olympic Peninsula. In (p. 1288)

Peters, D.P.C., Yao, J., Huenneke, L.F., Gibbens, R.P., Havstad, K.M., Herrick, J.E., Rango, A., & Schlesinger, W.H. (2006). A framework and methods for simplifying complex landscapes to reduce uncertainty in predictions. In J. Wu, K.B. Jones, H. Li & O.L. Loucks (Eds.), *Scaling and Uncertainty Analysis in Ecology: Methods and Applications* (pp. 131-146). Dordrecht: Springer

Pickup, G., Chewings, V.H., & Nelson, D.J. (1993). Estimating changes in vegetation cover over time in arid rangelands using landsat MSS data. *Remote Sensing of Environment, 43*, 243-263

Pike, J.G. (1971). The Development of Water Resources of the Okavango Delta. *Botswana Notes and Records, Special Edition, 1*, 35-40

Pinty, B., & Verstraete, M.M. (1992). GEMI: a non-linear index to monitor global vegetation from satellites. *Plant Ecology, 101*, 15-20

Plaza, A., Martinez, P., Pérez, R., & Plaza, J. (2004). A quantitative and comparative analysis of endmember extraction algorithms from hyperspectral data. *Geoscience and Remote Sensing, IEEE Transactions on, 42*, 650-663

Polley, H.W., Mayeux, H.S., Johnson, H.B., & Tischler, C.R. (1997). Viewpoint: Atmospheric CO2, soil water, and shrub/grass ratios on rangelands. *Journal of Range Management, 50*, 278-284

Poole, G.C. (2002). Fluvial landscape ecology: addressing uniqueness within the river discontinuum. *Freshwater Biology, 47*, 641-660

Powell, R.L., Roberts, D.A., Dennison, P.E., & Hess, L.L. (2007). Sub-pixel mapping of urban land cover using multiple endmember spectral mixture analysis: Manaus, Brazil. *Remote Sensing of Environment, 106*, 253-267

Privette, J.L., & Roy, D.P. (2005). Southern Africa as a remote sensing test bed: the SAFARI 2000 Special Issue overview. *International Journal of Remote Sensing, 26*, 4141-4158

Privette, J.L., Tian, Y., Roberts, G., Scholes, R.J., Wang, Y., Caylor, K.K., Frost, P., & Mukelabai, M. (2004). Vegetation structure characteristics and relationships of Kalahari woodlands and savannas. *Global Change Biology, 10*, 281-291

Radeloff, V.C., Mladenoff, D.J., & Boyce, M.S. (2000). Effects of interacting disturbances on landscape patterns: budworm defoliation and salvage logging. In (p. 233)

Reed, M., & Dougill, A. (2010). Linking degradation assessment to sustainable land management: A decision support system for Kalahari pastoralists. *Journal of Arid Environments, 74*, 149-155

Reed, M.S., Dougill, A.J., & Taylor, M.J. (2007). Integrating local and scientific knowledge for adaptation to land degradation: Kalahari rangeland management options. *Land Degradation & Development, 18*, 249-268

Richardson, A.J., & Wiegand, C.L. (1977). Distinguishing Vegetation from Soil Background Information. *Photogrammetric Engineering and Remote Sensing, 43*, 1541-1552

Richter, R., & Schläpfer, D. (2008). Atmospheric/Topographic Correction for Satellite Imagery. ATCOR-2/3 User Guide, Version 6.4. In

Ringrose, S., Jellema, A., Huntsman-Mapila, P., Baker, L., & Brubaker, K. (2005). Use of remotely sensed data in the analysis of soil-vegetation changes along a drying gradient peripheral to the Okavango Delta, Botswana. *International Journal of Remote Sensing, 26*, 4293-4319

Ringrose, S., Matheson, W., & Vanderpost, C. (1998). Analysis of soil organic carbon and vegetation cover trends along the Botswana Kalahari Transect. *Journal of Arid Environments, 38*, 379-396

Ringrose, S., Matheson, W., Wolski, P., & Huntsman-Mapila, P. (2003). Vegetation cover trends along the Botswana Kalahari transect. *Journal of Arid Environments, 54*, 297-317

Roberts, D.A., Dennison, P.E., Gardner, M.E., Hetzel, Y., Ustin, S.L., & Lee, C.T. (2003). Evaluation of the potential of Hyperion for fire danger assessment by

comparison to the Airborne Visible/Infrared Imaging Spectrometer. *Geoscience and Remote Sensing, IEEE Transactions on, 41*, 1297-1310

Roberts, D.A., Gardner, M., Church, R., Ustin, S., Scheer, G., & Green, R.O. (1998). Mapping Chaparral in the Santa Monica Mountains Using Multiple Endmember Spectral Mixture Models. *Remote Sensing of Environment, 65*, 267-279

Roberts, D.A., Gardner, M., Church, R., Ustin, S.L., & Green, R.O. (1997a). Optimum strategies for mapping vegetation using multiple endmember spectral mixture models. In M.R. Descour & S.S. Shen (Eds.), *Imaging Spectrometry Iii* (pp. 108-119). Bellingham: Spie - Int Soc Optical Engineering

Roberts, D.A., Green, R.O., & Adams, J.B. (1997b). Temporal and spatial patterns in vegetation and atmospheric properties from AVIRIS. *Remote Sensing of Environment, 62*, 223-240

Roberts, D.A., Smith, M.O., & Adams, J.B. (1993). Green Vegetation, Nonphotosynthetic. Vegetation, and Soils in AVIRIS Data. *Remote Sensing of Environment, 44*, 255-269

Román, M.O., Schaaf, C.B., Woodcock, C.E., Strahler, A.H., Yang, X., Braswell, R.H., Curtis, P.S., Davis, K.J., Dragoni, D., & Goulden, M.L. (2009). The MODIS (Collection V005) BRDF/albedo product: Assessment of spatial representativeness over forested landscapes. *Remote Sensing of Environment, 113*, 2476-2498

Ross, K. (1987). *Okavango: jewel of the Kalahari*: Struik

Roy, D.P., Boschetti, L., & Giglio, L. (2011). Remote Sensing of Global Savanna Fire Occurence, Extent and Properties. In M.J. Hill & N.P. Hanan (Eds.), *Ecosystem Function in Savannas: Measurement and Modeling at Landscape to Global Scales*: CRC Press

Running, S.W., Loveland, T.R., Pierce, L.L., Nemani, R., & Hunt Jr, E. (1995). A remote sensing based vegetation classification logic for global land cover analysis. *Remote Sensing of Environment, 51*, 39-48

Sala, O., & Lauenroth, W. (1982). Small rainfall events: an ecological role in semiarid regions. *Oecologia, 53*, 301-304

Sankaran, M., Hanan, N.P., Scholes, R.J., Ratnam, J., Augustine, D.J., Cade, B.S., Gignoux, J., Higgins, S.I., Le Roux, X., Ludwig, F., Ardo, J., Banyikwa, F., Bronn, A., Bucini, G., Caylor, K.K., Coughenour, M.B., Diouf, A., Ekaya, W., Feral, C.J., February, E.C., Frost, P.G.H., Hiernaux, P., Hrabar, H., Metzger, K.L., Prins, H.H.T., Ringrose, S., Sea, W., Tews, J., Worden, J., & Zambatis, N. (2005). Determinants of woody cover in African savannas. *Nature, 438*, 846-849

Sankaran, M., Ratnam, J., & Hanan, N.P. (2004). Tree-grass coexistence in savannas revisited - insights from an examination of assumptions and mechanisms invoked in existing models. *Ecology Letters, 7*, 480-490

Scanlon, T.M., Albertson, J.D., Caylor, K.K., & Williams, C.A. (2002). Determining land surface fractional cover from NDVI and rainfall time series for a savanna ecosystem. *Remote Sensing of Environment, 82*, 376-388

Scanlon, T.M., Caylor, K.K., Levin, S.A., & Rodriguez-Iturbe, I. (2007). Positive feedbacks promote power-law clustering of Kalahari vegetation. *Nature, 449*, 209-212

Scanlon, T.M., Caylor, K.K., Manfreda, S., Levin, S.A., & Rodriguez-Iturbe, I. (2005). Dynamic response of grass cover to rainfall variability: implications for the function and persistence of savanna ecosystems. *Advances in Water Resources, 28*, 291-302

Schlesinger, W.H., Reynolds, J.F., Cunningham, G.L., Huenneke, L.F., Jarrell, W.M., Virginia, R.A., & Whitford, W.G. (1990). Biological Feedbacks in Global Desertification. *Science, 247*, 1043-1048

Schmitz, O.J., Hambck, P.A., & Beckerman, A.P. (2000). Trophic cascades in terrestrial systems: a review of the effects of carnivore removals on plants. In (p. 141)

Scholes, R.J., & Archer, S.R. (1997). Tree-grass interactions in savannas. *Annual Review of Ecology and Systematics, 28*, 517-544

Scholes, R.J., Dowty, P.R., Caylor, K., Parsons, D.A.B., Frost, P.G.H., & Shugart, H.H. (2002). Trends in Savanna Structure and Composition along an Aridity Gradient in the Kalahari. *Journal of Vegetation Science, 13*, 419-428

Scholes, R.J., & Walker, B.H. (1993). Cambridge Studies in Applied Ecology and Resource Management: An African savanna: Synthesis of the Nylsvley study. *Cambridge Studies in Applied Ecology and Resource Management; An African savanna: Synthesis of the Nylsvley study* (p. xii+306p): Cambridge University Press; Cambridge University Press

Schwartz, M.K., Mills, L.S., Ortega, Y., Ruggiero, L.F., & Allendorf, F.W. (2003). Landscape location affects genetic variation of Canada lynx (Lynx canadensis). In (p. 1807)

Seagle, S.W. (2003). Can deer foraging in multiple-use landscapes alter forest nitrogen budgets. In (p. 230)

Sesnie, S.E., Gessler, P.E., Finegan, B., & Thessler, S. (2008). Integrating Landsat TM and SRTM-DEM derived variables with decision trees for habitat classification and change detection in complex neotropical environments. *Remote Sensing of Environment, 112*, 2145-2159

Shugart, H., Macko, S., Lesolle, P., Szuba, T., Mukelabai, M., Dowty, P., & Swap, R. (2004). The SAFARI 2000–Kalahari transect wet season campaign of year 2000. *Global Change Biology, 10*, 273-280

Sinclair, A.R.E. (1995). Serengeti past and present. *Serengeti II: Dynamics, management, and conservation of an ecosystem* (pp. 3-30): University of Chicago Press; University of Chicago Press

Sinclair, A.R.E., & Arcese, P. (1995). Population Consequences of Predation-Sensitive Foraging - the Serengeti Wildebeest. *Ecology, 76*, 882-891

Skarpe, C. (1990). Shrub Layer Dynamics Under Different Herbivore Densities in an Arid Savanna, Botswana. *Journal of Applied Ecology, 27*, 873-885

Skarpe, C. (1991). Impact of Grazing in Savanna Ecosystems. *Ambio, 20*, 351-356

Smith, M.O., Ustin, S.L., Adams, J.B., & Gillespie, A.R. (1990). Vegetation in deserts: I. A regional measure of abundance from multispectral images. *Remote Sensing of Environment, 31*, 1-26

Solomon, S., D. , Qin, M., Manning, Z., Chen, M., Marquis, K.B., Averyt, M., & Tignor, H.L. (Eds.) (2007). *Climate Change : The Physical Science Basis, Contribution of Working Group I to the Fourth Assessment Report of the Intergovernmental Panel on Climate Change*. Cambridge: Cambridge Univeristy press

Somers, B., Asner, G.P., Tits, L., & Coppin, P. (2011). Endmember variability in spectral mixture analysis: A review. *Remote Sensing of Environment, 115*, 1603-1616

Sonka, M., Hlavac, V., Boyle, R., & Ray, L.A. (1996). Image processing, analysis and machine vision. *Journal of Electronic Imaging, 5*, 423

Soranno, P.A., Webster, K.E., Riera, J.L., Kratz, T.K., & Baron, J.S. (1999). Spatial variation among lakes within landscapes: ecological organization along lake chains. In (p. 395)

Southworth, J., Nagendra, H., & Tucker, C. (2002). Fragmentation of a Landscape: incorporating landscape metrics into satellite analyses of land-cover change. In (pp. 253 - 269): Routledge

Southworth, J., Rigg, L., Gibbes, C., Waylen, P., Zhu, L., McCarragher, S., & Cassidy, L. (2013). Integrating Dendrochronology, Climate and Satellite Remote Sensing to Better Understand Savanna Landscape Dynamics in the Okavango Delta, Botswana. *Land, 2*, 637-655

Spearman, C. (1904). The proof and measurement of association between two things. *American Journal of Psychology, 15*, 72-101

Spies, T.A., Ripple, W.J., & Bradshaw, G.A. (1994). Dynamics and pattern of a managed coniferous forest landscape in Oregon. In (p. 555)

Steen, D.A., & Gibbs, J.P. (2004). Effects of roads on the structure of freshwater turtle populations. *Conservation Biology, 18*, 1143-1148

Steenkamp, K., Wessels, K., Archibald, S., & von Maltitz, G. (2008). Long-Term Phenology and Variability of Southern African Vegetation. In, *Geoscience and Remote Sensing Symposium, 2008. IGARSS 2008. IEEE International* (pp. III - 816-III - 819)

Steffan-Dewenter, I., Munzenberg, U., Burger, C., Thies, C., & Tscharntke, T. (2002). Scale-dependent effects of landscape context on three pollinator guilds. In (p. 1421)

Steven, M., Biscoe, P., Jaggard, K., & Paruntu, J. (1986). Foliage cover and radiation interception. *Field Crops Research, 13*, 75-87

Stewart, G., Johnson, P., & Mark, A. (1989). Monitoring terrestrial vegetation for biological conservation. In, *Symposium on Environmental Monitoring in New Zealand with Emphasis on Protected Areas. Dunedin (New Zealand). May 1989.*

Stocker, A.D., & Schaum, A.P. (1997). Application of stochastic mixing models to hyperspectral detection problems. In A.E. Iverson & S.S. Shen (Eds.), *Algorithms for Multispectral and Hyperspectral Imagery Iii* (pp. 47-60). Bellingham: Spie - Int Soc Optical Engineering

Stott, P. (1991). Recent Trends in the Ecology and Management of the Worlds Savanna Formations. *Progress in Physical Geography, 15*, 18-28

Strayer, D.L., Beighley, R.E., Thompson, L.C., Brooks, A., & Nilsson, C. (2003a). Effects of land cover on stream ecosystems: roles of empirical models and scaling issues. In (p. 407)

Strayer, D.L., Ewing, H.A., & Bigelow, S. (2003b). What kind of spatial and temporal details are required in models of heterogeneous systems. In (p. 654)

Strohbach, B.J., Strohbach, J., Katuahuripa, J.T., & Mouton, H.D. (2004). A reconnaissance of the landscapes, soils and vegetation in the eastern communal areas. In. Namibia, Windhoek

Swain, H., & Davis, S.M. (1978). *Remote Sensing: The Quantitative Approach*. New York: McGraw- Hill

Swap, R.J., Annegarn, H.J., Suttles, J.T., King, M.D., Platnick, S., Privette, J.L., & Scholes, R.J. (2003). Africa burning: a thematic analysis of the Southern African Regional Science Initiative (SAFARI 2000). *Journal of Geophysical Research, 108*, 8465

Tallmon, D.A., Jules, E.S., Radke, N.J., & Mills, L.S. (2003). Of mice and men and trillium: cascading effects of forest fragmentation. In (p. 1193)

Tangestani, M.H., Mazhari, N., Agar, B., & Moore, F. (2008). Evaluating Advanced Spaceborne Thermal Emission and Reflection Radiometer (ASTER) data for alteration zone enhancement in a semi-arid area, northern Shahr-e-Babak, SE Iran. *International Journal of Remote Sensing, 29*, 2833-2850

Taylor, T. (2003). *The Timaeus and Critias of Plato*: Kessinger Publishing

Tews, J., Blaum, N., & Jeltsch, F. (2004). Structural and Animal Species Diversity in Arid and Semi-arid Savannas of the Southern Kalahari. *Annals of Arid Zone, 42*, 1-13

Tews, J., Esther, A., Milton, S.J., & Jeltsch, F. (2006). Linking a population model with an ecosystem model: Assessing the impact of land use and climate change on savanna shrub cover dynamics. *Ecological Modelling, 195*, 219-228

Thenkabail, P.S., Lyon, J.G., & Huete, A. (2012). *Hyperspectral remote sensing of vegetation*: CRC Press Boca Raton, FL

Theseira, M., Thomas, G., & Sannier, C. (2002). An evaluation of spectral mixture modelling applied to a semi-arid environment. *International Journal of Remote Sensing, 23*, 687-700

Thomas, D.S.G. (1984). Late Quaternary environmental change in central Southern Africa with particular reference to extensions of the arid zones. In: University of Oxford

Thomas, D.S.G. (2002). Sand, grass, thorns, and ... cattle: the modern Kalahari environment. In D. Sporton & D.S.G. Thomas (Eds.), *In Sustainable Livelihoods in Kalahari. Environments: Contributions to Global Debates* (pp. 39-66): Oxford University Press

Thomas, D.S.G., Knight, M., & Wiggs, G.F.S. (2005). Remobilization of southern African desert dune systems by twenty-first century global warming. *Nature, 435*, 1218-1221

Thomas, D.S.G., & Shaw, P.A. (1991). *The Kalahari Environment*: Cambridge University Press

Thomas, D.S.G., & Shaw, P.A. (1993). The evolution and characteristics of the Kalahari, southern Africa. *Journal of Arid Environments, 25*, 97-108

Thomas, D.S.G., & Sporton, D. (1997). Understanding the dynamics of social and environmental variability : The impacts of structural land use change on the environment and peoples of the Kalahari, Botswana. *Applied Geography, 17*, 11-27

Thomas, D.S.G., & Twyman, C. (2004). Good or bad rangeland? Hybrid knowledge, science, and local understandings of vegetation dynamics in the Kalahari. *Land Degradation & Development, 15*, 215-231

Thompson, M. (1996). Standard land-cover classification scheme for remote-sensing applications in South Africa

Thouless, C.R. (1998). Large mammals inside and outside protected areas in the Kalahari. *Transactions of the Royal Society of South Africa, 53*, 245-255

Tietjen, B., & Jeltsch, F. (2007). Semi-arid grazing systems and climate change: a survey of present modelling potential and future needs. *Journal of Applied Ecology, 44*, 425-434

Tompkins, S., Mustard, J.F., Pieters, C.M., & Forsyth, D.W. (1997). Optimization of endmembers for spectral mixture analysis. *Remote Sensing of Environment, 59*, 472-489

Trimble (2011a). *Ecognition developer 8.0 reference book*. Munchen, Germany

Trimble (2011b). eCognition® Developer 8.64. 1 User Guide. In: Trimble Germany GmbH Munich, Germany

Trombulak, S.C., & Frissell, C.A. (2000). Review of ecological effects of roads on terrestrial and aquatic communities. *Conservation Biology, 14*, 18-30

Trzcinski, M.K., Fahrig, L., & Merriam, G. (1999). Independent effects of forest cover and fragmentation on the distribution of forest breeding birds. In (p. 586)

Turner, B.L., Lambin, E.F., & Reenberg, A. (2007). The emergence of land change science for global environmental change and sustainability. *Proceedings of the National Academy of Sciences, 104*, 20666-20671

Turner, M.G. (1989). Landscape ecology: the effect of pattern on process. In (p. 171)

Turner, M.G. (2005). Landscape ecology in North America: past, present and future. In (p. 1967)

Turner, M.G., Pearson, S.M., Bolstad, P., & Wear, D.N. (2003). Effects of land-cover change on spatial pattern of forest communities in the southern Appalachian Mountains (USA). In (p. 449)

Turner, M.G., Romme, W.H., Gardner, R.H., O'Neill, R.V., & Kratz, T.K. (1993). A revised concept of landscape equilibrium: disturbance and stability on scaled landscapes. In (p. 213)

Turner, M.G., Tinker, D.B., Romme, W.H., Kashian, D.M., & Litton, C.M. (2004). Landscape patterns of sapling density, leaf area, and aboveground net primary production in postfire lodgepole pine forests, Yellowstone National Park (USA). In (p. 751)

Twyman, C. (2000). Livelihood Opportunity and Diversity in Kalahari Wildlife Management Areas, Botswana: Rethinking Community Resource Management. *Journal of Southern African Studies, 26*, 783-806

Tyson, P., Cooper, G., & McCarthy, T. (2002). Millennial to multi-decadal variability in the climate of southern Africa. *International Journal of Climatology, 22*, 1105-1117

Tyson, P.D., Dyer, T.G., & Mametse, M. (1975). Secular changes in South African rainfall: 1880 to 1972. *Quarterly Journal of the Royal Meteorological Society, 101*, 817-833

Urban, D., Goslee, S., Pierce, K., & Lookingbill, T. (2002). Extending community ecology to landscapes. In (p. 200)

Urban, D.L., O'Neill, R.V., & Shugart, H.H. (1987). Landscape ecology. In (p. 119)

Ustin, S.L., Roberts, D.A., Gamon, J.A., Asner, G.P., & Green, R.O. (2004). Using imaging spectroscopy to study ecosystem processes and properties. *Bioscience, 54*, 523-534

van Bommel, F.P.J., Heitkonig, I.M.A., Epema, G.F., Ringrose, S., Bonyongo, C., & Veenendaal, E.M. (2006). Remotely sensed habitat indicators for predicting distribution of impala (Aepyceros melampus) in the Okavango Delta, Botswana. *Journal of Tropical Ecology, 22*, 101-110

van Langevelde, F., van de Vijver, C., Kumar, L., van de Koppel, J., de Ridder, N., van Andel, J., Skidmore, A.K., Hearne, J.W., Stroosnijder, L., Bond, W.J., Prins, H.H.T., & Rietkerk, M. (2003). Effects of fire and herbivory on the stability of savanna ecosystems. *Ecology, 84*, 337-350

Van Rooyen, N., Bezuidenhout, D., Theron, G.K., & Bothma, J.D.P. (1990). Monitoring of the vegetation around artificial watering points (windmills) in the Kalahari Gemsbok National Park. *Koedoe, 33*, 63-88

van Rooyen, N., & van Rooyen, M.W. (1998). Vegetation of the south-western arid Kalahari: An overview. *Transactions of the Royal Society of South Africa, 53*, 113-140

Vane, G., Green, R.O., Chrien, T.G., Enmark, H.T., Hansen, E.G., & Porter, W.M. (1993). The Airborne Visible Infrared Imaging Spectrometer (Aviris). *Remote Sensing of Environment, 44*, 127-143

Vitousek, P.M. (1994). Beyond global warming: ecology and global change. *Ecology, 75*, 1861-1876

Vos, C.C., Verboom, J., Opdam, P.F.M., & Ter Braak, C.J.F. (2001). Toward ecologically scaled landscape indices. In (p. 24)

Walker, B.H., Ludwig, D., Holling, C.S., & Peterman, R.M. (1981). Stability of Semi-Arid Savanna Grazing Systems. *Journal of Ecology, 69*, 473-498

Wang, L., Sousa, W.P., Gong, P., & Biging, G.S. (2004). Comparison of IKONOS and QuickBird images for mapping mangrove species on the Caribbean coast of Panama. *Remote Sensing of Environment, 91*, 432-440

Warren, P.L., & Hutchinson, C.F. (1984). Indicators of Rangeland Change and Their Potential for Remote-Sensing. *Journal of Arid Environments, 7*, 107-126

Watkins, R.Z., Chen, J.Q., Pickens, J., & Brosofske, K.D. (2003). Effects of forest roads on understory plants in a managed hardwood landscape. *Conservation Biology, 17*, 411-419

Weare, P., & Yalala, A. (1971). Provisional vegetation map of Botswana. *Botswana Notes and Records, 3*, 1-1

Weller, D.E., Jordan, T.E., & Correll, D.L. (1998). Heuristic models for material discharge from landscapes with riparian buffers. In (p. 1156)

Wells, T.C., Sheail, J., Ball, D.F., & Ward, L.K. (1976). Ecological studies on the Porton Ranges: relationships between vegetation, soils and land-use history. In (p. 589)

Werger, M.J.A. (1973). Notes on the phytogeographical affinities of the southern Kalahari. *Bathalia, 11*, 177-180

Westhoff, V., & Van Der Maarel, E. (1980). *The Braun-Blanquet approach*: Springer

White, D., Minotti, P.G., Barczak, M.J., Sifneos, J.C., & Freemark, K.E. (1997). Assessing risks to biodiversity from future landscape change. In (p. 349)

Whiteside, T.G., Boggs, G.S., & Maier, S.W. (2011). Comparing object-based and pixel-based classifications for mapping savannas. *International Journal of Applied Earth Observation and Geoinformation, 13*, 884-893

Wickham, J.D., & Riitters, K.H. (1995). Sensitivity of landscape metrics to pixel size. In (p. 3585)

Wiegand, K., Saltz, D., & Ward, D. (2006). A patch-dynamics approach to savanna dynamics and woody plant encroachment - Insights from an arid savanna. *Perspectives in Plant Ecology, Evolution and Systematics, 7*, 229-242

Wiegand, K., Ward, D., & Saltz, D. (2005). Multi-scale patterns and bush encroachment in an and savanna with a shallow soil layer. *Journal of Vegetation Science, 16*, 311-320

Wigley, B.J., Bond, W.J., & Hoffman, M. (2010). Thicket expansion in a South African savanna under divergent land use: local vs. global drivers? *Global Change Biology, 16*, 964-976

Wu, H., & Li, Z.L. (2009). Scale Issues in Remote Sensing: A Review on Analysis, Processing and Modeling. *Sensors, 9*, 1768-1793

Wu, J. (2007). Past, present and future of landscape ecology. *Landscape Ecology, 22*, 1433-1435

Wu, J., & Marceau, D. (2002). Modeling complex ecological systems: an introduction. *Ecological Modelling, 153*, 1-6

Wu, J.G., & Loucks, O.L. (1995). From balance of nature to hierarchical patch dynamics: A paradigm shift in ecology. *Quarterly Review of Biology, 70*, 439-466

Wulder, M.A., Hall, R.J., Coops, N.C., & Franklin, S.E. (2009). High Spatial Resolution Remotely Sensed Data for Ecosystem Characterization. *Bioscience, 54*, 511-521

Wyk, B.V., Wyk, Piet van (1997). *Field guide to trees of Southern Africa*: Struik Publishers

Xiao, J.F., & Moody, A. (2005). A comparison of methods for estimating fractional green vegetation cover within a desert-to-upland transition zone in central New Mexico, USA. *Remote Sensing of Environment, 98*, 237-250

Xie, Y.C., Sha, Z.Y., & Yu, M. (2008). Remote sensing imagery in vegetation mapping: a review. *Journal of Plant Ecology-Uk, 1*, 9-23

Yan, G., Mas, J.F., Maathuis, B., Xiangmin, Z., & Van Dijk, P. (2006). Comparison of pixel-based and object-oriented image classification approaches—a case study in a coal fire area, Wuda, Inner Mongolia, China. *International Journal of Remote Sensing, 27*, 4039-4055

Yang, J., Weisberg, P.J., & Bristow, N.A. (2012). Landsat remote sensing approaches for monitoring long-term tree cover dynamics in semi-arid woodlands: comparison of vegetation indices and spectral mixture analysis. *Remote Sensing of Environment, 119*, 62-71

Yu, Q., Gong, P., Clinton, N., Biging, G., Kelly, M., & Schirokauer, D. (2006). Object-based detailed vegetation classification. with airborne high spatial resolution remote sensing imagery. *Photogrammetric Engineering and Remote Sensing, 72*, 799-811

Yu, Q., Gong, P., Tian, Y.Q., Pu, R., & Yang, J. (2008). Factors affecting spatial variation of classification uncertainty in an image object-based vegetation mapping. *Photogrammetric Engineering and Remote Sensing, 74*, 1007-1018

Zhu, L., & Southworth, J. (2013). Disentangling the relationships between net primary production and precipitation in southern Africa savannas using satellite observations from 1982 to 2010. *Remote Sensing, 5*, 3803-3825

Zimmermann, J., Higgins, S.I., Grimm, V., Hoffmann, J., & Linstadter, A. (2010). Grass mortality in semi-arid savanna: The role of fire, competition and self-shading. *Perspectives in Plant Ecology Evolution and Systematics, 12*, 1-8